MULTISEGMENT FOOT AND LOWER EXTREMITY BIOMECHANICS DURING WALKING IN YOUNGER AND OLDER ADULTS

by

Nayeli Guadalupe Marcial Muñoz

Biomedical Engineering, Tecnológico de Monterrey, 2018

A Thesis Submitted in Partial Fulfillment
of the Requirements for the Degree of

Master's of Science in Mechanical Engineering

in the Graduate Academic Unit of Mechanical Engineering

Supervisors: Victoria Chester, PhD, Faculty of Kinesiology
Usha Kuruganti, PhD, Faculty of Kinesiology
Edmund Biden, D.Phil., Department of Mechanical Engineering, Faculty of Engineering

Examining Board: Tiger Jeans, PhD, Department of Mechanical Engineering, Chair
Gobinda Saha, PhD, Department of Mechanical Engineering
Mohsen Mohammadi, PhD, Department of Mechanical Engineering
Emily Read, PhD, Faculty of Nursing

This thesis is accepted by the
Dean of Graduate Studies

THE UNIVERSITY OF NEW BRUNSWICK

January 2022

©Nayeli Marcial, 2022

ABSTRACT

The purpose of this study was to investigate differences in multisegment foot (MSF) and lower extremity biomechanics between young and older adults during walking at five different speeds, independent of speed, and as a function of foot structure and mobility. A 3D scanner was used to collect foot anthropometric data on 16 younger (18-35 years old) and 15 older (+65 years old) adults. A Vicon motion capture system and Kistler force plates were used to quantify trunk, pelvis, and lower limb kinematic and kinetic data. As a function of speed, older adults exhibited significant ($p<.05$) differences in temporospatial variables, reduced hip moment compensated by increased anterior pelvic tilting and knee flexion, as well as decreased foot mobility and propulsive capacity. Independent of speed, significant ($p<.05$) differences in MSF kinematics were found in older adults. Significant ($p<.05$) differences as a function of foot structure and mobility indicated that planus and rectus foot posture have a distinct motion pattern. Overall, findings of the study were mainly an age-related change, altering the gait pattern of older adults. To our knowledge, no single study has examined MSF and lower limb joint kinematics and kinetics across age, speed and foot structure and mobility. Results of this study improved our understanding of age-related differences in MSF mechanics.

DEDICATION

I dedicate this thesis to my family and many friends. A special feeling of gratitude to my loving parents for their support since day one and for their encouragement during the challenges of graduate school and life. They have taught me to work hard for the things that I aspire to achieve. Thank you to my sisters for always being there for me. Both have been my best cheerleaders.

I also dedicate this work to my many friends and lab mates who have supported me throughout the process. I will always appreciate all they have done.

Thank you to my academic supervisors under whose constant guidance I have completed this thesis. They not only enlightened me with academic knowledge but also gave me valuable advice when I needed it the most.

Last but not least, I dedicate this work to Almighty God, my strong pillar, for giving me strength, inspiration and motivation throughout this program.

Table of Contents

ABSTRACT ii
DEDICATION iii
Table of Contents iv
List of Tables xi
List of Figures xxviii
List of Symbols, Nomenclature or Abbreviations xliv
1.0 Introduction 1
1.1 Purpose 7
2.0 Literature Review 8
2.1 Significance of study 8
2.2 Age-related changes in kinematics and kinetics 8
2.3 Effect of Walking Speed on Gait Kinematics and Kinetics 14
2.3.1 Effect of Walking Speed using a Single Segment Foot Model 14
2.3.2 Effect of Walking Speed using a Multisegment Foot Model 18
2.4 Single segment foot models 24
2.5 Multisegment foot models 24
2.6 Effects of foot structure and mobility on gait 26
2.6.1 Age-related changes in foot structure 27
2.6.2 Age-related changes on foot mobility and posture 28
2.6.3 Arch height 32
2.8 Summary 32
3.0 Methods 33
3.1 Participants 33
3.2 Instrumentation 34

3.2.1 3D Scanner 34
3.2.2 Motion Capture System 36
3.2.3 Marker Placement 37
3.2.5 Force Plates 38
3.2.6 Visual3D 38
3.2.7 Laser trip timer 39
3.2.8 Custom-made foot measurement device 39
3.3 Experimental Procedure 39
3.3.1 3D Scanning Phase 40
3.3.2 Motion Capture Phase 41
3.3.3 Dynamic Trials Phase 42
3.4 Data Analysis 43
3.4.1 Data processing and analysis 43
3.4.2 Kinematic Data 44
3.4.3 Mechanical Model 44
3.4.5 Anatomical and Embedded coordinate systems 45
3.4.6 Kinetic Data 46
3.4.7 Foot Structure and Mobility Data 46
3.4.8 Method for controlling gait speed 47
3.4.9 Dimensionless Speed 47

3.4.10 Speed Group Division 48

3.4.11 Statistical Analysis 49

4.0 Results 50

4.1 Age-related Differences in MSF and Lower Extremity Kinematic and Kinetic Variables as a Function of Speed 50

4.1.1 Age-related Differences in Temporospatial Variables 50

4.1.2 Summary of temporospatial results 52

4.1.3 Age-related Differences in Relative Angles Between the Foot and Shank 52

4.1.4 Age-related Differences in Relative Angles Between the Midfoot and Calcaneus 67

4.1.5 Age-related Differences in Relative Angles Between the Shank and Calcaneus 85

4.1.6 Age-related Differences in Relative Angles Between the Midfoot and Forefoot 99

4.1.7 Age-related Differences in Relative Angles Between the Calcaneus and Forefoot 112

4.1.8 Summary of MSF kinematics' results 133

4.1.9 Age-related Differences in Planar Angles of the Foot 134

4.1.10 Summary of Planar Angles Results 147

4.1.11 Age-related Differences in Ankle Kinetics 148

4.1.12 Summary of Ankle Kinetics Results 157

4.1.13 Age-related Differences in Knee Kinetics and Kinematics 158

4.1.14 Summary of Knee Kinetics and Kinematics Results 178

4.1.15 Age-related Differences in Hip Kinetics and Kinematics..... 179

4.1.16 Summary of Hip Kinetics and Kinematics Results..... 204

4.1.17 Age-related Differences in Pelvic Kinematics..... 206

4.1.18 Summary of Pelvic Kinematics Results..... 220

4.1.19 Age-related Differences in Torso Kinematics 220

4.1.20 Summary of Torso Kinematics Results 235

4.1.21 Age-related Differences in Ground Reaction Forces..... 235

4.1.22 Summary of Ground Reaction Forces Results..... 241

4.2 Age-related Differences in MSF and Lower Extremity Kinematic and Kinetic Variables Independent of Speed 241

4.2.1 Age-related Differences in Temporospatial Variables Independent of Speed242

4.2.2 Summary of Temporospatial Results..... 242

4.2.3 Age-related Differences in Relative Angles Between the Foot and Shank Independent of Speed..... 243

4.2.4 Age-related Differences in Relative Angles Between the Midfoot and Calcaneus Independent of Speed..... 247

4.2.5 Age-related Differences in Relative Angles Between the Shank and Calcaneus Independent of Speed..... 250

4.2.6 Age-related Differences in Relative Angles Between the Midfoot and Forefoot Independent of Speed..... 255

4.2.7 Age-related Differences in Relative Angles Between the Calcaneus and Forefoot Independent of Speed..... 259

4.2.8 Summary of MSF Kinematics Results..... 262

4.2.9 Age-related Differences in Planar Angles of the Foot Independent of Speed264

4.2.10 Summary of Planar Angles Results 271

4.2.11 Age-related Differences in Ankle Kinetics Independent of Speed..... 272

4.2.12 Summary of Ankle Kinetics Results..... 274

4.2.13 Age-related Differences in Knee Kinetics and Kinematics Independent of Speed..... 274

4.2.14 Summary of Knee Kinetics and Kinematics Results 280

4.2.15 Age-related Differences in Hip Kinetics and Kinematics Independent of Speed 281

4.2.16 Summary of Hip Kinetics and Kinematics Results..... 287

4.2.17 Age-related Differences in Pelvic Kinematics Independent of Speed..... 288

4.2.18 Summary of Pelvic Kinematics Results..... 290

4.2.19 Age-related Differences in Torso Kinematics Independent of Speed 290

4.2.20 Summary of Torso Kinematics Results 292

4.2.21 Age-related Differences in Ground Reaction Forces Independent of Speed293

4.2.22 Summary of Ground Reaction Forces Results 296

4.3 Age-related Differences in MSF and Lower Extremity Kinematic and Kinetic Variables as a Function of Foot Structure and Mobility Independent of Speed 297

4.3.1 Age, Foot Type and Foot Mobility Differences in Relative Angles Between the Foot and Shank Independent of Speed 297

4.3.2 Age, Foot Type and Foot Mobility Differences in Relative Angles Between the Calcaneus and Forefoot Independent of Speed 298

4.3.3 Age, Foot Type and Foot Mobility Differences in Planar Angles of the Foot Independent of Speed 299

4.4 Summary of MSF Kinematics and Planar Angles Results 300

5.0 Discussion 301

5.1 Differences in MSF and Lower Extremity Kinematic and Kinetic Variables Between Age Groups as a Function of Speed 301

5.1.1 Temporospatial Variables 301

5.1.2 Ankle Kinetics and Kinematics 304

5.1.3 Multisegment Foot Kinematics 308

5.1.4 Knee Kinetics and Kinematics 320

5.1.5 Hip Kinetics and Kinematics 321

5.1.6 Pelvic Kinematics 324

5.1.7 Torso Kinematics 326

5.1.8 Ground Reaction Forces 327

5.2 Differences in MSF and Lower Extremity Kinematic and Kinetic Variables Between Age Groups Independent of Speed 328
5.2.1 Temporospatial Variables Independent of Speed 328
5.2.2 MSF Kinematics and Planar Angles Independent of Speed 328
5.2.3 Knee Kinetics and Kinematics Independent of Speed 330
5.2.4 Hip Kinetics and Kinematics Independent of Speed 330
5.2.5 Ground Reaction Forces 331
5.3 Differences in MSF and Lower Extremity Kinematic and Kinetic Variables Between Age Groups as a Function of Foot Structure and Mobility and Independent of Speed 332
5.4 Limitations of the study 334
5.5 Future recommendations 335
6.0 Conclusion 336
7.0 Significance and Impact of the Study 338
Bibliography 339
Curriculum Vitae

List of Tables

Table 1. Independent and Dependent Variables. 49

Table 2. Significant p-values of the mean temporospatial variables across five walking speeds. 50

Table 3. Significant p-values of the mean maximum DF/PF angles (∠) of the foot-shank during stance and swing phase, as well as their respective time of occurrence in the gait cycle across five walking speeds. 53

Table 4. DF/PF ROM data for the foot-shank during stance and swing phase across five walking speeds and their respective significant p-values. 59

Table 5. Significant p-values of the mean min and max ADD/ABD angles (∠) of the foot-shank during stance and swing phase, as well as their respective time of occurrence in the gait cycle across five walking speeds. 60

Table 6. Significant ADD/ABD ROM data for the foot-shank during stance and swing phase across five walking speeds and their respective significant p-values. 66

Table 7. Significant p-values of the mean min and max DF/PF angles (∠) of the mid-cal during stance and swing phase, as well as their respective time of occurrence in the gait cycle across five walking speeds. 67

Table 8. Significant DF/PF ROM data for the mid-cal during stance and swing phase across five walking speeds and their respective significant p-values. 70

Table 9. Significant p-values of the mean min and max EVE/INV angles (∠) of the mid-cal during stance and swing phase, as well as their respective time of occurrence in the gait cycle across five walking speeds. 72

Table 10. Significant EVE/INV ROM data for the mid-cal during stance and swing phase across five walking speeds and their respective significant p-values. 77
Table 11. Significant p-values of the mean min and max ADD/ABD angles (∠) of the mid-cal during stance and swing phase, as well as their respective time of occurrence in the gait cycle across five walking speeds. 79
Table 12. Significant ADD/ABD ROM data for the mid-cal during stance and swing phase across five walking speeds and their respective significant p-values. 84
Table 13. Significant p-values of the mean min and max DF/PF angles (∠) of the sha-cal during stance and swing phase, as well as their respective time of occurrence in the gait cycle across five walking speeds. 85
Table 14. Significant DF/PF ROM data for the sha-cal during stance and swing phase across five walking speeds and their respective significant p-values. 91
Table 15. Significant p-values of the mean min and max ADD/ABD angles (∠) of the sha-cal during stance and swing phase, as well as their respective time of occurrence in the gait cycle across five walking speeds. 92
Table 16. Significant ADD/ABD ROM data for the sha-cal during stance and swing phase across five walking speeds and their respective significant p-values. 98
Table 17. Significant p-values of the mean min and max DF/PF angles (∠) of the mid-met during stance and swing phase, as well as their respective time of occurrence in the gait cycle across five walking speeds. 99
Table 18. Significant DF/PF ROM data for the mid-met during stance and swing phase across five walking speeds and their respective significant p-values. 105

Table 19. Significant p-values of the mean min and max ADD/ABD angles (∠) of the mid-met during stance and swing phase, as well as their respective time of occurrence in the gait cycle across five walking speeds. 106
Table 20. Significant ADD/ABD ROM data for the mid-met during stance and swing phase across five walking speeds and their respective significant p-values. 111
Table 21. Significant p-values of the mean min and max DF/PF angles (∠) of the cal-met during stance and swing phase, as well as their respective time of occurrence in the gait cycle across five walking speeds. 112
Table 22. Significant DF/PF ROM data for the cal-met during stance and swing phase across five walking speeds and their respective significant p-values. 118
Table 23. Significant p-values of the mean min and max EVE/INV angles (∠) of the cal-met during stance and swing phase, as well as their respective time of occurrence in the gait cycle across five walking speeds. 120
Table 24. Significant EVE/INV ROM data for the cal-met during stance and swing phase across five walking speeds and their respective significant p-values. 126
Table 25. Significant p-values of the mean min and max ADD/ABD angles (∠) of the cal-met during stance and swing phase, as well as their respective time of occurrence in the gait cycle across five walking speeds. 127
Table 26. Significant ADD/ABD ROM data for the cal-met during stance and swing phase across five walking speeds and their respective significant p-values. 132
Table 27. Significant p-values of the mean min and max F2Pt angles (∠) during stance phase, as well as their respective time of occurrence in the gait cycle across five walking speeds. 135

Table 28. Significant F2Pt ROM data during stance phase across five walking speeds and their respective significant p-values..... 137

Table 29. Significant p-values of the mean min and max V2G angles (∠) during stance phase, as well as their respective time of occurrence in the gait cycle across five walking speeds..... 138

Table 30. Significant p-values of the mean min and max F2G angles (∠) during stance phase, as well as their respective time of occurrence in the gait cycle across five walking speeds..... 140

Table 31. Significant p-values of the mean min and max S2G angles (∠) during stance phase, as well as their respective time of occurrence in the gait cycle across five walking speeds..... 142

Table 32. Significant p-values of the mean min and max F2Ps angles (∠) during stance phase, as well as their respective time of occurrence in the gait cycle across five walking speeds..... 143

Table 33. Significant F2Ps ROM data for the cal-met during stance phase across five walking speeds..... 144

Table 34. Significant p-values of the mean min and max MLA angles (∠) during stance phase, as well as their respective time of occurrence in the gait cycle across five walking speeds..... 145

Table 35. Significant MLA ROM data for the cal-met during stance phase across five walking speeds and their respective significant p-values..... 147

Table 36. Significant p-values of the mean min and max DF/PF moments ((N·m)/kg) of the ankle during stance and swing phase, as well as their respective time of occurrence in the gait cycle across five walking speeds. 149
Table 37. Significant p-values of the mean max eccentric and concentric power (W/Kg) of the ankle during stance and swing phase, as well as their respective time of occurrence in the gait cycle across five walking speeds. 153
Table 38. Significant p-values of the mean min and max FLEX/EXT moments ((N·m)/kg) of the knee during stance and swing phase, as well as their respective time of occurrence in the gait cycle across five walking speeds. 159
Table 39. Significant p-values of the mean max eccentric and concentric power (W/Kg) of the knee during stance and swing phase, as well as their respective time of occurrence in the gait cycle across five walking speeds. 164
Table 40. Significant p-values of the mean min and max FLEX/EXT angles (∠) of the knee during stance and swing phase, as well as their respective time of occurrence in the gait cycle across five walking speeds. 169
Table 41. Significant FLEX/EXT ROM data for the knee during stance and swing phase across five walking speeds. 174
Table 42. Significant p-values of the mean min and max INT/EXTL rotation angles (∠) of the knee during stance and swing phase, as well as their respective time of occurrence in the gait cycle across five walking speeds. 175
Table 43. Significant internal/ER ROM data for the knee during stance and swing phase across five walking speeds. 178

Table 44. Significant p-values of the mean max FLEX/EXT moments ((N·m)/kg) of the hip during stance and swing phase, as well as their respective time of occurrence in the gait cycle across five walking speeds. 180
Table 45. Significant p-values of the mean min and max eccentric and concentric power (W/Kg) of the hip during stance and swing phase, as well as their respective time of occurrence in the gait cycle across five walking speeds. 187
Table 46. Significant p-values of the mean min and max FLEX/EXT angles (∠) of the hip during stance and swing phase, as well as their respective time of occurrence in the gait cycle across five walking speeds. 189
Table 47. Significant FLEX/EXT ROM data for the hip during stance and swing phase across five walking speeds. 194
Table 48. Significant p-values of the mean max ADD/ABD angles (∠) of the hip during stance and swing phase, as well as their respective time of occurrence in the gait cycle across five walking speeds. 196
Table 49. Significant ADD/ABD ROM data for the hip during stance and swing phase across five walking speeds and their respective significant p-values. 199
Table 50. Significant p-values of the mean max INT/EXTL rotation angles (∠) of the hip during stance and swing phase, as well as their respective time of occurrence in the gait cycle across five walking speeds. 200
Table 51. Significant internal/ER ROM data for the hip during stance and swing phase across five walking speeds and their respective significant p-values. 204

Table 52. Significant p-values of the mean min and max ANT/POST tilt angles (∠) of the pelvis during stance and swing phase, as well as their respective time of occurrence in the gait cycle across five walking speeds. 206
Table 53. Significant anterior/posterior tilt ROM data for the pelvis during stance and swing phase across five walking speeds and their respective significant p-values. 212
Table 54. Significant p-values of the mean max UP/DOWN obliquity angles (∠) of the pelvis during stance and swing phase, as well as their respective time of occurrence in the gait cycle across five walking speeds. 213
Table 55. Significant UP/DOWN obliquity ROM data for the pelvis during stance and swing phase across five walking speeds and their respective significant p-values. 219
Table 56. Significant p-values of the mean min and max ANT/POST tilt angles (∠) of the torso during stance and swing phase, as well as their respective time of occurrence in the gait cycle across five walking speeds. 221
Table 57. Significant anterior/POST tilt ROM data for the torso during stance and swing phase across five walking speeds and their respective significant p-values. 227
Table 58. Significant p-values of the mean max IPSI/CONTRA lean angles (∠) of the torso during stance and swing phase, as well as their respective time of occurrence in the gait cycle across five walking speeds. 228
Table 59. Significant IPSI/CONTRA lean ROM data for the torso during stance and swing phase across five walking speeds and their respective significant p-values. 234
Table 60. Significant p-values of the mean min and max antero-posterior ground reaction forces (%Body Weight) during stance and swing phase, as well as their respective time of occurrence in the gait cycle across five walking speeds. 236

Table 64. Significant p-values of the mean min and max vertical ground reaction forces (%Body Weight) during stance and swing phase, as well as their respective time of occurrence in the gait cycle across five walking speeds. 238
Table 62. Significant p-values of the mean temporospatial variables independent of WS. 242
Table 63. Temporospatial variables, independent of WS, found similar/different to the first hypothesis. 242
Table 64. Significant p-values of the mean max DF/PF angles (∠) of the foot-shank during stance and swing phase, as well as their respective time of occurrence in the gait cycle independent of WS. 243
Table 65. Foot-shank DF/PF angles, independent of WS, found similar/different to the first hypothesis. 243
Table 66. Significant p-values of the mean min and max EVE/INV angles (∠) of the foot-shank during stance and swing phase, as well as their respective time of occurrence in the gait cycle independent of WS. 244
Table 67. Foot-shank EVE/INV angles, independent of WS, found similar/different to the first hypothesis. 245
Table 68. Significant p-values of the mean min and max ADD/ABD angles (∠) of the foot-shank during stance and swing phase, as well as their respective time of occurrence in the gait cycle independent of WS. 246
Table 69. Foot-shank ADD/ABD angles, independent of WS, found similar/different to the first hypothesis. 246

Table 70. Significant p-values of the mean min and max DF/PF angles (∠) of the mid-cal during stance and swing phase, as well as their respective time of occurrence in the gait cycle independent of WS. 247
Table 71. Midfoot-calcaneus DF/PF angles, independent of WS, found similar/different to the first hypothesis. 247
Table 72. Significant p-values of the mean min and max EVE/INV angles (∠) of the mid-cal during stance and swing phase, as well as their respective time of occurrence in the gait cycle independent of WS. 248
Table 73. Midfoot-calcaneus EVE/INV angles, independent of WS, found similar/different to the first hypothesis. 248
Table 74. Significant p-values of the mean min and max ADD/ABD angles (∠) of the mid-cal during stance and swing phase, as well as their respective time of occurrence in the gait cycle independent of WS. 249
Table 75. Midfoot-calcaneus ADD/ABD angles, independent of WS, found similar/different to the first hypothesis. 250
Table 76. Significant p-values of the mean min and max DF/PF angles (∠) of the sha-cal during stance and swing phase, as well as their respective time of occurrence in the gait cycle independent of WS. 251
Table 77. Shank-calcaneus DF/PF angles, independent of WS, found similar/different to the first hypothesis. 251
Table 78. Significant p-values of the mean min and max EVE/INV angles (∠) of the sha-cal during stance and swing phase, as well as their respective time of occurrence in the gait cycle independent of WS. 252

Table 79. Shank-calcaneus EVE/INV angles, independent of WS, found similar/different to the first hypothesis. 252
Table 80. Significant p-values of the mean min and max ADD/ABD angles (∠) of the sha-cal during stance and swing phase, as well as their respective time of occurrence in the gait cycle independent of WS. 253
Table 81. Shank-calcaneus ADD/ABD angles, independent of WS, found similar/different to the first hypothesis. 253
Table 82. Significant p-values of the mean min and max DF/PF angles (∠) of the mid-met during stance and swing phase, as well as their respective time of occurrence in the gait cycle independent of WS. 255
Table 83. Midfoot-forefoot DF/PF angles, independent of WS, found similar/different to the first hypothesis. 255
Table 84. Significant p-values of the mean min and max EVE/INV angles (∠) of the mid-met during stance and swing phase, as well as their respective time of occurrence in the gait cycle independent of WS. 256
Table 85. Midfoot-forefoot EVE/INV angles, independent of WS, found similar/different to the first hypothesis. 256
Table 86. Significant p-values of the mean min and max ADD/ABD angles (∠) of the mid-met during stance and swing phase, as well as their respective time of occurrence in the gait cycle independent of WS. 258
Table 87. Midfoot-forefoot ADD/ABD angles, independent of WS, found similar/different to the first hypothesis. 258

Table 88. Significant p-values of the mean max DF/PF angles (∠) of the cal-met during stance and swing phase, as well as their respective time of occurrence in the gait cycle independent of WS. 259
Table 89. Calcaneus-forefoot DF/PF angles, independent of WS, found similar/different to the first hypothesis. 259
Table 90. Significant p-values of the mean min and max EVE/INV angles (∠) of the cal-met during stance and swing phase, as well as their respective time of occurrence in the gait cycle independent of WS. 260
Table 91. Calcaneus-forefoot EVE/INV angles, independent of WS, found similar/different to the first hypothesis. 261
Table 92. Significant p-values of the mean min and max ADD/ABD angles (∠) of the cal-met during stance and swing phase, as well as their respective time of occurrence in the gait cycle independent of WS. 262
Table 93. Calcaneus-forefoot ADD/ABD angles, independent of WS, found similar/different to the first hypothesis. 262
Table 94. Significant p-values of the mean min and max F2Pt angles (∠) during stance phase, as well as their respective time of occurrence in the gait cycle independent of WS. 264
Table 95. F2Pt angles, independent of WS, found similar/different to the first hypothesis. 264
Table 96. Significant p-values of the mean min and max V2G angles (∠) during stance phase, as well as their respective time of occurrence in the gait cycle independent of WS. 265

Table 97. V2G angles, independent of WS, found similar/different to the first hypothesis. 265

Table 98. Significant p-values of the mean min and max S2F angles (∠) during stance phase, as well as their respective time of occurrence in the gait cycle independent of WS. 266

Table 99. S2F angles, independent of WS, found similar/different to the first hypothesis. 266

Table 100. Significant p-values of the mean min and max S2V angles (∠) during stance phase, as well as their respective time of occurrence in the gait cycle independent of WS. 267

Table 101. S2V angles, independent of WS, found similar/different to the first hypothesis. 267

Table 102. Significant p-values of the mean min and max F2G angles (∠) during stance phase, as well as their respective time of occurrence in the gait cycle independent of WS. 268

Table 103. F2G angles, independent of WS, found similar/different to the first hypothesis. 268

Table 104. Significant p-values of the mean min and max S2G angles (∠) during stance phase, as well as their respective time of occurrence in the gait cycle independent of WS. 269

Table 105. S2G angles, independent of WS, found similar/different to the first hypothesis. 269

Table 106. Significant p-values of the mean min and max F2Ps angles (∠) during stance phase, as well as their respective time of occurrence in the gait cycle independent of WS. 270

Table 107. F2Ps angles, independent of WS, found similar/different to the first hypothesis. 270

Table 108. Significant p-values of the mean min and max MLA angles (∠) during stance phase, as well as their respective time of occurrence in the gait cycle independent of WS. 271

Table 109. MLA angles, independent of WS, found similar/different to the first hypothesis. 271

Table 110. Significant p-values of the mean min and max DF/PF ankle moments ((N·m)/kg) during stance and swing phase, as well as their respective time of occurrence in the gait cycle independent of WS. 272

Table 111. Ankle moment, independent of WS, found similar/different to the first hypothesis. 273

Table 112. Significant p-values of the mean max eccentric and concentric power (W/Kg) of the ankle during stance and swing phase, as well as their respective time of occurrence in the gait cycle independent of WS. 273

Table 113. Ankle power, independent of WS, found similar/different to the first hypothesis. 274

Table 114. Significant p-values of the mean min and max FLEX/EXT moments ((N·m)/kg) of the knee during stance and swing phase, as well as their respective time of occurrence in the gait cycle independent of WS. 275

Table 115. Knee moment, independent of WS, found similar/different to the first hypothesis. 275
Table 116. Significant p-values of the mean max eccentric and concentric power (W/Kg) of the knee during stance and swing phase, as well as their respective time of occurrence in the gait cycle independent of WS. 276
Table 117. Knee power, independent of WS, found similar/different to the first hypothesis. 276
Table 118. Significant p-values of the mean min and max FLEX/EXT angles (∠) of the knee during stance and swing phase, as well as their respective time of occurrence in the gait cycle independent of WS. 277
Table 119. Knee FLEX/EXT angles, independent of WS, found similar/different to the first hypothesis. 277
Table 120. Significant p-values of the mean min and max INT/EXTL rotation angles (∠) of the knee during stance and swing phase, as well as their respective time of occurrence in the gait cycle independent of WS. 278
Table 121. Knee INT/EXTL rotation angles, independent of WS, found similar/different to the first hypothesis. 279
Table 122. Significant p-values of the mean max FLEX/EXT moments ((N·m)/kg) of the hip during stance and swing phase, as well as their respective time of occurrence in the gait cycle independent of WS. 281
Table 123. Hip FLEX/EXT moments, independent of WS, found similar/different to the first hypothesis. 281

Table 124. Significant p-values of the mean min and max eccentric and concentric power (W/Kg) of the hip during stance and swing phase, as well as their respective time of occurrence in the gait cycle independent of WS. 282
Table 125. Hip concentric-eccentric FLEX/EXT power, independent of WS, found similar/different to the first hypothesis. 282
Table 126. Significant p-values of the mean min and max FLEX/EXT angles (∠) of the hip during stance and swing phase, as well as their respective time of occurrence in the gait cycle independent of WS. 284
Table 127. Hip FLEX/EXT angles, independent of WS, found similar/different to the first hypothesis. 284
Table 128. Significant p-values of the mean max ADD/ABD angles (∠) of the hip during stance and swing phase, as well as their respective time of occurrence in the gait cycle independent of WS. 285
Table 129. Hip ADD/ABD angles, independent of WS, found similar/different to the first hypothesis. 285
Table 130. Significant p-values of the mean max INT/EXTL rotation angles (∠) of the hip during stance and swing phase, as well as their respective time of occurrence in the gait cycle independent of WS. 286
Table 131. Hip INT/EXTL rotation angles, independent of WS, found similar/different to the first hypothesis. 286
Table 132. Significant p-values of the mean min and max ANT/POST tilt angles (∠) of the pelvis during stance and swing phase, as well as their respective time of occurrence in the gait cycle independent of WS. 288

Table 133. Pelvic ANT/POST tilt angles, independent of WS, found similar/different to the first hypothesis. 289
Table 134. Significant p-values of the mean max UP/DOWN obliquity angles (∠) of the pelvis during stance and swing phase, as well as their respective time of occurrence in the gait cycle independent of WS. 289
Table 135. Pelvic UP/DOWN obliquity angles, independent of WS, found similar/different to the first hypothesis. 290
Table 136. Significant p-values of the mean min and max ANT/POST tilt angles (∠) of the torso during stance and swing phase, as well as their respective time of occurrence in the gait cycle independent of WS. 291
Table 137. Torso ANT/POST tilt angles, independent of WS, found similar/different to the first hypothesis. 291
Table 138. Significant p-values of the mean max IPSI/CONTRA lean angles (∠) of the torso during stance and swing phase, as well as their respective time of occurrence in the gait cycle independent of WS. 292
Table 139. Torso IPSI/CONTRA lean angles, independent of WS, found similar/different to the first hypothesis. 292
Table 140. Significant p-values of the mean min and max antero-posterior ground reaction forces (%Body Weight) during stance and swing phase, as well as their respective time of occurrence in the gait cycle independent of WS. 293
Table 141. Antero-posterior GRFs, independent of WS, found similar/different to the first hypothesis. 293

Table 142. Significant p-values of the mean min and max medial-lateral ground reaction forces (%Body Weight) during stance and swing phase, as well as their respective time of occurrence in the gait cycle independent of WS. 294
Table 143. Medial-lateral GRFs, independent of WS, found similar/different to the first hypothesis. 295
Table 144. Significant p-values of the mean min and max vertical ground reaction forces (%Body Weight) during stance and swing phase, as well as their respective time of occurrence in the gait cycle independent of WS. 296
Table 145. Vertical GRFs, independent of WS, found similar/different to the first hypothesis. 296

List of Figures

Figure 1. Mean dorsiflexion-plantarflexion for the foot-shank of the OG versus the YG at each walking speed. 53

Figure 2. Mean max PF angle of the foot-shank during stance phase for the YG and OG across walking speeds at the 95% confidence interval (VS: Very Slow, S: Slow, T: Typical, F: Fast, VF: Very Fast). 54

Figure 3. Mean max PF angle of the foot-shank during swing phase for the YG and OG across walking speeds at the 95% confidence interval (VS: Very Slow, S: Slow, T: Typical, F: Fast, VF: Very Fast). 55

Figure 4. Mean max DF angle of the foot-shank during stance phase for the YG and OG across walking speeds at the 95% confidence interval (VS: Very Slow, S: Slow, T: Typical, F: Fast, VF: Very Fast). 57

Figure 5. Mean max DF angle of the foot-shank during swing phase for the YG and OG across walking speeds at the 95% confidence interval (VS: Very Slow, S: Slow, T: Typical, F: Fast, VF: Very Fast). 58

Figure 6. Mean adduction-abduction for the foot-shank of the OG versus the YG at each walking speed..... 60

Figure 7. Mean min ADD angle of the foot-shank during stance phase for the YG and OG across walking speeds at the 95% confidence interval (VS: Very Slow, S: Slow, T: Typical, F: Fast, VF: Very Fast). 61

Figure 8. Mean min ADD angle of the foot-shank during swing phase for the YG and OG across walking speeds at the 95% confidence interval (VS: Very Slow, S: Slow, T: Typical, F: Fast, VF: Very Fast). 62

Figure 9. Mean max ADD angle of the foot-shank during stance phase for the YG and OG across walking speeds at the 95% confidence interval (VS: Very Slow, S: Slow, T: Typical, F: Fast, VF: Very Fast). 63

Figure 10. Mean max ADD angle of the foot-shank during swing phase for the YG and OG across walking speeds at the 95% confidence interval (VS: Very Slow, S: Slow, T: Typical, F: Fast, VF: Very Fast). 65

Figure 11. Mean dorsiflexion-plantarflexion for the mid-cal of the OG versus the YG at each walking speed. 67

Figure 12. Mean max DF angle of the mid-cal during swing phase for the YG and OG across walking speeds at the 95% confidence interval (VS: Very Slow, S: Slow, T: Typical, F: Fast, VF: Very Fast). 68

Figure 13. Mean eversion-inversion for the mid-cal of the OG versus the YG at each walking speed..... 71

Figure 14. Mean min EVE angle of the mid-cal during stance phase for the YG and OG across walking speeds at the 95% confidence interval (VS: Very Slow, S: Slow, T: Typical, F: Fast, VF: Very Fast). 73

Figure 15. Mean min EVE angle of the mid-cal during swing phase for the YG and OG across walking speeds at the 95% confidence interval (VS: Very Slow, S: Slow, T: Typical, F: Fast, VF: Very Fast). 74

Figure 16. Mean max EVE angle of the mid-cal during stance phase for the YG and OG across walking speeds at the 95% confidence interval (VS: Very Slow, S: Slow, T: Typical, F: Fast, VF: Very Fast). 75

Figure 17. Mean max EVE angle of the mid-cal during swing phase for the YG and OG across walking speeds at the 95% confidence interval (VS: Very Slow, S: Slow, T: Typical, F: Fast, VF: Very Fast). 76

Figure 18. Mean adduction-abduction for the mid-cal of the OG versus the YG at each walking speed..... 78

Figure 19. Mean min ADD angle of the mid-cal during stance phase for the YG and OG across walking speeds at the 95% confidence interval (VS: Very Slow, S: Slow, T: Typical, F: Fast, VF: Very Fast). 80

Figure 20. Mean min ADD angle of the mid-cal during swing phase for the YG and OG across walking speeds at the 95% confidence interval (VS: Very Slow, S: Slow, T: Typical, F: Fast, VF: Very Fast). 81

Figure 21. Mean max ADD angle of the mid-cal during stance phase for the YG and OG across walking speeds at the 95% confidence interval (VS: Very Slow, S: Slow, T: Typical, F: Fast, VF: Very Fast). 82

Figure 22. Mean max ADD angle of the mid-cal during swing phase for the YG and OG across walking speeds at the 95% confidence interval (VS: Very Slow, S: Slow, T: Typical, F: Fast, VF: Very Fast). 83

Figure 23. Mean dorsiflexion-plantarflexion for the sha-cal of the OG versus the YG at each walking speed. 85

Figure 24. Mean min PF angle of the sha-cal during stance phase for the YG and OG across walking speeds at the 95% confidence interval (VS: Very Slow, S: Slow, T: Typical, F: Fast, VF: Very Fast)..... 86

Figure 25. Mean min PF angle of the sha-cal during swing phase for the YG and OG across walking speeds at the 95% confidence interval (VS: Very Slow, S: Slow, T: Typical, F: Fast, VF: Very Fast)..... 87

Figure 26. Mean max DF angle of the sha-cal during stance phase for the YG and OG across walking speeds at the 95% confidence interval (VS: Very Slow, S: Slow, T: Typical, F: Fast, VF: Very Fast). 89

Figure 27. Mean max DF angle of the sha-cal during swing phase for the YG and OG across walking speeds at the 95% confidence interval (VS: Very Slow, S: Slow, T: Typical, F: Fast, VF: Very Fast)..... 90

Figure 28. Mean adduction-abduction for the sha-cal of the OG versus the YG at each walking speed..... 92

Figure 29. Mean min ADD angle of the sha-cal during stance phase for the YG and OG across walking speeds at the 95% confidence interval (VS: Very Slow, S: Slow, T: Typical, F: Fast, VF: Very Fast). 93

Figure 30. Mean min ADD angle of the sha-cal during swing phase for the YG and OG across walking speeds at the 95% confidence interval (VS: Very Slow, S: Slow, T: Typical, F: Fast, VF: Very Fast). 94

Figure 31. Mean max ADD angle of the sha-cal during stance phase for the YG and OG across walking speeds at the 95% confidence interval (VS: Very Slow, S: Slow, T: Typical, F: Fast, VF: Very Fast). 95

Figure 32. Mean max ADD angle of the sha-cal during swing phase for the YG and OG across walking speeds at the 95% confidence interval (VS: Very Slow, S: Slow, T: Typical, F: Fast, VF: Very Fast). 97

Figure 33. Mean dorsiflexion-plantarflexion for the mid-met of the OG versus the YG at each walking speed. 99
Figure 34. Mean min PF angle of the mid-met during stance phase for the YG and OG across walking speeds at the 95% confidence interval (VS: Very Slow, S: Slow, T: Typical, F: Fast, VF: Very Fast). 100
Figure 35. Mean min PF angle of the mid-met during swing phase for the YG and OG across walking speeds at the 95% confidence interval (VS: Very Slow, S: Slow, T: Typical, F: Fast, VF: Very Fast). 101
Figure 36. Mean max PF angle of the mid-met during stance phase for the YG and OG across walking speeds at the 95% confidence interval (VS: Very Slow, S: Slow, T: Typical, F: Fast, VF: Very Fast). 103
Figure 37. Mean max PF angle of the mid-met during swing phase for the YG and OG across walking speeds at the 95% confidence interval (VS: Very Slow, S: Slow, T: Typical, F: Fast, VF: Very Fast). 104
Figure 38. Mean adduction-abduction for the mid-met of the OG versus the YG at each walking speed..... 106
Figure 39. Mean max ABD angle of the mid-met during stance phase for the YG and OG across walking speeds at the 95% confidence interval (VS: Very Slow, S: Slow, T: Typical, F: Fast, VF: Very Fast). 107
Figure 40. Mean max ABD angle of the mid-met during swing phase for the YG and OG across walking speeds at the 95% confidence interval (VS: Very Slow, S: Slow, T: Typical, F: Fast, VF: Very Fast). 108

Figure 41. Mean min ABD angle of the mid-met during stance phase for the YG and OG across walking speeds at the 95% confidence interval (VS: Very Slow, S: Slow, T: Typical, F: Fast, VF: Very Fast). 109
Figure 42. Mean min ABD angle of the mid-met during swing phase for the YG and OG across walking speeds at the 95% confidence interval (VS: Very Slow, S: Slow, T: Typical, F: Fast, VF: Very Fast). 110
Figure 43. Mean dorsiflexion-plantarflexion for the cal-met of the OG versus the YG at each walking speed. 112
Figure 44. Mean max PF angle of the cal-met during stance phase for the YG and OG across walking speeds at the 95% confidence interval (VS: Very Slow, S: Slow, T: Typical, F: Fast, VF: Very Fast). 113
Figure 45. Mean max PF angle of the cal-met during swing phase for the YG and OG across walking speeds at the 95% confidence interval (VS: Very Slow, S: Slow, T: Typical, F: Fast, VF: Very Fast)..... 115
Figure 46. Mean min PF angle of the cal-met during stance phase for the YG and OG across walking speeds at the 95% confidence interval (VS: Very Slow, S: Slow, T: Typical, F: Fast, VF: Very Fast)..... 116
Figure 47. Mean min PF angle of the cal-met during swing phase for the YG and OG across walking speeds at the 95% confidence interval (VS: Very Slow, S: Slow, T: Typical, F: Fast, VF: Very Fast)..... 117
Figure 48. Mean eversion-inversion for the cal-met of the OG versus the YG at each walking speed..... 119

Figure 49. Mean min EVE angle of the cal-met during stance phase for the YG and OG across walking speeds at the 95% confidence interval (VS: Very Slow, S: Slow, T: Typical, F: Fast, VF: Very Fast). 121

Figure 50. Mean min EVE angle of the cal-met during swing phase for the YG and OG across walking speeds at the 95% confidence interval (VS: Very Slow, S: Slow, T: Typical, F: Fast, VF: Very Fast). 122

Figure 51. Mean max EVE angle of the cal-met during stance phase for the YG and OG across walking speeds at the 95% confidence interval (VS: Very Slow, S: Slow, T: Typical, F: Fast, VF: Very Fast). 123

Figure 52. Mean max EVE angle of the cal-met during swing phase for the YG and OG across walking speeds at the 95% confidence interval (VS: Very Slow, S: Slow, T: Typical, F: Fast, VF: Very Fast). 125

Figure 53. Mean adduction-abduction for the cal-met of the OG versus the YG at each walking speed..... 127

Figure 54. Mean min ADD angle of the cal-met during stance phase for the YG and OG across walking speeds at the 95% confidence interval (VS: Very Slow, S: Slow, T: Typical, F: Fast, VF: Very Fast). 128

Figure 55. Mean min ADD angle of the cal-met during swing phase for the YG and OG across walking speeds at the 95% confidence interval (VS: Very Slow, S: Slow, T: Typical, F: Fast, VF: Very Fast). 129

Figure 56. Mean max ADD angle of the cal-met during stance phase for the YG and OG across walking speeds at the 95% confidence interval (VS: Very Slow, S: Slow, T: Typical, F: Fast, VF: Very Fast). 130

Figure 57. Mean max ADD angle of the cal-met during swing phase for the YG and OG across walking speeds at the 95% confidence interval (VS: Very Slow, S: Slow, T: Typical, F: Fast, VF: Very Fast). 131
Figure 58. Mean F2Pt planar angle of the OG versus the YG at each walking speed.... 135
Figure 59. Mean max F2Pt angle during stance phase for the YG and OG across walking speeds at the 95% confidence interval (VS: Very Slow, S: Slow, T: Typical, F: Fast, VF: Very Fast)..... 136
Figure 60. Mean V2G planar angle of the OG versus the YG at each walking speed. .. 138
Figure 61. Mean max V2G angle during stance phase for the YG and OG across walking speeds at the 95% confidence interval (VS: Very Slow, S: Slow, T: Typical, F: Fast, VF: Very Fast)..... 139
Figure 64. Mean F2G planar angle of the OG versus the YG at each walking speed. ... 140
Figure 65. Mean S2G planar angle of the OG versus the YG at each walking speed. ... 141
Figure 66. Mean F2Ps planar angle of the OG versus the YG at each walking speed. .. 143
Figure 67. Mean MLA planar angle of the OG versus the YG at each walking speed. . 145
Figure 68. Mean dorsiflexion-plantarflexion moment for the ankle of the OG versus the YG at each walking speed..... 148
Figure 69. Mean max PF moment of the foot-shank during stance phase for the YG and OG across walking speeds at the 95% confidence interval (VS: Very Slow, S: Slow, T: Typical, F: Fast, VF: Very Fast). 150
Figure 70. Mean max PF moment of the foot-shank during swing phase for the YG and OG across walking speeds at the 95% confidence interval (VS: Very Slow, S: Slow, T: Typical, F: Fast, VF: Very Fast). 151

Figure 71. Mean dorsiflexion-plantarflexion power for the ankle of the OG versus the YG at each walking speed. 153
Figure 72. Mean max ECC power of the foot-shank during swing phase for the YG and OG across walking speeds at the 95% confidence interval (VS: Very Slow, S: Slow, T: Typical, F: Fast, VF: Very Fast). 154
Figure 73. Mean max CNC power of the foot-shank during stance phase for the YG and OG across walking speeds at the 95% confidence interval (VS: Very Slow, S: Slow, T: Typical, F: Fast, VF: Very Fast). 155
Figure 74. Mean max CNC power of the foot-shank during swing phase for the YG and OG across walking speeds at the 95% confidence interval (VS: Very Slow, S: Slow, T: Typical, F: Fast, VF: Very Fast). 156
Figure 75. Mean flexion-extension moment for the knee of the OG versus the YG at each walking speed..... 158
Figure 76. Mean min FLEX moment of the knee during stance phase for the YG and OG across walking speeds at the 95% confidence interval (VS: Very Slow, S: Slow, T: Typical, F: Fast, VF: Very Fast). 160
Figure 77. Mean max EXT moment of the knee during stance phase for the YG and OG across walking speeds at the 95% confidence interval (VS: Very Slow, S: Slow, T: Typical, F: Fast, VF: Very Fast). 161
Figure 78. Mean max EXT moment of the knee during swing phase for the YG and OG across walking speeds at the 95% confidence interval (VS: Very Slow, S: Slow, T: Typical, F: Fast, VF: Very Fast). 162

Figure 79. Mean dorsiflexion-plantarflexion power for the knee of the OG versus the YG at each WS. 164
Figure 80. Mean max ECC power of the knee during swing phase for the YG and OG across walking speeds at the 95% confidence interval (VS: Very Slow, S: Slow, T: Typical, F: Fast, VF: Very Fast). 165
Figure 81. Mean max CNC power of the knee during stance phase for the YG and OG across walking speeds at the 95% confidence interval (VS: Very Slow, S: Slow, T: Typical, F: Fast, VF: Very Fast). 166
Figure 82. Mean max CNC power of the knee during swing phase for the YG and OG across walking speeds at the 95% confidence interval (VS: Very Slow, S: Slow, T: Typical, F: Fast, VF: Very Fast). 167
Figure 83. Mean flexion-extension for the knee of the OG versus the YG at each walking speed. 169
Figure 84. Mean min FLEX angle of the knee during stance phase for the YG and OG across walking speeds at the 95% confidence interval (VS: Very Slow, S: Slow, T: Typical, F: Fast, VF: Very Fast). 170
Figure 85. Mean min FLEX angle of the knee during swing phase for the YG and OG across walking speeds at the 95% confidence interval (VS: Very Slow, S: Slow, T: Typical, F: Fast, VF: Very Fast). 171
Figure 86. Mean max FLEX angle of the knee during stance phase for the YG and OG across walking speeds at the 95% confidence interval (VS: Very Slow, S: Slow, T: Typical, F: Fast, VF: Very Fast). 172

Figure 87. Mean internal-external rotation for the knee of the OG versus the YG at each walking speed..... 175

Figure 88. Mean min ER angle of the knee during stance phase for the YG and OG across walking speeds at the 95% confidence interval (VS: Very Slow, S: Slow, T: Typical, F: Fast, VF: Very Fast)..... 176

Figure 89. Mean flexion-extension moment for the hip of the OG versus the YG at each WS..... 180

Figure 90. Mean max FLEX moment of the hip during stance phase for the YG and OG across walking speeds at the 95% confidence interval (VS: Very Slow, S: Slow, T: Typical, F: Fast, VF: Very Fast). 181

Figure 91. Mean max FLEX moment of the hip during swing phase for the YG and OG across walking speeds at the 95% confidence interval (VS: Very Slow, S: Slow, T: Typical, F: Fast, VF: Very Fast). 182

Figure 92. Mean max EXT moment of the hip during stance phase for the YG and OG across walking speeds at the 95% confidence interval (VS: Very Slow, S: Slow, T: Typical, F: Fast, VF: Very Fast). 184

Figure 93. Mean max EXT moment of the hip during swing phase for the YG and OG across walking speeds at the 95% confidence interval (VS: Very Slow, S: Slow, T: Typical, F: Fast, VF: Very Fast). 185

Figure 94. Mean flexion-extension power for the hip of the OG versus the YG at each walking speed..... 186

Figure 95. Mean min ECC power of the hip during stance phase for the YG and OG across walking speeds at the 95% confidence interval (VS: Very Slow, S: Slow, T: Typical, F: Fast, VF: Very Fast)..... 187
Figure 96. Mean flexion-extension for the hip of the OG versus the YG at each walking speed. 189
Figure 97. Mean max EXT angle of the hip during stance phase for the YG and OG across walking speeds at the 95% confidence interval (VS: Very Slow, S: Slow, T: Typical, F: Fast, VF: Very Fast)..... 190
Figure 98. Mean min FLEX angle of the hip during swing phase for the YG and OG across walking speeds at the 95% confidence interval (VS: Very Slow, S: Slow, T: Typical, F: Fast, VF: Very Fast)..... 191
Figure 99. Mean max FLEX angle of the hip during stance phase for the YG and OG across walking speeds at the 95% confidence interval (VS: Very Slow, S: Slow, T: Typical, F: Fast, VF: Very Fast)..... 192
Figure 100. Mean max FLEX angle of the hip during swing phase for the YG and OG across walking speeds at the 95% confidence interval (VS: Very Slow, S: Slow, T: Typical, F: Fast, VF: Very Fast). 193
Figure 101. Mean adduction-abduction for the hip of the OG versus the YG at each walking speed. 195
Figure 102. Mean max ABD angle of the hip during stance phase for the YG and OG across walking speeds at the 95% confidence interval (VS: Very Slow, S: Slow, T: Typical, F: Fast, VF: Very Fast)..... 196

Figure 103. Mean max ABD angle of the hip during swing phase for the YG and OG across walking speeds at the 95% confidence interval (VS: Very Slow, S: Slow, T: Typical, F: Fast, VF: Very Fast)..... 198
Figure 104. Mean internal-external rotation for the hip of the OG versus the YG at each walking speed..... 200
Figure 105. Mean max ER angle of the hip during stance phase for the YG and OG across walking speeds at the 95% confidence interval (VS: Very Slow, S: Slow, T: Typical, F: Fast, VF: Very Fast)..... 201
Figure 106. Mean max IR angle of the hip during stance phase for the YG and OG across walking speeds at the 95% confidence interval (VS: Very Slow, S: Slow, T: Typical, F: Fast, VF: Very Fast)..... 202
Figure 107. Mean anterior-posterior tilt for the pelvis of the OG versus the YG at each walking speed..... 206
Figure 108. Mean min ANT tilt angle of the pelvis during stance phase for the YG and OG across walking speeds at the 95% confidence interval (VS: Very Slow, S: Slow, T: Typical, F: Fast, VF: Very Fast). 207
Figure 109. Mean min ANT tilt angle of the pelvis during swing phase for the YG and OG across walking speeds at the 95% confidence interval (VS: Very Slow, S: Slow, T: Typical, F: Fast, VF: Very Fast). 208
Figure 110. Mean max ANT tilt angle of the pelvis during stance phase for the YG and OG across walking speeds at the 95% confidence interval (VS: Very Slow, S: Slow, T: Typical, F: Fast, VF: Very Fast). 209

Figure 111. Mean max ANT tilt angle of the pelvis during swing phase for the YG and OG across walking speeds at the 95% confidence interval (VS: Very Slow, S: Slow, T: Typical, F: Fast, VF: Very Fast). 211

Figure 112. Mean upward-downward obliquity for the pelvis of the OG versus the YG at each walking speed. 213

Figure 113. Mean max DOWN obliquity angle of the pelvis during stance phase for the YG and OG across walking speeds at the 95% confidence interval (VS: Very Slow, S: Slow, T: Typical, F: Fast, VF: Very Fast). 214

Figure 114. Mean max DOWN obliquity angle of the pelvis during swing phase for the YG and OG across walking speeds at the 95% confidence interval (VS: Very Slow, S: Slow, T: Typical, F: Fast, VF: Very Fast)..... 215

Figure 115. Mean max UP obliquity angle of the pelvis during stance phase for the YG and OG across walking speeds at the 95% confidence interval (VS: Very Slow, S: Slow, T: Typical, F: Fast, VF: Very Fast). 216

Figure 116. Mean max UP obliquity angle of the pelvis during swing phase for the YG and OG across walking speeds at the 95% confidence interval (VS: Very Slow, S: Slow, T: Typical, F: Fast, VF: Very Fast). 218

Figure 117. Mean anterior-posterior tilt for the torso of the OG versus the YG at each walking speed..... 221

Figure 118. Mean max POST tilt angle of the torso during stance phase for the YG and OG across walking speeds at the 95% confidence interval (VS: Very Slow, S: Slow, T: Typical, F: Fast, VF: Very Fast). 222

Figure 119. Mean max POST tilt angle of the torso during swing phase for the YG and OG across walking speeds at the 95% confidence interval (VS: Very Slow, S: Slow, T: Typical, F: Fast, VF: Very Fast). 223
Figure 120. Mean min POST tilt angle of the torso during stance phase for the YG and OG across walking speeds at the 95% confidence interval (VS: Very Slow, S: Slow, T: Typical, F: Fast, VF: Very Fast). 225
Figure 121. Mean min POST tilt angle of the torso during swing phase for the YG and OG across walking speeds at the 95% confidence interval (VS: Very Slow, S: Slow, T: Typical, F: Fast, VF: Very Fast). 226
Figure 122. Mean ipsilateral-contralateral lean for the torso of the OG versus the YG at each walking speed. 228
Figure 123. Mean max CONTRA lean angle of the torso during stance phase for the YG and OG across walking speeds at the 95% confidence interval (VS: Very Slow, S: Slow, T: Typical, F: Fast, VF: Very Fast)..... 229
Figure 124. Mean max CONTRA lean angle of the torso during swing phase for the YG and OG across walking speeds at the 95% confidence interval (VS: Very Slow, S: Slow, T: Typical, F: Fast, VF: Very Fast)..... 230
Figure 125. Mean max IPSI lean angle of the torso during stance phase for the YG and OG across walking speeds at the 95% confidence interval (VS: Very Slow, S: Slow, T: Typical, F: Fast, VF: Very Fast). 231
Figure 126. Mean max IPSI lean angle of the pelvis during swing phase for the YG and OG across walking speeds at the 95% confidence interval (VS: Very Slow, S: Slow, T: Typical, F: Fast, VF: Very Fast). 233

Figure 127. Mean antero-posterior ground reaction force of the OG versus the YG at each walking speed..... 236
Figure 128. Mean max A/P GRF during stance phase for the YG and OG across walking speeds at the 95% confidence interval (VS: Very Slow, S: Slow, T: Typical, F: Fast, VF: Very Fast)..... 237
Figure 129. Mean vertical ground reaction force of the OG versus the YG at each walking speed. 238
Figure 130. Mean min vertical GRF during stance phase for the YG and OG across walking speeds at the 95% confidence interval (VS: Very Slow, S: Slow, T: Typical, F: Fast, VF: Very Fast)..... 239
Figure 131. Mean max vertical GRF during stance phase for the YG and OG across walking speeds at the 95% confidence interval (VS: Very Slow, S: Slow, T: Typical, F: Fast, VF: Very Fast)..... 240

List of Symbols, Nomenclature or Abbreviations

3D Three-dimensional

A/D Analog/Digital

ABD/ADD Abduction/adduction

AHR Arch Height Ratio

AI Arch Index

ANCOVA Analysis of Covariance

ANOVA Analysis of Variance

C1 Cluster marker 1, top right corner of plate

C2 Cluster marker 2, bottom right corner of plate

C3 Cluster marker 3, bottom left corner of plate

C4 Cluster marker 4, top left corner of plate

DAH Dorsal Arch Height

DF/PF Dorsiflexion/plantarflexion

DOF Degrees of Freedom

EVE/INV Eversion/inversion

F2Ps Angle for the hallux in the sagittal plane

FFW Forefoot Width

FMM Foot Mobility Magnitude

FPI Foot Posture Index

GCS Global Coordinate System

GRF Ground Reaction Forces

IR/ER Internal/External Rotation

LSCL	Left Shank Cluster
LTCL	Left Thigh Cluster
MFW	Midfoot Width
ML	Medial-Lateral
MLA	Medial Longitudinal Arch
MSF	Multi-segment Foot
NNHt	Normalized Navicular Height Truncated
OA	Older Adults
OFM	Oxford Foot Model
OG	Older Group
PLA	Polylactic Acid
RFM	Rizzoli Foot Model
RFW	Rearfoot Width
ROM	Range of Motion
RSCL	Right Shank Cluster
RTCL	Right Thigh Cluster
S2G	Angle for the second metatarsal in the sagittal plane
TFL	Truncated Foot Length
TO	Toe-Off
V2G	Angle for the fifth metatarsal in the sagittal plane
WS	Walking Speed
YA	Younger Adults
YG	Younger Group

1.0 Introduction

The human foot is a complex structure that consists of 26 bones, 33 joints, and over 100 muscles and soft tissue structures. During gait, the foot and ankle functions to attenuate shock at impact, provide stability and support of the lower limb, and aid in forward propulsion of the body. Given the important role of the ankle/foot complex in gait, it is plausible that changes in foot function may result in impaired movement patterns. While previous studies have reported that physical impairment increases with age and is related to changes in mobility and gait (Aboutorabi et al., 2016; Guralnik et al., 2000; Trombetti et al., 2015), the interrelationship between age-related changes in foot mechanics and physical function are not clear (Arnold et al., 2014). Further, the mechanics of the foot and ankle during gait are poorly understood. Further research examining mechanical models of the foot and age-related changes in foot mechanics are warranted.

Currently, research on age-related changes to foot and ankle mechanics during walking has shown: 1) altered ankle joint motion (Legault-Moore et al., 2012; Scott et al., 2007), 2) reduced ankle joint plantarflexion (PF) range of motion (ROM), 3) reduced ankle dorsiflexion (DF) at initial contact, 4) reduced ankle PF at toe-off (TO) (Judge et al., 1996; Kerrigan et al., 1998), 5) decreased ankle power (DeVita & Hortobagyi, 2000; McGibbon & Krebs, 1999; Monaco et al., 2009), and 6) decreased ankle plantarflexor moment (Crenna & Frigo, 2011; Monaco et al., 2009) for older adults (OA) when compared to younger adults (YA). All of these changes are indicative of a less propulsive gait pattern in the elderly population. However, the majority of previous research has used single segment foot models, neglecting important information about intrinsic foot motion. The use of multisegment foot (MSF) models could provide insight about the functional significance

of motion occurring within the foot as well as alterations due to age. More recently, researchers have been using MSF models for clinical groups in older populations (Caravaggi et al., 2021; Fritz et al., 2021; Kim et al., 2020; Kyung et al., 2020; Shin et al., 2019).

To date, only a few studies (Arnold et al., 2014; Lee et al., 2017; Legault-Moore et al., 2012; Van Hoeve et al., 2017) have used an MSF model to investigate age-related changes in healthy adults in foot kinematics during walking. Legault-Moore et al. (2012), compared age-related changes to MSF kinematics and self-selected walking speed (WS) between young (24.0 ± 3 years old) and OA (65.0 ± 4.2 years old) using a 4-segment foot model and reported no significant differences. Similar foot mechanics between the two age groups may be a function of the small sample size and/or the age of the participants in the study. In their study, the older group (OG) was defined as participants aged 55 years or older, however, their sample was between the age 61-69 (mean age 65.0 ± 4.2 years). Further, due to available motion capture camera resolution at the time, the midfoot segment was excluded from the foot model and only male participants with a minimum shoe size of 9 were recruited.

The study by Arnold et al. (2014) examined the age-related differences in MSF kinematics in 20 YA and 20 OA during gait. Their study used a 5-segment mechanical model of the foot, which included the midfoot segment. As foot kinematics are speed-dependent, and WS typically declines with age (Bohannon, 1997; Caravaggi et al., 2010; Dubbeldam et al., 2010), it is important to consider speed-mediated effects on age-related changes in foot kinematics. Arnold et al. compared differences in foot kinematics between OA (mean age 73.2 ± 5.1 years) walking at a self-selected preferred WS and YA (23.0 ± 3

years old) walking at both a self-selected preferred and self-selected slow WS. Compared to YA, the OA walked with decreased PF of the calcaneus at TO, decreased sagittal ROM of the midfoot, and decreased ROM of the metatarsus. The results of this study showed that speed only influenced the differences in sagittal plane ROM of the calcaneus and hallux, suggesting that independent of WS, significant differences in MSF kinematics between young and OA exist, leading to reduced ROM and propulsion. This suggests that physical impairments increase with age, and are related to changes in mobility and gait.

Limitations of the study by Arnold et al. (2014) must be considered. The self-selected slower WS of the younger group (YG) was actually slower than the self-selected preferred WS of the OA. To identify age-related changes in MSF kinematics from speed-mediated effects, further research examining a broader range of WSs is warranted.

Van Hoeve et al. (2017) assessed the effect of age and speed on foot and ankle kinematics by comparing results during slow and fast walking. A group of healthy YA (22.4±1.3) and a group of OA (57.5±3.9) were recruited. Also, the interaction between age and speed was analyzed. Their study used a 4-segment mechanical model of the foot. The results showed that WS had a significant influence on several kinematic parameters leading to higher ROM, especially on the ankle joint (ROM between hindfoot and tibia). However, similar to Legault-Moore et al. (2012), there was no significant effect of age on foot and ankle kinematics. Nonetheless, this result was contradictory to the findings of Arnold et al. (2014).

Lee et al. (2007) evaluated the differences in inter-segmental motion of the foot between young (27 ± 4 years old) and old (64.6 ± 2.9 years old) adult healthy females during barefoot gait. The researchers used a 4-segment foot mechanical model (Henley et

al., 2008) and arch data was also collected. Participants were asked to walk at a faster and slower WS. Their results showed that speed, stride length, and step width were significantly lower in the OG. Conversely to Arnold et al. (2014), who demonstrated that some changes in foot kinematics between different age groups could be explained by altered WS, Lee et al. (2017) showed that differences in the inter-segmental motion of the foot between both age groups were not related to differences in speed. Additionally, several parameters in the OG suggested flattening of the longitudinal arch: 1) In the sagittal plane, forefoot was in a dorsiflexed position relative to the hindfoot, 2) in the coronal plane, the position of the hindfoot was more pronated, and consequently the forefoot was more supinated. Their findings agree with the association of aging with pes planus (flattening of the foot). Despite their results, limitations in the study were present. It has been previously shown that at the age of 60 years, 85% of people present a normal gait, but as age increases (85 years or older) this proportion drops to 18% (Sudarsky, 2000). However, the age range for the old group in the study by Lee et al. (2017) was narrow (mean age 64.6 ± 2.9 years old). Therefore, besides examining a broader range of WSs, a broader range of age for the old group must be examined.

Previous research has identified age-related differences in lower limb and single foot kinetics of OA during walking (Aboutorabi et al., 2016) including, decreased concentric strength of the ankle plantarflexor muscles (Thelen et al., 1996) and decreased ankle joint power during preswing (DeVita & Hortobagyi, 2000; Kerrigan et al., 1998). In addition, OA have exhibited decreased hip flexion torque (DeVita & Hortobagyi, 2000; Monaco et al., 2009), increased hip extension torque (DeVita & Hortobagyi, 2000), and increased hip power generation (DeVita & Hortobagyi, 2000; Monaco et al., 2009; Silder

et al., 2008). Further, OA have shown decreased initial peak vertical forces and increased vertical forces at mid-stance (Alcock et al., 2013). For fast WS, OA significantly increase knee and hip moment contributions for hip linear power to levels comparable to those of young participants at a similar speed (Riley et al., 2001). Last, elderly groups translate their center of gravity slower than the YG when walking at the same cadence (McGibbon & Krebs, 1999). More recently, research in MSF kinetics has identified an overestimation of up to 53% in ankle peak power when implementing a single segment model (Bruening et al., 2012b), misestimating foot contributions. However, technological limitations to study MSF kinetics exist. Thus, different methodological approaches have been developed (Bruening et al., 2012b; Saraswat et al., 2014), although these methods imply estimations that carry errors in the data calculation. Therefore, for the study only a single foot kinetic model and MSF kinematic model were studied.

As joint kinematics and kinetics are interrelated, comprehensive studies that measure both sets of mechanical parameters across ages and speed conditions are lacking with most studies examining only the effect of age and speed on kinematics, or the effect of age on kinetics. There is a need to examine the effect of age and speed on MSF and lower limb kinematics and kinetics, which provides a more comprehensive understanding of the age-related changes in gait to the literature. Thus, age-related changes on MSF kinematics and single foot kinetics were studied.

In addition to age-related changes in foot mechanics, previous research has also suggested that changes in foot structure, function and mobility occur with age. Changes in foot structure with age include lowering of the transverse arch (Hsu, 1971; Scott et al., 2007), increased soft tissue stiffness (Menz, 2014), toe deformities, as well as flatter,

longer, and wider feet than YA (Frey, 2000; Scott et al., 2007). Calcaneal eversion is linked to low arch and it has been proposed to decrease the inclination of the subtalar joint axis of rotation (Arangio et al., 1998; Blackwood et al., 2005). In addition, increased forefoot DF and decreased forefoot adduction (Van Boerum & Sangeorzan, 2003) have been predicted in individuals with low arches. Age-related changes in foot function include decreased proprioception (Stevens & Choo, 1996), and decreased muscle strength, such as ankle and toe plantarflexor weakness (Edelstein, 1988; Endo et al., 2002; Scott et al., 2007). Toe plantarflexor weakness effects the grasping function of the toes in OA when executing weight-bearing activities, resulting in impaired balance and functional ability (Menz, 2014). Age-related changes in foot mobility include decreased ROM of the ankle and 1st metatarsophalangeal (MTP1) joints (Edelstein, 1988; Endo et al., 2002; James & Parker, 1989; Nigg et al., 1992; Scott et al., 2007), a decreased subtalar joint inversion-eversion ROM, a more pronated posture of the foot as well as a more pronated position with reduced joint mobility and less efficient propulsion when walking (Menz, 2014). Due to the important role played by the foot in adapting to uneven terrain, a reduced ROM in the joints of the foot and ankle is strongly associated with impaired balance and functional ability in older people (Menz et al., 2005; Spink et al., 2011). Such age-related changes may lead to alterations in foot mechanics and could impact an individual's quality of life.

No single study has examined MSF and lower limb joint kinematics and kinetics across age, speed and foot structure and mobility. This research helped improve our understanding about the foot mechanics in YA and OA, providing a more comprehensive knowledge about the age-related changes in MSF and lower limb biomechanics. Further, the data provided can be used as a reference of normal gait parameters to distinguish

abnormal and pathological gait patterns, e.g., patients with planus and cavus feet, diabetic foot, or after stroke. Hence, the findings may provide guidance to improve gait performance. Findings from this study may also contribute to an accurate engineering design for wearable device technology, e.g., footwear, prostheses, orthoses and exoskeletons.

1.1 Purpose

To address the limitations of current work and increase our understanding of age-related changes in MSF and lower extremity biomechanics, the purpose of the study was to investigate differences in MSF kinematics and lower extremity kinematics and kinetics between young and OA during walking. To separate speed-mediated effects from age-related changes in motion, data were recorded across five walking speeds at self-selected speeds (very slow, slow, typical, fast and very fast speeds). The relationship between age-related changes in foot kinematics/kinetics and foot structure and mobility was also explored. The following hypotheses were tested:

1. There would be significant differences in MSF and lower extremity kinematic and kinetic variables (e.g. calcaneus-tibia plantarflexion angle, hallux angle (F2Ps), medial longitudinal arch (MLA) angle, stance phase, cadence, double support time, etc.) between age groups as a function of speed.
2. Independent of speed, there would be significant differences in MSF and lower limb kinematic and kinetic variables (e.g. maximum foot-tibia angle, calcaneus-tibia, midfoot-calcaneus, and planar angles of the foot, as well as time to maximum angle, ankle plantarflexor moment, etc.) between the younger and older adults.

3. There would be significant differences in MSF and lower extremity kinematic and kinetic variables (e.g. ROM of the ankle joint, midfoot and metatarsophalangeal joints, vertical ground reaction force, step length, etc.) between age groups as a function of foot structure and mobility.

2.0 Literature Review

The review below discusses the existing literature of the age-related changes in the lower limb kinematics and kinetics, as well as the effects of WS, foot structure and mobility on gait in younger and older adults.

2.1 Significance of study

Physical impairment increases with age. This is related to changes in physical mobility and walking (Aboutorabi et al., 2016; Guralnik et al., 2000; Trombetti et al., 2015). "Walking is one of the more frequently performed sensorimotor tasks in everyday life. Gait disorders are common in the elderly populations, and their prevalence increases with age" (Aboutorabi et al., 2016, p. 393). Nonetheless, the influence of age on foot kinematics and kinetics, and what role may play in the context of changes to physical function with ageing remains unclear (Arnold et al., 2014). Pursuing this was beneficial because it contributed to our brief knowledge about the age-related changes on lower limb kinematics and kinetics. Therefore, it enhanced our knowledge on gait mechanics in the elderly population.

2.2 Age-related changes in kinematics and kinetics

Previous research has investigated age-related differences in foot kinematics using an MSF model. In 2012, Legault-Moore et al. studied age-related changes in MSF

kinematics during walking between younger (24 ± 3 years old) and older males (65 ± 4.2 years old). The Rizzoli Foot Model (RFM) was used with the following exceptions: 1) the midfoot segment was excluded due to difficulties with consistent tracking of the navicular and cuboid markers, and 2) a neutral calcaneus was formed using a laser level technique to guide marker placement. They examined differences in mean temporal-spatial data, mean ROM, and mean peak joint angle data between both groups. Participants were asked to walk at a self-selected speed. As part of their results, they did not find significant differences between the younger and older age groups for the mean temporal-spatial or mean joint angle data. However, the lack of observable significant differences may had been due to several reasons including: 1) the recruited older participants formed a group with a narrow age range, 2) all participants had a minimum shoe size of nine to facilitate marker tracking and autolabeling, and 3) female participants were excluded. This decision was made for two reasons: 1) to eliminate any sex effects associated with foot kinematics, and 2) because females have smaller feet than males, which increases the probability of marker merging and tracking problems. These limitations suggested that a broader range of age in the OG should be studied, as well as both sexes and a variety of foot sizes.

In 2014, Arnold et al. conducted a study investigating the differences in foot kinematics between YA and OA during walking using the RFM MSF model. The mean age of the YG was 23 ± 3 years old, while the mean age of the OG was 73 ± 5 years old. The participants were asked to walked at a preferred and slow WS. They found that the OG had a less plantarflexed calcaneus at TO, a smaller sagittal plane ROM of the midfoot, and a smaller coronal plane ROM of the metatarsus. They concluded that WS did not influence these differences, since they remained present when groups walked at comparable speeds.

Thus, the findings of this study indicated that independent of WS, the OG exhibited significant differences in foot kinematics compared to the YG. Gait patterns of the OG were characterised by less propulsion and reduced mobility of multiple foot segments. However, this conclusion was questionable since the researchers did not look at the differences in foot structure or foot mobility between groups.

Lee et al. (2017) evaluated the differences in inter-segmental motion of the foot between young (27 ± 4 years old) and older (64 ± 3 years old) adult healthy females during gait and considered the structure of the foot. The researchers used an MSF model (Henley et al., 2008) and arch data was also collected. Participants were asked to walk at their self-selected WS. Both the young and OG were divided into two different speed groups: 1) faster and 2) slower. To determine the speed group, they cut-off the speeds (1.25 m/s in the young group and 1.10 m/s in the OG). Their results showed that WS, stride length, and step width were significantly lower in the OG. They also showed that differences in the inter-segmental motion of the foot between both groups was not related to differences in WS. Further, several parameters in the OG suggested flattening of the longitudinal arch: 1) In the sagittal plane, forefoot was in a DF position relative to the hindfoot, 2) in the coronal plane, the position of the hindfoot was more pronated, and consequently the forefoot was more supinated. Although they implemented a MSF model and took into account the arch of the foot, researchers did not include the male group and the range of age for the OG was narrow (64 ± 3 years old).

The aforementioned studies showed inconsistencies in their results in foot kinematics as a function of age. A decrement in WS and increments in stance duration and double support time with increasing age may indicate a trend towards a safer, more

dynamically stable, gait pattern (Wall et al., 1991; Winter et al., 1990) and are clearly consequences of the aging process, but not necessarily indicative of functional limitations.

With respect to age-related changes in kinetics, Brown et al. (1995) suggested that muscle and link-segment power analyses may be more sensitive to functional limitations than time-distance or kinematic measures. Net muscle power is defined as the instantaneous angular power component of muscle torque. Calculations of net muscle power are highly dependent upon body size (mass, stature) and the kinematics (velocity) of movement (McGibbon & Krebs, 1999). Therefore, because OA generally walk slower than YA, a reduction in muscle power generated and absorbed would be expected. In addition, research has shown the effect of age on single foot kinetics such as reduced ankle PF power in OA (DeVita & Hortobagyi, 2000; Judge & Davis, 1996; McGibbon & Krebs, 1999; Monaco et al., 2009; Riley et al., 2001; Silder et al., 2008; Winter et al., 1990). Furthermore, decreased hip flexion torque (DeVita & Hortobagyi, 2000; Monaco et al., 2009), increased hip extension torque (DeVita & Hortobagyi, 2000), and increased hip power generation (DeVita & Hortobagyi, 2000; Monaco et al., 2009; Silder et al., 2008) in OA have been reported; however, changes in ankle and hip kinetics are not always observed together (Kerrigan et al., 1998; Winter et al., 1990). It has also been reported that OA may be unable to produce sufficient ankle power during push-off, specifically at faster WS (Judge et al., 1996; Kerrigan et al., 1998). DeVita and Hortobagyi (2000) suggested that OA compensate for reduced ankle PF (decreased ankle torque) and reduced power generation at the ankle by adopting a gait strategy that encourages the use of the proximal hip extensors. The researchers pointed out that this compensation was a neuromuscular adaptation distinguished by a distal-to-proximal shift in motor control strategy (DeVita &

Hortobagyi, 2000). This hypothesis has been supported by further research that found differences in joint kinetics (Monaco et al., 2009; Silder et al., 2008) and muscle activity (Schmitz et al., 2009) between age groups during walking at different speeds. Further, OA tend to walk at a slower WS which is related to decreased initial peak vertical forces and peak powers, and increased vertical forces at mid-stance (Alcock et al., 2013).

McGibbon and Krebs (1999) conducted a study to investigate whether power calculations from motion analysis data were sensitive to impairments beyond the differences expected with ageing. They recruited 20 healthy young women (27 ± 4.2 years), 16 healthy older women (72.5 ± 5.6 years), and 24 functionally limited older women (73.5 ± 7.2 years). Their gait data was analyzed during stance phase at a moderate-speed paced using a single foot model. They calculated the net muscle power and work of the leg joints (ankle, knee and hip), and selected time-distance parameters (center of gravity velocity, stance duration, and single support time). Researchers found that both elderly groups translated their center of gravity slower than the YG when walking at the same cadence. Also, their results suggested that decreased ankle plantar-flexor (PF) power in late stance of gait may be an impairment-related characteristic more than age-related characteristic.

However, research in MSF kinetics has identified an overestimation of up to 53% in ankle peak power when implementing a single segment model (Bruening et al., 2012b), misestimating foot contributions (Zelik et al., 2018). Also, it has been shown that the Chopart joint encompasses power absorption and generation, whilst the Lisfranc joint mainly contributes to power generation (Deschamps et al., 2017). These findings suggest that both joints have a similar peak power generation as the ankle joint, showing the contribution of the foot in the lower limb kinetics. To our knowledge, only one study has

examined changes in MSF kinetics as a function of speed. Eerdekens et al. (2019) studied the effect of WS on joint kinetics obtained from a three-segment and four-segment kinetic foot model at self-selected and fast WS (1.28 m/s and 1.76 m/s respectively) among male adults. They found that when WS increases, peak power generation and positive work increases. Additionally, the absorption at the ankle declines with increasing WS, whereas the influence of the MTP1 joint on relative power absorption increases. Moreover, the Chopart and MTP1 joints combined produce small amounts of the total power generation (21% and 23% during self-selected WS and highest possible WS respectively). Furthermore, they also found increases in peak power generation and absorption of the Lisfranc and Chopart joints throughout the propulsion phase. Their findings also showed that as WS increases, higher power output and mechanical work in different foot joints is needed, and that the foot joints must produce net positive mechanical work in order to walk at normal WS. This study provided the first attempt towards gaining insight into MSF kinetic patterns during self-selected and high-speed walking. Eerdekens et al. (2019) concluded that future studies should examine a broader range of WS to increase our understanding of MSF kinetics and provide more suitable control data for clinical studies. But limitations of studying MSF kinetics must be considered. Currently there are different methodological approaches (Bruening et al., 2012b; MacWilliams et al., 2003; Saraswat et al., 2014) to compute MSF kinetics such as the proportionality scheme (Saraswat et al., 2014) which derives, for all foot segments, the center of pressure and resultant ground reaction force (GRF) for each frame of the segmented pressure data by estimating subarea shear forces and normal moment as a proportion of the measured normal force. However, this method carries an estimation error of maximum 3% for all shear forces. Another

method proposed (Bruening et al., 2012b) consists on asking the participant to target the force plate, which might alter the natural gait pattern of the participant, inducing different results when comparing to a non-targeted walking.

Nonetheless, a more detailed study should be conducted including the age-related changes on the foot as well as the inclusion of broader range of speeds. This is needed because the influence of age in foot kinematics and kinetics, and what role may play in the context of changes to physical function with ageing, remains unclear. There are different foot models described in the literature that can be applied to better understand the foot mechanics changes with ageing and they will be discussed below.

2.3 Effect of Walking Speed on Gait Kinematics and Kinetics

2.3.1 Effect of Walking Speed using a Single Segment Foot Model

Research studying the effect of WS on foot kinematics have showed that speed significantly influences foot and ankle kinematics. The study of different WSs at different age groups is important because in older adults' gait patterns, WS often differs from the YA. Older adults tend to walk at a slower speed when compared to YA, although is not always the case. Discrepancies exist of how different the WS is between YA and OA (Hollman et al, 2011; Oh-Park et al, 2010; Samson et al, 2001), and furthermore, whether WS is significantly different between both age groups (Silder et al., 2008). Further, it can be difficult to determine whether differences in walking patterns are age-related or simply due to the speed at which the person was walking. Therefore, it is important to study a wide range of speeds to be able to separate speed-mediated effects from those due to age. The appreciation of speed-mediated effects is critical for increasing our understanding of foot

mechanics in young and OA. The study of slow and fast WSs will aid to solve the discrepancies mentioned above.

Several studies have noted the effect of WS on lower extremity kinematics and kinetics in YA and OA. For example, using single segment foot models (Ardestani et al., 2016; Chehab et al., 2017; Røislien et al., 2009; Schwartz et al., 2008; Stansfield et al., 2001) researchers have found that stride length and cadence increase as WS increases (Kirtley, 2006) and stance phase and double support time decrease as WS increases in healthy adults (Kirtley et al., 1985; Røislien et al., 2009). Gait kinematic parameters have shown a strong correlation with speed. As WS increases, the ROM at the hip joint is increased (Haight, 2012), producing increased hip flexion in early stance, and hip extension in late stance (Murray et al., 1984). Similarly, increased WS has been shown to increase knee joint ROM (Kirtley et al., 1985), therefore, increasing knee flexion (Riley et al., 2001; Schwartz et al., 2008). While the ROM at the knee and hip joints increases at faster WS, it has been shown that the ROM of the ankle does not increase significantly with WS (Murray et al., 1984). Further, the ROM of the ankle was shown to be lower at the highest stride rate. Through the late stance phase and the swing phase, peak angular velocities were greater at a higher stride rate in the hip and the knee, but not in the ankle (Umberger & Martin, 2007).

In 2009, Røislien et al. found that WS, age, and gender significantly affect kinematic gait data in healthy adults (23 – 62 years old). Participants walked at their self-selected speed (range from .98 – 1.94 m/s) and it was found that there was a significantly earlier TO at a high WS in the pre-swing phase. They also noted a higher knee flexion velocity and an earlier maximum knee flexion at a higher WS, as well as an earlier

maximum plantar flexion at TO. Furthermore, as WS increased, they found a higher degree of DF in initial contact, loading response and mid stance, as well as more PF in terminal stance. Increasing WS also affected kinematics of the ankle. They found a higher degree of PF angle during terminal stance, while the DF angle increased during initial contact, loading response and midstance. Their results showed that WS was the primary factor that significantly affected kinematic gait data.

Likewise, kinetic parameters of gait show a strong correlation with WS. In 2001, Riley et al. investigated the relationship of hip, knee and ankle function to gait speed in healthy elderly participants. They recruited 16 young (29.4±4.3 years) and 14 elderly (72.9±5.6) participants and asked them to walk at a self-selected speed and at a fast speed. Results about the elderly participants during free speed gait showed a decreased linear power transfer from the leg to the upper body due to the hip and knee moments compared to the young participants. Nonetheless, when they were asked to walk at a fast speed, older adults significantly increased knee and hip moment contributions to hip linear power to levels comparable to those of young participants at a similar speed. These results supported previous findings indicating that kinematic alterations at the hip are a cause of reduced gait speed in the elderly.

Furthermore, Lelas et al. (2003) found that peak external hip flexion moment swing, peak external knee flexion moment loading response, peak external knee flexion moment pre-swing and peak external knee extension moment terminal stance increase with faster speeds. Furthermore, it has been shown that vertical and horizontal GRF are significantly affected by WS, especially during the loading response phase and mid-stance phase (White et al., 1996). In 2001, Stansfield et al. examined the importance of speed in the

characterization of ground reaction forces (GRF) and found that WS was the primary determinant of kinematic and kinetic changes in growing children.

In 2009, Monaco et al. conducted a study comparing lower limb kinetics between YA and OA. They recruited 9 young (26.4 ± 2.3 years old) and 8 elderly (70.4 ± 5.3 years old) healthy subjects. Participants were asked to walk on a treadmill at five normalized speeds (from 0.5 to 1.3 m/s). Researchers found that in elderly participants, hip and knee concentric powers during the stance phase were higher than those in young participants despite their decreased ankle plantar flexor kinetics.

Schwartz et al. (2008) provided a comprehensive study on the effects of WS on joint kinematics and kinetics of typically developing children at a wide variety of speeds (very slow (VS), slow, self-selected comfortable, and fast WS) using a single foot model. It was found that ankle DF at TO exhibited a plateau at low WS and maximum hip extension decreased as WS increased. It was also found that pelvic tilt ROM increased as WS increased. Further, peak-braking force was nearly linear and peak propulsive force exhibited a plateau at high WS. Additionally, it was shown that maximum knee flexion moment in late swing exhibited a plateau at low WS, and peak hip power generation in early stance exceeded linear growth. The power generation in the ankle increased at higher WS, while power absorption decreased. Thus, their study showed that WS had a significant influence on 3D lower extremity joint kinematics and kinetics (GRF, net internal joint moment and net joint power) in a pediatric population.

In 2020, da Silva et al. investigated the association between aging and ankle-foot power output considering the effect of gait speed. Researchers studied the gait data from an open dataset previously published. This dataset included data from younger (27.6 ±

4.4 years) and older (62.7 ± 8.0 years) adults, walking at their self-selected speed, then at speeds 30% faster and 30% slower than the self-selected speed. Da Silva et al. (2020) found that OA absorb more power during the early stages of the stance phase compared to YA. Researchers concluded that WS significantly affects both the ankle and foot mechanical power output profiles. Conversely, researchers found that age did not affect either ankle or foot power profiles.

2.3.2 Effect of Walking Speed using a Multisegment Foot Model

The aforementioned studies modeled the foot as a single rigid segment permitting only foot progression angle and dorsi/plantarflexion to be measured (Carson et al., 2001). Using such models has shown that WS influences ankle, knee and hip motion. However, relatively little is known about the effects of WS on subsegment foot kinematics. Hence, researchers have recently developed MSF kinematic models to further understand foot mechanics and function in YA and OA (Dubbeldam et al., 2010; Grant & Chester, 2015; Pohl et al., 2007; Sun et al., 2018; Tulchin et al., 2009; Van Hoeve et al., 2017).

In 2010, Dubbeldam et al. used an MSF model to examine the effect of WS on forefoot, hindfoot and ankle kinematics among healthy adults (43 ± 8 years old) walking at comfortable and clinically relevant slower speeds. The participants walked at three different WS: 1.28 m/s, 0.97 m/s and 0.65 m/s. The WS was computed from the recordings, but to adjust the speed, it was also measured manually during the recordings and communicated to the test participant. The variations in WS significantly affected the foot and ankle joint ROM in the sagittal and transverse planes and it mainly influenced these joint motions at TO. In the sagittal plane, researchers found that the minimum tibio-talar PF and maximum hallux DF at TO decreased significantly (between 3° and 9°) with

decreasing WS. Additionally, they showed that increasing WS resulted in decreased stance phase duration, increased cadence, and decreased double support time (Dubbeldam et al., 2010). The minimum medial arch at TO, as well as the minimum midfoot supination at mid-stance, were significantly affected by the WS. In the frontal plane, significant differences only occurred in the midfoot, at foot loading or at midstance. Increases in peak supination angles of the midfoot with respect to hindfoot were found with increasing WS throughout the loading phase. The motion of the hindfoot was not significantly affected by the WS, even though the hindfoot is initially slightly (0.5°–1°) less everted for lower WS. In the transversal plane, significant differences in joint ROM between different WS were observed for the hallux adduction only. Also, more motion in forefoot adduction with respect to the hindfoot and more external leg rotation were observed at higher WS, and both were related to increased stride length. However, fast WS were not tested in this study and a broader range of WS is needed to provide speed-matched data when evaluating a patient (Grant & Chester, 2015).

A more comprehensive study conducted by Grant and Chester (2015) used a modified version of the RFM to examine a broader range of WS (VS, slow, free, fast, and very fast (VF)) among healthy adults (23 ± 2.6 years old) in order to replicate WS routinely observed in typical and atypical gait on foot kinematics. They found that all of the temporal-spatial parameters showed significant differences. For example, as WS increased, time to TO decreased, whereas single leg stance time, stride length, and cadence increased. Moreover, increasing WS affected the relative angles between the calcaneus and tibia in the sagittal plane; the mean maximum DF angle decreased, while the mean maximum PF angle increased. These findings are similar to Dubbeldam et al. (2010), who analyzed the

talus with respect to the tibia, and found that the PF angles increased at TO as WS increased. They also found that pronation of the midfoot relative to the calcaneus increased during midstance with a reduction in WS. Additionally, in the sagittal plane, mean maximum absolute angles of the metatarsals and the hallux presented significant differences between speed groups. As WS increased, the mean maximum absolute angle for the fifth metatarsal (V2G), the second metatarsal (S2G) and the hallux (F2Ps) increased. Conversely, the medial longitudinal arch (MLA) angle decreased as WS increased.

Grant and Chester (2015) found similar results as Schwartz et al. (2008), which used a single foot model, for mean ankle DF at TO when walking at slow speed. The agreement of the results is interesting since the foot model used differed, and Schwartz et al. (2008) studied children (10.5 ± 3.5 years old). Contrary to Dubbeldam et al. (2010), researchers (Grant & Chester, 2015) found significant changes in mean maximum PF of the midfoot relative to the calcaneus over changes in WS although they also used an MSF model. One of the reasons could be the age group, where Grant and Chester (2015) studied healthy adults (23 ± 2.6 years old) and Dubbeldam et al. (2010) recruited OA (43 ± 8 years old). The relative angles of the foot (as a single segment) with respect to the tibia were similar to that of the calcaneus relative to the tibia. As WS increased, the mean maximum DF angle decreased. These results were also found by Schwartz et al. (2008). Additionally, there was an increase in the mean maximum PF angle as WS increased (from 15.05° at VS to 22.73° at VF). Differences in the results compared to Schwartz were found, since they reported a mean PF angle from 4°, at a VS speed, to 22° at a VF WS. These variations found may be due to the varying WS between studies, as well as the age group. Similar to the single rigid body model studies, WS was found to affect MSF kinematics.

Van Hoeve et al. (2017) assessed the effect of age and speed on foot and ankle kinematics by comparing results during slow walking and fast walking. A group of healthy YA (22.4±1.3) and a group of OA (57.5±3.9) were recruited. The interaction between age and speed was also analyzed. With a stopwatch, time and speed were controlled by the researcher. This study used a 4-segment mechanical model of the foot. The results showed that, regarding speed, there was a significant difference between forefoot/hindfoot motion in the sagittal plane (flexion/ extension) during both loading- and push-off phase. Additionally, there was a significant difference between hindfoot/tibia for all parameters except for motion in the sagittal plane (flexion/extension) during push-off phase. However, their results showed that age did not significantly influence kinematics. There were no significant differences between the younger and older adults' groups regarding the ROM between the forefoot and hindfoot in the sagittal, frontal, and transverse planes, neither during the loading phase nor during the push-off phase. Nor were there significant differences between the two groups in ROM between the hindfoot and tibia in the sagittal, frontal, and transverse planes, neither during the loading phase nor during the push-off phase. Further, there was no interaction between age and WS. There were no significant interactions found between WS and age for the ROM between the forefoot and hindfoot in the sagittal, frontal, and transverse planes, neither during the loading phase nor during the push-off phase. Nor were there significant interactions found between WS and age for the ROM between the hindfoot and tibia in the sagittal, frontal, and transverse planes, neither during the loading phase nor during the push-off phase. In summary, their analysis found that WS significantly influenced the kinematic outcome parameters (more pronounced in the ankle joint) and no significant differences were found between younger and older

healthy participants. Their findings agree with Legault-Moore et al. (2012), who found no significant effect of age on foot and ankle kinematics and there was no interaction between age and speed.

In 2018, Sun et al., studied the effect of WS on the foot inter-segment kinematics, GRF and lower limb joint moments among healthy male adults. They implemented a modified version of the OFM and found that with increasing WS, the cadence and the stride length increased, while the stance duration, stance phase and stride time decreased (Sun et al., 2018). These findings are similar to previous studies which used a single foot model (Kirtley et al.,1985; Kirtley, 2006). Sun et al. also examined the hindfoot relative to the tibia motion and found that, in the sagittal plane, fast WS showed a significantly higher heel contact, DF, peak DF, and DF/PF. They also found a significant increase of the peak values of hindfoot relative to the tibia DF as WS increased. In the frontal plane, as WS increases, researchers found a significant increase in eversion at heel contact during stance phase, whereas peak inversion angle was found lower as WS increases. Likewise, in the transverse plane, significant changes in peak external rotation (ER) and ROM were found in fast WS. They also examined the forefoot relative to hindfoot motion and found that the DF angle was significantly greater at a fast WS in the sagittal plane, but the peak PF angle was found to be significantly higher in neutral WS. Additionally, they found a significantly larger supination in slow and neutral WS at heel contact in the frontal plane. In the transverse plane, adduction/abduction ROM and adduction angles at initial contact were found significant at slow WS. However, maximum abduction angle was significant at a fast WS. Moreover, they studied the forefoot relative to the tibia motion and found that fast WS showed more DF at initial contact in the sagittal plane. Peak PF was found significant

at a neutral WS. Further, as WS increased, the ROM (DF/PF) increased. Their results did not show a significant difference in peak supination and supination/pronation ROM. In the transverse plane, the adduction angle at initial contact and maximum adduction angle were significant at a slow and neutral WS, while the peak abduction and adduction/abduction ROM were found significant at fast WS.

Researchers also examined the hallux relative to the forefoot motion and they only found that the hallux was less dorsiflexed at a fast WS in the sagittal plane. Additionally, DF/PF ROM in slow and neutral speed were found significant. Regarding GRF, their results showed that peak braking force together with peak propulsive force was significant at fast WS compared to slow WS in the anterior-posterior (A/P) direction, and that peak vertical forces at a fast WS were significantly higher than neutral WS. Speed had a significant effect on the sagittal and frontal plane joint moments of the knee and ankle. In the sagittal plane, the peak knee flexion and extension moment, peak ankle DF moment in early stance and peak ankle PF moment in late stance phase were found significantly higher at a fast WS. In the frontal plane, peak knee adduction and peak ankle eversion moments were significant at a fast WS. As WS increased, knee and ankle joint moments in the sagittal and frontal planes increased, suggesting a positive linear correlation between WS and joint moments.

The aforementioned studies provided insight into MSF kinematic patterns and improved the knowledge of the effects of WS in foot kinematics and kinetics of the different segments of the foot, while the single segment foot models could not provide that information. However, there were some disparities in the results found between the previous studies demonstrating that the effects of speed on foot and ankle kinematics in

gait studies using MSF models are not fully understood. The discrepancies are mostly due to different age groups, the speed groups selected, as well as the method to control the speed. To resolve for these differences, standard methods should be developed. Currently, most researchers are using the same MSF model (RFM), although the method to control speed still differs greatly.

2.4 Single segment foot models

In the past, most gait research has modeled the foot as a single rigid segment consisting of two rotational degrees of freedom. Thereby, only foot progression angle and dorsi/plantarflexion can be measured. When modeling the foot as a single-segment, a minimum of three retro-reflective markers are placed on the foot. The simplicity of the single rigid segment model allows for easier marker configuration and this represents an advantage when the movement of each segment of the foot is not of interest. However, the foot is comprised of 26 bones and several joints connecting them. Thus, a standard kinematic protocol based on three markers is inadequate in describing the complex foot biomechanics when a detailed level is required. Therefore, to fully understand what is occurring within the foot during gait, an MSF model should be used.

2.5 Multisegment foot models

To increase our knowledge of the mechanics of the typical and atypical foot, multisegment mechanical models of the foot have recently been developed (Dubbeldam et al., 2010; Grant & Chester, 2015; Pohl et al., 2007; Sun et al., 2018; Tulchin et al., 2009; Van Hoeve et al., 2017). These models divide the foot into multiple compartments or segments allowing the relative motion between segments to be measured (e.g., forefoot vs

hindfoot). The importance of studying each segment of the foot stems from having a better understanding of the typical and pathological movement within the foot.

Motion in all three planes (sagittal, frontal and transversal) of the forefoot, midfoot and hindfoot can be tracked using an MSF model. This allows the identification of any deviations in motion and their underlying causes. Such information could be beneficial for determining the most appropriate treatment to restore foot and ankle function. A disadvantage of using an MSF model is its complexity. The markers are usually located near one another on the foot, thus, lower resolution motion capture cameras may have difficulty distinguishing markers. In addition, an MSF model requires more training to be able to apply the markers correctly. The navicular and cuboid, specifically, can be difficult to palpate, thus the person applying the markers must be well versed in the locations of these landmarks.

For the proposed study, the Rizzoli Foot Model (RFM) was used due to its validity and reliability (Leardini & Caravaggi, 2016). A few studies have compared the performance of the most popular MSF models. Mahaffey et al. (2013) used intraclass correlation coefficients to assess the OFM, the RFM, and the Kinfoot model. Results showed that MSF kinematics were quite repeatable, even in pediatric feet. A standard error of measurement greater than 5° was found in 26%, 15% and 44% of the kinematic parameters, respectively for the OFM, RFM and the Kinfoot model. The RFM resulted in moderate repeatability and reasonable test-retest error similar to that of the OFM, but with original additional data also on midfoot kinematics. Later, DiMarco et al. (2015a, 2015b) performed a more comprehensive comparative analysis of the OFM, RFM, the Sawacha et al. (2009) and Saraswat et al. (2012) models. The best coefficient of multiple correlation

between-sessions of the kinematic parameters during ground and treadmill walking was observed for the RFM (range 0.83-0.95).

2.6 Effects of foot structure and mobility on gait

While there has been significant research regarding age-related changes in foot mechanics, challenges remain. In addition, very few studies examined the impact of foot structure on gait mechanics. However, the major limitation of these studies is that foot structure variables, other than arch heigth, are not often considered. Foot structure refers to the external shape or morphology of the foot. Common variables to examine foot structure are foot length, truncated foot length (TFL), arch height ratio (AHR) and dorsal arch height (DAH), among others. Examining the effect of different structures of the foot within and between the various structural components is fundamental for comprehending their respective function during gait and will also allow a better understanding of different disorders (Gefen et al., 2000).

Further, the assessment of foot mobility has received less attention in the literature and is usually linked to the foot posture. Foot mobility parameters, such as foot mobility magnitude (FMM), forefoot width (FFW), midfoot width (MFW), and rearfoot width (RFW), have been found to be positively correlated to MSF kinematics and kinetics (Buldt et al., 2015; Maharaj et al., 2018). Impairments in intrinsic foot mobility have been recognized as significant potential contributors to altered foot function. Nonetheless, the role of foot mobility in gait continues to be poorly understood (Rao et al., 2007).

Therefore, a more detailed understanding of age-related differences in foot function could be obtained by measuring both structure and mobility in YA and OA during gait.

2.6.1 Age-related changes in foot structure

Previous studies performed on different population groups have reported that foot morphology undergoes age-dependent changes and foot development and maturation is accompanied by variations in its shape and function. Younger people (18 – 35 years old) tend to have a smaller foot circumference compared to OA (Kouchi, 1998). The elderly (+65 years old) are reported to have flatter, longer, and wider feet than YA (Frey, 2000; Scott et al., 2007). In addition, when the foot is loaded by the body weight, the foot structure experiences deformations such as hindfoot pronation/supination, modification of the widening between the first and fifth metatarsal, flexion of the phalanges in the late stance phase, lowering of the medial arch, and many other intrinsic movements occurring both in the stance and swing phases (Farinelli et al., 2019). Lowering of the transverse arch (Hsu, 1971; Scott et al., 2007), increased soft tissue stiffness (Menz, 2014) and toe deformities are also changes in foot structure due to age. Calcaneal eversion is linked to low arch and it has been proposed to decrease the inclination of the subtalar joint axis of rotation (Arangio et al., 1998; Blackwood et al., 2005). In addition, increased forefoot DF and decreased forefoot adduction (Van Boerum & Sangeorzan, 2003) have been predicted in individuals with low arches.

In 2007, Scott et al. studied the age related differences in foot structure and function. The purpose of the study was to compare foot characteristics and plantar force in young (20.9±2.6 years old) and OA (80.2±5.7 years old). However, they did not implement a MSF model or a motion capture system. Instead, foot and ankle characteristics were assessed with different equipment such as a pressure aesthesiometer and an isometric device. Speed, cadence and average step length were recorded with a stopwatch. Plantar

forces and pressures were recorded using a pressure mat. They found that the OG exhibited flatter feet, reduced ROM of the ankle and MTP1 joints, as well as toe plantarflexor weakness. They also found that older participants exhibited a slower WS and shorter step length. Thus, it was suggested that foot structure in OA could alter their foot function.

2.6.2 Age-related changes on foot mobility and posture

The Foot Mobility Magnitude (FMM) is a composite measure of the vertical and medial-lateral (ML) mobility of the midfoot under weight-bearing and non-weight bearing conditions, i.e., ΔDAH, which represents the change in the vertical mobility of the midfoot, and ΔMFW, which represents the change in the ML mobility of the midfoot. In 2009, McPoil et al. conducted a study to determine the reliability of the FMM. They showed good to high levels on intra-rater and inter-rater reliability. Their results were valid when compared to radiographs. In addition, they noted that the greater the vertical change in AHR, the greater the amount of foot mobility. However, FMM is a measure of the mobility of the midfoot only, thus, to provide a better understanding of the foot mobility in each segment, studies should also measure the mobility of the forefoot and rearfoot.

Currently, there are four static foot posture measures presented in the literature that have been validated against angular measurements from radiographs and considered to be the 'gold standard' measurement technique (Menz & Munteanu, 2006; McPoil et al., 2008a; Williams & McClay, 2000). These measures include the Foot Posture Index (FPI), the Arch Index (AI), normalized navicular height truncated (NNHt) and the AHR. In addition, by measuring foot mobility, it is possible to describe the response of structures such as DAH to the load applied during the measurement of foot posture and thus, be more valid in predicting dynamic function than static measurements (Menz, 1998). The Foot

Mobility Magnitude (FMM) has been found to be the most reliable of the current measures of foot mobility (McPoil et al., 2009). As a result, the use of these measures (i.e. FPI, AI, NNHt, DAH and FMM) may provide useful insights into the variances in the motion of the foot during gait due to aging.

In 2011, Cornwall and McPoil conducted a study that examined the relationship between the static foot posture and foot mobility. They hypothesized that feet with a high arched static foot posture would have minimal foot mobility, whereas feet with low arch static foot posture would have increased foot mobility. They assessed the foot posture using four different measurements, including the Foot Posture Index, the DAH, DAH ratio, and MFW. Each measurement was taken in two different positions: 1) Participants were in their relaxed stance position, distributing equal weight on both feet (weight bearing), 2) Participants were asked to sit on the end of a table with ankles slightly plantar flexed (non-weight bearing). They also assessed the foot mobility of each participant using the FMM. The results of their study substantiate their hypothesis by showing a relationship between static foot posture as measured by either DAH or MFW, and the amount of foot mobility as measured by FMM. Thus, participants with greater mobility as measured by the FMM, had lower dorsal arch heights and greater MFW compared to participants with less mobility. This study compared two different foot postures in YA (25.6 ± 3.8 years old) to analyze its relationship with foot mobility, however, in-depth research about the foot mobility including other age groups and the sex factor should be performed.

In 2015, Buldt et al. examined the associations of clinical measures of static foot posture and mobility with foot kinematics during walking. A five-segment foot model was used to measure 3D motion of the rearfoot, midfoot, medial forefoot, lateral forefoot and

hallux. The participants were healthy adults (24.4 ± 6.2 years old), and they were asked to walk at their self-selected speed. Peak and ROM variables throughout load acceptance and midstance/propulsion phases of gait were extracted for segment to segment motion calculations (Buldt et al., 2015). According to their findings, AHR, anthropometric and spatiotemporal variables were found to influence variations in abduction ROM of the hallux (between 0-20% of the gait cycle), as well as in the eversion ROM of the midfoot (between 20-70% of the gait cycle). AHR also explained variations in peak midfoot DF and adduction and FMM explained 8% of the variation in peak hindfoot abduction. In other words, these measures explained between 3.9-20.0% of the variation in peak kinematic variables of the hindfoot, midfoot, lateral forefoot and hallux. Foot posture measures were more strongly correlated with foot peak angle kinematic variables compared to ROM kinematic variables, e.g. a more planus foot posture was associated with increased peak adduction and inversion of the rearfoot (i.e. a more supinated position) during propulsion. While the associations between static foot posture measures and ROM kinematic variables were weak, there were findings that may be significant from a functional perspective, e.g. a foot with greater cavus posture score displayed greater eversion motion of the midfoot on the rearfoot during the propulsive phase of gait, while a more planus foot posture score displayed less motion. According to the researchers, such findings question the theory that the midfoot and forefoot can withstand increased loading during propulsion by increasing 'rigidity' of the foot (Elftman, 1960) and, instead, suggest that the midfoot undergoes coordinated eversion motion during propulsion that may vary according to static foot posture. However, they had several limitations including the recruitment of healthy YA only, thus their findings may not be generalizable to older populations.

According to the previous research, the foot posture, i.e. low arch and high arch, affects the mobility of the foot, and this may influence the walking kinematic and kinetic patterns. As mentioned before, it has been found that older people tend to have a lower arch. Thus, further research is needed since there is still a poor understanding to which extent the foot mobility and posture affects the mechanics of the foot in different age groups and at different WSs.

The posture of the foot is characterized by the external shape of the foot. During standing, foot posture is a measure of the response of the foot to relatively static external and internal forces (Buldt et al., 2015). However, during dynamic tasks, such as walking, the forces applied are typically greater than during standing and vary over time. The measurement of the static posture of the foot and its dynamic function is important because certain variations may predispose individuals to injury (e.g. planus foot posture has been identified as a risk factor for patellofemoral pain and Achilles tendinopathy). The mechanism relating static foot posture and dynamic foot function to injuries has been attributed to altered foot kinematics and loading rates, resulting in the development of excessive stress within musculoskeletal tissues (Buldt et al., 2015). It is believed that planus feet generally over-pronate, causing the GRF to move medially during the stance phase of gait, whereas cavus feet over-supinates, making the GRF to move laterally during stance (Hillstrom et al., 2013). According to previous findings (Buldt, et al., 2015; Cornwall & McPoil, 2011), the foot posture, i.e. low arch and high arch, affects the mobility of the foot, and this may influence the walking kinematic and kinetic patterns. Therefore, further research is needed since there is still a poor understanding to which

extent the foot mobility and structure affect the mechanics of the foot, particularly in different age groups and across different WSs which can influence the walking patterns.

2.6.3 Arch height

Foot arches vary across individuals due to factors such as age, sex and weight (Pfeiffer et al., 2006; Tomassoni et al., 2014; Zhao et al., 2017). It has been suggested that individuals with low-arched feet are usually more flexible, and those with high-arched feet tend to be stiffer (Zifchock et al., 2006). Thus, a flexible, low-arched foot tends to stretch the soft tissues of the foot as it attempts to produce enough moment for toe-off (TO). Conversely, individuals with high-arched feet tend to be less mobile. However, there is limited evidence supporting this information, thus, it is necessary to further investigate the influence of the arch height on kinematic variables of the lower limb in individuals across different arch heights, considering broader age groups and a broader range of WSs. Although a specific foot type, i.e. low arch, normal arch and high arch, was not targeted, it was recorded for the purpose of this study.

2.8 Summary

One of the important needs in biomechanic research is to examine MSF and lower limb joint kinematics and kinetics across age, speed and foot structure and mobility. Previous research has focused on the effect of age and speed on kinematics alone or the effect of age on kinetics alone. A more thorough approach is to examine the kinematics and kinetics together along with foot structure to obtain a more comprehensive foot model. This work addressed the limitations of current work and increased our understanding of age-related changes in MSF motion by examining differences in MSF kinematics and lower extremity kinematics and kinetics between young and OA during walking. Speed-

mediated effects were separated from age-related changes. Additionally, the relationship between age-related changes and foot structure and mobility were explored. The study helped improve our understanding about the foot mechanics in YA and OA, providing a more comprehensive knowledge about the age-related changes in MSF kinematics, and lower limb kinematics and kinetics.

3.0 Methods

The following section will provide information regarding the research project's participants, procedure, instrumentation and data analysis.

3.1 Participants

Participants were recruited through word of mouth, emails, and posters. The proposed study was approved by the Research Ethics Board at the University of New Brunswick (REB #2019-049). Two groups of participants were recruited for the study. Group 1 consisted of 16 adults (8 male, 8 female) aged 18 – 35 years old (YG) and Group 2 consisted of 15 OA (8 females, 7 males) aged over 65 years old (OG). A power test was conducted and determined a sample size of 21 participants with a large effect size of 0.5 and power of 0.80, however, due to the duration of the test and the amount of equipment that was used, the aim was at least 14 participants per group (power = 0.65), as this seemed to be a feasible amount of participants to recruit and was near the sample size calculated. In order to participate, individuals had to meet the exclusion/inclusion criteria. The inclusion criteria was that the participant was able to stand and walk barefoot at least 10 meters without an assistive device and at various speeds. The exclusion criteria included no foot trauma or foot pathology (fractures, bunions, ulcers, etc.), joint replacement surgery or an orthopaedic surgery of the lower limb and/or spine, a neurodegenerative disease such

as diabetes, any physical or neurological condition that resulted in abnormal gait such as rheumatoid arthritis, osteoarthritis affecting the foot, Parkinson's disease, peripheral vascular disease, history of stroke, chronic pain, and edema, and any pain, aching or stiffness in their feet, knees or hips in the past 30 days.

Participants were asked to complete a questionnaire called "Participant Characteristics Questionnaire". The questionnaire asked questions about the participants' medical history (e.g. injuries and/or surgeries of the lower limb) and it helped to ensure their participation.

3.2 Instrumentation

A combination of instruments was used for the study. A 3D white-light body segment scanner (TechMed 3D Inc., Quebec City, QC) was used to obtain bilateral anthropometric foot measurements of each participant while weightbearing (standing) and non-weightbearing (sitting). Further, a passive optical motion capture system (Vicon, Oxford Metrics Group, Oxford, UK) was used to measure the kinematics of the body during walking. Additionally, two high-speed Basler digital video cameras (Basler Inc., Ahrensburg, Germany) were used to obtain front and side images of each participant during the trials. Six force plates (Kistler Instruments Ltd, Michigan, USA) were used to determine the temporal-spatial data and GRF data for kinetics. To ensure that the participants speed groups did not overlap, a system of laser beams were used. Each component involved in the data collection were discussed in the following sections.

3.2.1 3D Scanner

A white-light 3D body segment scanner (TechMed 3D Inc., Quebec City, QC) was used to measure different anthropometrics of the foot in an efficient and accurate fashion.

One advantage of using this system is that it deducts automatically specific height, width and circumference measures at different percentage lengths of the foot. The 3D scanner used in the study captures 13 frames per second. Its resolution is automatically set to 2 mm but can range from 1mm-10mm. However, the smaller resolution is recommended since the distance between each point of the mesh was smaller, which generated a more detailed model of the foot. Thus, a 1mm resolution was used. A checkered fabric (white and black) was used as a backdrop and placed over the floor to mask the floor or any other unwanted surface (i.e., to ensure a clear image of the foot was collected when the participants were in a stance/stand position). The pattern of the checkered fabric is invisible to the white light of the scanner; thus, the 3d scanner did not pick up images of the floor. The reliability and validity test was conducted at the Human Performance Laboratory and it was found to be highly reliable. An inter-rater test (ICC = .74 - .99) and intra-rater test (ICC = 0.66 to 0.99) were performed.

Six scanner markers were used to assist in scanning the FFW, the MFW and the RFW. These markers have a circular 6 mm diameter reflective surface and have a 2 mm (width) black border. The scanner identified the centroid of the reflective surface and the markers were projected onto the exact same location in the 3D model of the foot. The foot measures collected in this study included FFW, MFW, RFW, foot length, TFL, DAH and AHR. The FFW corresponded to the width between the most medial portion of the MTP1 joint and the most lateral portion of the MTPJ5. The MFW corresponded to the width perpendicular to 50% of the foot length on both the medial and lateral sides of the foot (Witana et al., 2006). And RFW corresponded to the the width at 16% of the foot length on both the medial and lateral sides of the foot (Lee et al., 2014). The DAH corresponded

to the distance between the supporting surface and the highest point of the instep taken at 50% foot length (Hill et al., 2017).

The scanner was used simultaneously with MSoft (MSoft 3.0, TechMed 3D Inc., Quebec City, QC), which is a data acquisition tool that renders the 3D image of the scanned body segment. Scans of the foot were recorded at a scan height of approximately 500 mm, using the uniform texture setting in MSoft.

3.2.2 Motion Capture System

To capture the movement of the body, a Vicon T160 system (Oxford Metrics Group, Oxford, UK) was used. Vicon is considered the gold standard due to its high reliability and validity. The tests have shown that the system has a hight test-retest and inter-tester reliability in the sagittal plane (R_a= 0.971 to 0.994), the frontal plane (R_a= 0.759 to 0.977), and the transverse plane (R_a= 0.729 to 0.899) (Sushima et al., 2003). The system consisted of 12 cameras with a resolution of 16 megapixels and a sampling frequency of 100 Hz. Cameras were mounted on an aluminum speed rail system, via clamps, around the lab. This configuration allowed the cameras to focus on the measurement space at the center of the laboratory where the force plates were located. This space corresponded to the capture volume and its size is 9m x 16m x 7m. Within this volume, the 3D trajectory of the markers placed on the skin were tracked by at least two cameras. The cameras sent infrared light pulses from the diodes placed around the lens of each camera causing the markers to reflect the light back to the cameras. When the reflection was detected by the cameras, the centroid of each marker was calculated and a set of three-dimensional coordinates for each marker was generated. It was important that, throughout the static trial, the cameras captured all the markers and clusters. The coordinates were relayed to

the computer where they were recorded in a binary file (*.c3d). If a marker was not seen by at least two cameras, then the coordinates were not recorded.

The calibration of the system was conducted using an active wand. The latter consisted of five recessed diodes in the wand that strobed for recognition by the cameras. The calibration procedure was performed before the participant arrived. The wand was waved quickly and evenly through the capture volume and just outside the radius of the capture volume to increase the possibility of marker recognition during the walking trials. The origin of the capture volume was set by placing the active wand square to edges of the bottom right corner of the second force plate, with the diodes set to strobe. It was important to ensure that the wand was level to the floor to ensure the accuracy of the collected marker coordinates.

3.2.3 Marker Placement

A total of twenty 14 mm diameter retroreflective markers, and twenty-four 9.5 mm diameter retroreflective markers, as well as four clusters, were placed on the participant's skin to track the motion of the body during gait. The cluster markers consisted of four 14mm diameter markers fixed to a rigid plate lined with Velcro for fixation to the body and were used to minimize skin motion (RTCL = Right thigh cluster; LTCL = Left thigh cluster; RSCL = Right shank cluster; LSCL = Left shank cluster). They were placed on the distal third of the thigh and shank segments of the left and right leg. The markers on each plate were simply numbered C1, C2, C3 and C4 in a clockwise orientation starting with the marker in the top right of the plate. The placement of each marker of the foot was based on a modified version of the Rizzoli Foot Model (Leardini, et al., 2007). Modifications included: the cuboid was not assumed to coincide with the base of the fifth metatarsal.

Likewise, the rest of the markers were placed based on a full body gait analysis model.. A model template (.vst), consisting on a full body multi-segment foot model was created before bringing any participant. This pre-defined template was saved and applied through a scaling mechanism to each of the participants. The purpose of the template was to provide automatically labeled markers for each dynamic trial captured.

3.2.5 Force Plates

Six embedded force plates (Kistler 9281E, Kistler Instruments, Winterthur, Switzerland) in the center of the laboratory floor were used to determine gait events (e.g. heel strike and toe-off) and measure the three-dimensional ground reaction forces (GRF), moments, and center of pressure in each trial. The force plates were integrated and synchronized to the motion caption system through a 128-channel Vicon A/D board. The sampling frequency of each force plate was 1000 Hz. The Kistler force plates are considered the gold standard due to its high reliability and validity. When the participant struke a force plate, the three-dimensional forces, moments and vertical torque data were detected and sent to the A/D board, which relayed the information to the computer. Data were exported in a c3d file for further analysis.

3.2.6 Visual3D

Visual 3D (C-Motion, Inc. Germantown, MD) is a biomechanical analysis tool used to measure movement and force data collected by any motion capture system. It was used to analyze the data specific of the biomechanic computation. The .c3d file exported from Vicon was imported to Visual3D for the analysis. Refer to data analysis section for detailed description about the computation.

3.2.7 Laser trip timer

To ensure a separation of .20 m/s between each speed condition across trials for each participant, a laser trip timer was used. The setup consisted of two laser beams, three meters apart, along the direction of progression, integrated to a laptop. The latter was used to run a custom-made Arduino code designed to calculate the speed of each participant. Once the participant's tibia intersected the first laser beam, the timer started counting, and it stopped when the second laser was cut. Since distance was known, and time was measured, the velocity was calculated and used to ensure that the participant was, in fact, walking at a faster or slower speed.

3.2.8 Custom-made foot measurement device

A custom-made device was used to measure the 50% of the foot length (midfoot) and the 16% of the foot length (calcaneus). This custom 3D printed device was printed using the Pro2 3D Printer (Raise 3D Technologies Inc, California, USA). The material used was polylactic acid (PLA). A previous reliability and validity test was performed to test the custom-made foot measurement device against a digital caliper (Marcial et al., 2021). The latter was considered the gold standard as manual measurement techniques are commonly used for obtaining foot anthropometrics in research and clinical setting. The custom-made foot measurement device was accurate to 0.2mm, while the digital caliper had a resolution of 0.01mm and was accurate to 0.02mm.

3.3 Experimental Procedure

All data collection for each participant took place in a single session of approximately 2.5 hours at the Andrew and Marjorie McCain Human Performance

Laboratory in the Richard J. Currie Center located on the University of New Brunswick campus Fredericton throughout the months of July-August 2019.

At the beginning of the session, the principal investigator explained the scope of the research to the participants and the tasks they would be performing in order to obtain consent. Participants had the opportunity to ask any questions or voice concerns that they may had before, during or after the study. After the participant gave consent, a "Participant Characteristics Questionnaire" was filled. Subsequently, they were asked to change into shorts and a t-shirt or tank top.

3.3.1 3D Scanning Phase

Following the completion of the questionnaire and consent forms, height and weight were measured using a weight scale and stadiometer. Afterwards, anthropometrics of the foot were obtained using the Techmed 3D scanner. However, prior to scanning the foot, the participant was asked to stand with their feet shoulder-width apart in order to place six scanner markers on six landmarks of each participant's foot. The participant had full notice of each marker placed prior to palpation such that they would not feel uncomfortable at any time. The scanner markers were placed on the first and fifth metatarsophalangeal joints, the medial and lateral aspect of the midfoot, and the medial and lateral aspect of the heel. The two markers for the metatarsophalangeal joints were identified through palpation, the two midfoot markers were placed according to 50% of foot length, and the two heel markers were placed according to 16% of foot length, both measured by the 3D printed device. The placement of markers was used to measure FFW, MFW and RFW respectively. The rest of the measurements were automatically measured by the 3D scanner. For

consistency and to reduce inter-operator errors, the same researcher was always responsible for placing the markers on each participant in the study.

Once the scanner markers were placed, participants were asked to complete two scans: 1) weightbearing and 2) non-weightbearing. The weightbearing scans were performed first. For the non-weightbearing scans, participants were asked to sit at the end of a table with both legs hanging in a perpendicular position from the knee to the ankle, perpendicular to the thigh and the floor with their hands at their sides and ankles slightly plantar flexed to have the foot in relatively the same position during sitting and standing (Cornwal & McPoil, 2011; Saghazadeh et al., 2015; Zhao et al., 2018). Once the position was reached, the scans of both feet were captured for a total of 4 scans (2 scans x 2 feet). Following the procedure, the scanner markers were removed. The duration of the scanner measurements was approximately 40 minutes.

3.3.2 Motion Capture Phase

Once both feet had been scanned, the retroreflective markers used for the motion capture system were placed on the participant's skin. Once the markers were applied, the principal investigator wrapped Neoprene-Velcro bands around the participant's thigh and shank of each leg at approximately the same height for fixation of the rigid cluster markers. The participant was asked about general comfort of the bands to ensure that the bands were at a comfortable tightness, preventing slippage during gait. Subsequently, the cluster plates were attached laterally on the band with Velcro in the vertical orientation. Once all of the markers were applied, the participant was asked to perform a series of 'warm-up' trials to allow time to adjust to the laboratory and marker set. Following this, the participant was asked to stand in the center of the capture volume for a static trial. When the static trial was

completed, the markers were labeled manually using the pre-defined marker template. The static trial allowed for the initiation of autolabel and calculation of joint centers. After the collection of the x, y, z marker coordinates, data were exported to a .c3d file. This file was used to calculate the temporal-spatial variables as well as calculate the angles for the segments using Visual3D (C-Motion, Inc. Germantown, MD).

3.3.3 Dynamic Trials Phase

Following this procedure, the participant was asked to go to the starting line in order to start recording the dynamic trials. A minimum of six successful trials (i.e. clean force plate strikes, marker visibility, and appropriate speed separation for both the left and right limb) were captured for each of the five speeds (VS, slow, self-selected, fast and VF) for a total of 60 trials per person (5 speeds x 2 limbs x 6 trials). Between each of the speed conditions, participants completed three free walking trials, which were not recorded, to aid in re-establishing the baseline WS. If needed, the participants were allowed to rest between the trials for a maximum of 10 minutes. Trials collected contained the necessary data for the left and right side. To ensure no overlap between the speed groups, two laser trip timers were used. A minimum separation threshold (.20 m/s) was used.

During the first set of trials, the participant was asked to walk at their self-selected speed. Afterwards, the participant was randomly asked to either start at a slow or fast speed group, using a coin toss to determine the starting speed. The slow speed group encompassed the slow and VS WS; the fast speed group encompassed the fast and VF WS. For example, if the slow speed group was randomly selected, VS speed was the next speed change. If the fast speed was randomly selected, the VF speed was the next speed change. After data for the determined speed group were collected, the participant was asked to walk

at their self-selected speed again. No data were recorded at this point since this procedure was only performed in order to familiarize the participant with their initial self-selected speed before starting on the next speed group. This allowed the participant to have a reference to what their free self-selected speed was before transitioning to the next speed group. To facilitate speed change, the participant was given verbal feedback to adjust speed accordingly (slightly faster, slightly slower, etc.) until the speed range was achieved. If a participant had difficulty reaching the target speed range, suggestions of particular activities such as rushing to a meeting, trying to catch the bus, going to a place you do not want to go, etc. were given. Once the participant had completed all tests, the markers were removed.

The next participant to enter the lab was asked to start with the speed group opposite to that with which the previous participant started (e.g. slow speed if the participant before started with fast speed after the self-selected trials). After this pair of participants, the coin flip was repeated with the next two participants etc. until all the data was collected. This method ensured that an equal number of participants started at slow and fast WSs.

3.4 Data Analysis

The following section will discuss how the kinematic and kinetic variables, as well as the foot structure and mobility variables, were analyzed.

3.4.1 Data processing and analysis

A static trial was captured to allow for the auto-labeling of markers in dynamic trials. The markers of the static trial were labeled based on the applied .vst template file. When a marker in the capture volume was seen by at least two cameras, a binary file (.c3d) containing the marker coordinates was relayed to the computer. Only markers tracked by

two or more cameras had three-dimensional coordinates. The Vicon system had the ability to fill gaps in collected data by predicting the trajectory of markers, depending on the sampling frequency. Once collected, the x, y, z coordinates were exported to a .c3d file and were used for the calculation of kinematic and kinetic parameters. Data were analyzed using Visual 3D software (C-Motion, Inc. Germantown, MD). All trajectories and analog data were filtered with a 2nd order low-pass Butterworth filter with 8Hz cut-off frequency.

3.4.2 Kinematic Data

The following kinematic variables were calculated: joint angles of the body and planar angles, specifically those between the multiple segments of the foot and the tibia, and the linear and angular accelerations and velocities of the body. The following temporal-spatial parameters were calculated: cadence, WS, stance time, step length and double limb support. Using a similar method as that outlined by Sutherland (1988), the mean WS was computed for the left leg trials, and the single walking trial that was closest to the mean value was used to represent the speed group for the left leg. This was repeated for the right leg. This resulted in each participant contributing two complete gait cycles, one for each leg, at each selected WS (5 x 12 = 60 trials per participant). The selected trials for the YG were pooled and the selected trials for the OG were pooled. Comparisons were made between both age groups.

3.4.3 Mechanical Model

The body was modeled as a series of connected rigid segments. The upper and lower body included the torso, pelvis and the right and left thigh, shank and foot. The foot was further divided into three segments: the hindfoot, the midfoot and the forefoot. The landmarks for each segment were as follows:

- Torso: Right and left shoulder (RSHO and LSHO) and the C7 vertebra.
- Pelvis: Right and left anterior superior iliac spine (LASI and RASI) and the sacrum (SACR).
- Thigh: Medial and lateral femoral epicondyle (MFEM and LFEM) and the greater trochanter (GTR).
- Shank: Medial and lateral epicondyles of the tibia (MTIB and LTIB) and medial and lateral malleoli (MMAL and LMAL).
- Hindfoot: Medial and lateral calcaneus (MCAL, LCAL) and the posterior calcaneus marker (HEEL).
- Midfoot: Navicular (NAVI), cuboid (CUBD) and proximal metatarsal 2 (PMT2)
- Forefoot: Distal metatarsal 1 (DMT1), distal metatarsal 2 (DMT2), distal metatarsal 5 (DMT5), proximal metatarsal 1 (PMT1), proximal metatarsal 2 (PMT2), proximal metatarsal 5 (PMT5) and the hallux (HALLX).

Joints included the hip joint center, and the left and right knee and ankle. The torso, pelvis, hip, knee and ankle allow for three degrees of freedom. The system does not allow for more than three degrees of freedom, thus, translational movement in this case was ignored. Ankle, hip and knee are capable of flexion-extension, internal-external rotation and abduction-adduction. The torso and pelvis are capable of the same motions, but are known as tilt, internal-external rotation and obliquity.

3.4.5 Anatomical and Embedded coordinate systems

The locations of the three non- collinear markers on each rigid segment were used to create embedded coordinate systems at the virtual joint centers. Joint angles were computed from the relative orientations of the embedded coordinate systems using Euler

angles in a y-x-z sequence, corresponding to flexion/ extension, adduction/abduction, and internal/external rotation. Joint angle data were normalized to 100% of the gait cycle (GC).

3.4.5.1 Anatomical System

The anatomical coordinate system was created for each segment based on the respective surface markers. Such segments included the torso, pelvis, thigh, shank, and foot (hindfoot, midfoot, forefoot).

3.4.6 Kinetic Data

The kinetic variables of interest to this study were ground reaction forces (GRF), joint moment and joint power. Inverse dynamics and the Newton-Euler equations of motion were used to compute the joint forces and moments. Joint power was calculated by multiplying the moment at the instant center of rotation (ICR) and joint angular velocity.

3.4.7 Foot Structure and Mobility Data

The structure variables of interest to this study were DAH, TFL, foot length, and AHR. The mobility variables of interest were rearfoot width (RFW), midfoot width (MFW), and forefoot width (FFW). To classify the posture of the foot, the AHR was used. The AHR, introduced by Williams and McClay (2000), is defined as the DAH divided by the TFL. The TFL corresponds to the distance between the pternion of the heel to the joint line of the MTP1 joint. Studies that looked at the reliability of the AHR have shown good intra-rater and inter-rater reliability (McPoil et al., 2008a; McPoil et al., 2009). To assess the mobility of the midfoot, the Foot Mobility Magnitude (FMM) was used. FMM is calculated by taking the square root of the sum of both variables after each has been squared (Maharaj et al., 2018).

3.4.8 Method for controlling gait speed

To identify speed-mediated differences in kinematics and kinetics between young and older walkers, a method of controlling gait speed during data collection is required. In the literature, several methods of obtaining gait patterns at a range of speeds have been used, such as treadmills, feedback control and free speed. For this study, the feedback control method was used. The method consisted on giving instant feedback to the participants as to whether they needed to speed up or slow down to reach the required speed. This method may have created a longer data collection process, however, the main benefit of implementing the feedback method was that participants, especially the elderly, were not forced to walk at a certain speed. This gave a natural gait pattern to analyze for each participant because the participant A was not forced to walk at the same speed as participant B.

3.4.9 Dimensionless Speed

In some cases, individuals may differ based on stature, which in turn can have an effect on gait. It is important to consider these differences when an individual will be compared to other individuals (Hof et al., 1996). To account for these individual differences, in this case the effect on speed, dimensionless gait speed was used. Hence, the dimensionless gait speed was distinct to the speed collected. The equation suggested by Hof (1996) to find dimensionless speed is as follows:

$$\hat{v} = \frac{v}{\sqrt{g l_o}} \quad (1)$$

Where v is the collected speed, g is gravity, and l_0 represents the leg length of the individual. The leg length was measured from the greater trochanter to the ground. The

objective of normalization was to attempt to minimize inter-individual differences due to anthropometry and assist in inter-individual comparisons. Speed ranges for each speed condition were determined with respect to these dimensionless values (See Section 3.4.10).

3.4.10 Speed Group Division

To define the ranges of speeds for each speed category (e.g. WSs for fast vs. VF conditions), speed groups were calculated using the percentage method following Grant and Chester (2015) protocol. These divisions of data were determined using a post hoc analysis, as it is difficult to know the distribution of data from self-selected trials. The selected trials were pooled and sorted from lowest to highest. Then, the median value was calculated and used as the midpoint of the free speed group. Due to the total number of gait trials, twenty percent of this midpoint value was calculated. Afterwards, this calculated value was added and subtracted from the midpoint to determine the upper and lower limit of the free speed group. The speed range of the free speed bin was determined and used to generate two slower speed bins and two faster speed bins. The negative percentiles were used to calculate the slow speed groups. The first speed trial outside the lower limit of the free speed group was the upper limit of the slow speed group. The VS speed group began at the first speed trial outside the lower limit of the slow speed group and contained all remaining slow speed trials. The positive percentiles were used to calculate the fast speed groups. The first speed trial outside the upper limit of the free speed group was the lower limit of the fast speed group. The VF speed group began at the first speed trial outside the upper limit of the fast speed group and contained all remaining fast speed trials. By sorting walking trials into speed groups using this method, the collected data were sorted into each group, leading to a more balanced distribution of data.

3.4.11 Statistical Analysis

Prior to undertaking inferential statistical testing, normality and equality of variances tests were performed to determine if parametric or non-parametric tests were appropriate. Differences in mean kinematic and kinetic data, such as mean maximum/minimum joint angles, mean temporal-spatial parameters, mean joint moments and powers, and mean ground reaction forces (GRFs) between OA and YA as a function of speed and foot structure were compared using a mixed model analysis of variance (ANOVA) or if indicated, a Kruskal-Wallis test. To test for significant differences in mean kinematic and kinetic data, independent of speed, an analysis of covariance (ANCOVA) was used, or if indicated, Quade's ANCOVA. An alpha level of 0.05 was used for all test of statistical significance.

3.4.11.1 Variables

A summary of the dependent and independent variables are shown in Table 1.

Table 1. Independent and Dependent Variables.

Independent Variables	Dependent Variables
Age • Younger group • Older group	Temporo-spatial • Cadence • Stride length • Single leg support time • Double leg support time • Time to toe-off • Cycle Time
Speed • Normal • Slow • Very Slow • Fast • Very Fast	Kinematics • Max./min. angle in stance • Time to max./min. angle in stance • Max./min. angle in swing • Time to max./min. angle in swing
Foot structure • Foot length – WB and NWB • Dorsal Arch Height – WB and NWB • Arch Height Ratio – WB and NWB	Kinetics • Ground Reaction Forces • Joint Moment • Joint Power
Foot Mobility • Foot mobility magnitude • Forefoot width • Midfoot width • Rearfoot width	
Left/right foot	

4.0 Results

4.1 Age-related Differences in MSF and Lower Extremity Kinematic and Kinetic Variables as a Function of Speed

The first purpose of the study was to investigate differences in MSF kinematics and lower extremity kinematics and kinetics between young and OA during walking. To separate speed-mediated effects from age-related changes in motion, data were recorded across five WSs at self-selected speeds (VS, slow, typical, fast, and VF speeds). Therefore, it was hypothesized that there would be significant differences in MSF and lower extremity kinematic and kinetic variables (e.g., calcaneus-tibia plantarflexion angle, hallux angle (F2Ps), medial longitudinal arch (MLA) angle, cadence, double support time, etc.) between age groups as a function of speed.

4.1.1 Age-related Differences in Temporospatial Variables

Table 2 presents the significant age-related differences in the mean temporospatial variables. The following section focuses on between-group differences.

Table 2. Significant p-values of the mean temporospatial variables across five walking speeds.

Walking speed group	Cadence p-value	Stride Length p-value	Single Leg Support Time p-value	Double Leg Support Time p-value	Time to Toe-off p-value	Cycle time p-value	Step Length p-value	Speed p-value
VS	-	.01	<.0001	-	<.0001	-	<.01	<.05
S	.03	<.001	<.01	.02	<.01	<.01	<.01	-
T	.02	<.01	<.01	-	<.01	-	-	-
F	<.01	<.01	<.001	.01	<.001	<.00001	<.001	-
VF	<.001	.01	<.001	-	<.001	<.001	-	-

Note: VS: Very Slow, S: Slow, T: Typical, F: Fast, VF: Very Fast.; '-' indicates no significant difference.

The YG had a significantly ($p<.05$) decreased mean cadence as WS increased from slow to VF WS (slow: 97.71±5.34 $\frac{\text{steps}}{\text{min}}$; VF: 142.61±20.80 $\frac{\text{steps}}{\text{min}}$) compared to the OG (slow: 104.67±11.96 $\frac{\text{steps}}{\text{min}}$; VF: 155.71±14.02 $\frac{\text{steps}}{\text{min}}$), as shown in Table 2. No significant

difference in mean cadence was found between YA and OA for the VS WS (Table 2). The YG had a significantly ($p<.05$) increased mean stride length across all speeds (VS: 0.98±0.16 m; VF: 1.71±0.19 m) compared to the OG (VS: 0.81±0.17 m; VF: 1.55±0.20 m). Similarly, the YG had a significantly ($p<.05$) increased mean single leg support time across all speeds (VS: 39.66±14.27 percent of GC; VF: 40.80±1.64 percent of GC) compared to the OG (VS: 30.40±5.37 percent of GC; VF: 39.39±1.61 percent of GC), as shown in Table 2.

The YG had a significantly ($p<.05$) decreased mean double leg support time for the slow and fast speeds only (slow: 23.93±2.75 percent of GC; fast: 19.50±2.20 percent of GC) compared to the OG (slow: 29.97±4.80 percent of GC; fast: 28.22±18.26 percent of GC). Moreover, the YG had a significantly ($p<.05$) decreased mean time to toe off across all speeds (VS: 64.12±2.29 percent of GC; VF: 59.20±1.63 percent of GC) compared to the OG (VS: 69.37±5.53 percent of GC; VF: 60.27±1.62 percent of GC).

The YG had a significantly ($p<.05$) decreased mean cycle time for the fast and VF speeds (fast: 53.39±23.07 percent of GC; VF: 65.48±13.59 percent of GC) compared to the OG (fast: 56.70±8.65 percent of GC; VF: 66.31±0.37 percent of GC). However, the YG had a significantly ($p<.05$) increased mean cycle time for the slow WS (slow: 69.94±19.61 percent of GC) compared to the OG (slow: 69.17±8.72 percent of GC). Further, the YG had a significantly ($p<.05$) increased mean step length for the VS, slow, and fast speeds only (VS: 0.46±0.06 m; slow: 0.58±0.06 m; fast: 0.77±0.05 m) compared to the OG (VS: 0.39±0.08 m; slow: 0.53±0.05 m; fast: 0.70±0.06 m), as shown in Table 2. In contrary, the

YG exhibited a significantly ($p<.05$) decreased mean collected VS WS (VS: 0.52±0.16 $\frac{m}{s}$) compared to the OG (VS: 0.60±0.12 $\frac{m}{s}$), as shown in Table 2.

4.1.2 Summary of temporospatial results

When the speed effect is being considered, there are significant differences in temporospatial variables between YA and OA. The key findings of the present study are as follows:

- Stride length and single leg support time were significantly increased for the YG across all speeds compared to the OG.
- Time to toe off was significantly decreased for the YG across all speeds compared to the OG.
- Cadence was significantly faster for the YG as WS increased from slow to VF WS compared to the OG.
- Double leg support time was significantly less for the YG for the slow and fast WSs compared to the OG.
- Step length was significantly increased for the YG for the VS, slow, and fast WSs compared to the OG.
- Cycle time was significantly decreased for the YG for the slow, fast, and VF WSs compared to the OG.
- The YG walked significantly slower at the VS collected WS compared to the OG.

4.1.3 Age-related Differences in Relative Angles Between the Foot and Shank

The mean relative angle for the foot-shank segment in the sagittal plane is presented in Figure 1. This is the ankle dorsiflexion-plantarflexion (DF/PF) angle defined by the

relative orientation between the foot and the shank (tibia) segments, which will be hereon referred to as the foot-shank. The following section focuses on between-group differences. Table 3 presents the significant age-related differences in the mean maximum (max) and minimum (min) DF/PF angles in stance and swing phase as well as their respective time of occurrence as a percentage of GC.

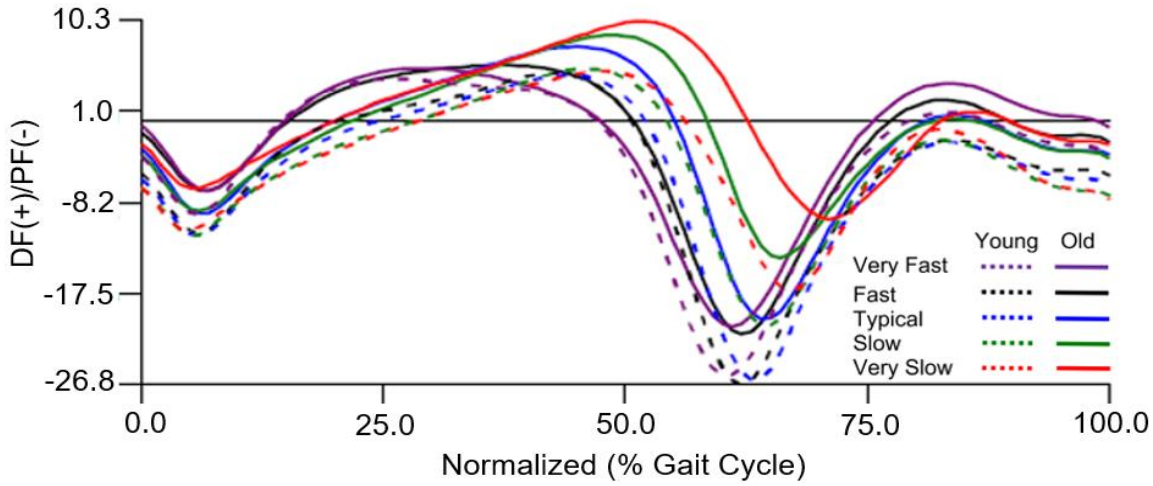


Figure 1. Mean dorsiflexion-plantarflexion for the foot-shank of the OG versus the YG at each walking speed.

Table 3. Significant p-values of the mean maximum DF/PF angles (∠) of the foot-shank during stance and swing phase, as well as their respective time of occurrence in the gait cycle across five walking speeds.

Walking speed group	Max PF ∠ in stance p-value	Time to max PF ∠ in stance p-value	Max PF ∠ in swing p-value	Time to max PF ∠ in swing p-value	Max DF ∠ in stance p-value	Time to max DF ∠ in stance p-value	Max DF ∠ in swing p-value	Time to max DF ∠ in swing p-value
VS	.01	<.01	<.01	<.001	<.0001	<.0001	.02	<.01
S	.03	-	.01	<.01	.02	<.0001	.03	-
T	<.01	<.01	.03	-	.02	-	<.01	-
F	-	.01	-	-	-	-	<.001	-
VF	-	<.01	-	-	-	-	<.01	-

Note: VS: Very Slow, S: Slow, T: Typical, F: Fast, VF: Very Fast.; '-' indicates no significant difference.

The mean max PF angle across WSs during stance, with error bars (95% confidence interval), is presented in Figure 2. Descriptively, the results showed that the mean max (peak) PF angle decreased with increasing WS for both groups, except for the VF WS in

the OG. In addition, the YG demonstrated lower mean max PF angles across speeds compared to the OG. The YG demonstrated more consistent patterns of variability for the max PF angles at each WS compared to the OG, as shown by the marginal error data in Figure 2.

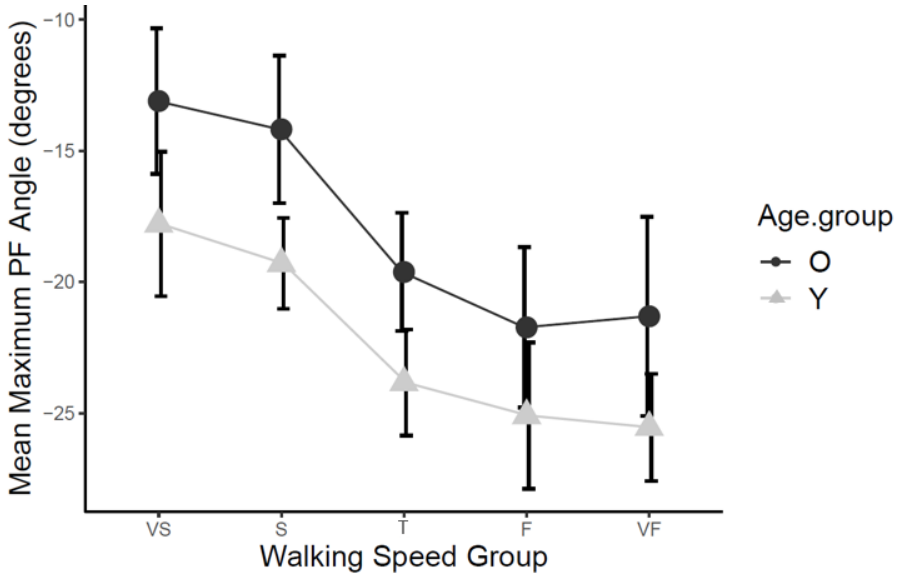


Figure 2. Mean max PF angle of the foot-shank during stance phase for the YG and OG across walking speeds at the 95% confidence interval (VS: Very Slow, S: Slow, T: Typical, F: Fast, VF: Very Fast).

The YG had a significantly ($p<.05$) increased mean max PF angle during stance (i.e., significantly higher peak PF) as WS increased from VS to typical speed (VS: -17.79°±7.39°; typical: -23.83° ±5.78°) compared to the OG (VS:-13.10°±7.95°; typical: -19.62°±6.66°), as shown in Table 3.

Significant differences in time to mean max PF ($p<.05$) during stance phase were found between YA and OA as WS increased (Figure 1, Table 3). The YG had a shorter time to mean max PF angle ($p<.05$) compared to the OG across all WSs, except for the slow WS. For the YG, max PF occurred at 48.45±26.23 percent GC at the VS WS, increasing to 59.15±1.51 percent GC at the VF WS. Whereas the OG showed max PF

angles at 51.15±30.69 percent GC at the VS WS, increasing to 60.39±1.83 percent GC at the VF WS. This result is consistent with the shorter time to toe off shown in Section 4.1.1 for the YG across all speeds.

The mean max PF angle across WSs during swing, with error bars (95% confidence interval), is presented in Figure 3. Descriptive results for the OG showed that the mean max PF angle during swing decreased with increasing WS except for the VF WS. The YG showed that the mean max PF angle decreased with increasing WS from VS to typical WS only, after which point, the mean max PF in swing phase began to increase. In addition, the YG demonstrated lower mean max PF angles across WSs compared to the OG. Both age groups displayed similar trends but at different magnitudes. However, the OG displayed a larger associated marginal error (Figure 3).

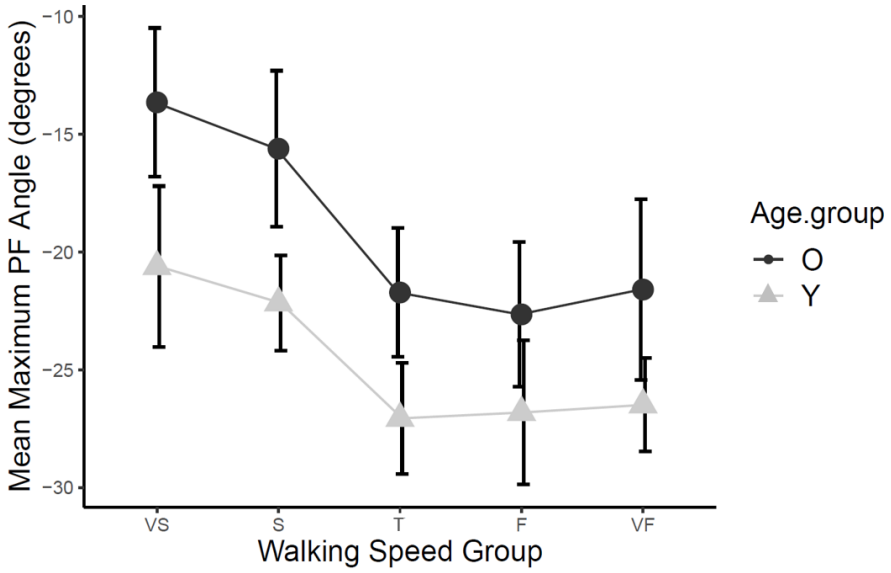


Figure 3. Mean max PF angle of the foot-shank during swing phase for the YG and OG across walking speeds at the 95% confidence interval (VS: Very Slow, S: Slow, T: Typical, F: Fast, VF: Very Fast).

Similar to the results of the stance phase, the YG had a significantly increased mean max PF angle ($p<.05$) during swing phase as WS increased from VS to typical WS (VS: -20.61°±9.14°; typical: -27.05°±6.74°) compared to the OG (VS: -13.64°± 9.05°; typical: -21.75° ±8.08°) as shown in Table 3.

Significant differences in time to mean max PF angle ($p<.05$) during swing phase were found between YA and OA as WS increased from the VS to slow speed. The YG had a significantly shorter time to mean max PF angle compared to the OG for the VS and slow speeds (Figure 1, Table 3). For the YG, the max PF occurred at 67.88±11.81 percent GC for the VS speed, decreasing to 64.83±3.46 at the slow speed. Whereas the OG demonstrated max PF angles at 73.36±8.18 percent GC for the VS speed, decreasing to 66.01±1.54 at the slow speed.

The mean max dorsiflexion (DF) angle across WSs during stance, with error bars (95% confidence interval), is presented in Figure 4. Descriptive results showed that the mean max DF angle decreased with increasing WS for the OG, whereas the angle was relatively consistent, with the smallest associated marginal error (Figure 4), across WSs for the YG. In addition, the YG demonstrated lower mean max DF angles across WSs compared to the OG. The YG had a significantly decreased mean max dorsiflexion (DF) angle ($p<.05$) during stance (i.e., significantly lower peak DF) as WS increased from VS to typical speed (VS: 6.15°±2.23°; typical: 5.65°±2.92°) compared to the OG (VS: 10.97°±3.88°; typical: 8.00°±4.06°) as shown in Table 3.

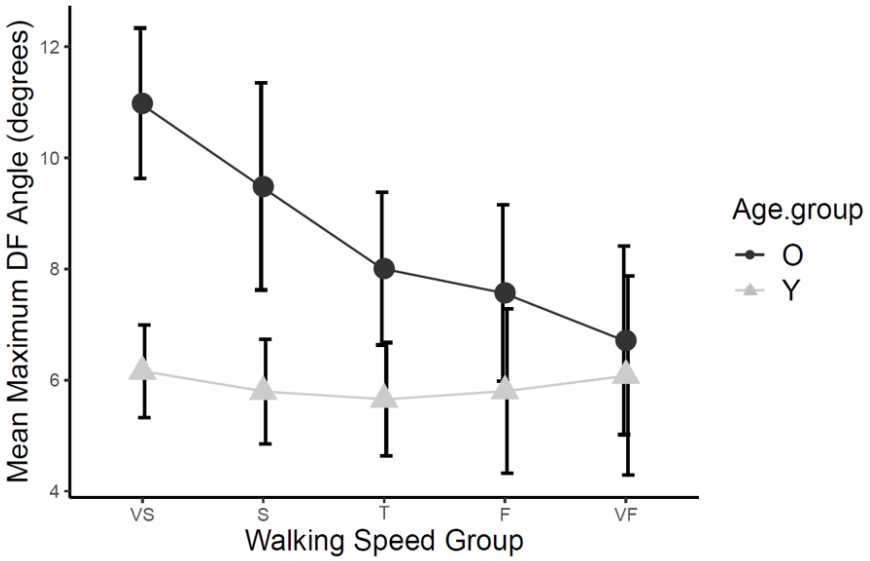


Figure 4. Mean max DF angle of the foot-shank during stance phase for the YG and OG across walking speeds at the 95% confidence interval (VS: Very Slow, S: Slow, T: Typical, F: Fast, VF: Very Fast).

Significant differences in time to mean max DF angle ($p<.05$) during stance phase were found between YA and OA as WS increased from the VS to slow speed (Figure 1, Table 3). The YG had a significantly shorter time to mean max DF ($p<.05$) compared to the OG for the VS and slow speeds. For the YG, the max PF occurred at 47.29±7.45 percent GC at the VS speed, decreasing to 44.66±4.29 at the slow speed. The OG demonstrated mean max PF angles at 52.10±3.64 percent GC at the VS speed, decreasing to 49.12±3.42 at the slow speed. This result is consistent with the decreased time to toe off exhibited in Section 4.1.1 for the YG across all speeds.

The mean max DF angle across WSs during swing, with error bars (95% confidence interval), is presented in Figure 5. Descriptive results for the YG showed that the mean max DF angle during swing decreased with increasing speed except for the fast and VF speeds. The OG showed that the mean max DF angle decreased from VS to slow speed

only, after which point, the mean max DF in swing phase began to increase. In addition, the OG demonstrated greater mean max DF angles across speeds compared to the OG. Overall, the older and YG displayed similar trends with relatively small marginal error (Figure 5). The YG had a significantly decreased mean max DF angle ($p<.05$) during swing as WS increased (VS: 0.04°±2.54°; VF: 1.45°±2.98°) compared to the OG (VS: 2.40°±2.89°; VF: 4.69°±3.56°) as shown in Table 3. Significant differences in time to mean max DF angle ($p<.05$) during swing phase were found between YA and OA for the VS speed only (Figure 1, Table 3). The YG had a significantly shorter time to mean min ADD angle ($p<.05$) for the slow speed. For the YG, the max PF occurred at 83.13±5.76 percent GC at the VS speed, whereas the OG demonstrated a max PF angle at 85.88±4.79 percent GC at the VS speed.

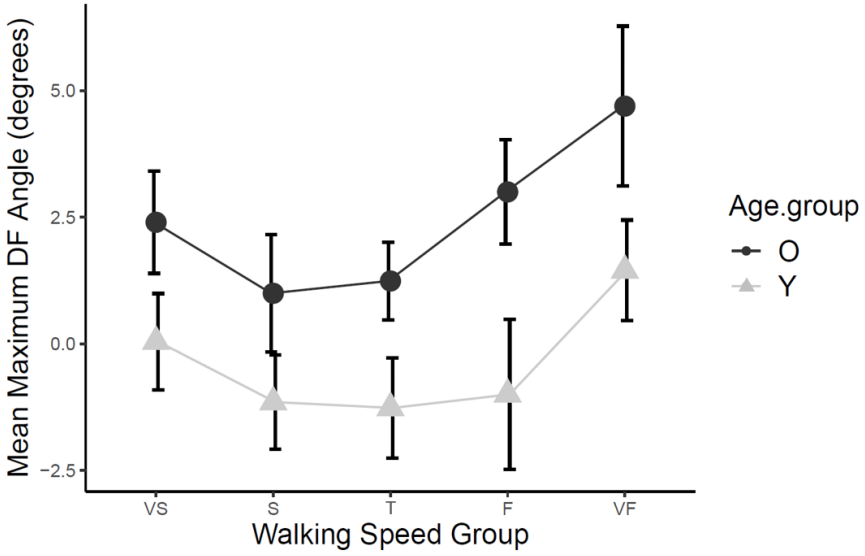


Figure 5. Mean max DF angle of the foot-shank during swing phase for the YG and OG across walking speeds at the 95% confidence interval (VS: Very Slow, S: Slow, T: Typical, F: Fast, VF: Very Fast).

Table 4 presents the significant ($p<.05$) age-related differences in the DF/PF range of motion (ROM) data for the foot-shank. In addition, relative DF/PF ROM data for the foot-shank are provided in Table 4. There were no significant ($p<.05$) age-related differences in the DF/PF ROM for the foot-shank during stance or swing (Table 4). Overall, the OG exhibited less DF/PF ROM for the foot shank during stance and swing compared to the YG, except for the VS speed in stance.

Table 4. DF/PF ROM data for the foot-shank during stance and swing phase across five walking speeds and their respective significant p-values.

DF/PF ROM Foot-Shank			
	Mean	± Std	P-value
Very Slow Young Stance	23 .94°	5.15°	-
Very Slow Old Stance	24.07°	4.07°	
Slow Young Stance	25.08°	2.41°	-
Slow Old Stance	23.66°	2.24°	
Typical Young Stance	29.49°	2.85°	-
Typical Old Stance	27.62°	2.60°	
Fast Young Stance	30.89°	2.87°	-
Fast Old Stance	29.29°	3.93°	
Very Fast Young Stance	31.62°	0.73°	-
Very Fast Old Stance	28.02°	4.72°	
Very Slow Young Swing	20.65°	6.60°	-
Very Slow Old Swing	16.04°	6.15°	
Slow Young Swing	21.00°	3.33°	-
Slow Old Swing	16.60°	5.08°	
Typical Young Swing	25.79°	3.90°	-
Typical Old Swing	22.95°	5.81°	
Fast Young Swing	25.80°	3.46°	-
Fast Old Swing	25.64°	5.45°	
Very Fast Young Swing	27.93°	2.94°	-
Very Fast Old Swing	26.28°	5.07°	

Note: Std: Standard deviation; '-' indicates no significant difference.

The mean relative angle gait curve for the foot-shank segment in the transverse plane is presented in Figure 6. This is the ankle adduction-abduction (ADD/ABD) angle defined by the relative orientation between the foot and the shank (tibia) segments, which

will be hereon referred to as the foot-shank. The following section focuses on between-group differences. Table 5 presents the significant age-related differences in the mean max and min ADD/ABD angles in stance and swing phase as well as their respective time of occurrence as a percentage of GC.

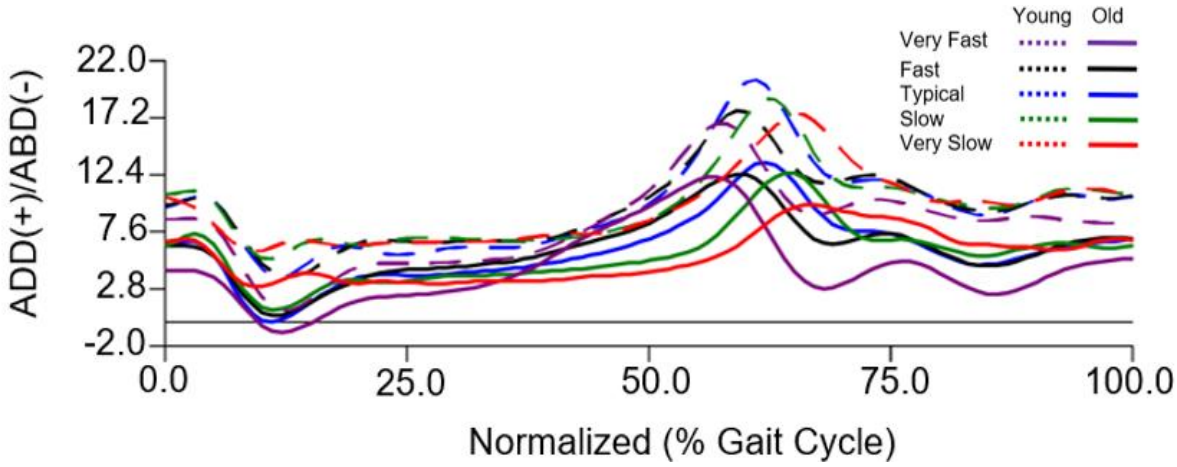


Figure 6. Mean adduction-abduction for the foot-shank of the OG versus the YG at each walking speed.

Table 5. Significant p-values of the mean min and max ADD/ABD angles (∠) of the foot-shank during stance and swing phase, as well as their respective time of occurrence in the gait cycle across five walking speeds.

Walking speed group	Min ADD ∠ in stance p-value	Time to min ADD ∠ in stance p-value	Min ADD ∠ in swing p-value	Time to min ADD ∠ in swing p-value	Max ADD ∠ in stance p-value	Time to max ADD ∠ in stance p-value	Max ADD ∠ in swing p-value	Time to max ADD ∠ in swing p-value
VS	.01	-	<.01	-	<.001	.01	<.001	<.01
S	<.01	-	<.01	-	<.00001	<.01	<.00001	<.01
T	.01	.01	<.00001	-	<.00001	<.001	<.0001	<.01
F	-	.01	<.001	-	<.01	-	<.01	-
VF	-	-	<.01	-	<.01	-	<.001	<.01

Note: VS: Very Slow, S: Slow, T: Typical, F: Fast, VF: Very Fast.; '-' indicates no significant difference.

The mean min ADD angle across WSs during stance, with error bars (95% confidence interval), is presented in Figure 7. Descriptive results for the OG showed that the mean min ADD angle during stance decreased from VS to typical speed only, after which point, the mean min ADD angle increased for the fast speed, and then decreased

again for the VF speed. The YG showed that the mean min ADD angle increased from VS to slow speed, after which point, the mean min ADD angle in stance phase began to decrease. In addition, the YG demonstrated greater mean min ADD angles across speeds compared to the OG. Both age groups demonstrated relatively consistent patterns of variability for the min ADD angles at each speed (Figure 7).

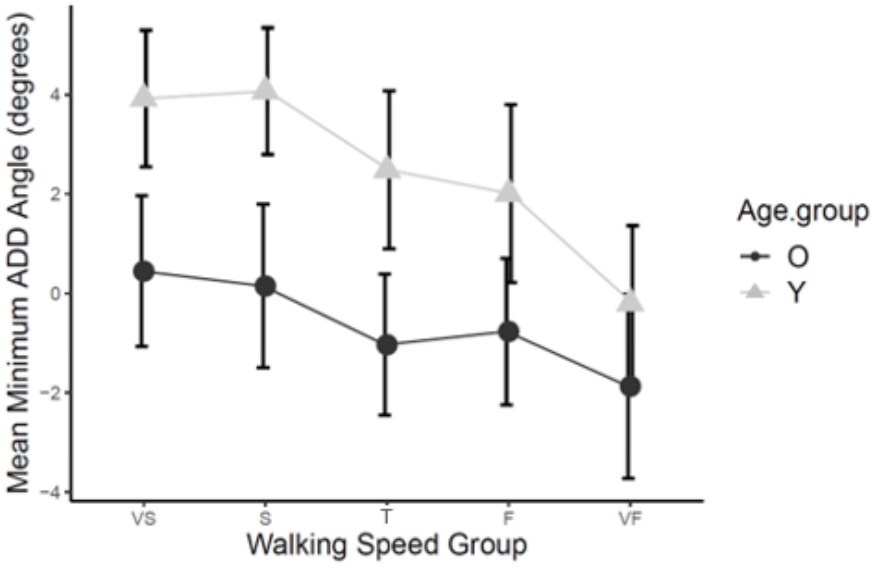


Figure 7. Mean min ADD angle of the foot-shank during stance phase for the YG and OG across walking speeds at the 95% confidence interval (VS: Very Slow, S: Slow, T: Typical, F: Fast, VF: Very Fast).

The YG had a significantly ($p<.05$) increased mean min ADD angle during stance (i.e., significantly higher peak ADD) as WS increased from VS to typical speed (VS: 3.92°±3.67°; typical: 2.48°±4.55°) compared to the OG (VS: 0.44°±4.35°; typical: -1.03°±4.20°), as shown in Table 5.

Significant differences in time to mean min ADD angle ($p<.05$) during stance phase were found between YA and OA for the typical and fast WSs (Figure 6, Table 5). The YG had a significantly longer time to mean min ADD angle ($p<.05$) compared to the OG for

the typical and fast speed. For the YG, the min ADD angle occurred at 17.70±10.59 percent GC at the typical speed, increasing to 18.72±10.36 percent GC at the fast speed. Whereas the OG demonstrated min ADD angles at 14.65±11.56 percent GC at the typical speed, increasing to 15.83±12.02 percent GC at the fast speed.

The mean min ADD angle across WSs during swing, with error bars (95% confidence interval), is presented in Figure 8. Descriptive results showed that the mean min ADD angle decreased with increasing WS for the OG, whereas the mean min ADD angle increased from VS to slow WS for the YG, after which point, the mean min ADD angle in swing phase began to decrease. In addition, the YG showed greater mean min ADD angles across speeds compared to the OG. Overall, both age groups demonstrated relatively consistent patterns of variability for the min ADD angles at each WS. However, the OG displayed a larger associated marginal error (Figure 8).

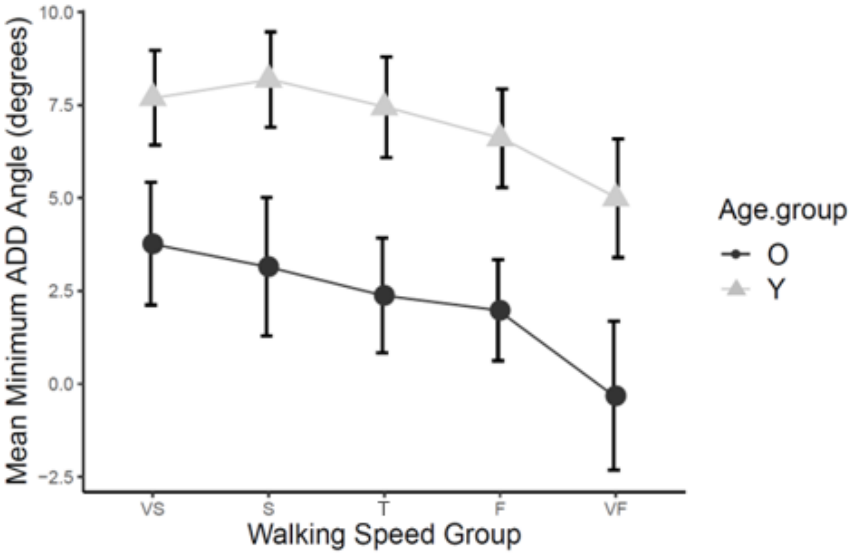


Figure 8. Mean min ADD angle of the foot-shank during swing phase for the YG and OG across walking speeds at the 95% confidence interval (VS: Very Slow, S: Slow, T: Typical, F: Fast, VF: Very Fast).

The YG had a significantly ($p<.05$) increased mean min ADD angle during swing (i.e., significantly higher peak PF) as WS increased across all speeds (VS: 7.69°±3.40°; VF: 4.99°±4.78°) compared to the OG (VS: 3.76°±4.72°; VF: -0.32°±4.51°), as shown in Table 5. Further, no significant differences in the time to mean min ADD angle during swing phase were found between YA and OA across all speeds (Table 5).

The mean max ADD angle across WSs during stance, with error bars (95% confidence interval), is presented in Figure 9. Descriptive results showed that the mean max (peak) ADD angle increased with increasing WS from VS to typical WS for both groups, after which point, the mean max ADD angle in stance phase began to decrease. Further, the YG demonstrated greater mean max ADD angles across WSs compared to the OG. Both age groups displayed similar trends but at different magnitudes. Overall, both age groups demonstrated relatively consistent patterns of variability for the max ADD angles at each WS. However, the OG displayed a larger associated marginal error.

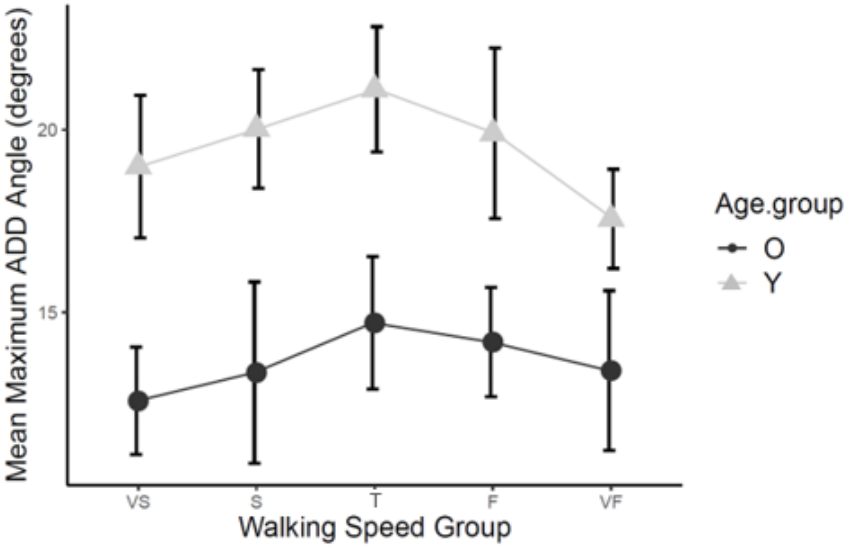


Figure 9. Mean max ADD angle of the foot-shank during stance phase for the YG and OG across walking speeds at the 95% confidence interval (VS: Very Slow, S: Slow, T: Typical, F: Fast, VF: Very Fast).

The YG had a significantly ($p<.05$) increased mean max ADD angle during stance (i.e., significantly higher peak ADD) as WS increased across all speeds (VS: 18.99°±5.22°; VF: 17.55°±4.07°) compared to the OG (VS: 12.56°±4.21°; VF: 13.40°±4.94°), as shown in Table 5.

Significant differences in time to mean max ADD angle ($p<.05$) during stance phase were found between YA and OA as WS increased from VS to typical WS. The YG had a significantly longer time to mean max ADD angle compared to the OG for the VS WS (Figure 6, Table 5). However, the YG had a significantly shorter time to mean max ADD angle compared to the OG for the slow and typical WSs (Figure 6, Table 5). For the YG, the max ADD occurred at 59.31±13.47 percent GC for the VS WS, decreasing to 55.18±14.59 at the typical WS. Whereas the OG showed max PF angles at 55.00±27.97 percent GC for the VS WS, increasing to 59.97±11.13 at the typical WS.

The mean max ADD angle across WSs during swing, with error bars (95% confidence interval), is presented in Figure 10. Descriptive results showed that the mean max (peak) ADD angle increased with increasing speed from VS to typical speed for both groups, after which point, the mean max ADD angle in swing phase began to decrease. In addition, the YG demonstrated greater mean max ADD angles across speeds compared to the OG. Both age groups displayed similar trends but at different magnitudes. Overall, both age groups demonstrated relatively consistent patterns of variability for the max ADD angles at each speed. However, the YG displayed a shorter associated marginal error (Figure 10). Similar to the results of the stance phase, the YG had a significantly ($p<.05$) increased mean max ADD angle during swing (i.e., significantly higher peak ADD) as WS

increased across all speeds (VS: 19.23°±5.04°; VF: 16.90°±4.51°) compared to the OG (VS: 12.43°±4.43°; VF: 10.80°±5.65°), as shown in Table 5.

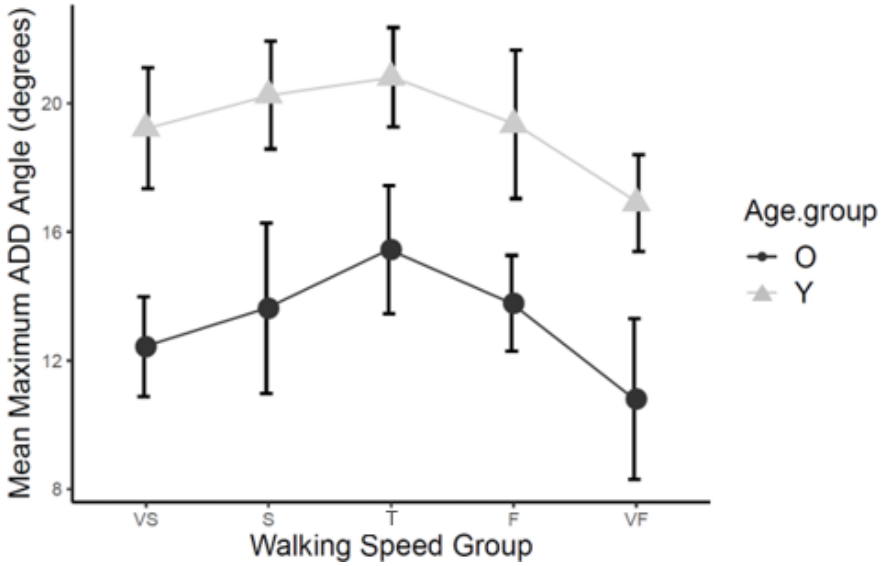


Figure 10. Mean max ADD angle of the foot-shank during swing phase for the YG and OG across walking speeds at the 95% confidence interval (VS: Very Slow, S: Slow, T: Typical, F: Fast, VF: Very Fast).

Significant differences in time to mean max ADD ($p<.05$) during swing phase were found between YA and OA as WS increased (Figure 6, Table 5). The YG had a significantly shorter time to mean max PF angle ($p<.05$) compared to the OG across all speeds, except for the fast speed. For the YG, the max ADD occurred at 67.73±8.13 percent GC at the VS speed, decreasing to 64.81±10.38 percent GC at the VF speed. Whereas the OG demonstrated max ADD angles at 73.76±8.95 percent GC at the VS speed, decreasing to 68.56±13.56 percent GC at the VF speed.

Table 6 presents the significant ($p<.05$) age-related differences in the ADD/ABD range of motion (ROM) data for the foot-shank. In addition, relative ADD/ABD ROM data for the foot-shank are provided in Table 6. The YG displayed the greatest ADD/ABD ROM (Figure 6) across all speeds during stance and swing compared to the OG. Table 6 presents

the between-group differences found for the ADD/ABD ROM during stance and swing phase. The YG exhibited a significantly ($p<.05$) greater ADD/ABD ROM during stance as WS increased from VS to fast speed (VS: 15.07°±1.55°; fast: 17.89°±1.18°) compared to the OG (VS: 12.12°±0.13°; fast: 14.95°±0.05°) as shown in Table 6. During swing phase, the YG exhibited a significantly ($p<.05$) greater ADD/ABD ROM for the VS speed only (VS: 11.53°±1.64°) compared to the OG (VS: 8.66°±0.28°) as shown in Table 6. During typical speed walking, the ADD/ABD ROM for the YA and OA increased most in the foot-shank during stance and swing.

Table 6. Significant ADD/ABD ROM data for the foot-shank during stance and swing phase across five walking speeds and their respective significant p-values.

ADD/ABD ROM Foot-Shank			
	Mean	± Std	P-value
Very Slow Young Stance	15.07°	1.55°	<.01
Very Slow Old Stance	12.12°	0.13°	
Slow Young Stance	15.95°	1.06°	<.05
Slow Old Stance	13.19°	1.99°	
Typical Young Stance	18.62°	0.36°	<.05
Typical Old Stance	15.74°	1.17°	
Fast Young Stance	17.89°	1.18°	<.05
Fast Old Stance	14.95°	0.05°	
Very Fast Young Stance	17.75°	0.59°	-
Very Fast Old Stance	15.27°	0.74°	
Very Slow Young Swing	11.53°	1.64°	<.01
Very Slow Old Swing	8.66°	0.28°	
Slow Young Swing	12.07°	1.20°	-
Slow Old Swing	10.47°	1.88°	
Typical Young Swing	13.37°	0.57°	-
Typical Old Swing	13.07°	1.33°	
Fast Young Swing	12.74°	2.15°	-
Fast Old Swing	11.80°	0.36°	
Very Fast Young Swing	11.91°	0.26°	-
Very Fast Old Swing	11.12°	1.13°	

Note: Std: Standard deviation.; '-' indicates no significant difference.

4.1.4 Age-related Differences in Relative Angles Between the Midfoot and Calcaneus

The mean relative angle gait curve for the midfoot-calcaneus (mid-cal) segment in the sagittal plane is presented in Figure 11. This is the mid-cal dorsiflexion-plantarflexion (DF/PF) angle defined by the relative orientation between the midfoot and the calcaneus segments. The following section focuses on between-group differences. Table 7 presents the significant age-related differences in the mean max and min DF/PF angles in stance and swing phase as well as their respective time of occurrence as a percentage of GC.

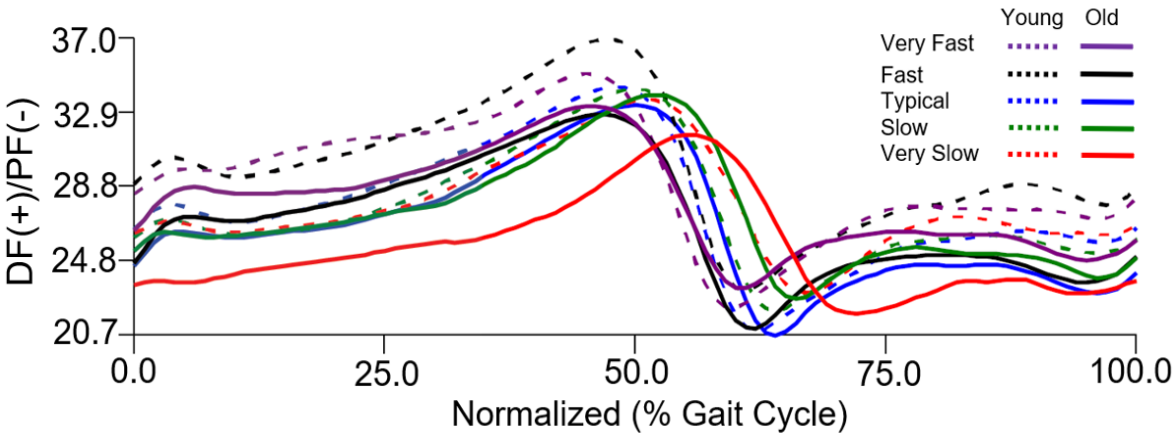


Figure 11. Mean dorsiflexion-plantarflexion for the mid-cal of the OG versus the YG at each walking speed.

Table 7. Significant p-values of the mean min and max DF/PF angles (∠) of the mid-cal during stance and swing phase, as well as their respective time of occurrence in the gait cycle across five walking speeds.

Walking speed group	Min DF ∠ in stance p-value	Time to min DF ∠ in stance p-value	Min DF ∠ in swing p-value	Time to min DF ∠ in swing p-value	Max DF ∠ in stance p-value	Time to max DF ∠ in stance p-value	Max DF ∠ in swing p-value	Time to max DF ∠ in swing p-value
VS	-	.03	-	<.001	-	<.001	.01	-
S	-	-	-	<.01	-	<.01	-	-
T	-	-	-	<.0001	-	-	-	.03
F	-	.01	-	.02	-	-	-	.03
VF	-	-	-	<.01	-	-	-	-

Note: VS: Very Slow, S: Slow, T: Typical, F: Fast, VF: Very Fast.; '-' indicates no significant difference.

The mean max DF angle across WSs during swing, with error bars (95% confidence interval), is presented in Figure 12. Descriptive results showed that the mean max (peak) DF angle increased with increasing speed for the OG. Whereas, for the YG the mean max DF angle decreased from VS to typical speed, after which point, the angle increased for the fast speed, and then decreased for the VF speed. In addition, the OG demonstrated lower mean max DF angles across speeds compared to the YG. Overall, both age groups demonstrated relatively consistent patterns of variability for the max DF angles at each speed with similar associated marginal error magnitude (Figure 12).

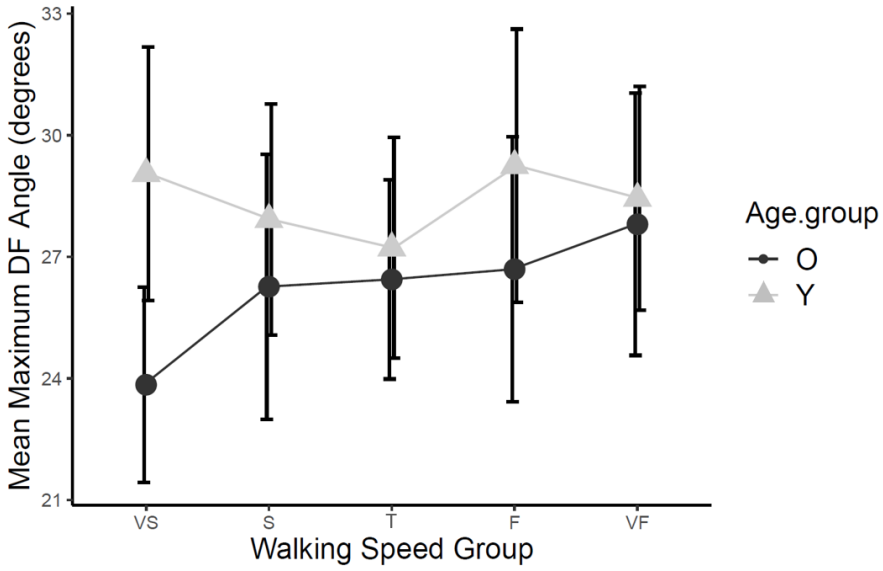


Figure 12. Mean max DF angle of the mid-cal during swing phase for the YG and OG across walking speeds at the 95% confidence interval (VS: Very Slow, S: Slow, T: Typical, F: Fast, VF: Very Fast).

The YG had a significantly ($p<.05$) increased mean max DF angle during swing (i.e., significantly higher peak DF) for the VS speed (VS: 29.05°±8.37°) compared to the OG (VS: 23.84°±6.91°). In addition, significant differences in time to mean max DF ($p<.05$) during swing phase were found between YA and OA as WS increased from typical

to fast speed (Figure 11, Table 7). The YG had a significantly longer time to mean max DF angle ($p<.05$) compared to the OG for the typical and fast speed. For the YG, the max PF occurred at 90.60±6.05 percent GC at the typical speed, increasing to 91.41±6.73 percent GC at the fast speed. Whereas the OG demonstrated max PF angles at 86.31±9.38 percent GC at the typical speed, decreasing to 84.51±11.14 percent GC at the fast speed.

Significant differences in time to mean max DF ($p<.05$) during stance phase were found between YA and OA as WS increased from VS to slow speed (Figure 11, Table 7). The YG had a significantly shorter time to mean max DF angle ($p<.05$) compared to the OG for the VS and slow speed. For the YG, the max DF occurred at 50.67±7.11 percent GC at the VS speed, decreasing to 50.36±4.77 percent GC at the slow speed. Whereas the OG demonstrated max DF angles at 55.63±3.57 percent GC at the VS speed, decreasing to 52.30±2.87 percent GC at the slow speed.

Significant differences in time to mean min DF ($p<.05$) during stance phase were found between YA and OA for the VS and fast WSs (Figure 11, Table 7). The YG had a significantly shorter time to mean min DF angle compared to the OG for the VS speed (Figure 11, Table 7). However, the YG had a significantly longer time to mean min DF angle compared to the OG for the fast speed (Figure 11, Table 7). For the YG, the min DF occurred at 42.78±25.42 percent GC at the VS speed, increasing to 58.55±5.77 percent GC at the fast speed. Whereas the OG demonstrated min DF angles at 47.12±31.09 percent GC at the VS speed, increasing to 55.21±16.91 percent GC at the fast speed.

Significant differences in time to mean min DF ($p<.05$) during swing phase were found between YA and OA as WS increased (Figure 11, Table 7). The YG had a significantly shorter time to mean min DF angle ($p<.05$) compared to the OG across all

speeds. For the YG, the min DF occurred at 67.92±11.50 percent GC at the VS speed, decreasing to 61.27±6.57 percent GC at the VF speed. Whereas the OG demonstrated min DF angles at 77.36±10.28 percent GC at the VS speed, decreasing to 72.71±16.15 percent GC at the VF speed.

Table 8 presents the significant ($p<.05$) age-related differences in the DF/PF range of motion (ROM) data for the mid-cal. In addition, relative DF/PF ROM data for the mid-cal are provided in Table 8. The YG displayed the greatest DF/PF ROM (Figure 11) across all speeds during stance and swing compared to the OG, except for the VS speed during stance. Table 8 presents the between-group differences found for the DF/PF ROM during stance and swing phase.

Table 8. Significant DF/PF ROM data for the mid-cal during stance and swing phase across five walking speeds and their respective significant p-values.

DF/PF ROM Midfoot-Calcaneus			
	Mean	± Std	P-value
Very Slow Young Stance	12.26°	0.41°	-
Very Slow Old Stance	12.63°	0.90°	
Slow Young Stance	12.34°	2.01°	-
Slow Old Stance	11.98°	1.63°	
Typical Young Stance	13.88°	1.02°	-
Typical Old Stance	13.34°	1.51°	
Fast Young Stance	14.03°	0.83°	-
Fast Old Stance	13.26°	1.69°	
Very Fast Young Stance	14.49°	1.12°	<.01
Very Fast Old Stance	11.07°	0.81°	
Very Slow Young Swing	6.86°	0.16°	-
Very Slow Old Swing	5.34°	0.35°	
Slow Young Swing	6.02°	0.93°	-
Slow Old Swing	4.97°	0.21°	
Typical Young Swing	7.38°	0.03°	<.05
Typical Old Swing	5.96°	0.66°	
Fast Young Swing	7.16°	0.74°	-
Fast Old Swing	6.60°	0.38°	
Very Fast Young Swing	8.73°	0.26°	<.05
Very Fast Old Swing	5.97°	0.47°	

Note: Std: Standard deviation.; '-' indicates no significant difference.

The YG exhibited a significantly ($p<.05$) greater DF/PF ROM during stance for the VF speed only (VF: 14.49°±1.12°) compared to the OG (VF: 11.07°±0.81°) as shown in Table 8. During swing phase, the YG exhibited a significantly ($p<.05$) greater DF/PF ROM for the typical and VF speed only (typical: 7.38°±0.03°; VF: 8.73°±0.26°) compared to the OG (typical: 5.96°±0.66°; VF: 5.97°±0.47°) as shown in Table 8.

The mean relative angle gait curve for the mid-cal segment in the frontal plane is presented in Figure 13. This is the mid-cal eversion-inversion (EVE/INV) angle defined by the relative orientation between the midfoot and the calcaneus segments. The following section focuses on between-group differences. Table 9 presents the significant age-related differences in the mean max and min EVE/INV angles in stance and swing phase as well as their respective time of occurrence as a percentage of GC.

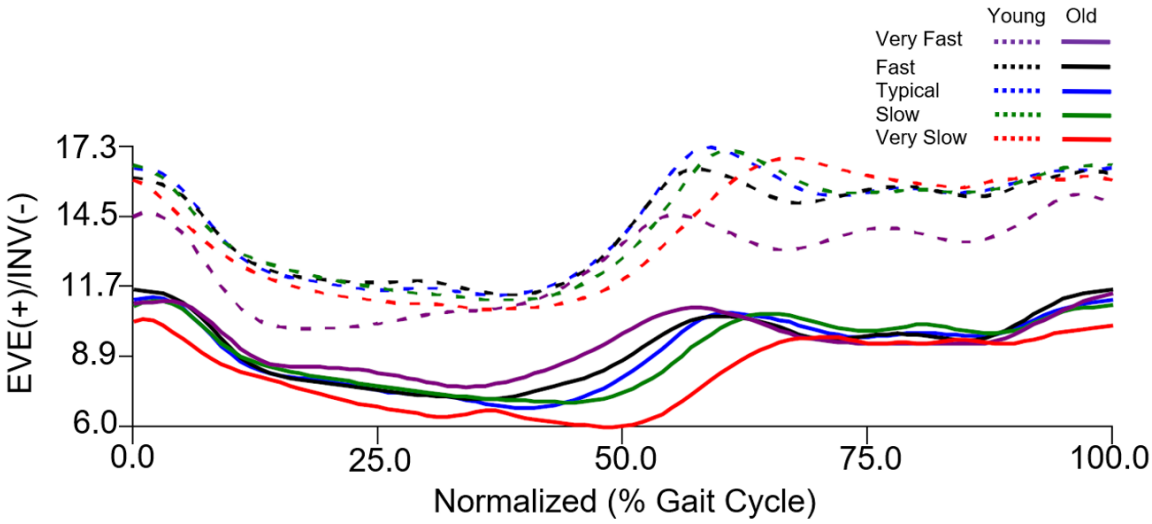


Figure 13. Mean eversion-inversion for the mid-cal of the OG versus the YG at each walking speed.

Table 9. Significant p-values of the mean min and max EVE/INV angles (∠) of the mid-cal during stance and swing phase, as well as their respective time of occurrence in the gait cycle across five walking speeds.

Walking speed group	Min EVE ∠ in stance p-value	Time to min EVE ∠ in stance p-value	Min EVE ∠ in swing p-value	Time to min EVE ∠ in swing p-value	Max EVE ∠ in stance p-value	Time to max EVE ∠ in stance p-value	Max EVE ∠ in swing p-value	Time to max EVE ∠ in swing p-value
VS	<.01	<.01	<.0001	-	<.001	-	<.001	.01
S	<.001	.02	<.0001	-	<.00001	-	<.0001	<.01
T	<.01	<.01	<.0001	-	<.0001	-	<.0001	<.01
F	<.01	-	<.01	-	.01	-	<.01	.02
VF	-	-	.01	-	<.001	-	<.01	-

Note: VS: Very Slow, S: Slow, T: Typical, F: Fast, VF: Very Fast.; '-' indicates no significant difference.

The mean min EVE angle across WSs during stance, with error bars (95% confidence interval), is presented in Figure 14. Descriptive results showed that the mean min EVE angle increased with increasing speed from VS to slow speed for the YG, after which point, the mean min EVE angle in stance phase began to decrease. The mean min EVE angle increased from VS to typical speed, after which point, the angle decreased for the fast speed, and then increased for the VF speed. In addition, the YG demonstrated greater mean min EVE angles across speeds compared to the OG. Overall, both age groups demonstrated relatively consistent patterns of variability for the min EVE angles at each speed, as shown by the marginal error data in Figure 14. The YG had a significantly ($p<.05$) increased mean min EVE angle during stance as WS increased from VS to fast WS (VS: 9.80°±3.75°; fast: 10.54°±3.95°) compared to the OG (VS: 5.67°±4.18°; fast:6.14°±4.73°), as shown in Table 9.

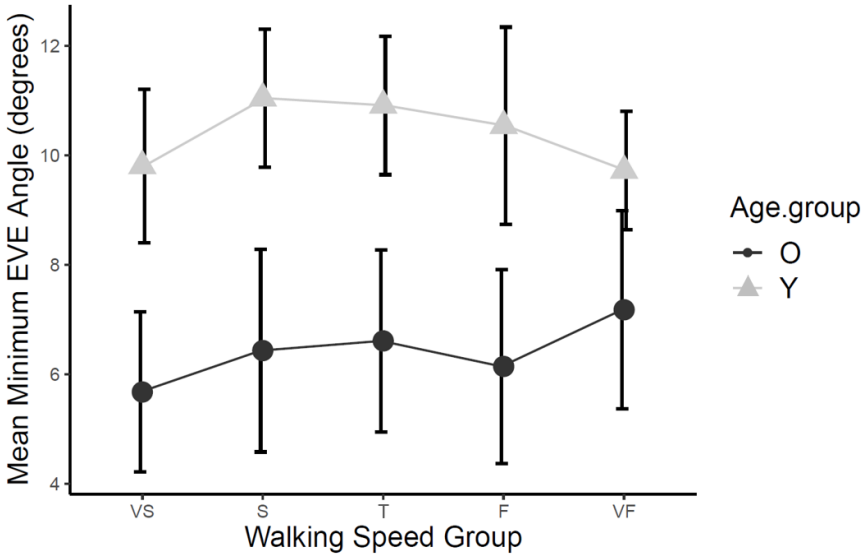


Figure 14. Mean min EVE angle of the mid-cal during stance phase for the YG and OG across walking speeds at the 95% confidence interval (VS: Very Slow, S: Slow, T: Typical, F: Fast, VF: Very Fast).

Significant differences in time to mean min EVE ($p<.05$) during stance phase were found between YA and OA as WS increased from VS to typical WS (Figure 13, Table 9). The YG had a significantly shorter time to mean min EVE angle compared to the OG for the VS, slow, and typical WS. For the YG, the min EVE occurred at 34.37±10.89 percent GC at the VS WS, decreasing to 31.82±9.31 percent GC at the typical WS. Whereas the OG showed min EVE angles at 42.63±9.07 percent GC at the VS WS, increasing to 38.87±8.96 percent GC at the typical WS.

The mean min EVE angle across WSs during swing, with error bars (95% confidence interval), is presented in Figure 15. Descriptive results showed that the mean min EVE angle increased with increasing WS from VS to slow WS for the YG, after which point, the mean min EVE angle in stance phase began to decrease, whereas the angle trend was relatively neutral for the OG across speeds. Overall, both age groups demonstrated relatively consistent patterns of variability for the mean min EVE angle. However, the OG

displayed the smallest associated marginal error (Figure 15). In addition, the YG demonstrated greater mean min EVE angles across WSs compared to the OG (Figure 15).

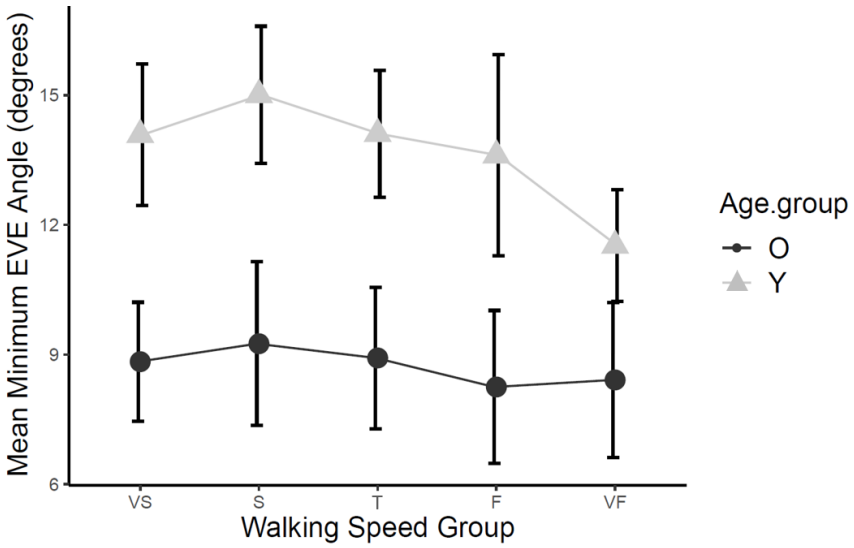


Figure 15. Mean min EVE angle of the mid-cal during swing phase for the YG and OG across walking speeds at the 95% confidence interval (VS: Very Slow, S: Slow, T: Typical, F: Fast, VF: Very Fast).

The YG had a significantly ($p<.05$) increased mean min EVE angle during swing as WS increased (VS: 14.08°±4.38°; VF: 11.52°±3.87°) compared to the OG (VS: 8.83°±3.94°; VF:8.41°±4.04°).

The mean max EVE angle across WSs during stance, with error bars (95% confidence interval), is presented in Figure 16. Descriptive results showed that the mean max EVE angle (peak) increased with increasing WS from VS to slow WS for the YG, after which point, the mean max EVE angle in stance phase began to decrease. The mean max EVE angle for the OG increased from VS to typical speed, after which point, the angle decreased for the fast WS, and then increased for the VF speed. Overall, both age groups showed relatively consistent patterns of variability for the mean max EVE angle at each

speed. Further, the YG showed greater mean max EVE angles across WSs compared to the OG (Figure 16).

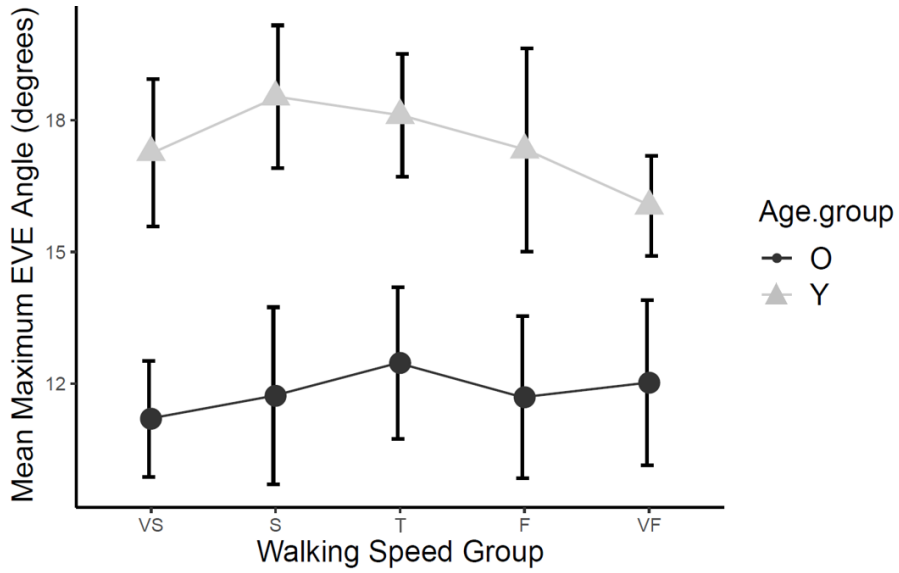


Figure 16. Mean max EVE angle of the mid-cal during stance phase for the YG and OG across walking speeds at the 95% confidence interval (VS: Very Slow, S: Slow, T: Typical, F: Fast, VF: Very Fast).

The YG had a significantly ($p<.05$) increased mean max EVE angle during stance (i.e., significantly higher peak EVE) as WS increased (VS: 17.26°±4.49°; VF: 16.04°±3.41°) compared to the OG (VS: 11.20°±3.79°; VF: 12.02°±4.24°).

The mean max EVE angle across WSs during swing, with error bars (95% confidence interval), is presented in Figure 17. Descriptive results showed that the mean max EVE angle (peak) increased with increasing speed from VS to slow speed for the YG, after which point, the mean max EVE angle in swing phase began to decrease. The mean max EVE angle for the OG increased from VS to typical speed, after which point, the angle decreased for the fast speed, and then increased for the VF speed. Overall, both age groups demonstrated relatively consistent patterns of variability for the mean max EVE angle

during swing, as shown by the marginal error data (Figure 17). In addition, the YG demonstrated greater mean max EVE angles across speeds compared to the OG.

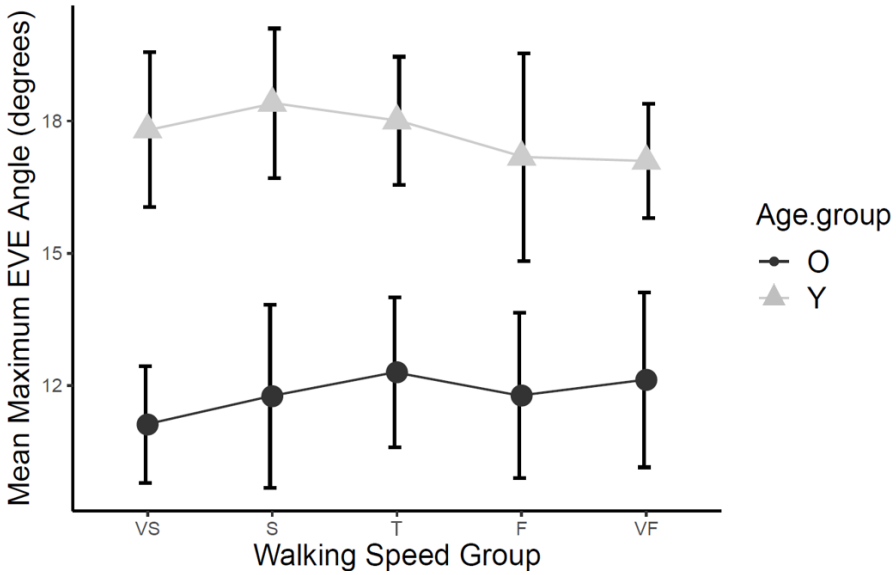


Figure 17. Mean max EVE angle of the mid-cal during swing phase for the YG and OG across walking speeds at the 95% confidence interval (VS: Very Slow, S: Slow, T: Typical, F: Fast, VF: Very Fast).

Similar to the results of the stance phase, the YG had a significantly ($p<.05$) increased mean max EVE angle during swing (i.e., significantly higher peak EVE) as WS increased (VS: 17.80°±4.69°; VF: 17.09°±3.88°) compared to the OG (VS: 11.11°±3.78°; VF: 12.12°±4.47°), as shown in Table 9.

Significant differences in time to mean max EVE ($p<.05$) during swing phase were found between YA and OA as WS increased (Figure 13, Table 9). The YG had a significantly shorter time to mean max EVE angle ($p<.05$) compared to the OG across all WSs, except for the VF speed. For the YG, the max EVE occurred at 78.45±12.35 percent GC at the VS speed, decreasing to 77.97±16.76 percent GC at the fast speed. Whereas the

OG demonstrated max EVE angles at 86.43±11.98 percent GC at the VS speed, increasing to 87.91±13.87 percent GC at the fast WS.

Table 10 presents the significant (p<.05) age-related differences in the EVE/INV range of motion (ROM) data for the mid-cal. In addition, relative EVE/INV ROM data for the mid-cal are provided in Table 10. The YG displayed the greatest EVE/INV ROM (Figure 13) across all speeds during stance and swing compared to the OG. Table 10 presents the between-group differences found for the EVE/INV ROM during stance and swing phase.

Table 10. Significant EVE/INV ROM data for the mid-cal during stance and swing phase across five walking speeds and their respective significant p-values.

EVE/INV ROM Midfoot-Calcaneus			
	Mean	± Std	P-value
Very Slow Young Stance	7.45°	0.73°	<.001
Very Slow Old Stance	5.52°	0.39°	
Slow Young Stance	7.48°	1.12°	<.001
Slow Old Stance	5.28°	0.39°	
Typical Young Stance	7.19°	0.38°	<.01
Typical Old Stance	5.85°	0.19°	
Fast Young Stance	6.77°	1.12°	<.05
Fast Old Stance	5.54°	0.21°	
Very Fast Young Stance	6.32°	0.16°	<.01
Very Fast Old Stance	4.84°	0.16°	
Very Slow Young Swing	3.71°	0.30°	<.001
Very Slow Old Swing	2.27°	0.15°	
Slow Young Swing	3.39°	0.32°	<.05
Slow Old Swing	2.50°	0.44°	
Typical Young Swing	3.90°	0.03°	-
Typical Old Swing	3.37°	0.17°	
Fast Young Swing	3.57°	0.06°	-
Fast Old Swing	3.52°	0.28°	
Very Fast Young Swing	5.57°	0.01°	<.05
Very Fast Old Swing	3.71°	0.42°	

Note: Std: Standard deviation.; '-' indicates no significant difference.

The YG exhibited a significantly (p<.05) greater EVE/INV ROM during stance as WS increased (VS: 7.45°±0.73°; VF: 6.32°±0.16°) compared to the OG (VS: 5.52°±0.39°;

VF: 4.84°±0.16°). During swing phase, the YG exhibited a significantly ($p<.05$) greater EVE/INV ROM for the VS, slow, and VF WSs (VS: 3.71°±0.30°; slow: 3.39°±0.32°; VF: 5.57°±0.01°) compared to the OG (VS: 2.27°±0.15°; slow: 2.50°±0.44°; VF: 3.71°±0.42°) as shown in Table 10.

The mean relative angle gait curve for the mid-cal segment in the transverse plane is presented in Figure 18. This is the mid-cal adduction-abduction (ADD/ABD) angle defined by the relative orientation between the midfoot and the calcaneus segments. The following section focuses on between-group differences. Table 11 presents the significant age-related differences in the mean max and min ADD/ABD angles in stance and swing phase as well as their respective time of occurrence as a percentage of GC.

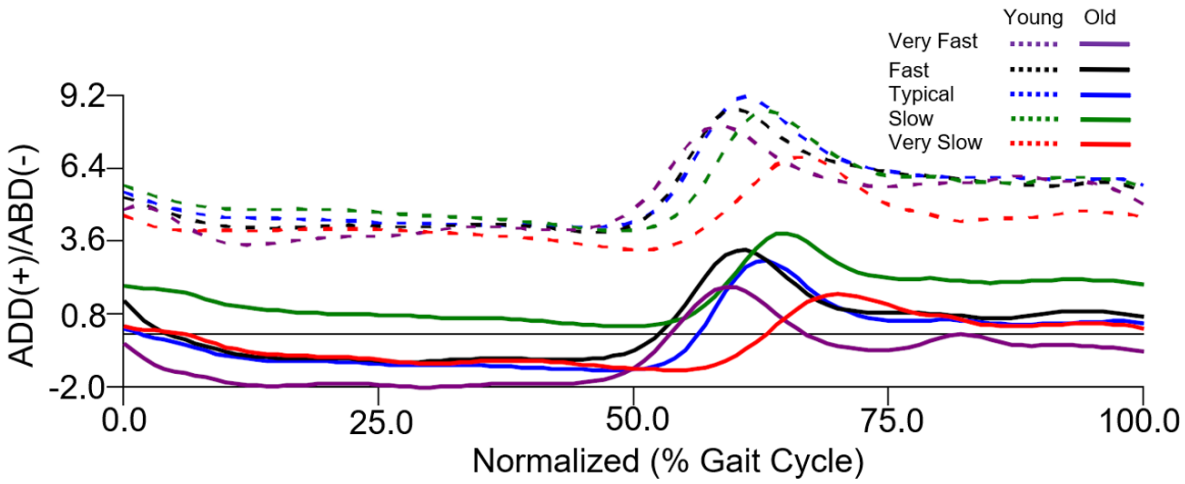


Figure 18. Mean adduction-abduction for the mid-cal of the OG versus the YG at each walking speed.

Table 11. Significant p-values of the mean min and max ADD/ABD angles (∠) of the mid-cal during stance and swing phase, as well as their respective time of occurrence in the gait cycle across five walking speeds.

Walking speed group	Min ADD ∠ in stance p-value	Time to min ADD ∠ in stance p-value	Min ADD ∠ in swing p-value	Time to min ADD ∠ in swing p-value	Max ADD ∠ in stance p-value	Time to max ADD ∠ in stance p-value	Max ADD ∠ in swing p-value	Time to max ADD ∠ in swing p-value
VS	-	-	.01	-	-	<.0001	.03	<.001
S	-	-	.01	-	.03	<.001	.04	.02
T	.01	-	-	-	<.01	<.01	<.01	.01
F	.03	-	.02	.04	.04	-	.03	.02
VF	.03	-	.03	-	.02	-	.01	-

Note: VS: Very Slow, S: Slow, T: Typical, F: Fast, VF: Very Fast.; '-' indicates no significant difference.

The mean min ADD angle across WSs during stance, with error bars (95% confidence interval), is presented in Figure 19. Descriptive results showed that the mean min ADD angle increased with increasing speed from VS to typical speed for the YG, after which point, the mean min ADD angle in stance phase began to decrease. The YG demonstrated more consistent patterns of variability for the min ADD angles at each speed compared to the OG, as shown by the marginal error data in Figure 19. The mean min ADD angle showed an inconsistent pattern for the OG, as the angle increased and decreased, in that order, as WS increased. In addition, the YG demonstrated greater mean min ADD angles across speeds compared to the OG (Figure 19). The YG had a significantly ($p<.05$) increased mean min ADD angle during stance as WS increased from typical to VF WS (typical: 4.09°±6.75°; VF: 3.18°±7.63°) compared to the OG (typical: -1.61°±5.82°; VF: -2.55°±6.34°), as shown in Table 11.

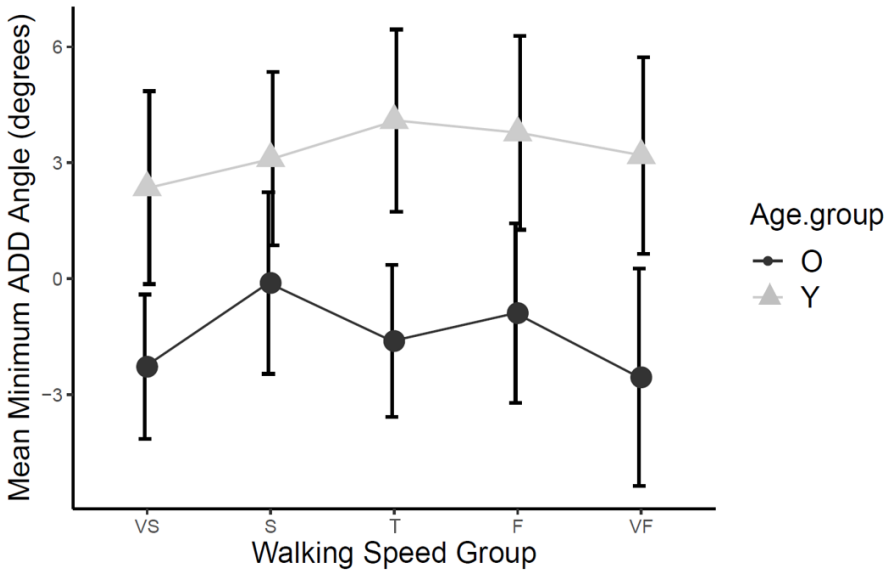


Figure 19. Mean min ADD angle of the mid-cal during stance phase for the YG and OG across walking speeds at the 95% confidence interval (VS: Very Slow, S: Slow, T: Typical, F: Fast, VF: Very Fast).

The mean min ADD angle across WSs during swing, with error bars (95% confidence interval), is presented in Figure 20. Descriptive results showed that the mean min ADD angle increased with increasing WS from VS to typical WS for the YG, after which point, the mean min ADD angle in stance phase began to decrease. The mean min ADD angle showed an inconsistent pattern for the OG, as the angle increased and decreased, in that order, as WS increased. In addition, the YG demonstrated greater mean min ADD angles across speeds compared to the OG (Figure 20). The YG had a significantly ($p<.05$) increased mean min ADD angle during swing as WS increased, except for the typical speed (VS: 3.18°±6.46°; VF: 4.33°±7.91°) compared to the OG (VS: -0.64°±5.27°; VF: -1.51° ±6.17°), as shown in Table 11.

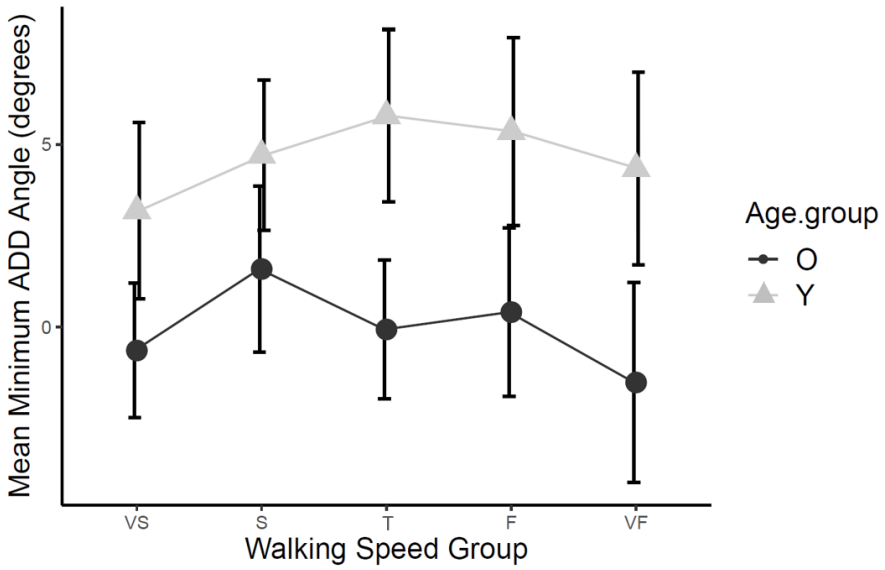


Figure 20. Mean min ADD angle of the mid-cal during swing phase for the YG and OG across walking speeds at the 95% confidence interval (VS: Very Slow, S: Slow, T: Typical, F: Fast, VF: Very Fast).

Significant differences in time to mean min ADD angle ($p<.05$) during swing phase were found between YA and OA for the fast WS only (Figure 18, Table 11). The YG had a significantly longer time to mean min ADD angle ($p<.05$) for the fast WS. For the YG, the min ADD occurred at 91.90±7.61 percent GC at the fast WS, whereas the OG showed a min ADD angle at 85.12±10.63 percent GC at the fast WS.

The mean max ADD angle across WSs during stance, with error bars (95% confidence interval), is presented in Figure 21. Descriptive results showed that the mean max ADD angle (peak) increased with increasing speed from VS to typical speed for the YG, after which point, the mean max ADD angle in stance phase began to decrease. The mean max ADD angle showed an inconsistent pattern for the OG, as the angle increased and decreased, in that order, as WS increased. In addition, the YG demonstrated greater mean max ADD angles across speeds compared to the OG (Figure 21).

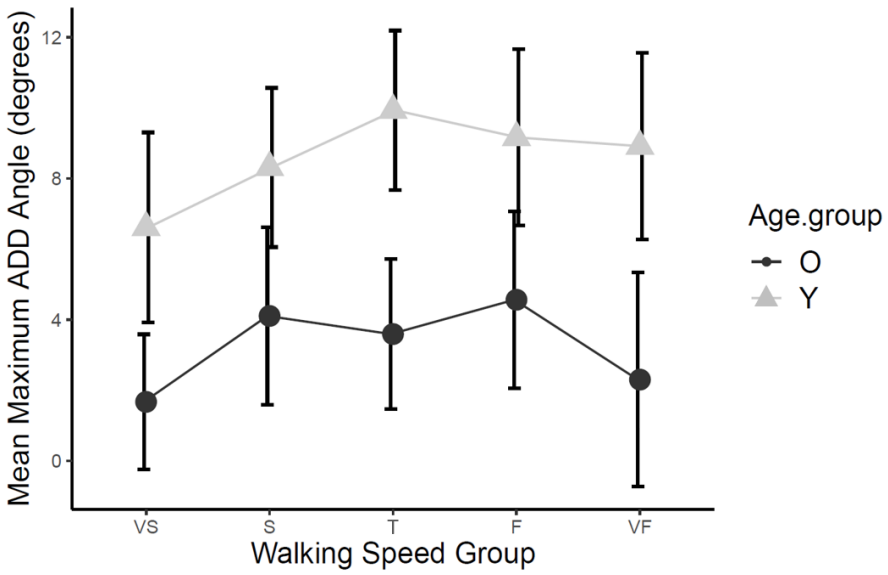


Figure 21. Mean max ADD angle of the mid-cal during stance phase for the YG and OG across walking speeds at the 95% confidence interval (VS: Very Slow, S: Slow, T: Typical, F: Fast, VF: Very Fast).

The YG had a significantly ($p<.05$) increased mean max ADD angle during stance (i.e., significantly higher peak ADD) as WS increased from slow to VF (slow: 8.31°±6.85°; VF: 8.91°±7.92°) compared to the OG (slow: 4.10°±5.96°; VF: 2.30°±6.83°).

Significant differences in time to mean max ADD ($p<.05$) during stance phase were found between YA and OA as WS increased from VS to typical WS (Figure 18, Table 11). The YG had a significantly shorter time to mean max ADD angle compared to the OG for the VS, slow, and typical WS. For the YG, the max ADD occurred at 57.25±12.42 percent GC at the VS WS, increasing to 59.49±5.32 percent GC at the typical WS. Whereas the OG demonstrated max ADD angles at 61.17±22.56 percent GC at the VS WS, decreasing to 59.96±8.41 percent GC at the typical WS.

The mean max ADD angle across WSs during swing, with error bars (95% confidence interval), is presented in Figure 22. Descriptive results showed that the mean max ADD angle (peak) increased with increasing speed from VS to typical speed for the

YG, after which point, the mean max ADD angle in stance phase began to decrease, and then increased again for the VF WS. The mean max ADD angle showed an inconsistent pattern for the OG, as the angle increased and decreased, in that order, as WS increased. In addition, the YG demonstrated greater mean max ADD angles across speeds compared to the OG (Figure 22).

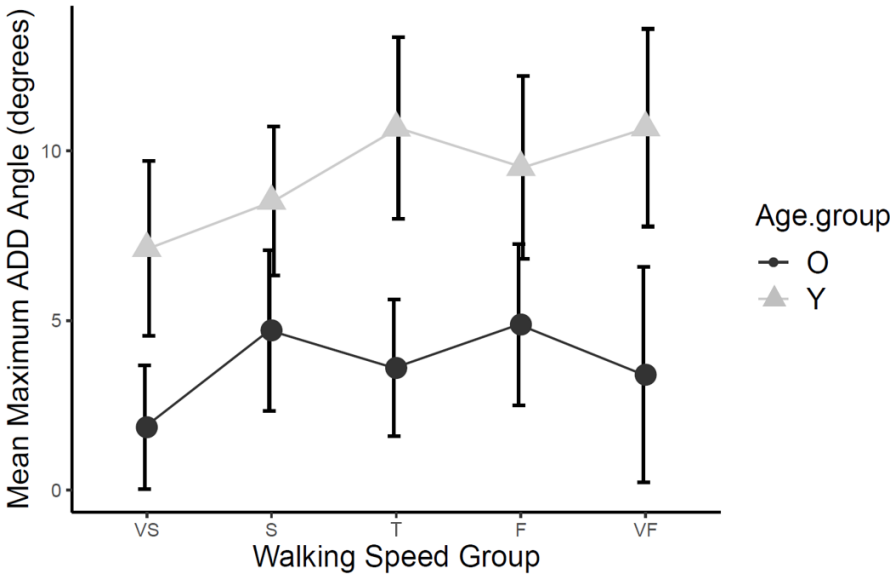


Figure 22. Mean max ADD angle of the mid-cal during swing phase for the YG and OG across walking speeds at the 95% confidence interval (VS: Very Slow, S: Slow, T: Typical, F: Fast, VF: Very Fast).

The YG had a significantly ($p<.05$) increased mean max ADD angle during swing (i.e., significantly higher peak ADD) as WS increased (VS: 7.12°±6.92°; VF: 10.68°±8.73°) compared to the OG (VS: 1.85°±5.24°; VF: 3.40°±7.17°).

Significant differences in time to mean max ADD ($p<.05$) during swing phase were found between YA and OA as WS increased from VS to fast WS (Figure 18, Table 11). The YG had a significantly shorter time to mean max ADD angle compared to the OG for the VS, slow, typical, and fast WS. For the YG, the max ADD occurred at 57.25±12.42 percent GC at the VS WS, increasing to 59.49±5.32 percent GC at the fast WS. Whereas

the OG demonstrated max ADD angles at 61.17±22.56 percent GC at the VS speed, decreasing to 59.96±8.41 percent GC at the fast WS.

Table 12 presents the significant ($p<.05$) age-related differences in the ADD/ABD range of motion (ROM) data for the mid-cal. In addition, relative ADD/ABD ROM data for the mid-cal are provided in Table 12 during stance and swing phase. The YG displayed the greatest ADD/ABD ROM (Figure 18) across all speeds during stance and swing compared to the OG. There were no significant ($p<.05$) age-related differences in the ADD/ABD ROM for the mid-cal during stance (Table 12). During swing phase, the YG exhibited a significantly ($p<.05$) greater ADD/ABD ROM for the VF speed only (VF: 6.34°±0.82°) compared to the OG (VF: 4.91°±0.99°) as shown in Table 12.

Table 12. Significant ADD/ABD ROM data for the mid-cal during stance and swing phase across five walking speeds and their respective significant p-values.

ADD/ABD ROM Midfoot-Calcaneus			
	Mean	± Std	P-value
Very Slow Young Stance	4.25°	0.52°	-
Very Slow Old Stance	3.95°	0.13°	
Slow Young Stance	5.20°	0.03°	-
Slow Old Stance	4.21°	0.39°	
Typical Young Stance	5.83°	0.27°	-
Typical Old Stance	5.20°	0.45°	
Fast Young Stance	5.38°	0.02°	-
Fast Old Stance	5.45°	0.51°	
Very Fast Young Stance	5.72°	0.28°	-
Very Fast Old Stance	4.85°	0.49°	
Very Slow Young Swing	3.94°	0.45°	-
Very Slow Old Swing	2.49°	0.03°	
Slow Young Swing	3.81°	0.43°	-
Slow Old Swing	3.11°	0.22°	
Typical Young Swing	4.89°	0.92°	-
Typical Old Swing	3.66°	0.35°	
Fast Young Swing	4.15°	0.28°	-
Fast Old Swing	4.47°	0.18°	
Very Fast Young Swing	6.34°	0.82°	<.01
Very Fast Old Swing	4.91°	0.99°	

Note: Std: Standard deviation.; '-' indicates no significant difference.

4.1.5 Age-related Differences in Relative Angles Between the Shank and Calcaneus

The mean relative angle gait curve for the shank-calcaneus (sha-cal) segment in the sagittal plane is presented in Figure 23. This is the sha-cal dorsiflexion-plantarflexion (DF/PF) angle defined by the relative orientation between the shank (tibia) and the calcaneus segments. The following section focuses on between-group differences. Table 13 presents the significant age-related differences in the mean max and min DF/PF angles in stance and swing phase as well as their respective time of occurrence as a percentage of GC.

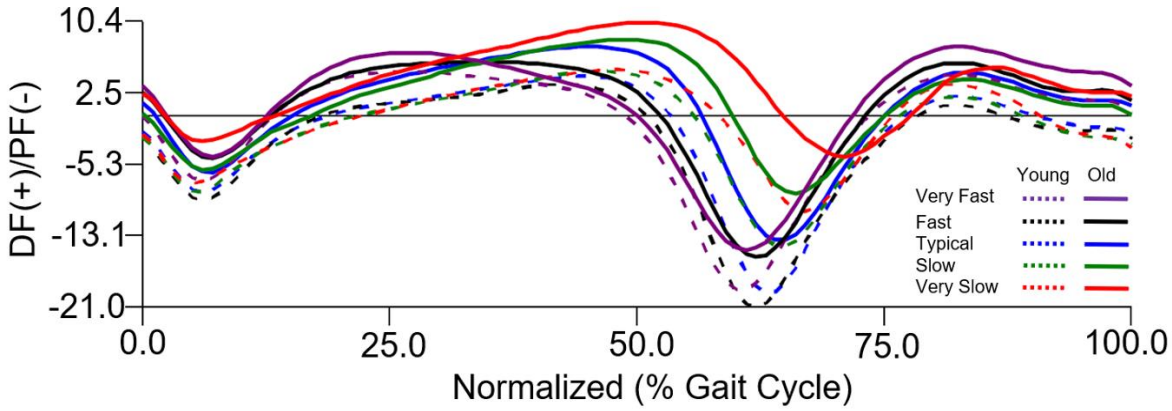


Figure 23. Mean dorsiflexion-plantarflexion for the sha-cal of the OG versus the YG at each walking speed.

Table 13. Significant p-values of the mean min and max DF/PF angles (∠) of the sha-cal during stance and swing phase, as well as their respective time of occurrence in the gait cycle across five walking speeds.

Walking speed group	Min PF ∠ in stance p-value	Time to min PF ∠ in stance p-value	Min PF ∠ in swing p-value	Time to min PF ∠ in swing p-value	Max DF ∠ in stance p-value	Time to max DF ∠ in stance p-value	Max DF ∠ in swing p-value	Time to max DF ∠ in swing p-value
VS	<.001	<.01	<.01	<.01	<.01	<.001	-	<.01
S	-	-	.04	<.01	-	<.001	-	-
T	-	-	.03	<.01	.04	-	.02	-
F	-	.01	-	-	-	-	<.01	-
VF	-	.02	-	-	-	-	-	-

Note: VS: Very Slow, S: Slow, T: Typical, F: Fast, VF: Very Fast.; '-' indicates no significant difference.

The mean min PF angle across WSs during stance, with error bars (95% confidence interval), is presented in Figure 24. Descriptively, the results showed that the mean min PF angle decreased with increasing WS for both groups, except for the VF WS. In addition, the YG demonstrated lower mean min PF angles across speeds compared to the OG. Both age groups displayed similar trends but at different magnitudes. Overall, both age groups demonstrated relatively consistent patterns of variability for the min PF angles at each WS. However, the OG displayed a larger associated marginal error (Figure 24). The YG had a significantly ($p<.05$) increased mean min PF angle during stance phase for the VS WS only (VS: -11.85°±6.10°) compared to the OG (VS:-6.68°±7.11°), as shown in Table 13.

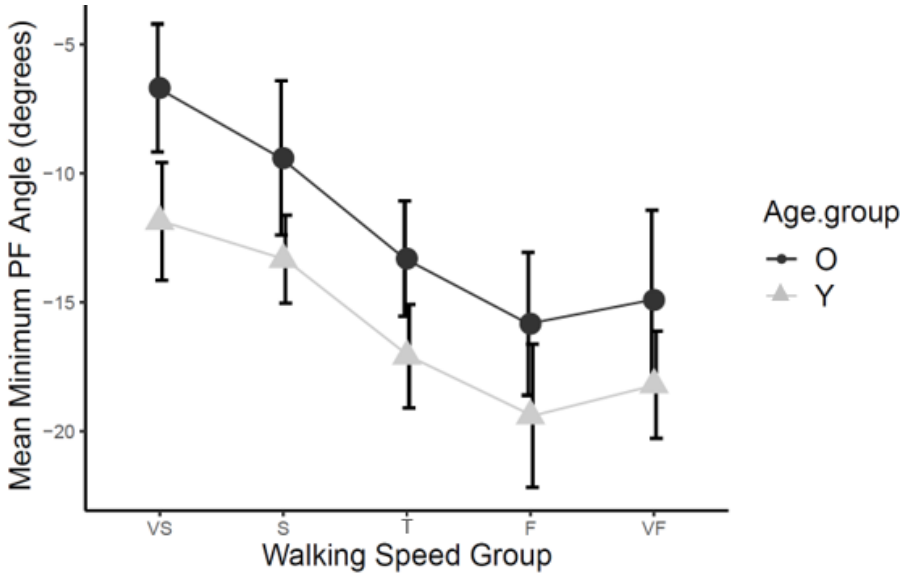


Figure 24. Mean min PF angle of the sha-cal during stance phase for the YG and OG across walking speeds at the 95% confidence interval (VS: Very Slow, S: Slow, T: Typical, F: Fast, VF: Very Fast).

Significant differences in time to mean min PF ($p<.05$) during stance phase were found between YA and OA as WS increased (Figure 23, Table 13). The YG had a significantly shorter time to mean min PF angle ($p<.05$) compared to the OG for the VS,

fast, and VF WSs. For the YG, the min PF occurred at 44.38±27.72 percent GC at the VS speed, increasing to 59.15±1.51 percent GC at the VF speed. Whereas the OG demonstrated min PF angles at 49.55±31.13 percent GC at the VS speed, increasing to 67.83±12.02 percent GC at the VF speed.

The mean min PF angle across WSs during swing, with error bars (95% confidence interval), is presented in Figure 25. Descriptively, the results showed that the mean min PF angle decreased with increasing speed for both groups, except for the VF speed. In addition, the YG demonstrated lower mean min PF angles across speeds compared to the OG. Both age groups displayed similar trends but at different magnitudes. Overall, both age groups demonstrated relatively consistent patterns of variability for the min PF angles at each speed. However, the OG displayed a larger associated marginal error (Figure 25).

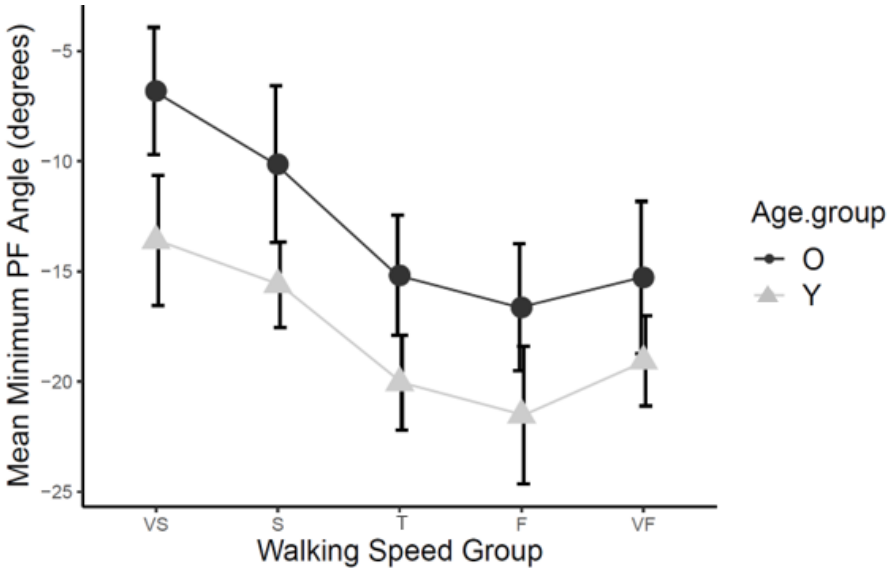


Figure 25. Mean min PF angle of the sha-cal during swing phase for the YG and OG across walking speeds at the 95% confidence interval (VS: Very Slow, S: Slow, T: Typical, F: Fast, VF: Very Fast).

The YG had a significantly ($p<.05$) increased mean min PF angle during swing phase as WS increased from VS to typical WS (VS: -13.60° ±7.90°; typical: -20.05°±6.15°) compared to the OG (VS:-6.81°±8.28°; typical: -15.18°±8.08°), as shown in Table 13.

Significant differences in time to mean min PF ($p<.05$) during swing phase were found between YA and OA as WS increased from VS to typical speed (Figure 23, Table 13). The YG had a significantly shorter time to mean min PF angle ($p<.05$) compared to the OG for the VS, slow, and typical WSs. For the YG, the min PF occurred at 68.98±12.61 percent GC at the VS speed, decreasing to 63.24±1.39 percent GC at the typical speed. Whereas the OG demonstrated min PF angles at 73.36±8.07 percent GC at the VS WS, decreasing to 65.07±4.17 percent GC at the typical speed.

The mean max DF angle across WSs during stance, with error bars (95% confidence interval), is presented in Figure 26. Descriptively, the results showed that the mean max DF angle (peak) decreased with increasing speed for the OG, except for the VF speed. The mean max DF angle showed a relatively neutral pattern of variability for the YG, as the speed increased from VS to fast speed. However, the YG displayed a larger associated marginal error. In addition, the YG demonstrated lower mean max DF angles across speeds compared to the OG (Figure 26). The YG had a significantly ($p<.05$) decreased mean max DF angle during stance phase at the VS and typical speed (VS: 5.71°±4.84°; typical: 5.25°±4.31°) compared to the OG (VS: 11.39°±4.52°; typical: 7.80°±4.60°), as shown in Table 13.

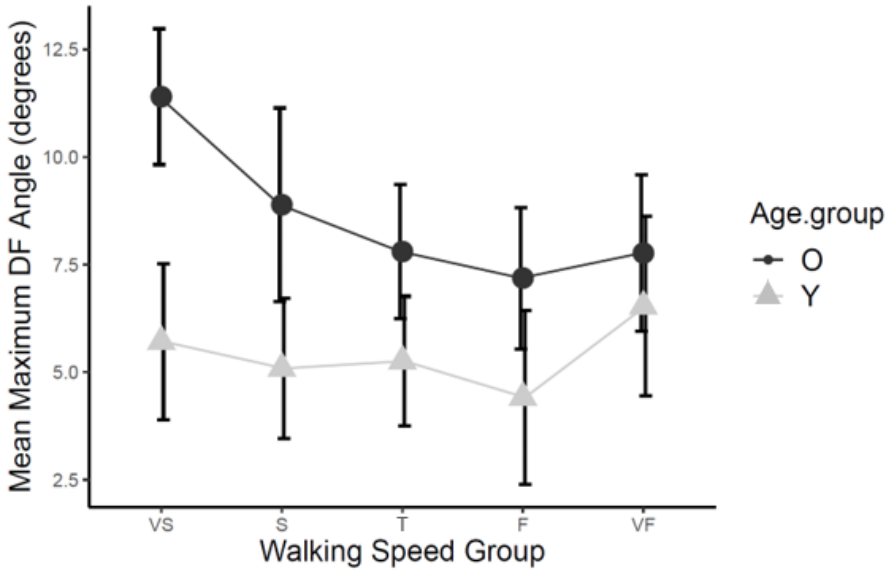


Figure 26. Mean max DF angle of the sha-cal during stance phase for the YG and OG across walking speeds at the 95% confidence interval (VS: Very Slow, S: Slow, T: Typical, F: Fast, VF: Very Fast).

Significant differences in time to mean max DF ($p<.05$) during stance phase were found between YA and OA as WS increased from VS to slow speed (Figure 23, Table 13). The YG had a significantly shorter time to mean max DF angle ($p<.05$) compared to the OG for the VS and slow WSs. For the YG, the max DF occurred at 44.61±8.07 percent GC at the VS speed, increasing to 44.67±7.57 percent GC at the slow speed. Whereas the OG demonstrated max DF angles at 50.92±3.90 percent GC at the VS speed, decreasing to 49.44±3.48 percent GC at the slow speed.

The mean max DF angle across WSs during swing, with error bars (95% confidence interval), is presented in Figure 27. Descriptive results for the OG showed that the mean max DF angle (peak) during swing decreased from VS to slow speed only, after which point, the mean max DF in swing phase began to increase. The mean max DF angle showed a less consistent pattern for the YG, as the angle decreased and increased, in that order, as WS increased. In addition, the YG demonstrated lower mean max DF angles across speeds

compared to the OG. The OG demonstrated more consistent patterns of variability, as shown by the marginal error data (Figure 27). The YG had a significantly ($p<.05$) decreased mean max DF angle during swing phase at the typical and fast WSs (typical: 3.03°±4.70°; fast: 1.92°±4.78°) compared to the OG (typical: 5.40°±4.14°; fast: 6.51°±4.01°).

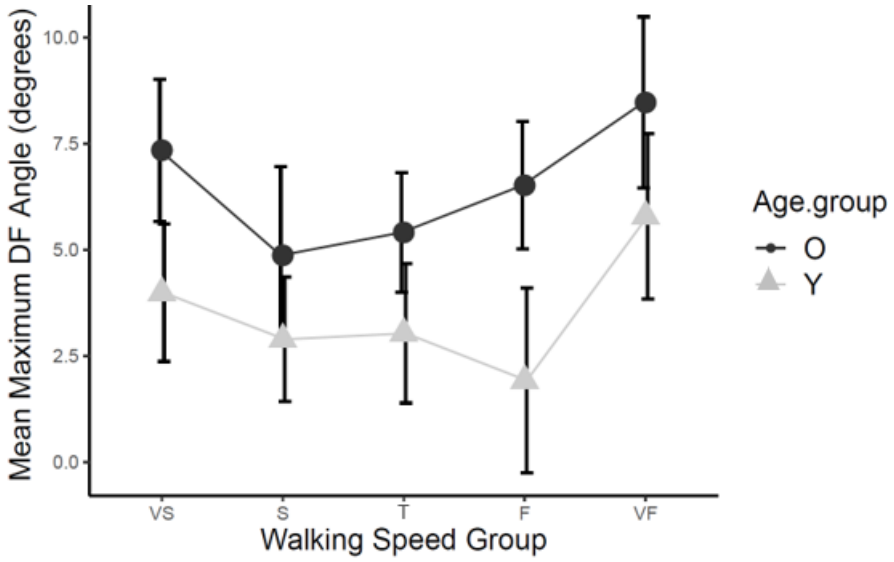


Figure 27. Mean max DF angle of the sha-cal during swing phase for the YG and OG across walking speeds at the 95% confidence interval (VS: Very Slow, S: Slow, T: Typical, F: Fast, VF: Very Fast).

Significant differences in time to mean max DF angle ($p<.05$) during swing phase were found between YA and OA for the VS speed only (Figure 23, Table 13). The YG had a significantly shorter time to mean max DF angle ($p<.05$) for the VS speed. For the YG, the max DF occurred at 82.89±5.46 percent GC at the VS speed, whereas the OG demonstrated a max DF angle at 85.49±4.31 percent GC at the VS speed.

Table 14 presents the significant ($p<.05$) age-related differences in the DF/PF range of motion (ROM) data for the sha-cal during stance and swing phase. In addition, relative DF/PF ROM data for the sha-cal are provided in Table 14. The YG displayed the greatest DF/PF ROM (Figure 23) across all speeds during stance and swing compared to the OG,

except for the VS WS during stance. There were no significant ($p<.05$) age-related differences in the DF/PF ROM for the sha-cal during stance. During swing phase, the YG showed a significantly ($p<.05$) greater DF/PF ROM for the slow WS only (slow: 18.49°±1.42°) compared to the OG (slow: 15.00°±3.50°) as shown in Table 14. During VF WS, the DF/PF ROM for the YA and OA increased most in the foot-shank during swing.

Table 14. Significant DF/PF ROM data for the sha-cal during stance and swing phase across five walking speeds and their respective significant p-values.

DF/PF ROM Shank-Calcaneus			
	Mean	± Std	P-values
Very Slow Young Stance	17.56°	1.25°	-
Very Slow Old Stance	18.08°	2.58°	
Slow Young Stance	18.42°	0.24°	-
Slow Old Stance	18.29°	1.76°	
Typical Young Stance	22.33°	1.45°	-
Typical Old Stance	21.10°	2.00°	
Fast Young Stance	23.80°	1.66°	-
Fast Old Stance	23.01°	3.02°	
Very Fast Young Stance	24.72°	0.05°	-
Very Fast Old Stance	22.66°	3.73°	
Very Slow Young Swing	17.59°	3.57°	-
Very Slow Old Swing	14.15°	3.48°	
Slow Young Swing	18.49°	1.42°	<.05
Slow Old Swing	15.00°	3.50°	
Typical Young Swing	23.08°	1.44°	-
Typical Old Swing	20.59°	3.93°	
Fast Young Swing	23.44°	2.08°	-
Fast Old Swing	23.15°	3.70°	
Very Fast Young Swing	24.85°	0.27°	-
Very Fast Old Swing	23.74°	3.24°	

Note: Std: Standard deviation.; '-' indicates no significant difference.

The mean relative angle gait curve for the sha-cal segment in the transverse plane is presented in Figure 28. This is the sha-cal adduction-abduction (ADD/ABD) angle defined by the relative orientation between the shank (tibia) and the calcaneus segments. The following section focuses on between-group differences. Table 15 presents the

significant age-related differences in the mean max and min ADD/ABD angles in stance and swing phase as well as their respective time of occurrence as a percentage of GC.

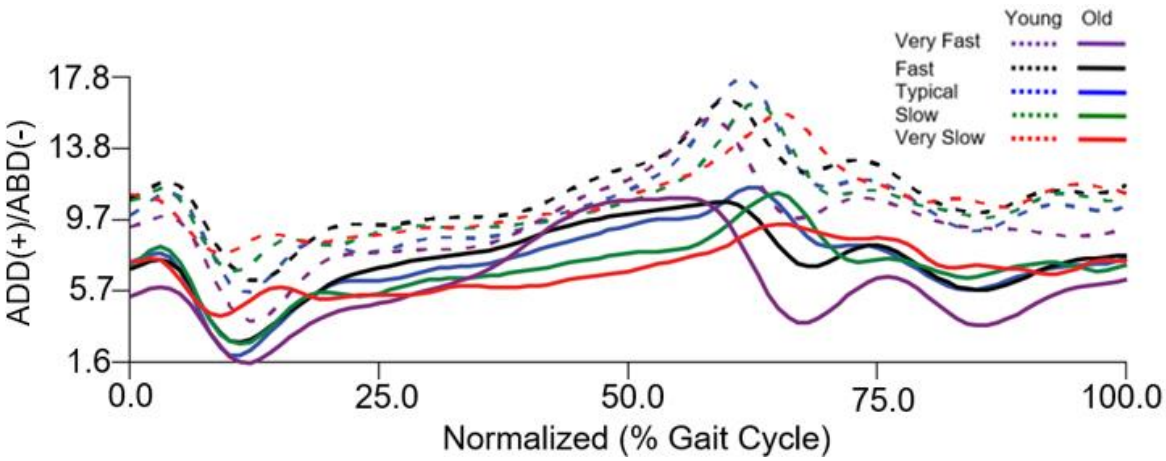


Figure 28. Mean adduction-abduction for the sha-cal of the OG versus the YG at each walking speed.

Table 15. Significant p-values of the mean min and max ADD/ABD angles (∠) of the sha-cal during stance and swing phase, as well as their respective time of occurrence in the gait cycle across five walking speeds.

Walking speed group	Min ADD ∠ in stance p-value	Time to min ADD ∠ in stance p-value	Min ADD ∠ in swing p-value	Time to min ADD ∠ in swing p-value	Max ADD ∠ in stance p-value	Time to max ADD ∠ in stance p-value	Max ADD ∠ in swing p-value	Time to max ADD ∠ in swing p-value
VS	.02	-	.01	-	<.01	-	<.01	<.01
S	<.01	-	.01	-	<.01	-	<.001	.03
T	.03	<.01	.01	-	<.001	-	<.01	.01
F	-	-	<.01	-	<.001	-	<.01	.04
VF	-	-	<.01	-	.01	-	<.01	-

Note: VS: Very Slow, S: Slow, T: Typical, F: Fast, VF: Very Fast.; '-' indicates no significant difference.

The mean min ADD angle across WSs during stance, with error bars (95% confidence interval), is presented in Figure 29. Descriptive results showed that the mean min ADD angle for both groups decreased with increasing speed from VS to typical speed only, after which point, the mean max PF in swing phase increased for the fast speed, and then decreased again for the VF WS. In addition, the YG demonstrated greater mean min ADD angles compared to the OG. Both age groups displayed similar trends but at different

magnitudes. However, the OG displayed a larger associated marginal error (Figure 29). The YG had a significantly ($p<.05$) decreased mean min ADD angle during stance phase at the VS speed (VS: 1.67°±5.30°) compared to the OG (VS: 2.18°±3.37°). However, as WS increased to typical speed, the YG had a significantly ($p<.05$) increased mean min ADD angle during stance phase (typical: typical: 2.44°±5.10°) compared to the OG (typical: 1.01°±3.61°), as shown in Table 15.

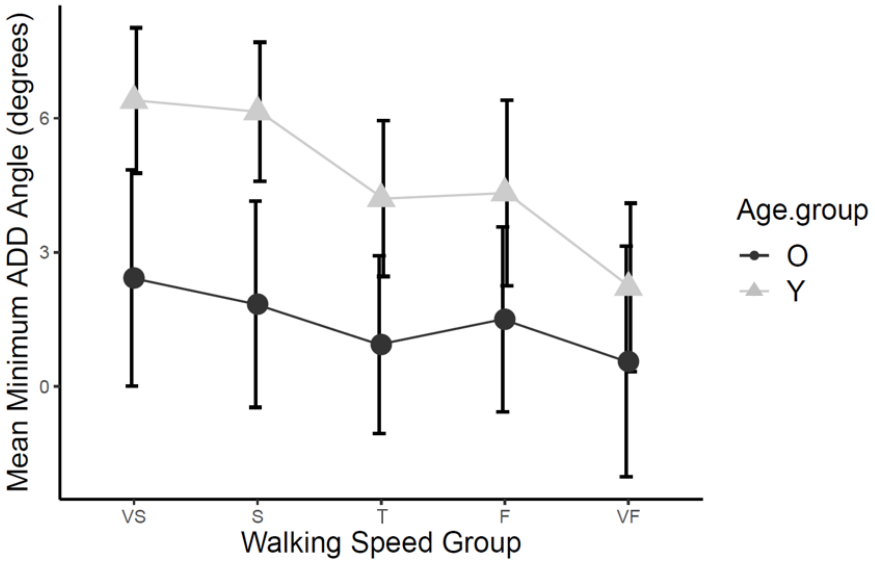


Figure 29. Mean min ADD angle of the sha-cal during stance phase for the YG and OG across walking speeds at the 95% confidence interval (VS: Very Slow, S: Slow, T: Typical, F: Fast, VF: Very Fast).

Significant differences in time to mean min ADD angle ($p<.05$) during stance phase were found between YA and OA for the typical speed only (Figure 28, Table 15). The YG had a significantly longer time to mean min ADD angle ($p<.05$) for the typical speed. For the YG, the min ADD occurred at 21.69±15.49 percent GC at the typical speed, whereas the OG demonstrated a min ADD angle at 20.80±12.61 percent GC at the typical speed.

The mean min ADD angle across WSs during swing, with error bars (95% confidence interval), is presented in Figure 30. Descriptive results showed that the mean min ADD angle decreased as WS increased for the OG. The OG displayed relatively consistent patterns of variability as WS increased from VS to fast speed The mean min ADD angle showed an inconsistent pattern for the YG, as the decreased with increasing speed from VS to typical speed only, after which point, the mean max PF in swing phase increased for the fast speed, and then decreased again for the VF WS. However, the YG displayed a smaller associated marginal error. In addition, the OG demonstrated greater mean min ADD angles compared to the YG (Figure 30).

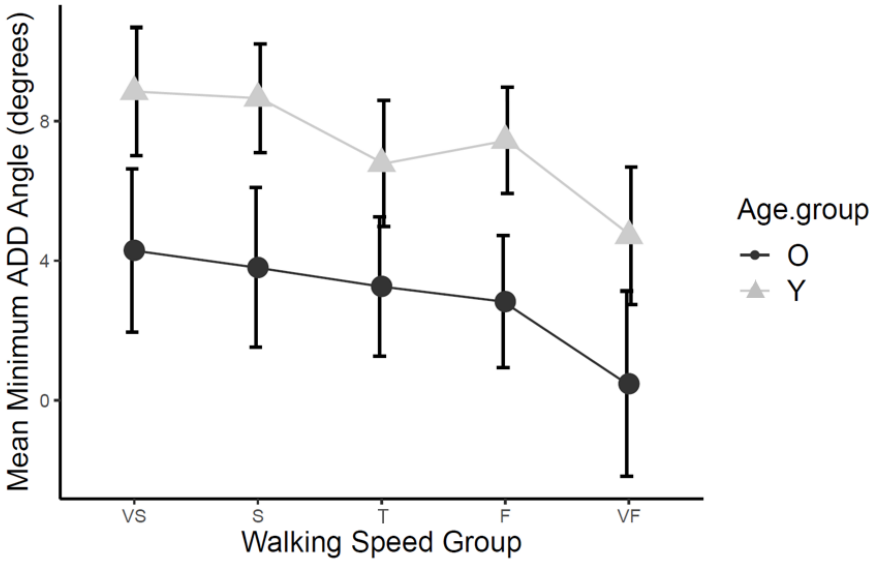


Figure 30. Mean min ADD angle of the sha-cal during swing phase for the YG and OG across walking speeds at the 95% confidence interval (VS: Very Slow, S: Slow, T: Typical, F: Fast, VF: Very Fast).

The YG had a significantly ($p<.05$) decreased mean min ADD angle during swing phase across all WSs (VS: 4.91°±5.24°; VF: 3.24°±4.54°) compared to the OG (VS: 6.83°±4.05°; VF: 4.19°±4.66°), as shown in Table 15. Further, no significant differences

in the time to mean min ADD angle during swing phase were found between YA and OA across all WSs.

The mean max ADD angle across WSs during stance, with error bars (95% confidence interval), is presented in Figure 31. Descriptive results showed that the mean max ADD angle (peak) for both groups increased as WS increased from VS to fast WS, after which point, the mean max ADD angle began to decrease. Both age groups displayed similar trends but at different magnitudes and demonstrated relatively consistent patterns of variability for the max ADD angles at each WS. However, the OG displayed a larger associated marginal error. In addition, the YG demonstrated greater mean max ADD angles compared to the OG.

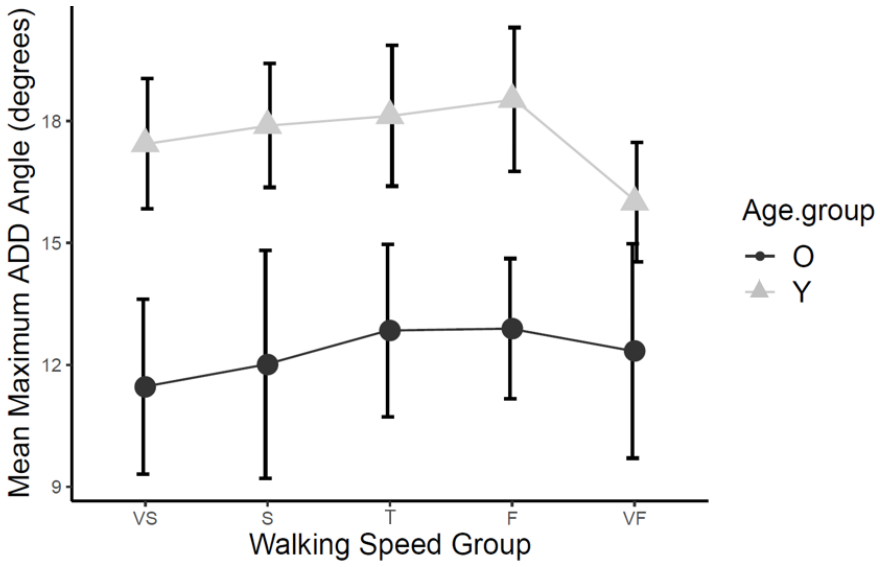


Figure 31. Mean max ADD angle of the sha-cal during stance phase for the YG and OG across walking speeds at the 95% confidence interval (VS: Very Slow, S: Slow, T: Typical, F: Fast, VF: Very Fast).

The YG had a significantly ($p<.05$) decreased mean max ADD angle during stance phase (i.e., significantly smaller peak ADD) at the VS and fast WSs (VS: 4.91°±5.24°; fast: 3.24°±4.54°) compared to the OG (VS: 6.83°±4.05°; fast: 4.19°±4.66°), as shown in Table

15. However, the YG had a significantly ($p<.05$) increased mean max ADD angle during stance phase (i.e. significantly higher peak ADD) at the slow, typical, and VF WSs (slow: 9.97°±5.83°; typical: 11.41°±5.85°; VF: 9.91°±5.29°) compared to the OG (slow: 9.95°±3.91°; typical: 10.68°±3.70°; VF: 9.30°±4.89°), as shown in Table 15. Further, no significant differences in the time to mean min ADD angle during stance phase were found between YA and OA across all speeds (Table 15).

The mean max ADD angle across WSs during swing, with error bars (95% confidence interval), is presented in Figure 32. Descriptive results showed that the mean max ADD angle (peak) for the OG increased as WS increased from VS to typical speed, after which point, the mean max ADD angle in swing began to decrease. The mean max ADD angle for the YG increased as WS increased from VS to fast speed, after which point, the mean max ADD angle in swing began to decrease. The YG demonstrated more consistent patterns of variability for the max ADD angles as speed increased from VS to fast WSs. The OG displayed a larger associated marginal error. In addition, the YG demonstrated greater mean max ADD angles compared to the OG (Figure 32). The YG had a significantly ($p<.05$) decreased mean max ADD angle during swing phase (i.e., significantly smaller peak ADD) as WS increased from VS to fast WSs (VS: 10.15°±6.06°; fast: 9.42°±4.96°) compared to the OG (VS: 10.81°±3.85°; fast: 10.63°±4.45°), as shown in Table 15.

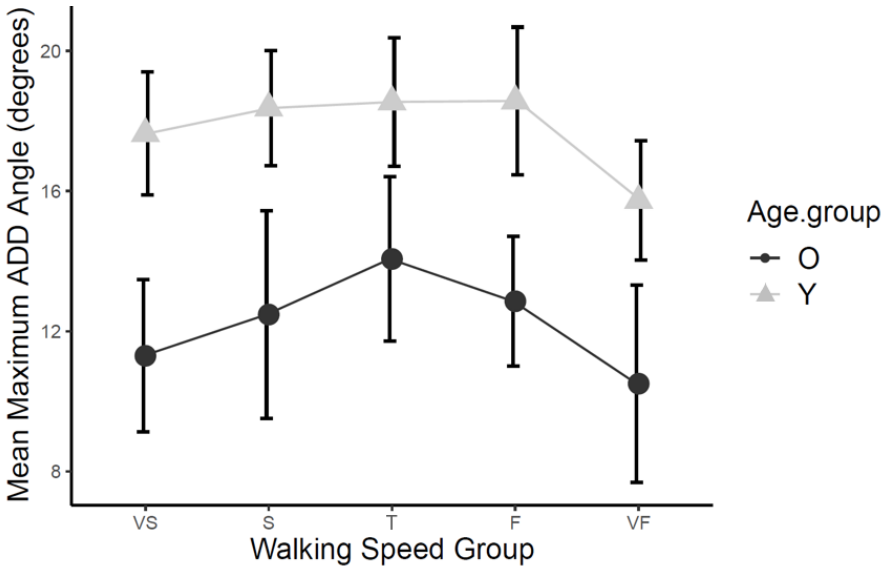


Figure 32. Mean max ADD angle of the sha-cal during swing phase for the YG and OG across walking speeds at the 95% confidence interval (VS: Very Slow, S: Slow, T: Typical, F: Fast, VF: Very Fast).

However, the YG had a significantly ($p<.05$) increased mean max ADD angle during swing phase (i.e. significantly higher peak ADD) at VF WS (VF: 10.74°±5.32°) compared to the OG (VF: 9.42°±4.93°).

Significant differences in time to mean max ADD ($p<.05$) during swing phase were found between YA and OA as WS increased from VS to fast speed (Figure 28, Table 15). The YG had a significantly shorter time to mean max ADD angle compared to the OG for the VS, slow, typical, and fast speed (Figure 28, Table 15). For the YG, the mean max ADD occurred at 77.55±10.46 percent GC at the VS speed, increasing to 92.39±8.41 percent GC at the fast WS. Whereas the OG demonstrated max ADD angles at 83.98±10.27 percent GC at the VS speed, increasing to 86.41±12.77 percent GC at the fast WS.

Table 16 presents the significant ($p<.05$) age-related differences in the ADD/ABD range of motion (ROM) data for the sha-cal. In addition, relative ADD/ABD ROM data for

the sha-cal are provided in Table 16. The YG displayed the greatest ADD/ABD ROM (Figure 28) across all speeds during stance and swing compared to the OG. Table 16 presents the between-group differences found for the ADD/ABD ROM during stance and swing phase. The YG exhibited a significantly ($p<.05$) greater ADD/ABD ROM during stance for the VS speed (VS: 8.19°±1.75°) compared to the OG (VS: 8.15°±0.91°). However, at the fast speed, the YG displayed a significantly ($p<.05$) smaller ADD/ABD ROM during stance (fast: 7.58°±1.04°) compared to the OG (fast: 9.35°±0.61°) as shown in Table 16. During swing phase, the YG exhibited a significantly ($p<.05$) greater ADD/ABD ROM for the VS WS only (VS: 5.23°±0.82°) compared to the OG (VS: 3.98°±0.20°) as shown in Table 16.

Table 16. Significant ADD/ABD ROM data for the sha-cal during stance and swing phase across five walking speeds and their respective significant p-values.

ADD/ABD ROM Shank-Calcaneus			
	Mean	± Std	P-value
Very Slow Young Stance	8.19°	1.75°	<.05
Very Slow Old Stance	8.15°	0.91°	
Slow Young Stance	7.89°	0.88°	-
Slow Old Stance	8.72°	0.05°	
Typical Young Stance	8.96°	0.75°	-
Typical Old Stance	9.66°	0.08°	
Fast Young Stance	7.58°	1.04°	<.05
Fast Old Stance	9.35°	0.61°	
Very Fast Young Stance	8.58°	0.97°	-
Very Fast Old Stance	9.51°	0.67°	
Very Slow Young Swing	5.23°	0.82°	<.05
Very Slow Old Swing	3.98°	0.20°	
Slow Young Swing	5.23°	0.87°	-
Slow Old Swing	4.43°	0.05°	
Typical Young Swing	6.22°	0.25°	-
Typical Old Swing	5.06°	0.03°	
Fast Young Swing	6.74°	0.31°	-
Fast Old Swing	5.08°	0.41°	
Very Fast Young Swing	7.50°	0.78°	-
Very Fast Old Swing	5.22°	0.27°	

Note: Std: Standard deviation.; '-' indicates no significant difference.

4.1.6 Age-related Differences in Relative Angles Between the Midfoot and Forefoot

The mean relative angle gait curve for the midfoot-forefoot (mid-met) segment in the sagittal plane is presented in Figure 33. This is the mid-met dorsiflexion-plantarflexion (DF/PF) angle defined by the relative orientation between the midfoot and the forefoot segments. The following section focuses on between-group differences. Table 17 presents the significant age-related differences in the mean max and min DF/PF angles in stance and swing phase as well as their respective time of occurrence as a percentage of GC.

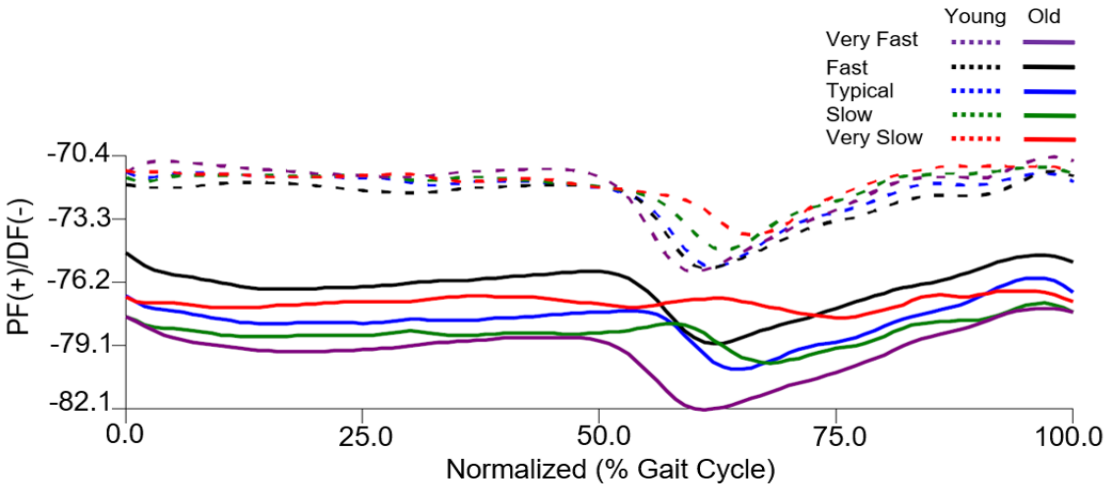


Figure 33. Mean dorsiflexion-plantarflexion for the mid-met of the OG versus the YG at each walking speed.

Table 17. Significant p-values of the mean min and max DF/PF angles (∠) of the mid-met during stance and swing phase, as well as their respective time of occurrence in the gait cycle across five walking speeds.

Walking speed group	Min PF ∠ in stance p-value	Time to min PF ∠ in stance p-value	Min PF ∠ in swing p-value	Time to min PF ∠ in swing p-value	Max PF ∠ in stance p-value	Time to max PF ∠ in stance p-value	Max PF ∠ in swing p-value	Time to max PF ∠ in swing p-value
VS	<.01	-	-	<.0001	-	<.001	.02	-
S	<.01	-	-	<.01	<.01	-	<.01	-
T	.01	-	.03	<.01	.01	-	.01	-
F	.01	-	-	.03	.01	-	.01	-
VF	<.01	-	.01	-	<.01	-	<.01	-

Note: VS: Very Slow, S: Slow, T: Typical, F: Fast, VF: Very Fast.; '-' indicates no significant difference.

The mean min PF angle across WSs during stance, with error bars (95% confidence interval), is presented in Figure 34. Descriptive results showed that the mean min PF angle for both groups decreased significantly as WS increased from VS to typical speed, after which point, the mean min PF angle increased for the fast speed, and then decreased again for the VF speed. Both age groups displayed similar trends but at different magnitudes. The YG demonstrated relatively consistent patterns of variability for the min PF angles at each speed. However, the OG displayed a larger associated marginal error. In addition, the YG demonstrated greater mean min PF angles compared to the OG (Figure 34).

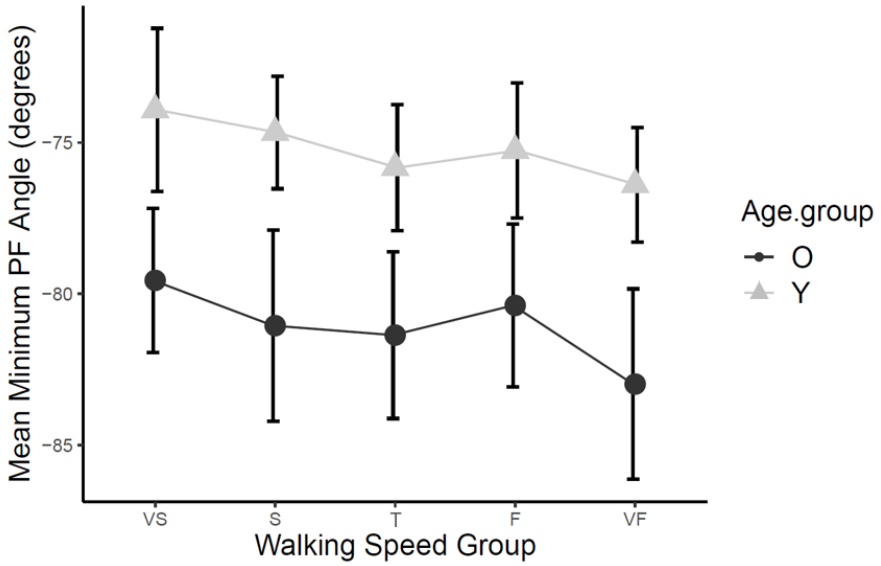


Figure 34. Mean min PF angle of the mid-met during stance phase for the YG and OG across walking speeds at the 95% confidence interval (VS: Very Slow, S: Slow, T: Typical, F: Fast, VF: Very Fast).

The YG had a significantly ($p<.05$) decreased mean min PF angle during stance phase as WS increased (VS: -73.91°±7.22°; VF: -76.39° ±5.67°) compared to the OG (VS: -79.55°±6.81°; VF: -82.98°±7.10°), as shown in Table 17. Further, no significant

differences in the time to mean min PF angle during stance phase were found between YA and OA across all WSs.

The mean min PF angle across WSs during swing, with error bars (95% confidence interval), is presented in Figure 35. Descriptive results showed that the mean min PF angle for both groups decreased as WS increased from VS to typical WS, after which point, the mean min PF angle increased for the fast speed, and then decreased again for the VF speed. Both age groups displayed similar trends but at different magnitudes. In addition, both age groups demonstrated relatively consistent patterns of variability for the min PF angles at each speed. However, the OG displayed a larger associated marginal error. In addition, the YG demonstrated greater mean min PF angles compared to the OG (Figure 35).

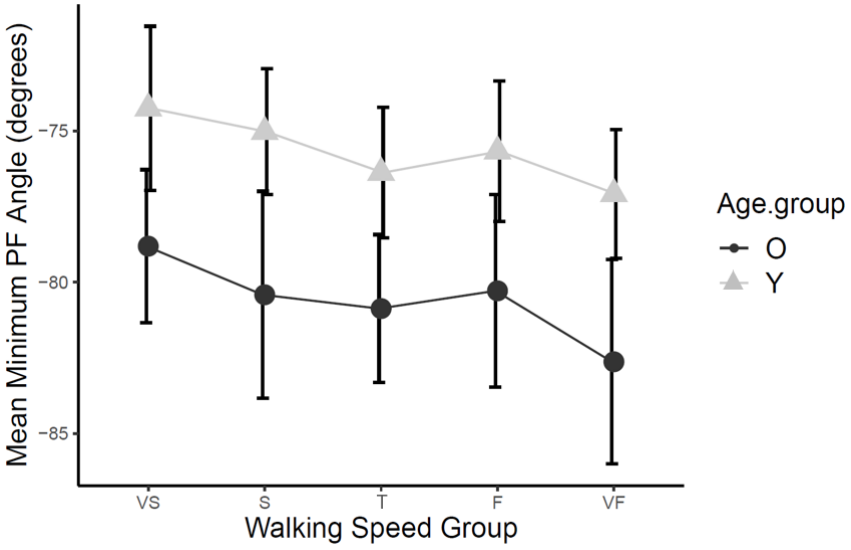


Figure 35. Mean min PF angle of the mid-met during swing phase for the YG and OG across walking speeds at the 95% confidence interval (VS: Very Slow, S: Slow, T: Typical, F: Fast, VF: Very Fast).

The YG had a significantly ($p<.05$) decreased mean min PF angle during swing phase at the typical and VF WSs (typical: -76.37°±6.17°; VF: -77.08°±6.38°) compared to the OG (typical: -80.87°±7.22°; VF: -82.62°±7.61°), as shown in Table 17.

Significant differences in time to mean min PF ($p<.05$) during swing phase were found between YA and OA as WS increased from VS to fast speed (Figure 33, Table 17). The YG had a significantly shorter time to mean min PF angle compared to the OG for the VS, slow, typical, and fast speed (Figure 33, Table 17). For the YG, the mean min PF occurred at 68.68±9.97 percent GC at the VS speed, decreasing to 63.68±5.80 percent GC at the fast speed. Whereas the OG demonstrated min PF angles at 79.16±10.90 percent GC at the VS speed, decreasing to 66.59±7.14 percent GC at the fast speed.

The mean max PF angle across WSs during stance, with error bars (95% confidence interval), is presented in Figure 36. Descriptive results showed that the mean max PF angle (peak) for the OG decreased as WS increased from VS to slow speed, after which point, the mean max PF angle began to increase until the fast speed, and then decreased again for the VF speed. The mean max PF was relatively consistent, with the smallest associated marginal error (Figure 36), across speeds for the YG. In addition, the YG demonstrated greater mean max PF angles compared to the OG (Figure 36). The YG had a significantly ($p<.05$) decreased mean max PF angle (i.e., significantly smaller peak PF) during stance phase as WS increased from slow to VF WSs (slow: -70.25°±5.58°; VF: -70.11°±6.09°) compared to the OG (slow: -76.43° ±7.12°; VF: -76.94°±6.56°), as shown in Table 17.

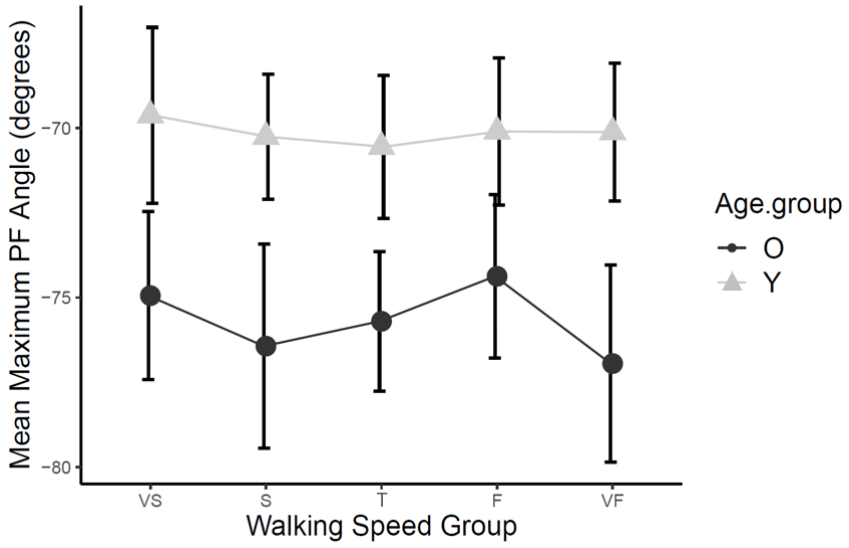


Figure 36. Mean max PF angle of the mid-met during stance phase for the YG and OG across walking speeds at the 95% confidence interval (VS: Very Slow, S: Slow, T: Typical, F: Fast, VF: Very Fast).

Significant differences in time to mean max PF angle ($p<.05$) during stance phase were found between YA and OA for the VS speed only (Figure 33, Table 17). The YG had a significantly shorter time to mean max PF angle ($p<.05$) for the VS WS. For the YG, the mean max PF occurred at 28.93±20.44 percent GC at the VS speed, whereas the OG demonstrated a max PF angle at 49.09±22.75 percent GC at the VS WS.

The mean max PF angle across WSs during swing, with error bars (95% confidence interval), is presented in Figure 37. Descriptive results showed that the mean max PF angle (peak) for the OG decreased as WS increased from VS to slow speed, after which point, the mean max PF angle began to increase until the fast speed, and then decreased again for the VF speed. The mean max PF was relatively consistent, with the smallest associated marginal error (Figure 37), across speeds for the YG. In addition, the YG demonstrated greater mean max PF angles compared to the OG (Figure 37).

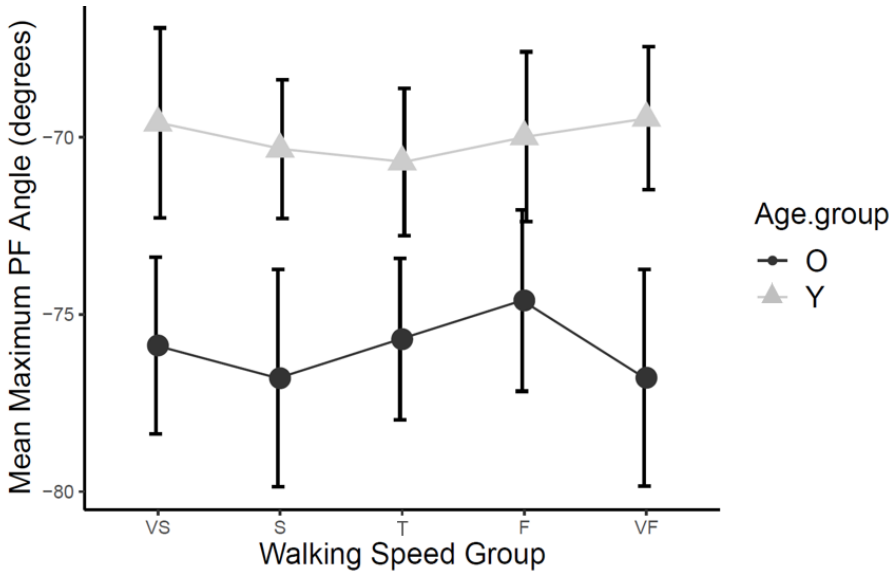


Figure 37. Mean max PF angle of the mid-met during swing phase for the YG and OG across walking speeds at the 95% confidence interval (VS: Very Slow, S: Slow, T: Typical, F: Fast, VF: Very Fast).

The YG had a significantly ($p<.05$) decreased mean max PF angle (i.e., significantly smaller peak PF) during swing phase as WS increased (VS: -69.59° ±7.18°; VF: -69.45°±6.06°) compared to the OG (VS: -75.87° ±7.16°; VF: -76.78°±6.91°), as shown in Table 17. Further, no significant differences in the time to mean max PF angle during swing phase were found between YA and OA across all speeds (Table 17).

Table 18 presents the significant ($p<.05$) age-related differences in the DF/PF range of motion (ROM) data for the mid-met. In addition, relative DF/PF range of motion (ROM) data for the mid-met are provided in Table 18. The YG displayed the greatest DF/PF ROM (Figure 33) across all speeds during stance and swing compared to the OG. Table 18 presents the between-group differences found for the DF/PF ROM during stance and swing phase. There were no significant ($p<.05$) age-related differences in the DF/PF ROM for the foot-shank during stance (Table 18). During swing phase, the YG exhibited a significantly

(p<.05) greater DF/PF ROM for the VS speed only (VS: 4.65°±0.07°) compared to the OG (VS: 2.93°±0.08°) as shown in Table 18.

Table 18. Significant DF/PF ROM data for the mid-met during stance and swing phase across five walking speeds and their respective significant p-values.

DF/PF ROM Midfoot-Forefoot			
	Mean	± Std	P-values
Very Slow Young Stance	4.28°	0.27°	-
Very Slow Old Stance	4.61°	0.29°	
Slow Young Stance	4.40°	0.06°	-
Slow Old Stance	4.62°	0.36°	
Typical Young Stance	5.27°	0.07°	-
Typical Old Stance	5.66°	2.08°	
Fast Young Stance	5.15°	0.15°	-
Fast Old Stance	6.01°	0.73°	
Very Fast Young Stance	6.27°	0.41°	-
Very Fast Old Stance	6.03°	0.53°	
Very Slow Young Swing	4.65°	0.07°	<.001
Very Slow Old Swing	2.93°	0.08°	
Slow Young Swing	4.69°	0.38°	-
Slow Old Swing	3.61°	0.83°	
Typical Young Swing	5.68°	0.22°	-
Typical Old Swing	5.17°	0.50°	
Fast Young Swing	5.69°	0.16°	-
Fast Old Swing	5.67°	1.64°	
Very Fast Young Swing	7.62°	0.31°	-
Very Fast Old Swing	5.84°	0.69°	

Note: Std: Standard deviation.; '-' indicates no significant difference.

The mean relative angle gait curve for the mid-met segment in the transverse plane is presented in Figure 38. This is the mid-met adduction-abduction (ADD/ABD) angle defined by the relative orientation between the midfoot and the forefoot (metatarsus) segments. The following section focuses on between-group differences. Table 19 presents the significant age-related differences in the mean max and min ADD/ABD angles in stance and swing phase as well as their respective time of occurrence as a percentage of GC.

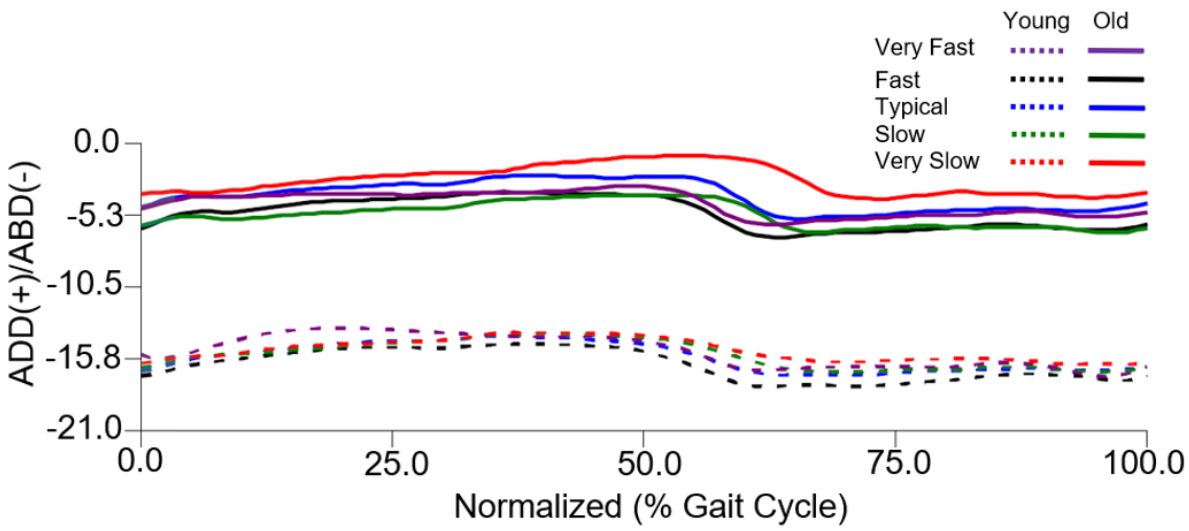


Figure 38. Mean adduction-abduction for the mid-met of the OG versus the YG at each walking speed.

Table 19. Significant p-values of the mean min and max ADD/ABD angles (∠) of the mid-met during stance and swing phase, as well as their respective time of occurrence in the gait cycle across five walking speeds.

Walking speed group	Max ABD ∠ in stance p-value	Time to max ABD ∠ in stance p-value	Max ABD ∠ in swing p-value	Time to max ABD ∠ in swing p-value	Min ABD ∠ in stance p-value	Time to min ABD ∠ in stance p-value	Min ABD ∠ in swing p-value	Time to min ABD ∠ in swing p-value
VS	<.0001	-	<.0001	-	<.0001	<.0001	<.0001	-
S	<.00001	-	<.001	-	<.001	.01	<.001	-
T	<.0001	-	<.0001	-	<.0001	.04	<.00001	-
F	<.001	-	<.001	-	<.001	-	<.001	-
VF	<.001	-	<.001	-	<.01	-	<.01	-

Note: VS: Very Slow, S: Slow, T: Typical, F: Fast, VF: Very Fast.; '-' indicates no significant difference.

The mean max abduction (ABD) angle across WSs during stance, with error bars (95% confidence interval), is presented in Figure 39. Descriptive results showed that the mean max ABD angle (peak) for the OG decreased and increased, in that order, as WS increased. Both age groups displayed similar trends but at different magnitudes. Overall, both age groups demonstrated relatively consistent patterns of variability for the max ABD angles at each speed. However, the OG displayed a larger associated marginal error. In

addition, the YG demonstrated greater mean max ABD angles across speeds compared to the OG (Figure 39).

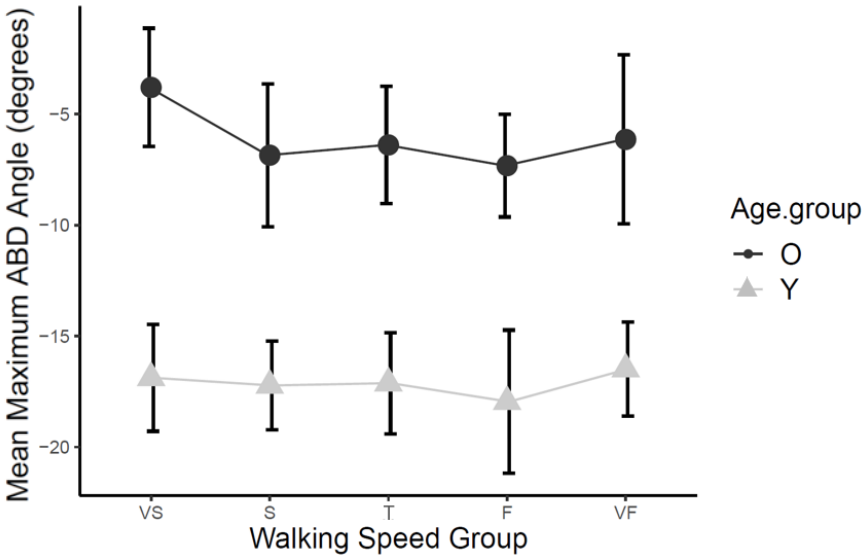


Figure 39. Mean max ABD angle of the mid-met during stance phase for the YG and OG across walking speeds at the 95% confidence interval (VS: Very Slow, S: Slow, T: Typical, F: Fast, VF: Very Fast).

The YG had a significantly ($p<.05$) increased mean max ABD angle (i.e., significantly higher peak ABD) during stance phase as WS increased (VS: -16.87°±6.44°; VF: -16.48 °±6.35°) compared to the OG (VS: -3.79° ±7.63°; VF: -6.13°±8.59°), as shown in Table 19. Further, no significant differences in the time to mean max ABD angle during stance phase were found between YA and OA across all speeds (Table 19).

The mean max abduction (ABD) angle across WSs during swing, with error bars (95% confidence interval), is presented in Figure 40. Descriptive results showed that the mean max ABD angle (peak) decreased from VS to slow speed, after which point, the angle was relatively consistent. Whereas for the YG, the mean max ABD angle was relatively consistent across speeds, with the smallest associated marginal error (Figure 40). In

addition, the YG demonstrated lower mean max ABD angles across speeds compared to the OG (Figure 40).

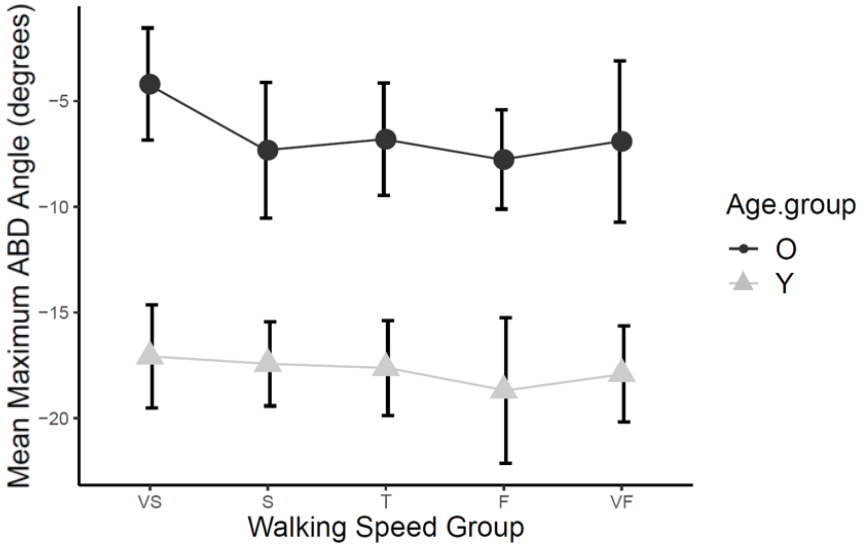


Figure 40. Mean max ABD angle of the mid-met during swing phase for the YG and OG across walking speeds at the 95% confidence interval (VS: Very Slow, S: Slow, T: Typical, F: Fast, VF: Very Fast).

Similar to the results of stance phase, the YG had a significantly ($p<.05$) increased mean max ABD angle (i.e., significantly higher peak ABD) during swing phase as WS increased (VS: -17.07°±6.52°; VF: -17.90°±6.79°) compared to the OG (VS: -4.20° ±7.61°; VF: -6.90°±8.60°), as shown in Table 19. Further, no significant differences in the time to mean max ABD angle during swing phase were found between YA and OA across all speeds (Table 19).

The mean min abduction (ABD) angle across WSs during stance, with error bars (95% confidence interval), is presented in Figure 41. Descriptive results showed that the mean min ABD angle decreased from VS to slow WS for the OG, after which point, the angle was relatively consistent, whereas for the YG the mean min ABD angle was

relatively consistent across speeds, except for the VF speed. The OG demonstrated a larger associated marginal error. In addition, the YG showed lower mean min ABD angles across speeds, with the smallest associated marginal error, compared to the OG (Figure 41).

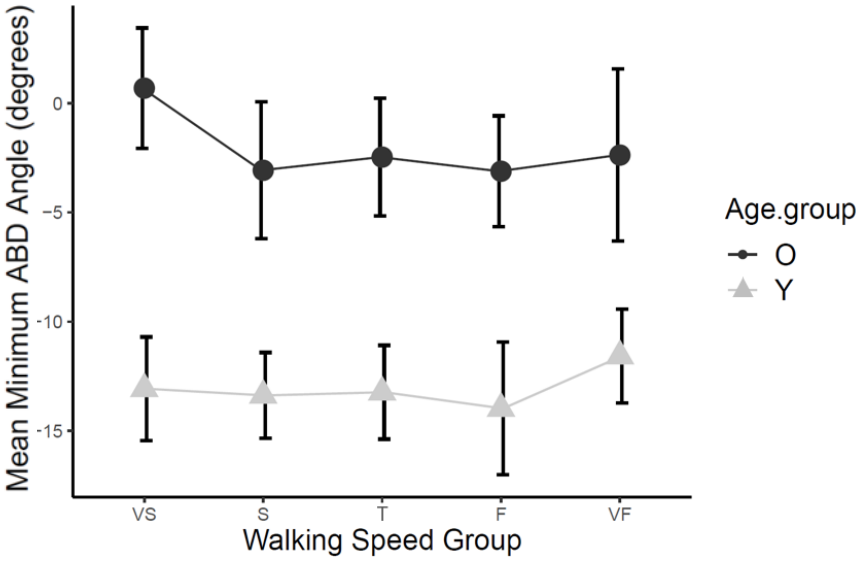


Figure 41. Mean min ABD angle of the mid-met during stance phase for the YG and OG across walking speeds at the 95% confidence interval (VS: Very Slow, S: Slow, T: Typical, F: Fast, VF: Very Fast).

The YG had a significantly ($p<.05$) increased mean min ABD angle during stance phase as speed increased (VS: -13.07°±6.35°; VF: -11.57°±6.42°) compared to the OG (VS: 0.69° ±7.89°; VF: -2.37°±8.88°), as shown in Table 19.

Significant differences in time to mean min ABD angle ($p<.05$) during stance phase were found between YA and OA as WS increased from VS to typical speed (Figure 38, Table 19). The YG had a significantly shorter time to mean min ABD angle ($p<.05$) for the VS, slow, and typical speed. For the YG, the min ABD occurred at 38.97±14.96 percent GC at the VS speed, increasing to 37.66±12.72 percent GC at the typical speed. Whereas

the OG demonstrated min ABD angles at 52.43±11.48 percent GC at the VS speed, decreasing to 42.14±17.10 percent GC at the typical speed.

The mean min abduction (ABD) angle across WSs during swing, with error bars (95% confidence interval), is presented in Figure 42. Descriptive results showed that the mean min ABD angle decreased from VS to slow speed for the OG, after which point, the angle was relatively consistent, whereas for the YG the mean min ABD angle was relatively consistent across WSs, except for the VF speed. In addition, the YG demonstrated lower mean min ABD angles across WSs, with the smallest associated marginal error, compared to the OG. Similar to the results of stance phase, the YG had a significantly ($p<.05$) increased mean min ABD angle during swing phase as WS increased (VS: -14.63°±6.24°; VF: -13.42°±7.17°) compared to the OG (VS: -1.77°±7.93°; VF: -3.62°±9.24°), as shown in Table 19. Further, no significant differences in the time to mean min ABD angle during swing phase were found between YA and OA across all WSs.

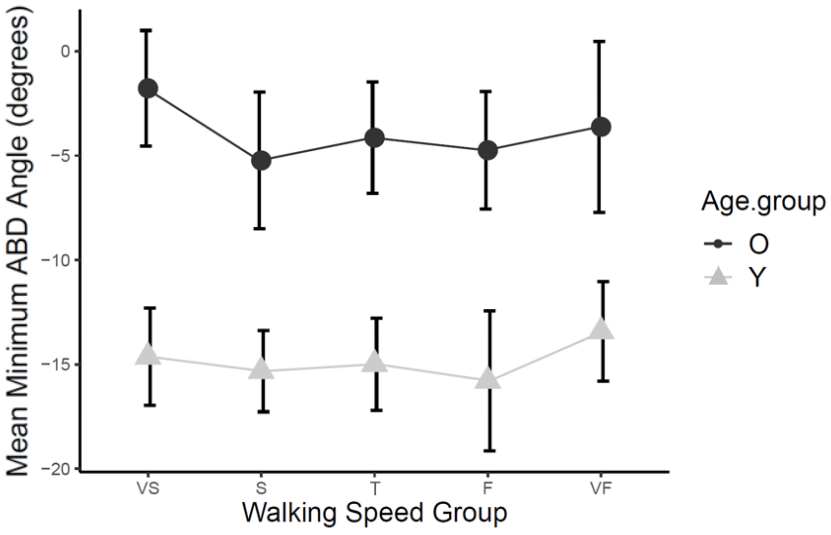


Figure 42. Mean min ABD angle of the mid-met during swing phase for the YG and OG across walking speeds at the 95% confidence interval (VS: Very Slow, S: Slow, T: Typical, F: Fast, VF: Very Fast).

Table 20 presents the significant (p<.05) age-related differences in the ADD/ABD range of motion (ROM) data for the mid-met. Relative ADD/ABD ROM data for the mid-met are provided in Table 20. The YG and OG exhibited similar ADD/ABD ROM data (Figure 38) across speeds during stance and swing. Table 20 presents the between-group differences found for the ADD/ABD ROM during stance and swing phase. At the VS speed, the YG exhibited a significantly (p<.05) reduced ADD/ABD ROM during stance (VS: 3.80°±0.08°) compared to the OG (VS: 4.48°±0.25°) as shown in Table 20. There were no significant (p<.05) age-related differences in the DF/PF ROM for the foot-shank during swing (Table 20).

Table 20. Significant ADD/ABD ROM data for the mid-met during stance and swing phase across five walking speeds and their respective significant p-values.

ADD/ABD ROM Midfoot-Forefoot			
	Mean	± Std	P-value
Very Slow Young Stance	3.80°	0.08°	<.05
Very Slow Old Stance	4.48°	0.25°	
Slow Young Stance	3.84°	0.09°	-
Slow Old Stance	3.77°	0.21°	
Typical Young Stance	3.88°	0.38°	-
Typical Old Stance	3.91°	0.17°	
Fast Young Stance	3.97°	0.41°	-
Fast Old Stance	4.20°	0.60°	
Very Fast Young Stance	4.90°	0.06°	-
Very Fast Old Stance	3.76°	0.29°	
Very Slow Young Swing	2.44°	0.28°	-
Very Slow Old Swing	2.42°	0.32°	
Slow Young Swing	2.10°	0.14°	-
Slow Old Swing	2.08°	0.15°	
Typical Young Swing	2.63°	0.11°	-
Typical Old Swing	2.66°	0.01°	
Fast Young Swing	2.89°	0.19°	-
Fast Old Swing	3.02°	1.25°	
Very Fast Young Swing	4.48°	0.38°	-
Very Fast Old Swing	3.28°	0.64°	

Note: Std: Standard deviation.; '-' indicates no significant difference.

4.1.7 Age-related Differences in Relative Angles Between the Calcaneus and Forefoot

The mean relative angle gait curve for the calcaneus-forefoot (cal-met) segment in the sagittal plane is presented in Figure 43. This is the cal-met dorsiflexion-plantarflexion (DF/PF) angle defined by the relative orientation between the calcaneus and the forefoot (metatarsus) segments. The following section focuses on between-group differences. Table 21 presents the significant age-related differences in the mean max and min DF/PF angles in stance and swing phase as well as their respective time of occurrence as a percentage of GC.

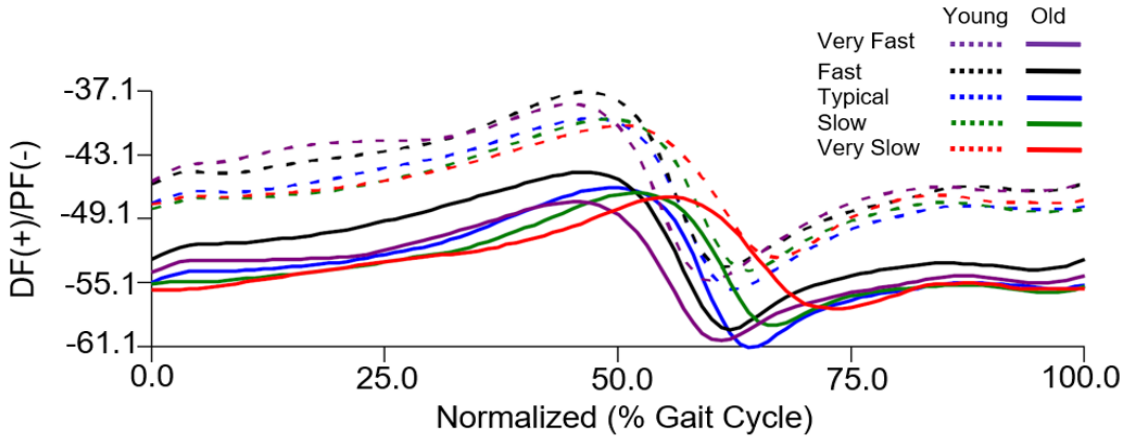


Figure 43. Mean dorsiflexion-plantarflexion for the cal-met of the OG versus the YG at each walking speed.

Table 21. Significant p-values of the mean min and max DF/PF angles (∠) of the cal-met during stance and swing phase, as well as their respective time of occurrence in the gait cycle across five walking speeds.

Walking speed group	Max PF ∠ in stance p-value	Time to max PF ∠ in stance p-value	Max PF ∠ in swing p-value	Time to max PF ∠ in swing p-value	Min PF ∠ in stance p-value	Time to min PF ∠ in stance p-value	Min PF ∠ in swing p-value	Time to min PF ∠ in swing p-value
VS	<.01	-	-	<.00001	-	<.00001	.01	-
S	-	-	-	<.0001	.01	<.0001	<.01	-
T	.03	<.01	.03	<.001	.01	<.01	<.01	-
F	<.01	<.01	<.01	<.01	<.01	-	<.01	.03
VF	-	-	-	.01	<.01	-	<.01	-

Note: VS: Very Slow, S: Slow, T: Typical, F: Fast, VF: Very Fast.; '-' indicates no significant difference.

The mean max plantarflexion (PF) angle across WSs during stance, with error bars (95% confidence interval), is presented in Figure 44. Descriptive results showed that the mean max PF angle showed an inconsistent pattern for the YG, as the angle decreased from VS to typical WS, after which point, the mean max PF angle increased for the fast WS, and then decreased again for the VF WS, whereas for the OG, the mean max PF angle was relatively consistent, with the smallest associated marginal error (Figure 44), across speeds. In addition, the YG showed greater mean max PF angles across speeds compared to the OG (Figure 44).

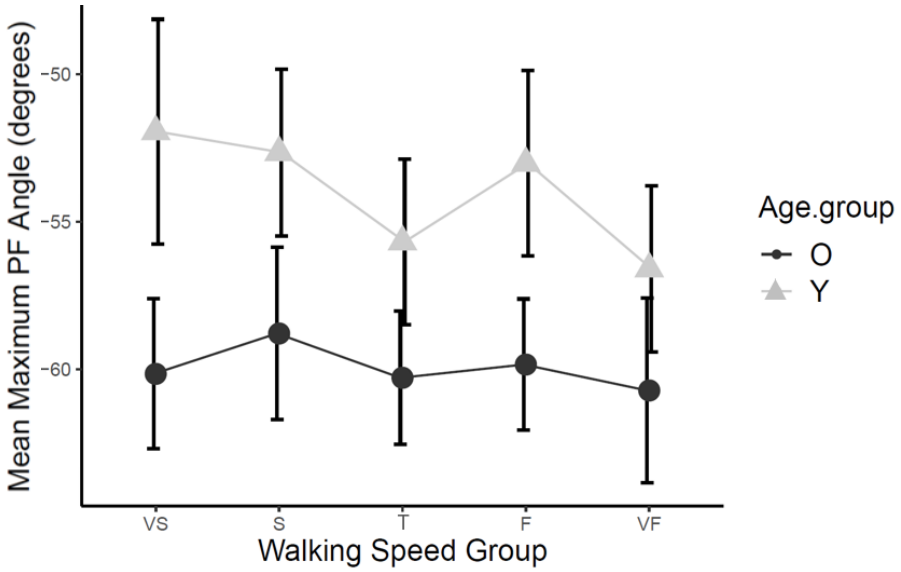


Figure 44. Mean max PF angle of the cal-met during stance phase for the YG and OG across walking speeds at the 95% confidence interval (VS: Very Slow, S: Slow, T: Typical, F: Fast, VF: Very Fast).

The YG had a significantly ($p<.05$) decreased mean max PF angle (i.e., significantly greater peak PF) during stance phase at the VS, typical and fast speeds (VS: -51.94°±10.18°; typical: -55.68°±8.02°; fast: -53.01°±6.88°) compared to the OG (VS: -60.15°±7.28°; typical: -60.28°±6.67°; fast: -59.84°±5.94°), as shown in Table 21.

Significant differences in time to mean max PF angle ($p<.05$) during stance phase were found between YA and OA as WS increased from typical to fast speed (Figure 43, Table 21). The YG had a significantly shorter time to mean max PF angle ($p<.05$) for the typical and fast speed. For the YG, the max PF occurred at 60.87±1.58 percent GC at the typical speed, decreasing to 58.42±5.90 percent GC at the fast speed. Whereas the OG demonstrated max PF angles at 61.62±3.24 percent GC at the typical speed, decreasing to 58.49±11.77 percent GC at the fast speed.

The mean max plantarflexion (PF) angle across WSs during swing, with error bars (95% confidence interval), is presented in Figure 45. Descriptive results showed that the mean max PF angle showed an inconsistent pattern for the YG, as the angle decreased from VS to typical speed, after which point, the mean max PF angle increased for the fast WS, and then decreased again for the VF WS, whereas for the OG, the mean max PF angle was relatively consistent, with the smallest associated marginal error (Figure 45), across WSs. Further, the YG showed greater mean max DF angles across WSs compared to the OG (Figure 45). The YG had a significantly ($p<.05$) decreased mean max PF angle (i.e., significantly greater peak PF) during swing phase at the typical and fast WSs (typical: -56.63°±7.71°; fast: -53.97°±7.04°) compared to the OG (typical: -61.06°±6.73°; fast: -60.33°±5.77°), as shown in Table 21.

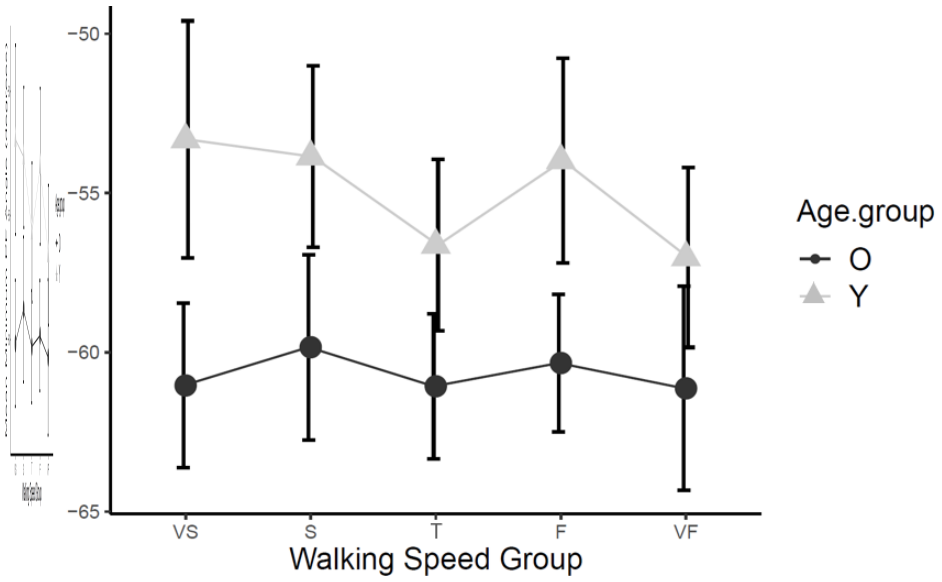


Figure 45. Mean max PF angle of the cal-met during swing phase for the YG and OG across walking speeds at the 95% confidence interval (VS: Very Slow, S: Slow, T: Typical, F: Fast, VF: Very Fast).

Significant differences in time to mean max PF angle ($p<.05$) during swing phase were found between YA and OA as WS increased (Figure 43, Table 21). The YG had a significantly shorter time to mean max PF angle ($p<.05$) across all speeds. For the YG, the max PF occurred at 66.96±8.66 percent GC at the VS speed, decreasing to 60.05±1.90 percent GC at the VF speed. Whereas the OG demonstrated max PF angles at 78.13±12.13 percent GC at the VS speed, decreasing to 63.36±8.42 percent GC at the VF speed.

The mean min plantarflexion (PF) angle across WSs during stance, with error bars (95% confidence interval), is presented in Figure 46. Descriptive results showed that the mean min PF angle (peak) showed an inconsistent pattern for the YG, as the angle decreased from VS to typical WS, after which point, the mean min PF angle increased for the fast speed, and then decreased again for the VF speed. The mean min PF angle for the OG increased as WS increased from VS to fast speed, after which point, began to decrease. Both age groups displayed different trends but similar associated marginal error. In

addition, the YG demonstrated greater mean min PF angles across speeds compared to the OG (Figure 46).

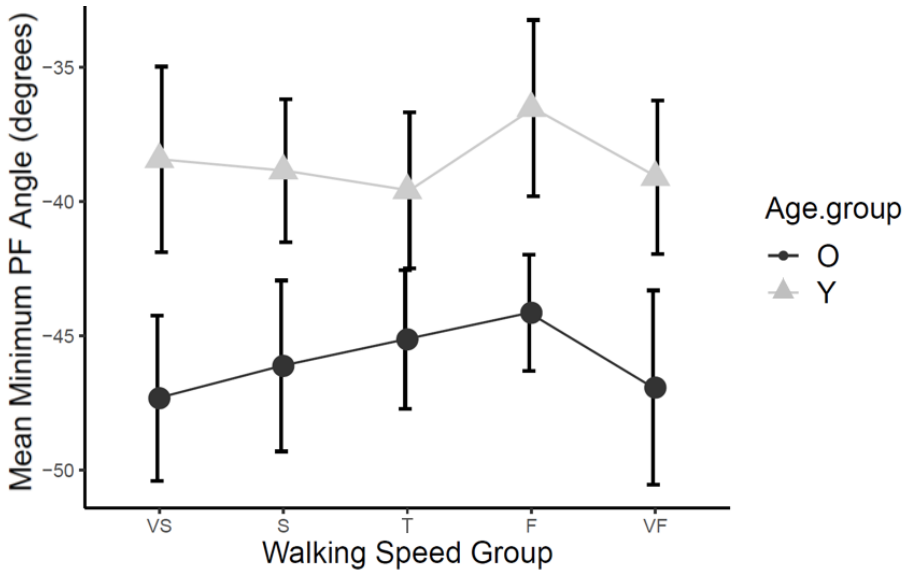


Figure 46. Mean min PF angle of the cal-met during stance phase for the YG and OG across walking speeds at the 95% confidence interval (VS: Very Slow, S: Slow, T: Typical, F: Fast, VF: Very Fast).

The YG had a significantly ($p<.05$) decreased mean min PF angle during stance phase as WS increased from slow to VF WSs (slow: -38.85°±8.08°; VF: -39.09°±8.59°) compared to the OG (slow: -46.11° ±7.53°; VF: -46.92°±8.16°), as shown in Table 21.

Significant differences in time to mean min PF angle ($p<.05$) during stance phase were found between YA and OA as WS increased from VS to typical speed (Figure 43, Table 21). The YG had a significantly shorter time to mean min PF angle ($p<.05$) for the VS, slow, and typical speed. For the YG, the min PF occurred at 49.04±6.97 percent GC at the VS speed, decreasing to 47.25±2.68 percent GC at the typical speed. Whereas the OG demonstrated min PF angles at 55.69±3.52 percent GC at the VS speed, decreasing to 49.18±2.64 percent GC at the typical speed.

The mean min plantarflexion (PF) angle across WSs during swing, with error bars (95% confidence interval), is presented in Figure 47. Descriptive results showed that the mean min PF angle (peak) showed an inconsistent pattern for the YG, as the angle decreased from VS to typical speed, after which point, the mean min PF angle increased for the fast speed, and then decreased again for the VF speed. The mean min PF angle for the OG demonstrated a more consistent pattern, where the angle increased as WS increased from VS to fast speed, after which point, began to decrease (Figure 47). However, both age groups displayed similar associated marginal error. In addition, the YG demonstrated greater mean min PF angles across speeds compared to the OG (Figure 47).

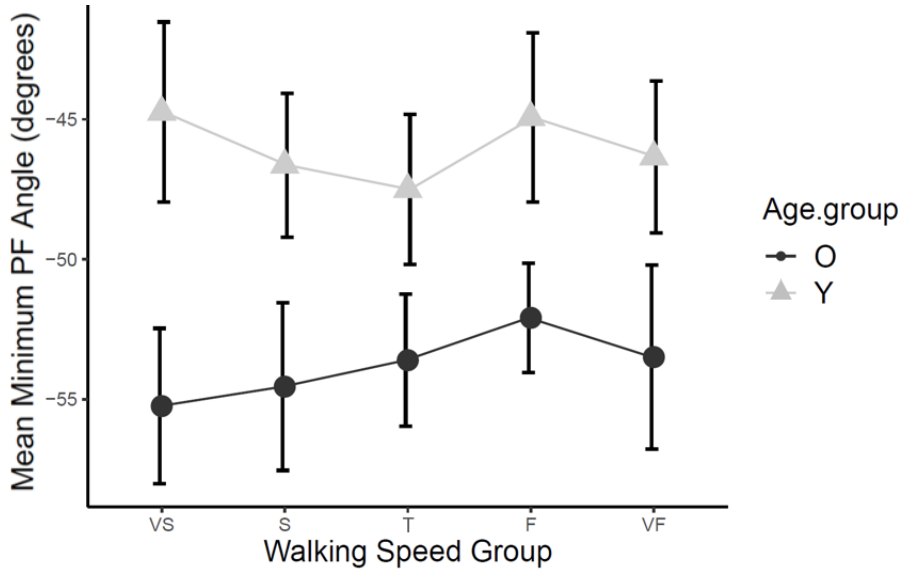


Figure 47. Mean min PF angle of the cal-met during swing phase for the YG and OG across walking speeds at the 95% confidence interval (VS: Very Slow, S: Slow, T: Typical, F: Fast, VF: Very Fast).

The YG had a significantly ($p<.05$) decreased mean min PF angle (i.e., significantly lower peak PF) during swing phase as WS increased (VS: -44.74° ±8.61°; VF: -46.34°±8.14°) compared to the OG (VS: -55.24°±7.95°; VF: -53.49°±7.41°), as shown in Table 21.

Significant differences in time to mean min PF angle ($p<.05$) during swing phase were found between YA and OA for the fast speed only (Figure 43, Table 21). The YG had a significantly longer time to mean min PF angle ($p<.05$) for the fast speed. For the YG, the mean min PF occurred at 94.44±6.32 percent GC at the fast speed, whereas the OG demonstrated a min PF angle at 88.52±10.24 percent GC at the fast speed.

Table 22 presents the significant ($p<.05$) age-related differences in the DF/PF range of motion (ROM) data for the cal-met. In addition, relative DF/PF ROM data for the cal-met are provided in Table 22. The YG displayed the greatest DF/PF ROM (Figure 43) across all speeds during stance and swing compared to the OG. Table 22 presents the between-group differences found for the DF/PF ROM during stance and swing phase.

Table 22. Significant DF/PF ROM data for the cal-met during stance and swing phase across five walking speeds and their respective significant p-values.

DF/PF ROM Calcaneus-Forefoot			
	Mean	± Std	P-value
Very Slow Young Stance	13.51°	0.93°	-
Very Slow Old Stance	12.83°	1.55°	
Slow Young Stance	13.80°	0.50°	-
Slow Old Stance	12.66°	0.61°	
Typical Young Stance	16.09°	0.29°	-
Typical Old Stance	15.15°	0.94°	
Fast Young Stance	16.49°	0.33°	-
Fast Old Stance	15.69°	0.17°	
Very Fast Young Stance	17.49°	0.16°	<.01
Very Fast Old Stance	13.79°	1.10°	
Very Slow Young Swing	8.57°	1.35°	<.01
Very Slow Old Swing	5.79°	0.54°	
Slow Young Swing	7.22°	0.84°	<.05
Slow Old Swing	5.28°	0.19°	
Typical Young Swing	9.12°	0.02°	<.05
Typical Old Swing	7.45°	0.22°	
Fast Young Swing	9.03°	0.41°	-
Fast Old Swing	8.24°	0.56°	
Very Fast Young Swing	10.68°	0.31°	<.01
Very Fast Old Swing	7.63°	0.19°	

Note: Std: Standard deviation.; '-' indicates no significant difference.

The YG exhibited a significantly ($p<.05$) greater DF/PF ROM during stance for the VF speed only (VF: 17.49°±0.16°) compared to the OG (VF: 13.79°±1.10°) as shown in Table 22. During swing phase, the YG exhibited a significantly ($p<.05$) greater DF/PF ROM as WS increased except for the fast speed (VS: 8.57°±1.35°; VF: 10.68°±0.31°) compared to the OG (VS: 5.79°±0.54°; VF: 7.63°±0.19°).

The mean relative angle gait curve for the cal-met segment in the frontal plane is presented in Figure 48. This is the cal-met eversion-inversion (EVE/INV) angle defined by the relative orientation between the calcaneus and the forefoot (metatarsus) segments. The following section focuses on between-group differences. Table 23 presents the significant age-related differences in the mean max and min EVE/INV angles in stance and swing phase as well as their respective time of occurrence as a percentage of GC.

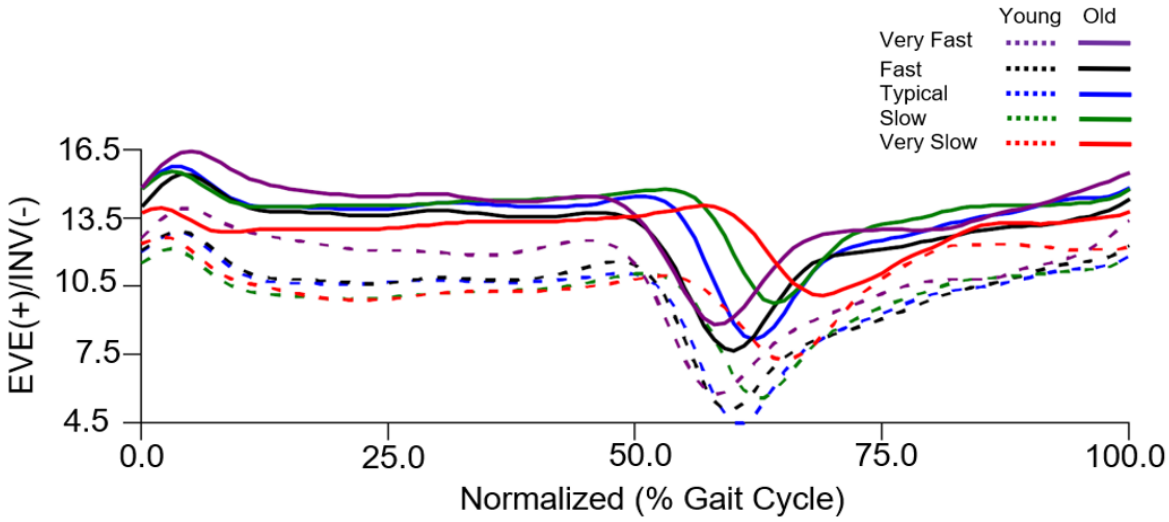


Figure 48. Mean eversion-inversion for the cal-met of the OG versus the YG at each walking speed.

Table 23. Significant p-values of the mean min and max EVE/INV angles (∠) of the cal-met during stance and swing phase, as well as their respective time of occurrence in the gait cycle across five walking speeds.

Walking speed group	Min EVE ∠ in stance p-value	Time to min EVE ∠ in stance p-value	Min EVE ∠ in swing p-value	Time to min EVE ∠ in swing p-value	Max EVE ∠ in stance p-value	Time to max EVE ∠ in stance p-value	Max EVE ∠ in swing p-value	Time to max EVE ∠ in swing p-value
VS	-	<.00001	-	<.0001	-	.03	-	.03
S	.04	<.00001	.04	<.01	.03	-	.04	-
T	<.01	<.01	<.01	.01	.01	-	.01	-
F	.04	.02	.03	<.001	-	-	-	-
VF	-	-	-	.02	-	-	-	-

Note: VS: Very Slow, S: Slow, T: Typical, F: Fast, VF: Very Fast.; '-' indicates no significant difference.

The mean min EVE angle across WSs during stance, with error bars (95% confidence interval), is presented in Figure 49. Descriptive results for the YG showed that the mean min EVE angle during stance decreased from VS to typical WS only, after which point, the mean min EVE angle increased for the fast speed, and then decreased again for the VF WS. The OG showed that the mean min EVE angle increased from VS to slow WS, after which point, the mean min EVE angle in stance phase began to decrease, except for the VF WS. Overall, the OG showed a relatively consistent pattern. Both age groups displayed similar associated marginal error data. In addition, the OG showed greater mean min EVE angles across speeds compared to the YG (Figure 49). The YG had a significantly ($p<.05$) decreased mean min EVE angle during stance phase as WS increased from slow to fast WSs (slow: 5.67°±6.69°; fast: 4.51°±4.35°) compared to the OG (slow: 9.40°±4.85°; fast: 7.29°±6.55°), as shown in Table 23.

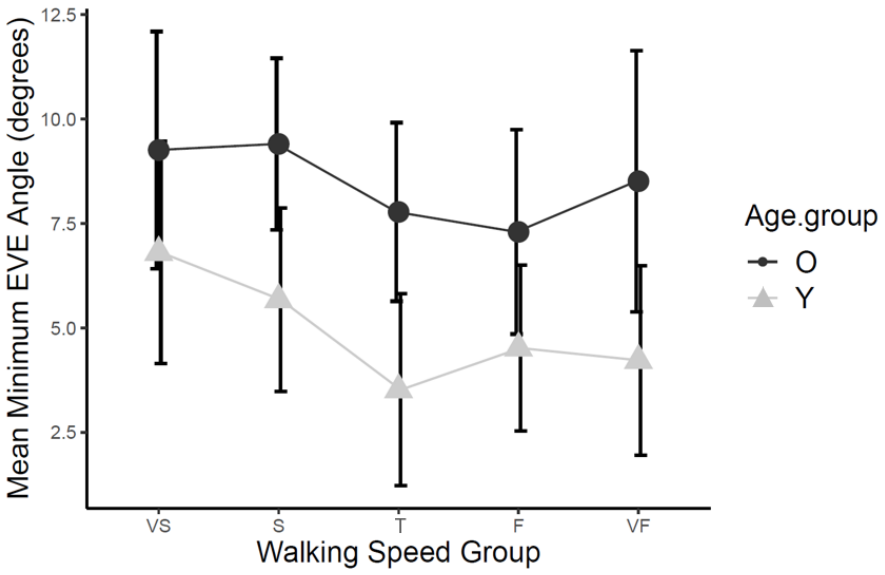


Figure 49. Mean min EVE angle of the cal-met during stance phase for the YG and OG across walking speeds at the 95% confidence interval (VS: Very Slow, S: Slow, T: Typical, F: Fast, VF: Very Fast).

Significant differences in time to mean min EVE angle ($p<.05$) during stance phase were found between YA and OA as WS increased from VS to fast WS (Figure 48, Table 23). The YG had a significantly shorter time to mean min EVE angle ($p<.05$) for the VS, slow, typical, and fast WSs. For the YG, the min EVE occurred at 55.31±14.38 percent GC at the VS speed, increasing to 58.11±4.77 percent GC at the fast speed. Whereas the OG demonstrated min EVE angles at 65.21±13.98 percent GC at the VS speed, decreasing to 59.08±4.90 percent GC at the fast speed.

The mean min EVE angle across WSs during swing, with error bars (95% confidence interval), is presented in Figure 50. Descriptive results for the YG showed that the mean min EVE angle during swing decreased from VS to typical speed only, after which point, the mean min EVE angle increased for the fast speed, and then decreased again for the VF speed. The OG showed that the mean min EVE angle increased from VS to slow speed, after which point, the mean min EVE angle in swing phase began to

decrease, except for the VF speed. Overall, the OG demonstrated a relatively consistent pattern. Both age groups displayed similar associated marginal error data. In addition, the OG demonstrated greater mean min EVE angles across speeds compared to the YG (Figure 50). The YG had a significantly ($p<.05$) decreased mean min EVE angle during swing phase as WS increased from slow to fast WSs (slow: 5.68°±6.68°; fast: 4.44°±4.63°) compared to the OG (slow: 9.26°±4.76°; fast: 7.61°±6.56°), as shown in Table 23. No significant differences in mean min EVE angle during swing were found between YA and OA for the VS and VF WSs (Figure 50).

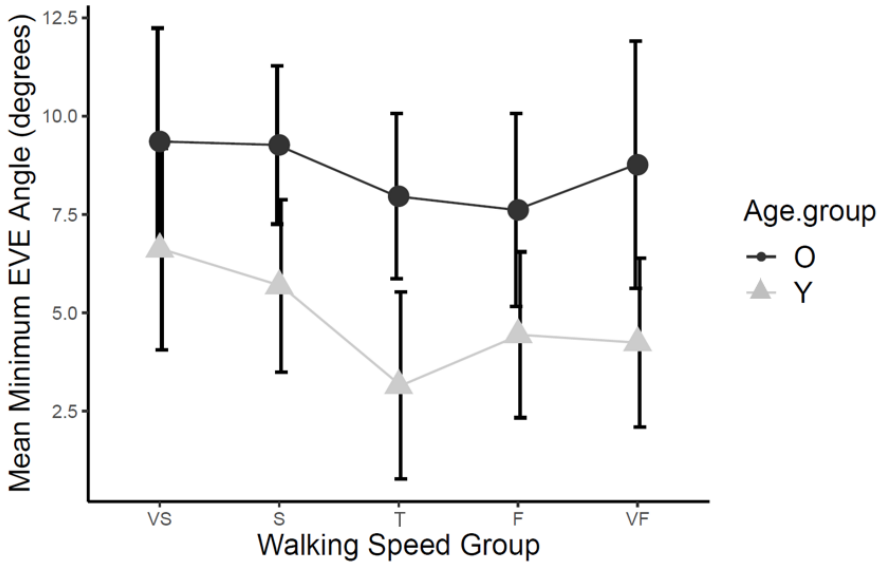


Figure 50. Mean min EVE angle of the cal-met during swing phase for the YG and OG across walking speeds at the 95% confidence interval (VS: Very Slow, S: Slow, T: Typical, F: Fast, VF: Very Fast).

Significant differences in time to mean min EVE angle ($p<.05$) during swing phase were found between YA and OA as WS increased (Figure 48, Table 23). The YG had a significantly shorter time to mean min EVE angle ($p<.05$) across all speeds. For the YG, the min EVE occurred at 65.18±9.04 percent GC at the VS speed, decreasing to 60.43±4.12

percent GC at the VF speed. Whereas the OG demonstrated min EVE angles at 70.59±6.23 percent GC at the VS speed, decreasing to 62.58±5.76 percent GC at the VF speed.

The mean max EVE angle across WSs during stance, with error bars (95% confidence interval), is presented in Figure 51. Descriptive results for the YG showed that the mean max EVE angle during stance decreased from VS to fast speed, after which point, the mean max EVE angle began to increase. The OG showed that the mean max EVE angle increased from VS to typical speed, after which point, the mean max EVE angle in stance decreased for the fast speed, and then increased for the VF speed. Overall, both age groups demonstrated a relatively consistent pattern with similar associated marginal error data. In addition, the OG demonstrated greater mean max EVE angles across speeds compared to the YG (Figure 51).

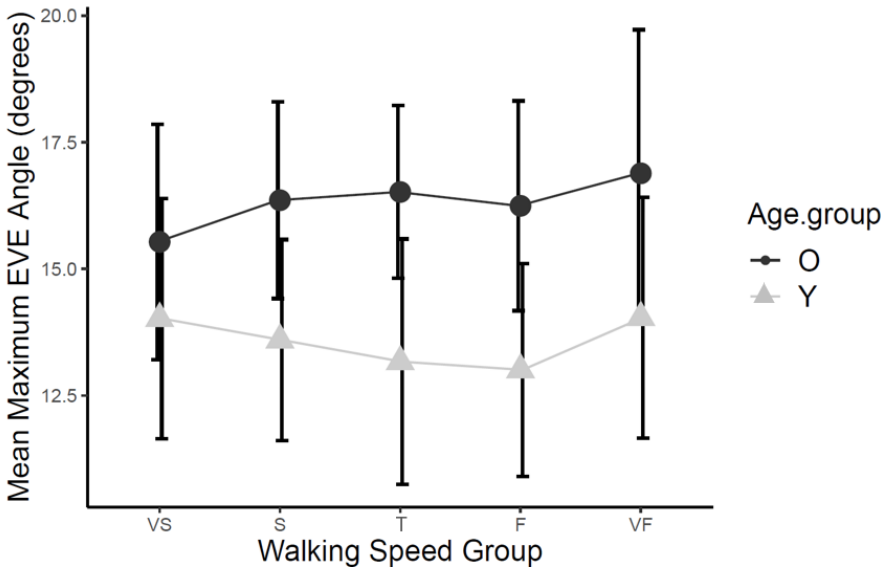


Figure 51. Mean max EVE angle of the cal-met during stance phase for the YG and OG across walking speeds at the 95% confidence interval (VS: Very Slow, S: Slow, T: Typical, F: Fast, VF: Very Fast).

The YG had a significantly ($p<.05$) decreased mean max EVE angle during stance phase as WS increased from slow to typical speed (slow: 13.59°±6.03°; typical: 13.16°±6.94°) compared to the OG (slow: 16.35°±4.59°; typical: 16.51°±5.03°), as shown in Table 23.

Significant differences in time to mean max EVE angle ($p<.05$) during stance phase were found between YA and OA for the VS WS only (Figure 48, Table 23). The YG had a significantly shorter time to mean max EVE angle ($p<.05$) for the VS WS. For the YG, the mean max EVE occurred at 18.78±25.36 percent GC at the VS speed, whereas the OG showed a max EVE angle at 32.88±27.14 percent GC at the VS WS.

The mean max EVE angle across WSs during swing, with error bars (95% confidence interval), is presented in Figure 52. Descriptive results for the YG showed that the mean max EVE angle during swing decreased from VS to typical speed, after which point, the mean max EVE angle began to increase. The OG demonstrated a relatively consistent pattern with a smaller associated marginal error. In addition, the OG demonstrated greater mean min EVE angles across speeds compared to the YG (Figure 52). The YG had a significantly ($p<.05$) decreased mean max EVE angle during swing phase as WS increased from slow to typical speed (slow: 12.37°±6.05°; typical: 11.54°±6.97°) compared to the OG (slow: 14.98°±4.33°; typical: 15.33°±4.96°), as shown in Table 23. No significant differences in mean max EVE angle during swing were found between YA and OA for the VS, fast, and VF WSs.

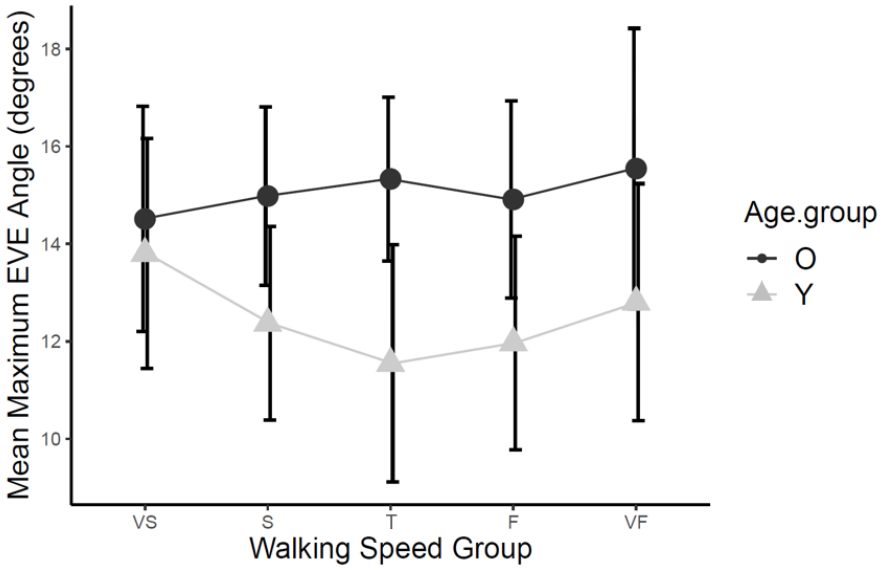


Figure 52. Mean max EVE angle of the cal-met during swing phase for the YG and OG across walking speeds at the 95% confidence interval (VS: Very Slow, S: Slow, T: Typical, F: Fast, VF: Very Fast).

Significant differences in time to mean max EVE angle ($p<.05$) during swing phase were found between YA and OA for the VS speed only (Figure 48, Table 23). The YG had a significantly shorter time to mean max EVE angle ($p<.05$) for the VS speed. For the YG, the mean max EVE occurred at 90.74±8.56 percent GC at the VS WS, whereas the OG demonstrated a max EVE angle at 95.35±5.38 percent GC at the VS WS.

Table 24 presents the significant ($p<.05$) age-related differences in the EVE/INV range of motion (ROM) data for the cal-met. In addition, relative EVE/INV ROM data for the cal-met are provided in Table 24. The YG displayed the greatest EVE/INV ROM (Figure 48) across all speeds during stance and swing compared to the OG. Table 24 presents the between-group differences found for the EVE/INV ROM during stance and swing phase. The YG exhibited a significantly ($p<.05$) greater EVE/INV ROM during stance for the VF speed only (VF: 9.81°±0.34°) compared to the OG (VF: 8.37°±0.66°) as

shown in Table 24. During swing phase, the YG exhibited a significantly ($p<.05$) greater EVE/INV ROM for the VS and VF speeds (VS: 7.18°±0.53°; VF: 8.56°±0.86°) compared to the OG (VS: 5.14°±1.62°; VF: 6.78°±0.58°) as shown in Table 24.

Table 24. Significant EVE/INV ROM data for the cal-met during stance and swing phase across five walking speeds and their respective significant p-values.

EVE/INV ROM Calcaneus-Forefoot			
	Mean	± Std	P-value
Very Slow Young Stance	7.21°	0.76°	-
Very Slow Old Stance	6.27°	1.47°	
Slow Young Stance	7.91°	0.65°	-
Slow Old Stance	6.95°	0.26°	
Typical Young Stance	9.64°	0.36°	-
Typical Old Stance	8.74°	1.28°	
Fast Young Stance	8.48°	0.26°	-
Fast Old Stance	8.94°	1.00°	
Very Fast Young Stance	9.81°	0.34°	<.05
Very Fast Old Stance	8.37°	0.66°	
Very Slow Young Swing	7.18°	0.53°	<.01
Very Slow Old Swing	5.15°	1.62°	
Slow Young Swing	6.68°	0.63°	-
Slow Old Swing	5.71°	0.43°	
Typical Young Swing	8.39°	0.17°	-
Typical Old Swing	7.36°	1.24°	
Fast Young Swing	7.52°	0.18°	-
Fast Old Swing	7.29°	1.14°	
Very Fast Young Swing	8.56°	0.86°	<.05
Very Fast Old Swing	6.78°	0.58°	

Note: Std: Standard deviation.; '-' indicates no significant difference.

The mean relative angle gait curve for the cal-met segment in the transverse plane is presented in Figure 53. This is the cal-met adduction-abduction (ADD/ABD) angle defined by the relative orientation between the calcaneus and the forefoot (metatarsus) segments. The following section focuses on between-group differences. Table 25 presents the significant age-related differences in the mean max and min ADD/ABD angles in stance and swing phase as well as their respective time of occurrence as a percentage of GC.

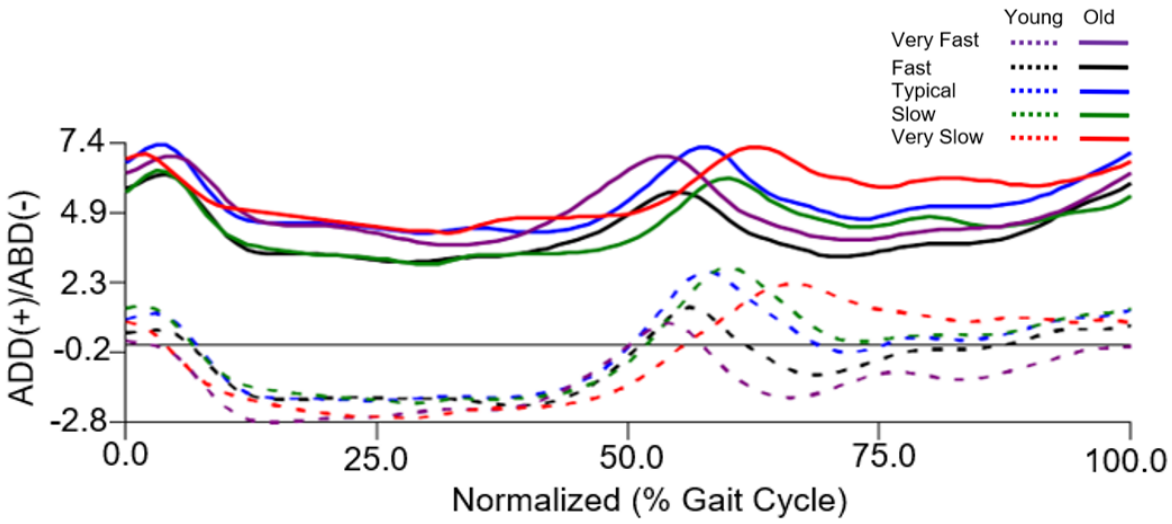


Figure 53. Mean adduction-abduction for the cal-met of the OG versus the YG at each walking speed.

Table 25. Significant p-values of the mean min and max ADD/ABD angles (∠) of the cal-met during stance and swing phase, as well as their respective time of occurrence in the gait cycle across five walking speeds.

Walking speed group	Min ADD ∠ in stance p-value	Time to min ADD ∠ in stance p-value	Min ADD ∠ in swing p-value	Time to min ADD ∠ in swing p-value	Max ADD ∠ in stance p-value	Time to max ADD ∠ in stance p-value	Max ADD ∠ in swing p-value	Time to max ADD ∠ in swing p-value
VS	<.0001	-	.02	-	.03	-	-	<.01
S	<.01	-	.03	-	.04	-	-	-
T	<.01	-	<.01	-	<.01	-	.01	.01
F	<.01	-	.03	-	.02	-	.02	<.01
VF	<.01	.03	<.01	-	<.01	-	.03	.04

Note: VS: Very Slow, S: Slow, T: Typical, F: Fast, VF: Very Fast.; '-' indicates no significant difference.

The mean min adduction (ADD) angle across WSs during stance, with error bars (95% confidence interval), is presented in Figure 54. Descriptive results showed that the mean min ADD angle for the YG increased from VS to slow speed, after which point, the mean min ADD angle was relatively consistent, as shown by the marginal error (Figure 54). The mean min ADD angle decreased from VS to slow speed for the OG, after which point, the angle was relatively consistent (Figure 54). In addition, the OG demonstrated greater mean min ADD angles across speeds compared to the YG (Figure 54). The YG had

a significantly (p<.05) decreased mean min ADD angle during stance phase as WS increased (VS: -3.87°±5.65°; VF: -3.07°±5.23°) compared to the OG (VS: 4.57°±7.35°; VF: 2.62°±6.66°), as shown in Table 25.

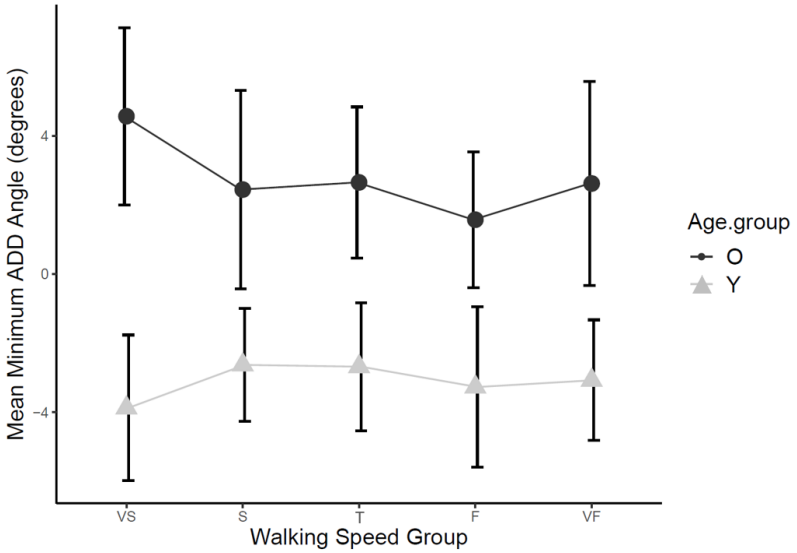


Figure 54. Mean min ADD angle of the cal-met during stance phase for the YG and OG across walking speeds at the 95% confidence interval (VS: Very Slow, S: Slow, T: Typical, F: Fast, VF: Very Fast).

Significant differences in time to mean min ADD angle (p<.05) during stance phase were found between YA and OA for the VF speed only (Figure 53, Table 25). The YG had a significantly shorter time to mean min ADD angle (p<.05) for the VF WS. For the YG, the mean min ADD occurred at 33.09±13.53 percent GC at the VF WS, whereas the OG showed a min ADD angle at 35.63±18.81 percent GC at the VF WS.

The mean min adduction (ADD) angle across WSs during swing, with error bars (95% confidence interval), is presented in Figure 55. Descriptive results showed that the mean min ADD angle for the YG increased from VS to slow WS, after which point, the mean min ADD angle began to decrease (Figure 55). The mean min ADD angle decreased

from VS to slow WS for the OG, after which point, the angle was relatively consistent. However, the OG demonstrated a larger associated marginal error. In addition, the OG showed greater mean min ADD angles across speeds compared to the YG (Figure 55).

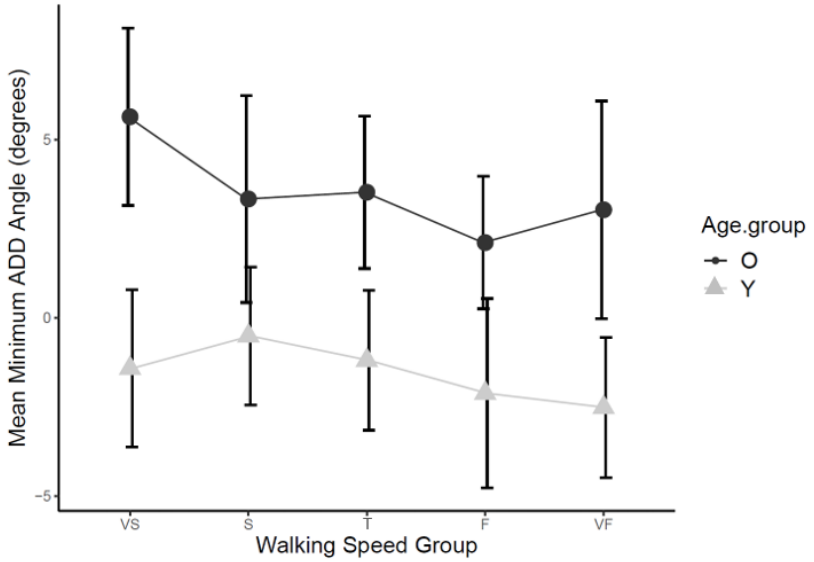


Figure 55. Mean min ADD angle of the cal-met during swing phase for the YG and OG across walking speeds at the 95% confidence interval (VS: Very Slow, S: Slow, T: Typical, F: Fast, VF: Very Fast).

The YG had a significantly ($p<.05$) decreased mean min ADD angle during swing phase as WS increased (VS: -1.41°±5.91°; VF: -2.51°±5.91°) compared to the OG (VS: 5.64°±7.13°; VF: 3.03°±6.88°), as shown in Table 25.

The mean max adduction (ADD) angle across WSs during stance, with error bars (95% confidence interval), is presented in Figure 56. Descriptive results showed that the mean max ADD angle increased from VS to slow speed for the YG, after which point, the mean max ADD angle in stance phase began to decrease with increasing speed, except for the VF speed (Figure 56). Overall, both age groups demonstrated relatively consistent patterns of variability for the mean max ADD angle at each speed, and similar associated

marginal error. In addition, the OG demonstrated greater mean max ADD angles across speeds compared to the YG (Figure 56).

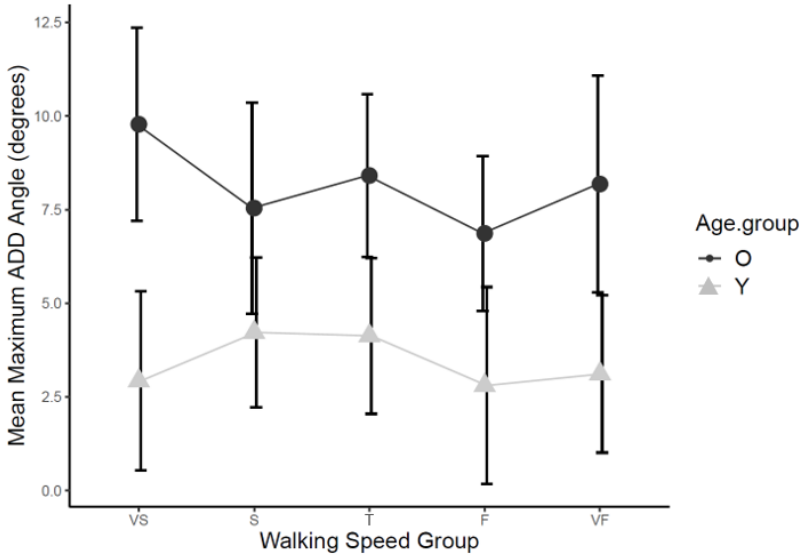


Figure 56. Mean max ADD angle of the cal-met during stance phase for the YG and OG across walking speeds at the 95% confidence interval (VS: Very Slow, S: Slow, T: Typical, F: Fast, VF: Very Fast).

The YG had a significantly ($p<.05$) decreased mean max ADD angle during stance phase as WS increased (VS: 2.92°±6.39°; VF: 3.11°±6.30°) compared to the OG (VS: 9.77°±7.39°; VF: 8.18°±6.52°).

The mean max adduction (ADD) angle across WSs during swing, with error bars (95% confidence interval), is presented in Figure 57. Descriptive results showed that the mean max ADD angle increased from VS to slow speed for the YG, after which point, the mean max ADD angle in stance phase began to decrease with increasing speed, except for the VF speed (Figure 57). Overall, the YG demonstrated relatively consistent pattern of variability for the mean max ADD angle. The mean max ADD angle showed a less consistent pattern for the OG, as the angle decreased and increased, in that order, as WS

increased. In addition, the OG demonstrated greater mean max ADD angles across speeds compared to the YG (Figure 57).

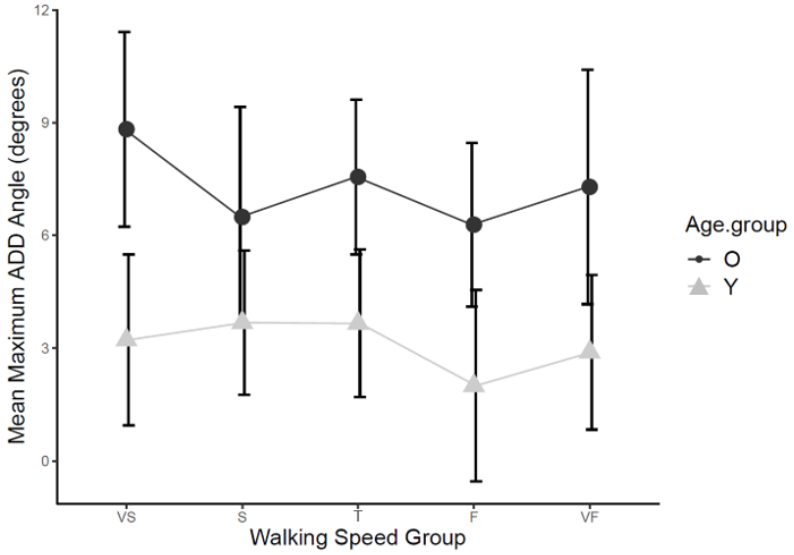


Figure 57. Mean max ADD angle of the cal-met during swing phase for the YG and OG across walking speeds at the 95% confidence interval (VS: Very Slow, S: Slow, T: Typical, F: Fast, VF: Very Fast).

The YG had a significantly ($p<.05$) decreased mean max ADD angle during swing phase as WS increased from typical to VF WS (typical: 3.65°±5.62°; VF: 2.89°±6.17°) compared to the OG (typical: 7.55°±6.08°; VF: 7.29°±7.03°), as shown in Table 25.

Significant differences in time to mean max ADD angle ($p<.05$) during swing phase were found between YA and OA as WS increased, except for the slow speed (Figure 53, Table 25). The YG had a significantly shorter time to mean max ADD angle ($p<.05$) for the VS, typical, fast, and VF WSs. For the YG, the max ADD occurred at 77.81±13.12 percent GC at the VS speed, increasing to 85.78±13.55 percent GC at the VF speed. Whereas, the OG demonstrated max ADD angles at 86.84±12.71 percent GC at the VS speed, increasing to 92.18±12.57 percent GC at the VF speed.

Table 26 presents the significant (p<.05) age-related differences in the ADD/ABD range of motion (ROM) data for the cal-met during stance and swing phase. In addition, relative ADD/ABD ROM data for the cal-met are provided in Table 26.

Table 26. Significant ADD/ABD ROM data for the cal-met during stance and swing phase across five walking speeds and their respective significant p-values.

ABD/ADD ROM Calcaneus-Forefoot			
	Mean	± Std	P-value
Very Slow Young Stance	6.80°	0.73°	<.01
Very Slow Old Stance	5.20°	0.04°	
Slow Young Stance	6.85°	1.11°	<.01
Slow Old Stance	5.09°	0.14°	
Typical Young Stance	6.81°	0.64°	<.05
Typical Old Stance	5.75°	0.04°	
Fast Young Stance	6.07°	0.68°	-
Fast Old Stance	5.28°	0.26°	
Very Fast Young Stance	6.18°	1.06°	-
Very Fast Old Stance	5.55°	0.13°	
Very Slow Young Swing	4.63°	0.17°	<.01
Very Slow Old Swing	3.18°	0.28°	
Slow Young Swing	4.18°	0.03°	<.05
Slow Old Swing	3.15°	0.04°	
Typical Young Swing	4.84°	0.01°	-
Typical Old Swing	4.03°	0.23°	
Fast Young Swing	4.11°	0.24°	-
Fast Old Swing	4.17°	0.86°	
Very Fast Young Swing	5.40°	0.25°	-
Very Fast Old Swing	4.25°	0.14°	

Note: Std: Standard deviation.; '-' indicates no significant difference.

The YG showed the greatest ADD/ABD ROM (Figure 53) across all WSs during stance and swing compared to the OG, except for the fast WS during swing. The YG showed a significantly (p<.05) greater ADD/ABD ROM during stance as WS increased from VS to typical speed (VS: 6.80°±0.73°; typical: 6.81°±0.64°) compared to the OG (VS: 5.20°±0.04°; typical: 5.75°±0.04°) as shown in Table 26. During swing phase, the YG showed a significantly (p<.05) greater ADD/ABD ROM for the VS and slow WSs (VS: 4.63°±0.17°; slow: 4.18°±0.03°) compared to the OG (VS: 3.18°±0.28°; slow:

3.15°±0.04°) as shown in Table 26. During VF speed walking, the ADD/ABD ROM for the YA and OA increased most in the cal-met during swing.

4.1.8 Summary of MSF kinematics' results

When the speed effect is being considered, there are significant differences in MSF angles between YA and OA. The key findings of the present study are as follows:

- Most differences in MSF angles between age groups were found in the sagittal and transverse plane.
- In the sagittal plane, the mean max shank-foot PF angle in stance and swing were significantly increased for the YG as a function of speed compared to the OG. Further, the mean max shank-foot DF angle in stance and swing were significantly decreased for the YA as a function of speed compared to the OA. The mean max mid-cal DF angle in swing was significantly increased for the YG for the VS speed only. The mean min sha-cal PF angle in both stance and swing were significantly increased for the YA as a function of speed compared to the OA. Further, the mean max sha-cal DF angle in stance and swing were significantly decreased for the YA as a function of speed compared to the OA. These latter results were similar to the shank-foot angles in the sagittal plane. The mean min and max mid-met PF angle in stance and swing were significantly decreased for the YG as a function of speed compared to the OG. Further, the mean min PF cal-met angle in stance and swing were significantly decreased for the YG, whereas the mean max PF cal-met angle in stance and swing were significantly increased for the YG as a function of speed compared to the OG.

- In the frontal plane, the mean min and max EVE mid-cal angle in stance and swing were significantly increased for the YA as WS increased from VS to VF speed compared to the OA. Further, the mean min EVE cal-met angle in stance and swing were significantly decreased for the YG, whereas the mean max EVE cal-met angle in stance and swing were significantly increased for the YG as a function of speed compared to the OG.
- In the transverse plane, the mean min and max ADD shank-foot angles in stance and swing were significantly increased for the YG as a function of speed compared to the OG. Similarly, the mean min and max ADD mid-cal angles in stance and swing phase were significantly increased for the YA as a function of speed compared to the OA. Conversely, the mean min and max ADD sha-cal angles in stance and swing were significantly decreased for the YG compared to the OG. Further, the mean min and max ABD mid-met angles in stance and swing were significantly increased for the YG as a function of speed compared to the OG. The mean min and max ADD calcaneus-metatarsus angles in stance and swing were significantly decreased for the YG compared to the OG.
- The mean min and max relative angles of the sha-cal and foot-shank in the sagittal and transverse plane were found very similar.

4.1.9 Age-related Differences in Planar Angles of the Foot

4.1.9.1 Age-related Differences in the F2Pt Planar Angle of the Foot

The mean relative angle gait curve for the F2Pt planar angle is presented in Figure 58. This is the angle defined between the projections of the line segments of the first distal and proximal metatarsal, and the first distal metatarsal and hallux segments. The following

section focuses on between-group differences. Table 27 presents the significant age-related differences in the mean max and min F2Pt angles in stance phase as well as their respective time of occurrence as a percentage of GC.

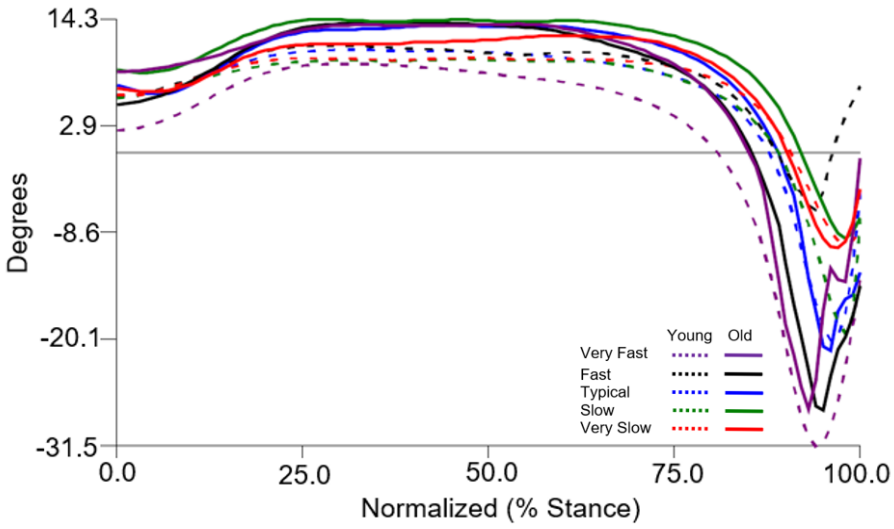


Figure 58. Mean F2Pt planar angle of the OG versus the YG at each walking speed.

Table 27. Significant p-values of the mean min and max F2Pt angles (∠) during stance phase, as well as their respective time of occurrence in the gait cycle across five walking speeds.

Walking speed group	Min F2Pt ∠ p-value	Time to min F2Pt ∠ p-value	Max F2Pt ∠ p-value	Time to max F2Pt ∠ p-value
VS	-	.02	-	.04
S	-	-	-	.02
T	-	-	-	<.01
F	-	-	-	-
VF	-	-	<.01	<.001

Note: VS: Very Slow, S: Slow, T: Typical, F: Fast, VF: Very Fast.; '-' indicates no significant difference.

The mean max F2Pt angle across WSs during stance, with error bars (95% confidence interval), is presented in Figure 59. Descriptive results showed that the mean max F2Pt angle (peak) increased from VS to fast WS for the YG, after which point, the mean max F2Pt angle in stance phase began to decrease (Figure 59). The mean max F2Pt angle showed a relatively inconsistent pattern for the OG, as the angle increased from VS to slow WS, then decreased at the typical WS, after which point, it began to increase. In

addition, the OG showed greater mean max F2Pt angles across speeds, except for the typical WS, compared to the YG. However, the OG had the largest associated marginal error (Figure 59). The YG had a significantly ($p<.05$) decreased mean max F2Pt angle during stance phase (i.e., significantly lower peak F2Pt) at the VF WS (VF: 11.79°±9.51°) compared to the OG (VF: 28.12°±35.85°).

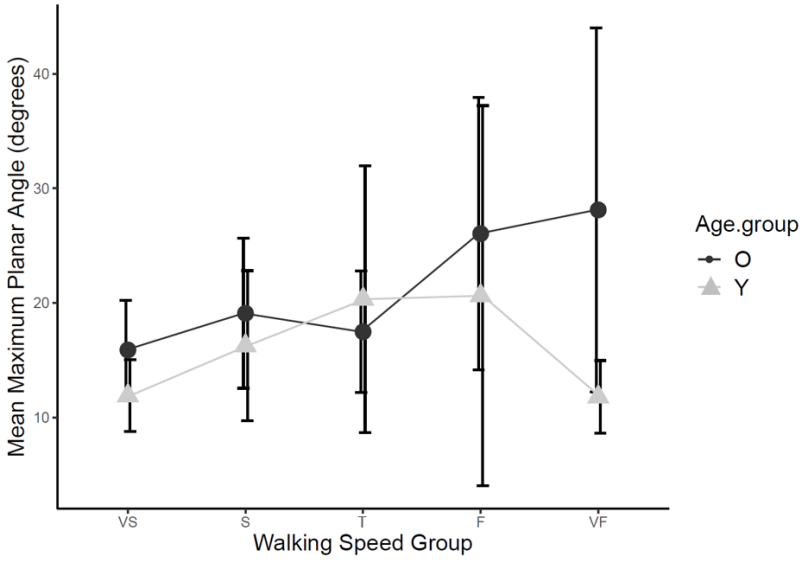


Figure 59. Mean max F2Pt angle during stance phase for the YG and OG across walking speeds at the 95% confidence interval (VS: Very Slow, S: Slow, T: Typical, F: Fast, VF: Very Fast).

Significant differences in time to mean max F2Pt angle ($p<.05$) during stance phase were found between YA and OA as WS increased, except for the fast speed (Figure 58, Table 27). The YG had a significantly shorter time to mean max F2Pt angle ($p<.05$) for the VS, slow, typical, and VF WSs. For the YG, the max F2Pt occurred at 27.79±15.54 percent GC at the VS speed, decreasing to 24.27±14.83 percent GC at the VF speed. Whereas the OG demonstrated max F2Pt angles at 37.83±21.99 percent GC at the VS speed, increasing to 38.32±17.06 percent GC at the VF speed.

Significant differences in time to mean min F2Pt angle ($p<.05$) during stance phase were found between YA and OA for the VS speed only (Figure 58, Table 27). The YG had a longer time to mean min F2Pt angle ($p<.05$) for the VS WS. For the YG, the mean min F2Pt occurred at 60.14±12.49 percent GC at the VS WS, whereas the OG demonstrated a min F2Pt angle at 56.96±22.61 percent GC at the VS WS.

Table 28 presents the significant ($p<.05$) age-related differences in the range of motion (ROM) data for the F2Pt planar angle. In addition, relative ROM data for the F2Pt planar angle are provided in Table 28. The OG displayed the greatest F2Pt ROM (Figure 58) across all speeds during stance compared to the YG. Table 28 presents the between-group differences found for the F2Pt ROM during stance phase. The YG exhibited a significantly ($p<.05$) reduced F2Pt ROM during stance for the fast speed only (fast: 33.22°±17.41°) compared to the OG (fast: 67.68°±23.40°) as shown in Table 28.

Table 28. Significant F2Pt ROM data during stance phase across five walking speeds and their respective significant p-values.

F2Pt Planar Angle ROM			
	Mean	± Std	P-value
Very Slow Young Stance	23.94°	8.01°	-
Very Slow Old Stance	32.24°	22.00°	
Slow Young Stance	33.87°	12.97°	-
Slow Old Stance	35.17°	14.65°	
Typical Young Stance	48.13°	5.24°	-
Typical Old Stance	50.20°	25.61°	
Fast Young Stance	33.22°	17.41°	<.05
Fast Old Stance	67.68°	23.40°	
Very Fast Young Stance	55.09°	32.62°	-
Very Fast Old Stance	63.24°	16.03°	

Note: Std: Standard deviation.; '-' indicates no significant difference.

4.1.9.2 Age-related Differences in the V2G Planar Angle of the Foot

The mean relative angle gait curve for the V2G planar angle is presented in Figure 60. This is the angle defined between the line segments of the fifth distal and proximal metatarsal, and the ground. The following section focuses on between-group differences. Table 29 presents the significant age-related differences in the mean max and min V2G angles in stance phase as well as their respective time of occurrence as a percentage of GC.

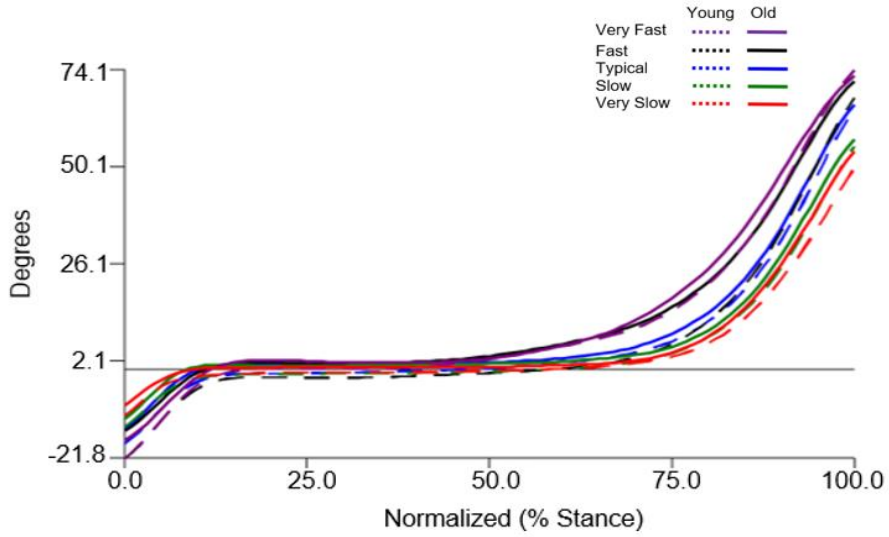


Figure 60. Mean V2G planar angle of the OG versus the YG at each walking speed.

Table 29. Significant p-values of the mean min and max V2G angles (∠) during stance phase, as well as their respective time of occurrence in the gait cycle across five walking speeds.

Walking speed group	Max V2G ∠ p-value	Time to max V2G ∠ p-value	Min V2G ∠ p-value	Time to min V2G ∠ p-value
VS	-	-	-	<.0001
S	-	-	-	.01
T	-	-	-	<.01
F	.03	-	-	.01
VF	-	-	-	.02

Note: VS: Very Slow, S: Slow, T: Typical, F: Fast, VF: Very Fast.; '-' indicates no significant difference.

The mean max V2G angle across WSs during stance, with error bars (95% confidence interval), is presented in Figure 61. Descriptive results showed that the mean

max V2G angle decreased as WS increased for both groups (Figure 61). In addition, the OG demonstrated greater mean max V2G angles across speeds compared to the YG, with a larger associated marginal error (Figure 61).

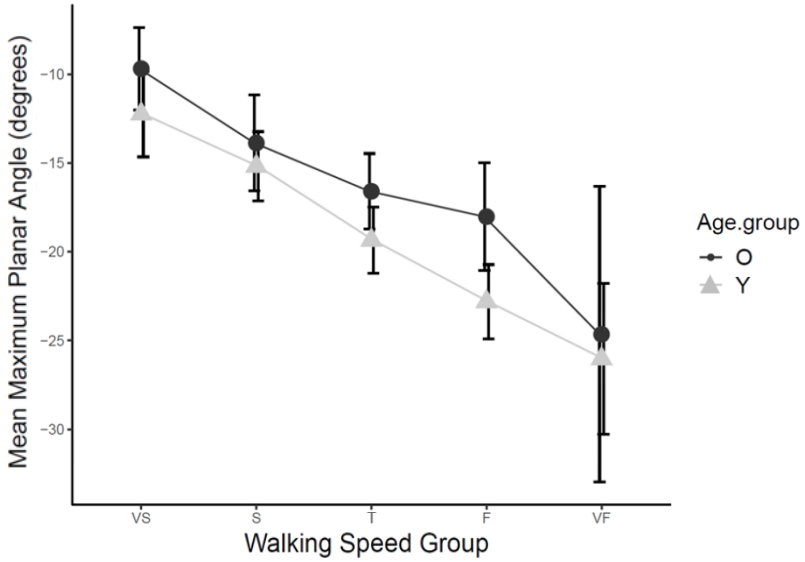


Figure 61. Mean max V2G angle during stance phase for the YG and OG across walking speeds at the 95% confidence interval (VS: Very Slow, S: Slow, T: Typical, F: Fast, VF: Very Fast).

The YG had a significantly ($p<.05$) increased mean max V2G angle during stance phase for the fast WS (fast: -22.81±4.59°) compared to the OG (fast: -18.02°±8.12°), as shown in Table 29.

Significant differences in time to mean min V2G angle ($p<.05$) during stance phase were found between YA and OA as WS increased (Figure 60, Table 29). The YG had a significantly shorter time to mean min V2G angle ($p<.05$) across all speeds. For the YG, the min V2G occurred at 64.45±2.25 percent GC at the VS speed, decreasing to 58.49±2.31 percent GC at the VF speed. Whereas the OG demonstrated min V2G angles at 68.00±7.98 percent GC at the VS speed, decreasing to 59.84±2.35 percent GC at the VF speed.

There were no significant ($p<.05$) age-related differences in the ROM for the V2G planar angle during stance or swing between groups.

4.1.9.3 Age-related Differences in the F2G Planar Angle of the Foot

The mean relative angle gait curve for the F2G planar angle is presented in Figure 62. This is the angle defined between the line segments of the first distal and proximal metatarsal, and the ground. The following section focuses on between-group differences. Table 30 presents the significant age-related differences in the mean max and min F2G angles in stance phase as well as their respective time of occurrence as a percentage of GC.

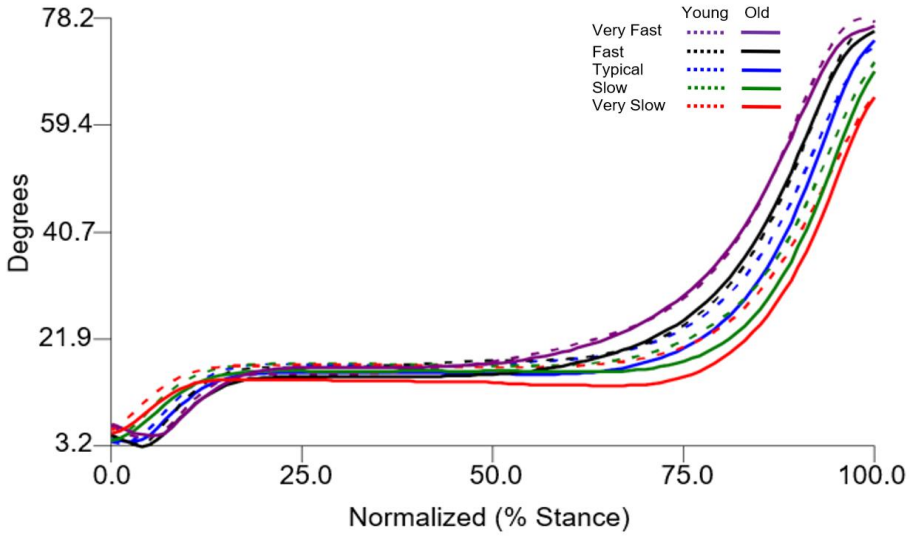


Figure 62. Mean F2G planar angle of the OG versus the YG at each walking speed.

Table 30. Significant p-values of the mean min and max F2G angles (∠) during stance phase, as well as their respective time of occurrence in the gait cycle across five walking speeds.

Walking speed group	Min F2G ∠ p-value	Time to min F2G ∠ p-value	Max F2G ∠ p-value	Time to max F2G ∠ p-value
VS	-	-	-	<.0001
S	-	-	-	.01
T	-	-	-	<.01
F	-	-	-	-
VF	-	-	-	.02

Note: VS: Very Slow, S: Slow, T: Typical, F: Fast, VF: Very Fast.; '-' indicates no significant difference.

Significant differences in time to mean max F2G angle ($p<.05$) during stance phase were found between YA and OA as WS increased, except for the fast speed (Figure 62, Table 30). The YG had a significantly shorter time to mean max F2G angle ($p<.05$) for the VS, slow, typical, and very fast WSs. For the YG, the max F2G occurred at 64.09±2.77 percent GC at the VS WS, decreasing to 56.10±5.74 percent GC at the VF WS. Whereas the OG showed max V2G angles at 68.11±6.93 percent GC at the VS WS, decreasing to 58.63±2.96 percent GC at the VF WS. There were no significant ($p>0.05$) age-related differences in the ROM for the F2G angle during stance or swing between YA and OA.

4.1.9.4 Age-related Differences in the S2G Planar Angle of the Foot

The mean relative angle gait curve for the S2G planar angle is presented in Figure 63. This is the angle defined between the line segments of the second distal and proximal metatarsal, and the ground. The following section focuses on between-group differences. Table 31 presents the significant age-related differences in the mean max and min S2G angles in stance phase as well as their respective time of occurrence as a percentage of GC.

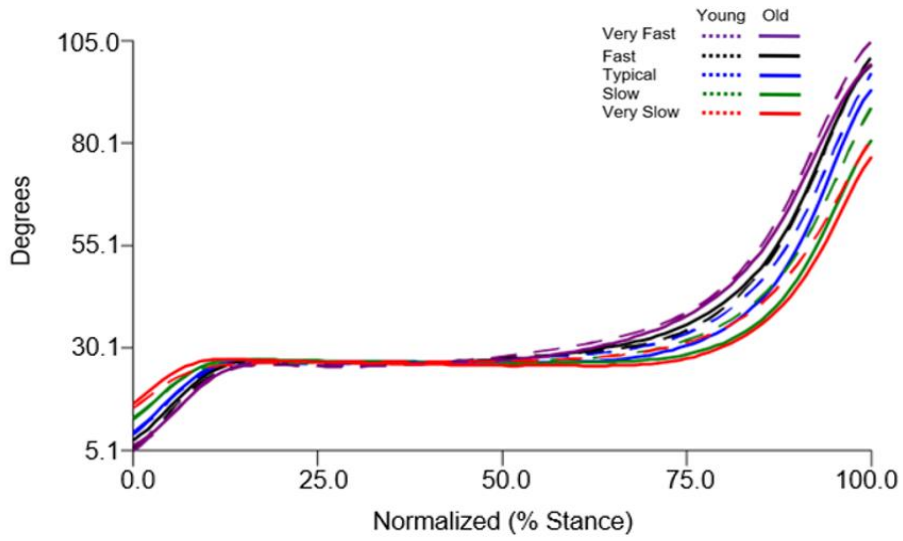


Figure 63. Mean S2G planar angle of the OG versus the YG at each walking speed.

Table 31. Significant p-values of the mean min and max S2G angles (∠) during stance phase, as well as their respective time of occurrence in the gait cycle across five walking speeds.

Walking speed group	Min S2G ∠ p-value	Time to min S2G ∠ p-value	Max S2G ∠ p-value	Time to max S2G ∠ p-value
VS	-	-	-	<.0001
S	-	-	-	.01
T	-	-	-	<.01
F	-	-	-	-
VF	-	-	-	-

Note: VS: Very Slow, S: Slow, T: Typical, F: Fast, VF: Very Fast.; '-' indicates no significant difference.

Significant differences in time to mean max S2G angle ($p<.05$) during stance phase were found between YA and OA as WS increased from VS to typical speed (Figure 63, Table 31). The YG had a significantly shorter time to mean max S2G angle ($p<.05$) for the VS, slow, and typical WSs. For the YG, the max S2G occurred at 64.01±2.86 percent GC at the VS speed, decreasing to 59.96±1.85 percent GC at the typical speed. Whereas the OG demonstrated max S2G angles at 67.70±8.14 percent GC at the VS speed, decreasing to 60.93±3.45 percent GC at the typical speed.

There were no significant ($p<.05$) age-related differences in the ROM for the S2G planar angle during stance or swing between YA and OA.

4.1.9.5 Age-related Differences in the F2Ps Planar Angle of the Foot

The mean relative angle gait curve for the F2Ps planar angle is presented in Figure 64. This is the angle defined between the line segments of the first distal and proximal metatarsal, and the first distal metatarsal and the hallux, i.e., dorsiflexion of the first metatarso-phalangeal joint. The following section focuses on between-group differences. Table 32 presents the significant age-related differences in the mean max and min F2Ps angles in stance phase as well as their respective time of occurrence as a percentage of GC.

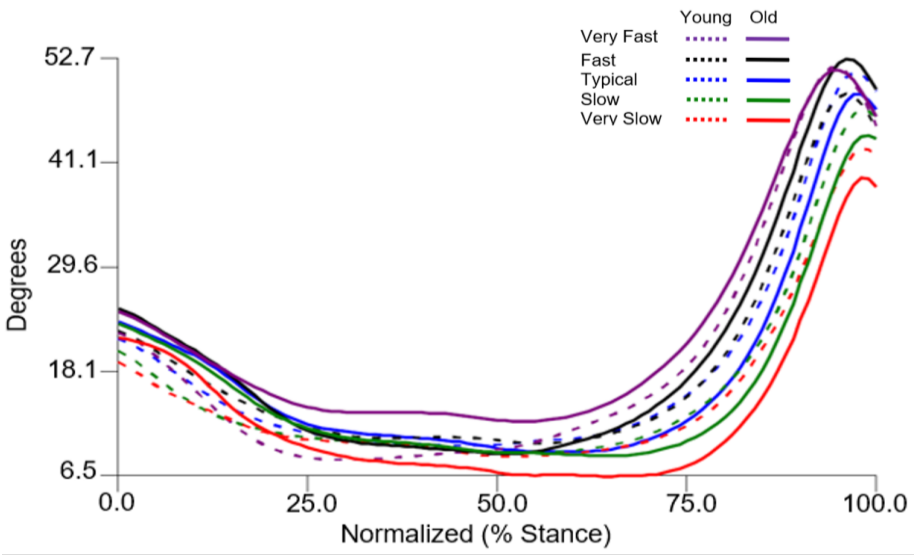


Figure 64. Mean F2Ps planar angle of the OG versus the YG at each walking speed.

Table 32. Significant p-values of the mean min and max F2Ps angles (∠) during stance phase, as well as their respective time of occurrence in the gait cycle across five walking speeds.

Walking speed group	Min F2Ps ∠ p-value	Time to min F2Ps ∠ p-value	Max F2Ps ∠ p-value	Time to max F2Ps ∠ p-value
VS	-	<.0001	-	<.0001
S	-	.03	-	.03
T	-	<.01	-	<.01
F	-	-	-	.03
VF	-	.03	-	-

Note: VS: Very Slow, S: Slow, T: Typical, F: Fast, VF: Very Fast.; '-' indicates no significant difference.

Significant differences in time to mean min F2Ps angle ($p<.05$) during stance phase were found between YA and OA as WS increased, except for the fast speed (Figure 64, Table 32). The YG had a significantly shorter time to mean min F2Ps angle ($p<.05$) for the VS, slow, typical, and VF WSs. For the YG, the min F2Ps occurred at 27.74±11.66 percent GC at the VS speed, decreasing to 22.56±9.68 percent GC at the VF speed. Whereas the OG demonstrated min F2Ps angles at 42.25±7.19 percent GC at the VS speed, decreasing to 28.27±9.81 percent GC at the VF speed.

Significant differences in time to mean max F2Ps angle ($p<.05$) during stance phase were found between YA and OA as WS increased, except for the VF speed (Figure 64, Table 32). The YG had a significantly shorter time to mean max F2Ps angle ($p<.05$) for the VS, slow, typical, and fast WSs. For the YG, the max F2Ps occurred at 63.07±3.02 percent GC at the VS speed, decreasing to 56.06±7.33 percent GC at the fast speed. Whereas the OG demonstrated max F2Ps angles at 66.03±11.01 percent GC at the VS speed, decreasing to 57.59±6.35 percent GC at the fast speed.

Table 33 presents the significant ($p<.05$) age-related differences in the range of motion (ROM) data for the F2Ps planar angle. In addition, relative ROM data for the F2Ps planar angle are provided in Table 33. The YG displayed the greatest F2Ps ROM (Figure 64) across all speeds during stance compared to the OG, except for the fast speed. Table 33 presents the between-group differences found for the F2Ps ROM during stance phase. The YG exhibited a significantly ($p<.05$) reduced F2Ps ROM during stance for the fast speed only (fast: 37.88°±9.18°) compared to the OG (fast: 45.87°±2.68°).

Table 33. Significant F2Ps ROM data for the cal-met during stance phase across five walking speeds.

F2Ps Planar Angle ROM			
	Mean	± Std	P-value
Very Slow Young Stance	37.78°	2.81°	-
Very Slow Old Stance	35.22°	4.06°	
Slow Young Stance	40.12°	4.77°	-
Slow Old Stance	38.40°	3.27°	
Typical Young Stance	43.68°	3.92°	-
Typical Old Stance	41.99°	3.29°	
Fast Young Stance	37.88°	9.18°	<.05
Fast Old Stance	45.87°	2.68°	
Very Fast Young Stance	46.88°	9.50°	-
Very Fast Old Stance	41.60°	4.07°	

Note: Std: Standard deviation.; '-' indicates no significant difference.

4.1.9.6 Age-related Differences in the MLA Planar Angle of the Foot

The mean relative angle gait curve for the Medial Longitudinal Arch (MLA) planar angle is presented in Figure 65. This is the angle defined between the projections of the line segments of the medial calcaneus and the heel, and the heel and the first distal metatarsal. The following section focuses on between-group differences. Table 34 presents the significant age-related differences in the mean max and min MLA angles in stance phase as well as their respective time of occurrence as a percentage of GC.

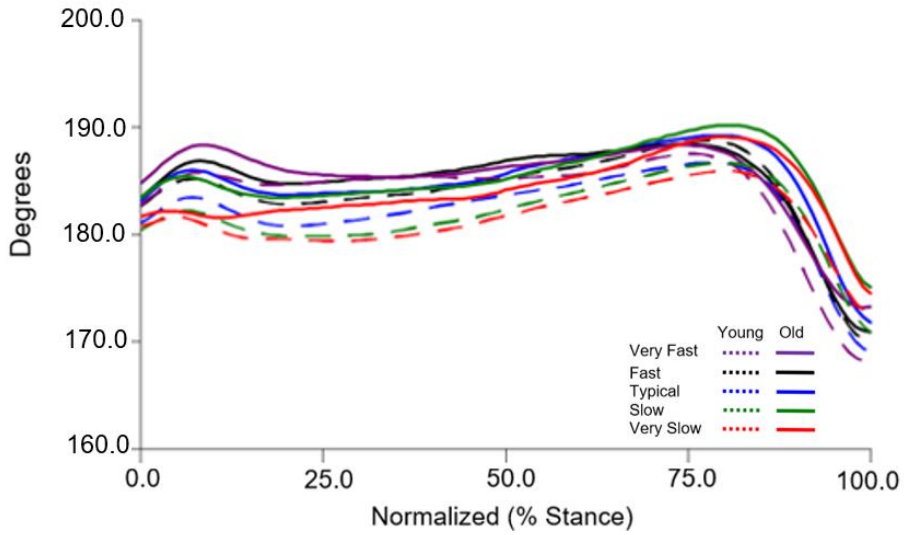


Figure 65. Mean MLA planar angle of the OG versus the YG at each walking speed.

Table 34. Significant p-values of the mean min and max MLA angles (∠) during stance phase, as well as their respective time of occurrence in the gait cycle across five walking speeds.

Walking speed group	Min MLA ∠ p-value	Time to min MLA ∠ p-value	Max MLA ∠ p-value	Time to max MLA ∠ p-value
VS	-	<.01	-	<.00001
S	-	<.001	-	<.01
T	-	<.001	-	-
F	-	-	-	-
VF	-	-	-	-

Note: VS: Very Slow, S: Slow, T: Typical, F: Fast, VF: Very Fast.; '-' indicates no significant difference.

Significant differences in time to mean min MLA angle ($p<.05$) during stance phase were found between YA and OA as WS increased from VS to typical speed (Figure 65, Table 34). The YG had a significantly shorter time to mean min MLA angle ($p<.05$) for the VS, slow, and typical WSs. For the YG, the min MLA occurred at 57.35±17.75 percent GC at the VS speed, increasing to 60.58±1.53 percent GC at the typical speed. Whereas the OG demonstrated min MLA angles at 59.70±22.42 percent GC at the VS speed, increasing to 62.64±4.06 percent GC at the typical speed.

Significant differences in time to mean max MLA angle ($p<.05$) during stance phase were found between YA and OA as WS increased from VS to slow WS (Figure 65, Table 34). The YG had a significantly shorter time to mean max MLA angle ($p<.05$) for the VS and slow WSs. For the YG, the max MLA occurred at 46.01±14.36 percent GC at the VS speed, decreasing to 42.78±15.51 percent GC at the slow speed. Whereas the OG demonstrated max MLA angles at 55.04±7.16 percent GC at the VS speed, decreasing to 49.08±11.17 percent GC at the slow speed.

Table 35 presents the significant ($p<.05$) age-related differences in the range of motion (ROM) data for the MLA planar angle during stance phase. In addition, relative ROM data for the MLA planar angle are provided in Table 35. The YG displayed the greatest MLA ROM (Figure 65) at the typical and VF speeds during stance compared to the OG. The YG exhibited a significantly ($p<.05$) greater MLA ROM during stance at the VF WS only (VF: 21.18°±1.12°) compared to the OG (VF: 17.33°±2.17°).

Table 35. Significant MLA ROM data for the cal-met during stance phase across five walking speeds and their respective significant p-values.

MLA Planar Angle ROM			
	Mean	± Std	P-value
Very Slow Young Stance	14.92°	1.93°	-
Very Slow Old Stance	15.32°	2.26°	
Slow Young Stance	15.48°	1.28°	-
Slow Old Stance	15.71°	0.88°	
Typical Young Stance	18.73°	0.55°	-
Typical Old Stance	18.39°	1.90°	
Fast Young Stance	18.50°	0.30°	-
Fast Old Stance	19.17°	1.88°	
Very Fast Young Stance	21.18°	1.12°	<.05
Very Fast Old Stance	17.33°	2.17°	

Note: Std: Standard deviation.; '-' indicates no significant difference.

4.1.10 Summary of Planar Angles Results

When the speed effect is being considered, there are fewer significant differences in planar angles between YA and OA. The key findings of the present study are as follows:

- Significant differences between YA and OA were found only for the F2Pt and V2G planar angles as a function of speed. The mean max F2Pt angle was significantly decreased for the YG for the VF speed only compared to the OG. Similarly, the mean max V2G angle was significantly decreased for the YA for the fast speed only compared to the OA.
- Planar angles, such as MLA, F2Ps, S2G and F2G, had significant differences between YA and OA for the temporal variables only, such as time to min and time to max mean angle.

4.1.11 Age-related Differences in Ankle Kinetics

4.1.11.1 Age-related Differences in Ankle Moment

The mean moment for the foot-shank in the sagittal plane is presented in Figure 66. This is the ankle dorsiflexion-plantarflexion (DF/PF) moment defined by the net muscle forces acting to modify the angular rotation of the joint between the foot and the shank (tibia) segments. The following section focuses on between-group differences. Table 36 presents the significant age-related differences in the mean max and min DF/PF moments in stance and swing phase as well as their respective time of occurrence as a percentage of GC.

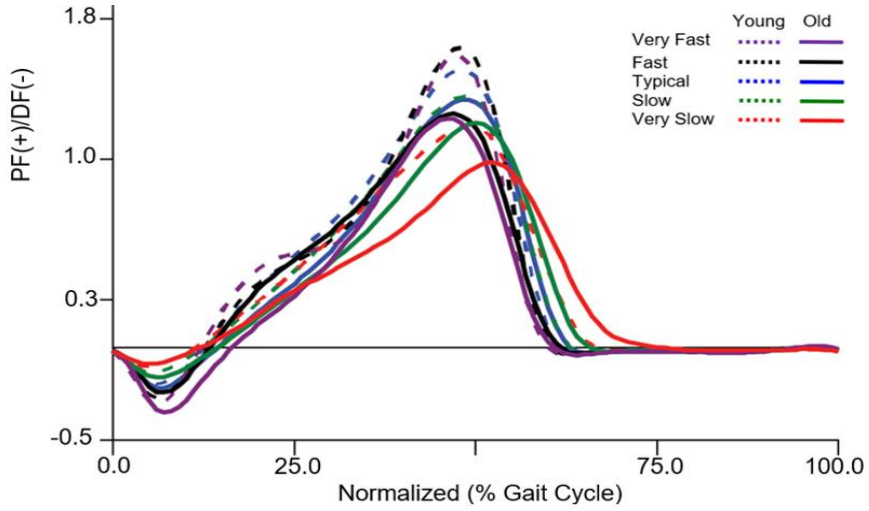


Figure 66. Mean dorsiflexion-plantarflexion moment for the ankle of the OG versus the YG at each walking speed.

Table 36. Significant p-values of the mean min and max DF/PF moments ((N·m)/kg) of the ankle during stance and swing phase, as well as their respective time of occurrence in the gait cycle across five walking speeds.

Walking speed group	Min DF moment in stance p-value	Time to min DF moment in stance p-value	Min DF moment in swing p-value	Time to min DF moment in swing p-value	Max PF moment in stance p-value	Time to max PF moment in stance p-value	Max PF moment in swing p-value	Time to max PF moment in swing p-value
VS	-	-	-	-	.03	<.0001	.03	-
S	-	-	-	-	-	<.001	-	-
T	-	-	-	-	.01	-	.01	-
F	-	<.001	-	-	<.001	-	-	.01
VF	-	<.001	-	<.01	<.001	-	-	.02

Note: VS: Very Slow, S: Slow, T: Typical, F: Fast, VF: Very Fast.; '-' indicates no significant difference.

The mean max PF moment across WSs during stance, with error bars (95% confidence interval), is presented in Figure 67. Descriptive results for the YG showed that the mean max PF moment during stance increased from VS to fast speed, after which point, the mean max PF moment began to decrease. The OG showed that the mean max PF moment increased from VS to slow speed, after which point, the mean max PF moment in stance was relatively consistent. In addition, the YG demonstrated greater mean min PF moment across speeds, except for the slow speed, compared to the YG. Both age groups demonstrated similar associated marginal error (Figure 67). The YG had a significantly ($p<.05$) increased mean max PF moment during stance phase (i.e. significantly higher peak PF) as WS increased from VS to VF, except for the slow speed (VS: 1.11±0.30 $\frac{N \cdot m}{kg}$; VF: 1.53±0.33 $\frac{N \cdot m}{kg}$) compared to the OG (VS: 1.04±0.18 $\frac{N \cdot m}{kg}$; VF: 1.22±0.28 $\frac{N \cdot m}{kg}$).

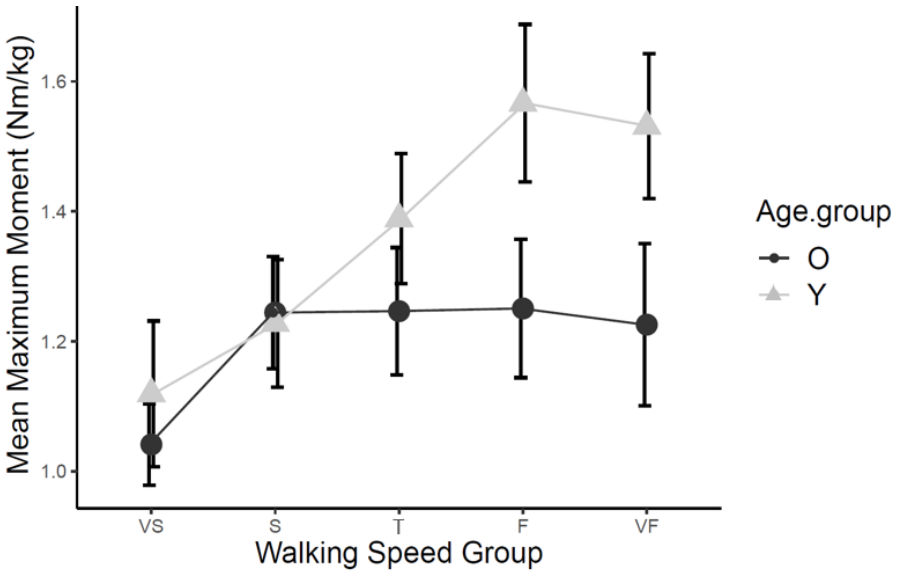


Figure 67. Mean max PF moment of the foot-shank during stance phase for the YG and OG across walking speeds at the 95% confidence interval (VS: Very Slow, S: Slow, T: Typical, F: Fast, VF: Very Fast).

Significant differences in time to mean max PF moment ($p<.05$) during stance phase were found between YA and OA as WS increased from VS to slow WS (Figure 66, Table 36). The YG had a significantly shorter time to mean max PF moment ($p<.05$) for the VS and slow WSs. For the YG, the max PF moment occurred at 45.96±8.65 percent GC at the VS speed, decreasing to 45.77±7.34 percent GC at the slow speed. Whereas the OG demonstrated max PF moments at 51.96±3.74 percent GC at the VS speed, increasing to 49.84±4.26 percent GC at the slow speed.

The mean max PF moment across WSs during swing, with error bars (95% confidence interval), is presented in Figure 68. Descriptive results for the YG showed that the mean max PF moment during swing decreased from VS to slow speed, after which point, the mean max PF moment was relatively consistent. The OG showed that the mean max PF moment during swing increased from VS to slow speed, after which point, the mean max PF moment was relatively consistent. In addition, the YG demonstrated greater

mean min PF moment at the VS, typical and VF speeds compared to the OG (Figure 68). The YG had a significantly ($p<.05$) increased mean max PF moment during swing phase (i.e. significantly higher peak PF) at the VS and typical WSs (VS: 0.03±0.03 $\frac{N \cdot m}{kg}$; typical: 0.02±0.01 $\frac{N \cdot m}{kg}$) compared to the OG (VS: 0.01±0.01 $\frac{N \cdot m}{kg}$; typical: 0.01±0.01 $\frac{N \cdot m}{kg}$), as shown in Table 36.

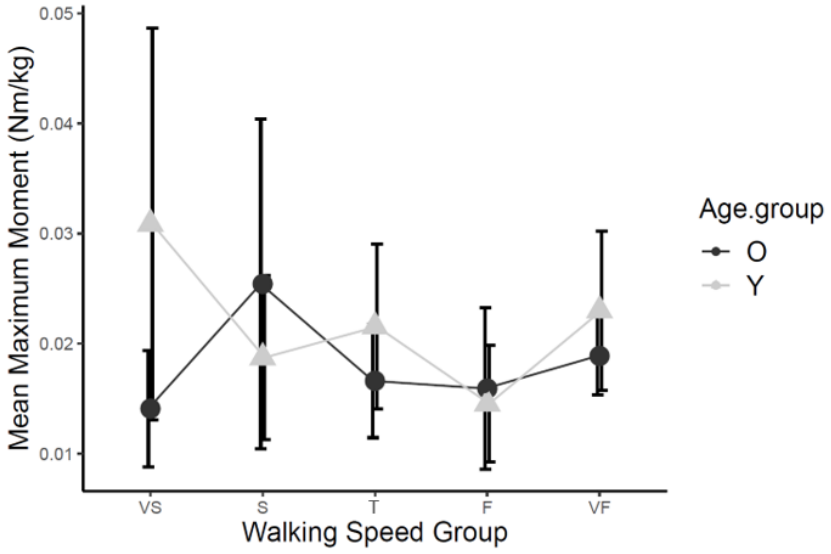


Figure 68. Mean max PF moment of the foot-shank during swing phase for the YG and OG across walking speeds at the 95% confidence interval (VS: Very Slow, S: Slow, T: Typical, F: Fast, VF: Very Fast).

Significant differences in time to mean max PF moment ($p<.05$) during swing phase were found between YA and OA as WS increased from fast to VF WS (Figure 66, Table 36). The YG had a significantly shorter time to mean max PF moment ($p<.05$) for the fast and VF WSs. For the YG, the max PF moment occurred at 78.30±15.51 percent GC at the fast speed, increasing to 80.91±17.00 percent GC at the VF speed. Whereas, the OG demonstrated max PF moments at 87.32±13.71 percent GC at the fast speed, increasing to 89.17±13.74 percent GC at the VF speed.

Significant differences in time to mean min PF moment ($p<.05$) during stance phase were found between YA and OA as WS increased from fast to VF WS (Figure 66, Table 36). The YG had a significantly shorter time to mean min PF moment ($p<.05$) for the fast and VF WSs. For the YG, the min PF moment occurred at 6.27±0.91 percent GC at the fast speed, increasing to 7.69±6.09 percent GC at the VF speed. Whereas the OG demonstrated min PF moments at 8.84±7.95 percent GC at the fast speed, increasing to 9.12±7.11 percent GC at the VF speed.

Significant differences in time to mean min PF moment ($p<.05$) during swing phase were found between YA and OA for the VF speed only (Figure 66, Table 36). The YG had a shorter time to mean min PF moment ($p<.05$) for the VF speed. For the YG, the mean min PF moment occurred at 61.48±4.71 percent GC at the VF WS, whereas the OG demonstrated a min PF moment at 64.39±8.92 percent GC at the VF speed.

4.1.11.2 Age-related Differences in Ankle Power

The mean power for the foot-shank in the sagittal plane is presented in Figure 69. This is the ankle concentric-eccentric power defined by the joint moment of force and joint angular velocity between the foot and the shank (tibia) segments. The following section focuses on between-group differences. Table 37 presents the significant age-related differences in the mean max and min DF/PF powers in stance and swing phase as well as their respective time of occurrence as a percentage of GC.

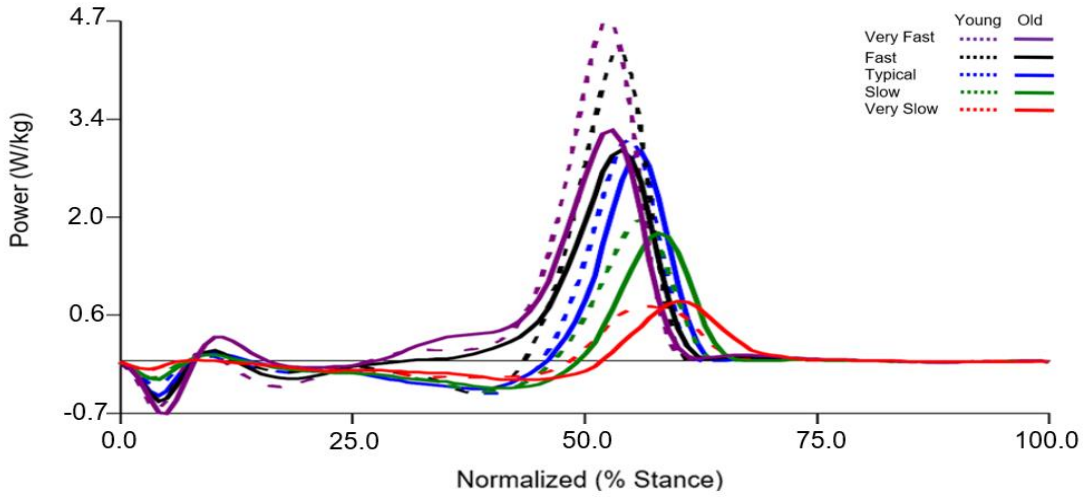


Figure 69. Mean dorsiflexion-plantarflexion power for the ankle of the OG versus the YG at each walking speed.

Table 37. Significant p-values of the mean max eccentric and concentric power (W/Kg) of the ankle during stance and swing phase, as well as their respective time of occurrence in the gait cycle across five walking speeds.

Walking speed group	Max eccentric power in stance p-value	Time to max eccentric power in stance p-value	Max eccentric power in swing p-value	Time to max eccentric power in swing p-value	Max concentric power in stance p-value	Time to max concentric power in stance p-value	Max concentric power in swing p-value	Time to max concentric power in swing p-value
VS	-	<.001	<.001	-	-	<.0001	<.01	<.0001
S	-	-	<.01	<.01	-	<.001	-	-
T	-	-	.01	<.01	-	<.01	<.01	<.01
F	-	-	.02	<.001	.01	-	-	<.001
VF	-	-	-	-	.01	-	-	<.01

Note: VS: Very Slow, S: Slow, T: Typical, F: Fast, VF: Very Fast.; '-' indicates no significant difference.

The mean max eccentric (ECC) power of the foot-shank across WSs during swing, with error bars (95% confidence interval), is presented in Figure 70. Descriptive results for both groups displayed similar trends but at different magnitudes. Both groups showed that the mean max ECC power during swing decreased from VS to typical speed, after which point, the mean max ECC power began to increase. In addition, the OG demonstrated greater mean max ECC power across speeds, with the smallest associated marginal error, compared to the YG.

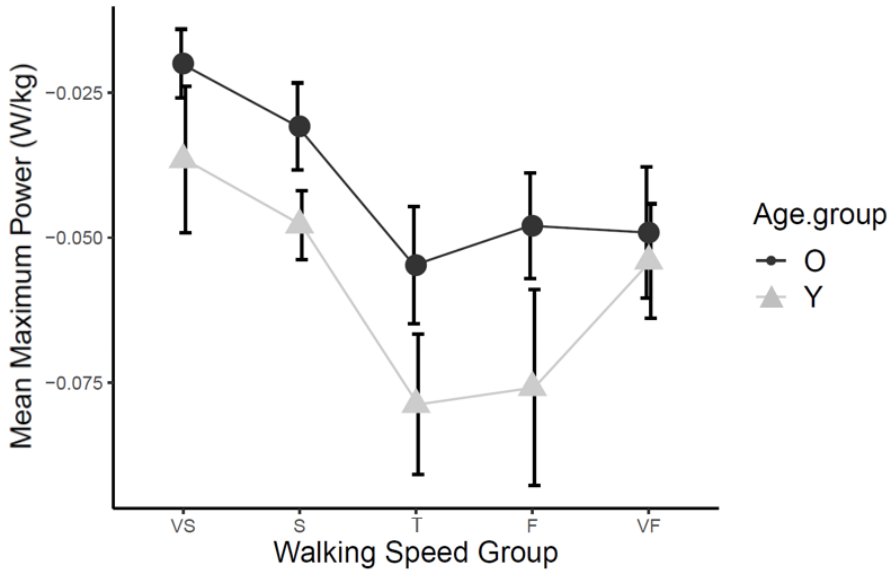


Figure 70. Mean max ECC power of the foot-shank during swing phase for the YG and OG across walking speeds at the 95% confidence interval (VS: Very Slow, S: Slow, T: Typical, F: Fast, VF: Very Fast).

The YG had a significantly ($p<.05$) increased mean max ECC power during swing phase as WS increased from VS to fast speed (VS: -0.03±0.03 $\frac{W}{Kg}$; fast: -0.07 ±0.03 $\frac{W}{Kg}$) compared to the OG (VS: -0.01±0.01 $\frac{W}{Kg}$; fast: -0.04±0.02 $\frac{W}{Kg}$), as shown in Table 37.

Significant differences in time to mean max ECC power ($p<.05$) during swing phase were found between YA and OA as WS increased from slow to fast WS (Figure 69, Table 37). The YG had a significantly shorter time to mean max ECC power ($p<.05$) for the slow, typical, and fast WSs. For the YG, the max ECC power occurred at 72.12±13.47 percent GC at the slow speed, increasing to 67.67±13.10 percent GC at the fast speed. Whereas the OG demonstrated max ECC power at 81.77±14.47 percent GC at the slow speed, increasing to 81.85±15.78 percent GC at the fast speed.

The mean max concentric (CNC) power of the foot-shank across WSs during stance, with error bars (95% confidence interval), is presented in Figure 71. Descriptive

results for both groups showed that the mean max CNC power during stance increased as WS increased. Both age groups displayed similar trends and very similar magnitudes. In addition, the YG demonstrated greater mean max CNC power at the typical, fast, and VF WSs, with the smallest associated marginal error, compared to the OG (Figure 71).

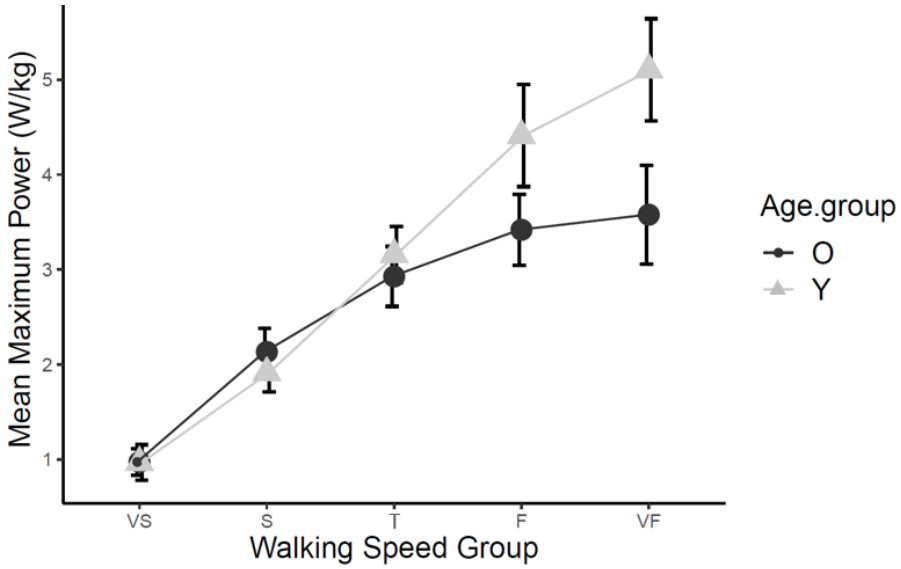


Figure 71. Mean max CNC power of the foot-shank during stance phase for the YG and OG across walking speeds at the 95% confidence interval (VS: Very Slow, S: Slow, T: Typical, F: Fast, VF: Very Fast).

The YG had a significantly ($p<.05$) increased mean max CNC power during stance phase as WS increased from fast to VF speed (fast: 4.41±1.18 $\frac{W}{Kg}$; VF: 5.10±1.61 $\frac{W}{Kg}$) compared to the OG (fast: 3.41±0.99 $\frac{W}{Kg}$; VF: 3.57±1.17 $\frac{W}{Kg}$), as shown in Table 37.

Significant differences in time to mean max CNC power ($p<.05$) during stance phase were found between YA and OA as WS increased from VS to typical WS (Figure 69, Table 37). The YG had a shorter time to mean max CNC power ($p<.05$) for the VS, slow, and typical WSs. For the YG, the max CNC power occurred at 52.48±9.36 percent GC at the VS WS, decreasing to 51.50±8.13 percent GC at the typical speed. Whereas the

OG showed max CNC power at 60.43±3.69 percent GC at the VS WS, decreasing to 53.71±9.84 percent GC at the typical WS.

The mean max CNC power of the foot-shank across WSs during swing, with error bars (95% confidence interval), is presented in Figure 72. Descriptive results for the OG showed that the mean max CNC power during swing increased as WS increased. The mean max CNC power showed an inconsistent pattern for the YG, as the angle decreased and increased, in that order, as WS increased. In addition, the YG demonstrated greater mean max CNC power across all speeds compared to the OG (Figure 72).

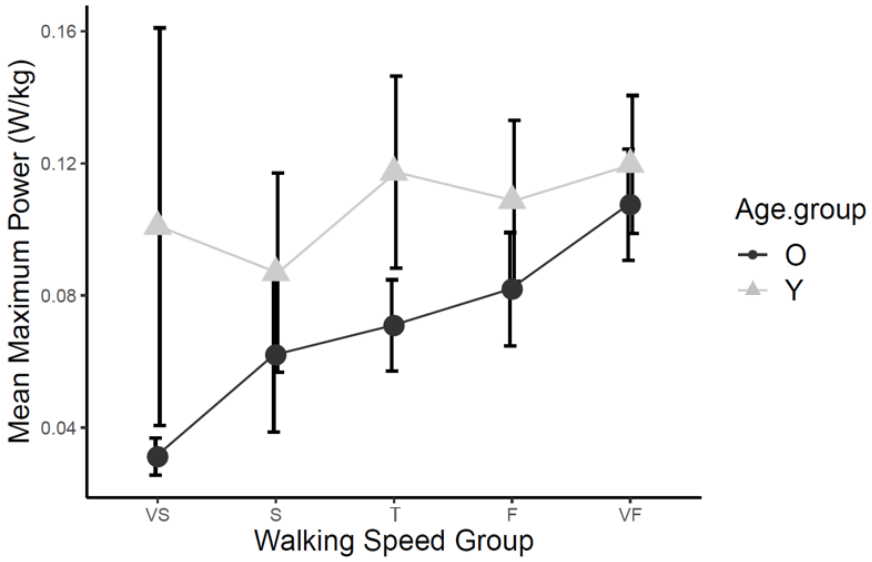


Figure 72. Mean max CNC power of the foot-shank during swing phase for the YG and OG across walking speeds at the 95% confidence interval (VS: Very Slow, S: Slow, T: Typical, F: Fast, VF: Very Fast).

The YG had a significantly ($p<.05$) increased mean max CNC power during swing phase as WS for the VS and typical WS (VS: 0.10±0.16 $\frac{W}{Kg}$; typical: 0.11±0.08 $\frac{W}{Kg}$) compared to the OG (VS: 0.03±0.01 $\frac{W}{Kg}$; typical: 0.07±0.04 $\frac{W}{Kg}$).

Significant differences in time to mean max CNC power ($p<.05$) during swing phase were found between YA and OA as WS increased, except for the slow speed (Figure 69, Table 37). The YG had a significantly shorter time to mean max CNC power ($p<.05$) for the VS, typical, fast, and VF WS. For the YG, the max CNC power occurred at 65.90±4.44 percent GC at the VS speed, decreasing to 63.39±2.70 percent GC at the VF speed. Whereas the OG demonstrated max CNC power at 71.39±5.44 percent GC at the VS speed, decreasing to 66.38±2.82 percent GC at the VF speed.

4.1.12 Summary of Ankle Kinetics Results

When the speed effect is being considered, there are significant differences in ankle kinetics between YA and OA. The key findings of the present study are as follows:

- The mean max PF moment in stance was significantly increased for the YG across all speeds except for the slow WS compared to the OG. Similarly, the mean max PF moment in swing was significantly increased for the YG for the VS and typical speeds compared to the OG.
- The mean min ECC power (i.e., ankle joint absorbed energy) in swing phase was significantly increased for the YG across all speeds compared to the OG. Similarly, the mean max CNC power (i.e., ankle joint generated energy) in stance phase was significantly increased for the YA as speed increased from fast to VF WS compared to the OA. The mean max CNC power in swing was also significantly greater for the YG for the VS and typical WSs compared to the OG.

4.1.13 Age-related Differences in Knee Kinetics and Kinematics

4.1.13.1 Age-related Differences in Knee Moment

The mean moment for the knee in the sagittal plane is presented in Figure 73. This is the knee flexion-extension (FLEX/EXT) moment defined by the net muscle forces acting to modify the angular rotation of the joint between the thigh and the shank (tibia) segments. The following section focuses on between-group differences. Table 38 presents the significant age-related differences in the mean max and min FLEX/EXT moments in stance and swing phase as well as their respective time of occurrence as a percentage of GC.

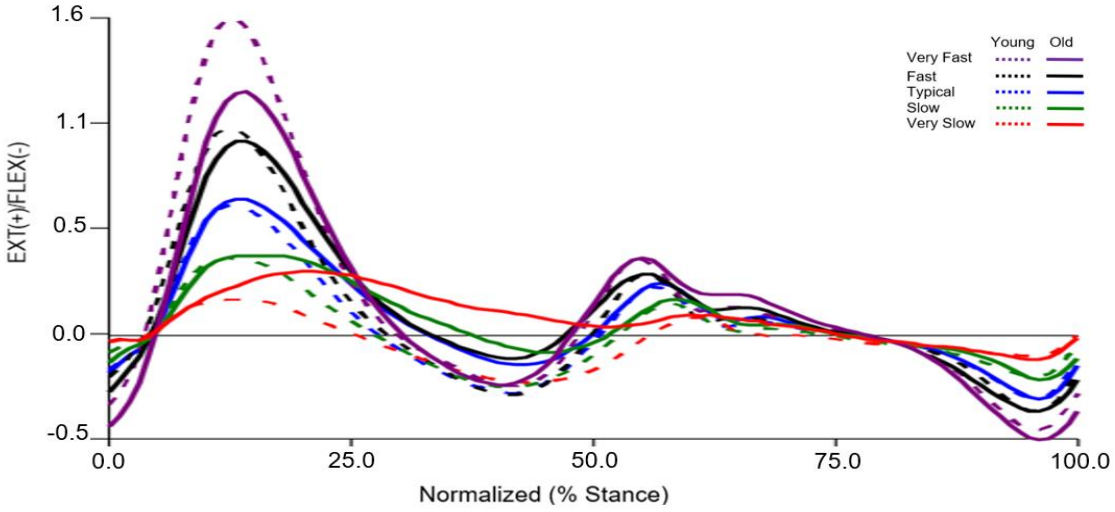


Figure 73. Mean flexion-extension moment for the knee of the OG versus the YG at each walking speed.

Table 38. Significant p-values of the mean min and max FLEX/EXT moments ((N·m)/kg) of the knee during stance and swing phase, as well as their respective time of occurrence in the gait cycle across five walking speeds.

Walking speed group	Min FLEX moment in stance p-value	Time to min FLEX moment in stance p-value	Min FLEX moment in swing p-value	Time to min FLEX moment in swing p-value	Max EXT moment in stance p-value	Time to max EXT in stance p-value	Max EXT moment in swing p-value	Time to max EXT moment in swing p-value
VS	<.001	-	-	-	.04	<.01	-	-
S	-	-	-	<.01	-	-	-	-
T	-	-	-	-	-	-	.02	-
F	-	.02	-	-	-	<.01	<.0001	.03
VF	-	<.01	-	-	-	.01	<.01	.01

Note: VS: Very Slow, S: Slow, T: Typical, F: Fast, VF: Very Fast.; '-' indicates no significant difference.

The mean min flexion (FLEX) moment across WSs during stance, with error bars (95% confidence interval), is presented in Figure 74. Descriptive results for the YG showed that the mean min FLEX moment during stance increased from VS to typical WS, after which point, the mean min FLEX moment began to decrease. The OG showed that the mean min FLEX moment decreased as WS increased. Overall, both age groups displayed a relatively consistent pattern as speed increased from slow to fast WS, however the YG displayed a larger associated marginal error. In addition, the OG showed greater mean min FLEX moment across speeds, except for the VF speed, compared to the YG (Figure 74). The YG had a significantly ($p<.05$) increased mean min FLEX moment during stance phase at the VS WS only (VS: -0.29±0.18 $\frac{N \cdot m}{kg}$) compared to the OG (VS: -0.12±0.09 $\frac{N \cdot m}{kg}$), as shown in Table 38.

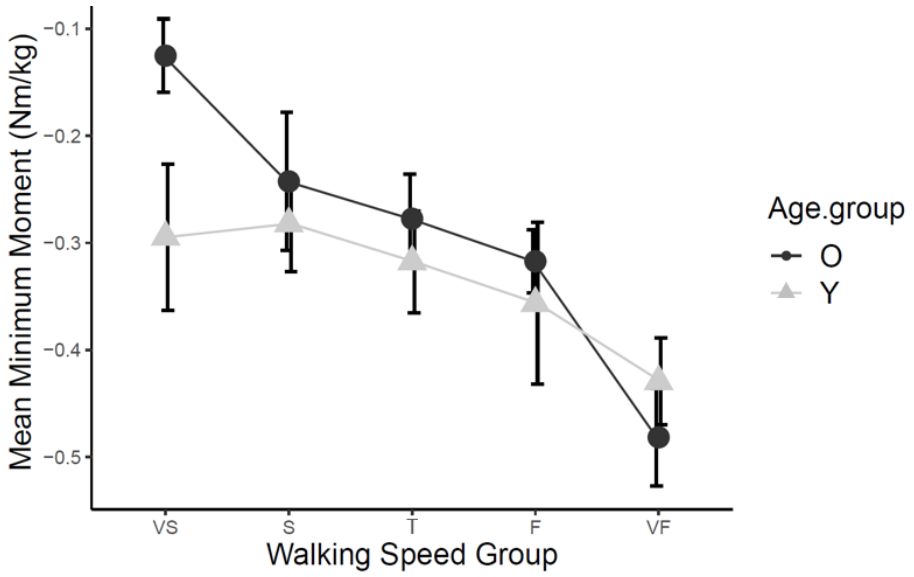


Figure 74. Mean min FLEX moment of the knee during stance phase for the YG and OG across walking speeds at the 95% confidence interval (VS: Very Slow, S: Slow, T: Typical, F: Fast, VF: Very Fast).

Significant differences in time to mean min FLEX moment ($p<.05$) during stance phase were found between YA and OA as WS increased from fast to VF WS (Figure 73, Table 38). The YG had a significantly longer time to mean min FLEX moment ($p<.05$) for the fast and VF WSs. For the YG, the min FLEX moment occurred at 26.88±20.14 percent GC at the fast speed, decreasing to 21.74±20.67 percent GC at the VF speed. Whereas the OG demonstrated min FLEX moments at 12.01±18.53 percent GC at the fast speed, decreasing to 6.44±14.46 percent GC at the VF speed.

Significant differences in time to mean min FLEX moment ($p<.05$) during swing phase were found between YA and OA at the slow speed only (Figure 73, Table 38). The YG had a significantly shorter time to mean min PF moment ($p<.05$) for the slow WS. For the YG, the min FLEX moment occurred at 95.17 ±1.36 percent GC at the slow WS, whereas the OG demonstrated min FLEX moments at 96.41±1.03 percent GC at the slow WS.

The mean max extension (EXT) moment across WSs during stance, with error bars (95% confidence interval), is presented in Figure 75. Descriptive results showed that the mean max EXT moment (peak) during stance increased as WS increased for both groups and at very similar magnitudes. However, the YG displayed a larger associated marginal error. In addition, the OG demonstrated greater mean max EXT moment across speeds, except for the fast and VF speeds, compared to the YG (Figure 75). The YG had a significantly ($p<.05$) decreased mean max EXT moment during stance phase (i.e., significantly lower peak PF) at the VS speed only (VS: 0.25±0.13 $\frac{N \cdot m}{kg}$) compared to the OG (VS: 0.36±0.17 $\frac{N \cdot m}{kg}$), as shown in Table 38.

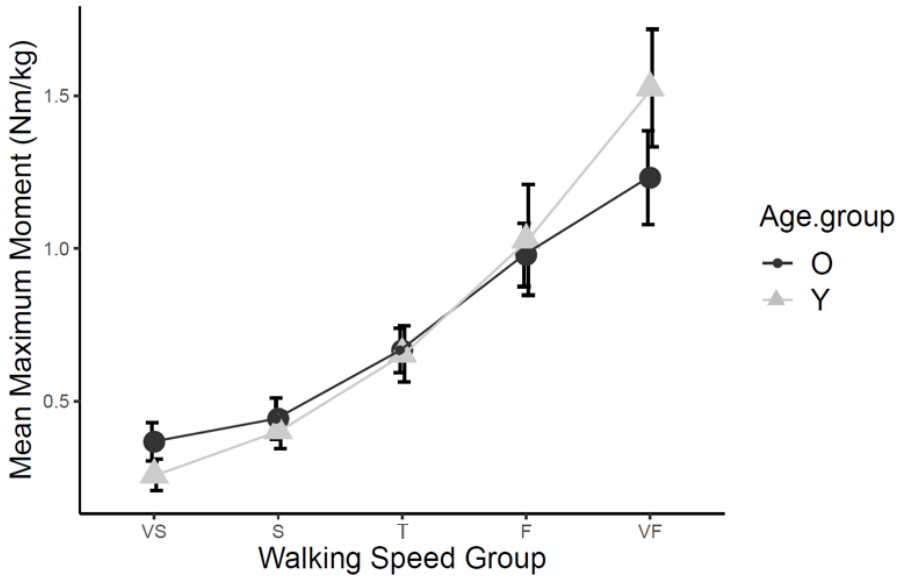


Figure 75. Mean max EXT moment of the knee during stance phase for the YG and OG across walking speeds at the 95% confidence interval (VS: Very Slow, S: Slow, T: Typical, F: Fast, VF: Very Fast).

Significant differences in time to mean max EXT moment ($p<.05$) during stance phase were found between YA and OA as WS increased, except for the slow and typical WS (Figure 73, Table 38). The YG had a significantly shorter time to mean max EXT

moment (p<.05) for the VS, fast, and VF WSs. For the YG, the max EXT moment occurred at 21.86±18.85 percent GC at the VS speed, decreasing to 14.44±6.11 percent GC at the VF speed. Whereas the OG demonstrated max EXT moments at 25.83±15.94 percent GC at the VS speed, decreasing to 14.83±5.56 percent GC at the VF speed.

The mean max EXT moment across WSs during swing, with error bars (95% confidence interval), is presented in Figure 76. Descriptive results showed that the mean max EXT moment (peak) during swing increased as WS increased for both groups. In addition, the OG demonstrated greater mean max EXT moment across speeds, except for the VS speed, compared to the YG. The latter displayed a larger associated marginal error (Figure 76).

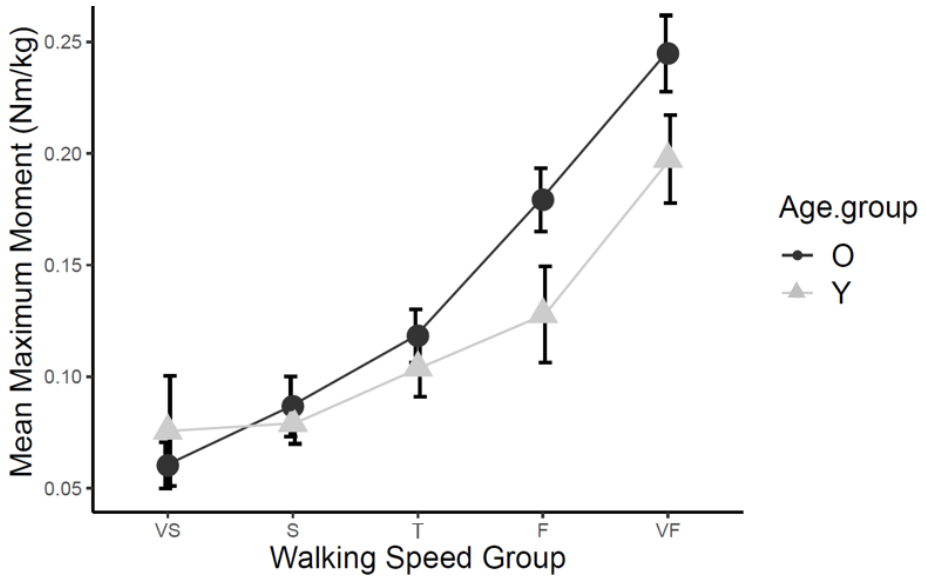


Figure 76. Mean max EXT moment of the knee during swing phase for the YG and OG across walking speeds at the 95% confidence interval (VS: Very Slow, S: Slow, T: Typical, F: Fast, VF: Very Fast).

The YG had a significantly (p<.05) decreased mean max EXT moment during swing phase (i.e. significantly lower peak PF) as WS increased from typical to VF speed

(typical: 0.10±0.03 $\frac{N \cdot m}{kg}$; VF: 0.19±0.05 $\frac{N \cdot m}{kg}$) compared to the OG (typical: 0.11±0.03 $\frac{N \cdot m}{kg}$; VF: 0.24±0.03 $\frac{N \cdot m}{kg}$), as shown in Table 38.

Significant differences in time to mean max EXT moment ($p<.05$) during swing phase were found between YA and OA at the fast and VF WSs (Figure 73, Table 38). The YG had a significantly shorter time to mean max EXT moment ($p<.05$) for the fast and VF WSs. For the YG, the max EXT moment occurred at 62.61±2.59 percent GC at the fast speed, decreasing to 61.37±3.09 percent GC at the VF speed. Whereas the OG demonstrated max EXT moments at 64.41±2.63 percent GC at the fast speed, decreasing to 64.12±2.30 percent GC at the VF speed.

4.1.13.2 Age-related Differences in Knee Power

The mean power for the knee in the sagittal plane is presented in Figure 77. This is the knee concentric-eccentric flexion-extension (FLEX/EXT) power defined by the joint moment of force and joint angular velocity between the thigh and the shank (tibia) segments. The following section focuses on between-group differences. Table 39 presents the significant age-related differences in the mean max and min flexion-extension powers in stance and swing phase as well as their respective time of occurrence as a percentage of GC.

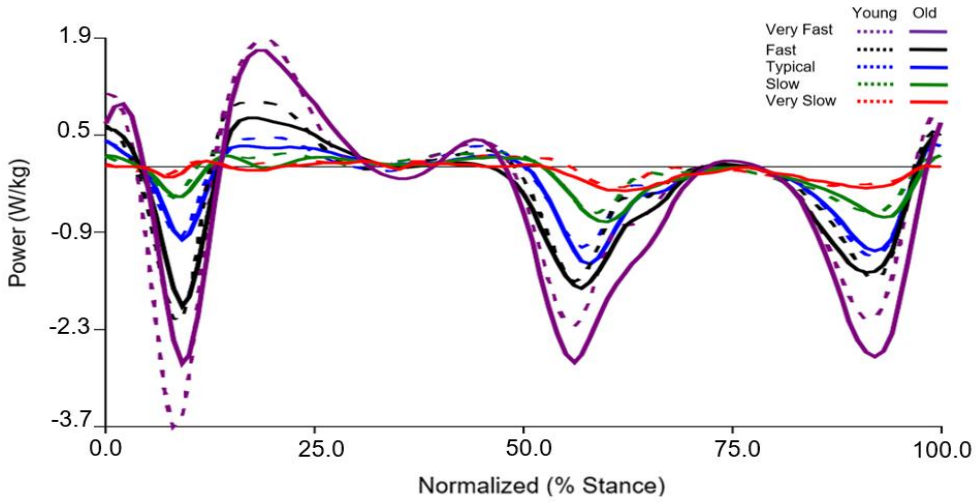


Figure 77. Mean dorsiflexion-plantarflexion power for the knee of the OG versus the YG at each WS.

Table 39. Significant p-values of the mean max eccentric and concentric power (W/Kg) of the knee during stance and swing phase, as well as their respective time of occurrence in the gait cycle across five walking speeds.

Walking speed group	Max ECC power in stance p-value	Time to max ECC power in stance p-value	Max ECC power in swing p-value	Time to max ECC power in swing p-value	Max CNC power in stance p-value	Time to max CNC power in stance p-value	Max CNC power in swing p-value	Time to max CNC power in swing p-value
VS	-	<.01	-	-	<.01	-	<.01	<.001
S	-	<.01	-	.03	-	-	-	<.001
T	-	.01	-	-	-	-	-	-
F	-	<.01	-	-	-	-	-	-
VF	-	-	.01	-	-	-	-	-

Note: VS: Very Slow, S: Slow, T: Typical, F: Fast, VF: Very Fast.; '-' indicates no significant difference.

The mean max ECC power of the knee across WSs during swing, with error bars (95% confidence interval), is presented in Figure 78. Descriptive results for both groups showed that the mean max ECC power during swing decreased as WS increased. Both age groups displayed similar magnitudes for the mean max ECC power, except for the VF WS. The OG showed a larger associated marginal error. In addition, the YG demonstrated greater mean max ECC power across speeds, except for the typical speed, compared to the OG. Additionally, at the VF speed, the OG exhibited a larger marginal error for the mean

max eccentric knee power during swing (Figure 78). This is due to the variations in sample size between YA and OA. As expected, the OG had a smaller sample size for the VF speed group. A small sample size causes a larger standard deviation. Consequently, the larger the standard deviation, the larger the confidence interval is. In this case, the marginal error.

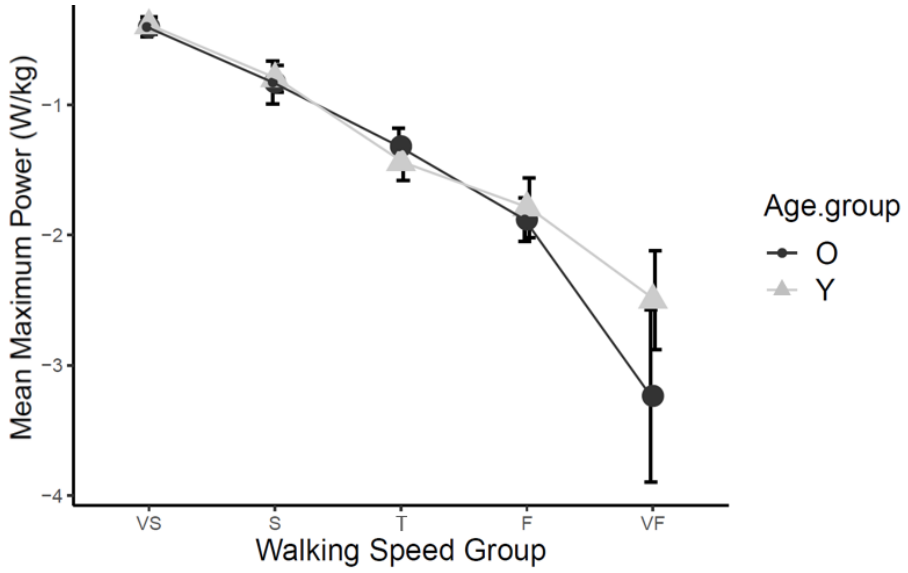


Figure 78. Mean max ECC power of the knee during swing phase for the YG and OG across walking speeds at the 95% confidence interval (VS: Very Slow, S: Slow, T: Typical, F: Fast, VF: Very Fast).

The YG had a significantly ($p<.05$) decreased mean max ECC power during swing phase at the VF speed only (VF: -2.49±1.13 $\frac{W}{Kg}$) compared to the OG (VF: -3.23±1.49 $\frac{W}{Kg}$), as shown in Table 39.

Significant differences in time to mean max ECC power ($p<.05$) during swing phase were found between YA and OA at the slow speed only (Figure 77, Table 39). The YG had a significantly shorter time to mean max ECC power ($p<.05$) for the slow speed. For the YG, the max ECC power occurred at 88.83±7.11 percent GC at the slow speed, whereas the OG demonstrated max ECC power at 90.83±7.21 percent GC at the slow WS.

Significant differences in time to mean max ECC power ($p<.05$) during stance phase were found between YA and OA as WS increased from VS to fast WS (Figure 77, Table 39). The YG had a significantly shorter time to mean max ECC power ($p<.05$) for the VS, slow, typical, and fast speeds. For the YG, the max ECC power occurred at 41.44±22.38 percent GC at the VS speed, decreasing to 29.49±23.09 percent GC at the fast speed. Whereas the OG showed max ECC power at 55.57±17.11 percent GC at the VS WS, decreasing to 39.46±22.49 percent GC at the fast speed.

The mean max CNC power of the knee across WSs during stance, with error bars (95% confidence interval), is presented in Figure 79. Descriptive results for both groups showed that the mean max CNC power during stance increased as WS increased. In addition, the YG demonstrated greater mean max CNC power at the typical, fast, and VF WSs, with the smallest associated marginal error, compared to the OG (Figure 79).

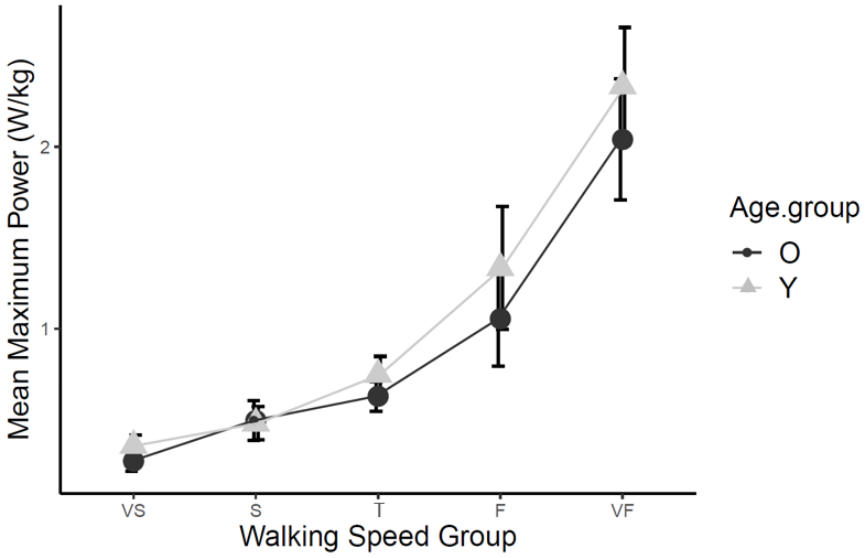


Figure 79. Mean max CNC power of the knee during stance phase for the YG and OG across walking speeds at the 95% confidence interval (VS: Very Slow, S: Slow, T: Typical, F: Fast, VF: Very Fast).

The YG had a significantly ($p<.05$) increased mean max CNC power during stance phase at the VS speed only (VS: 0.35±0.15 $\frac{W}{Kg}$) compared to the OG (VS: 0.27±0.16 $\frac{W}{Kg}$), as shown in Table 39.

The mean max CNC power of the knee across WSs during swing, with error bars (95% confidence interval), is presented in Figure 80. Descriptive results for both groups showed that the mean max CNC power during swing increased as WS increased. However, the OG displayed a larger associated marginal error. In addition, the YG demonstrated greater mean max CNC power as WS increased, except for the VF speed, compared to the OG. Additionally, at the VF speed, the OG exhibited a larger marginal error for the mean max concentric knee power during swing (Figure 80). This is due to the variations in sample size between YA and OA. As expected, the OG had a smaller sample size for the VF speed group and therefore a larger marginal error.

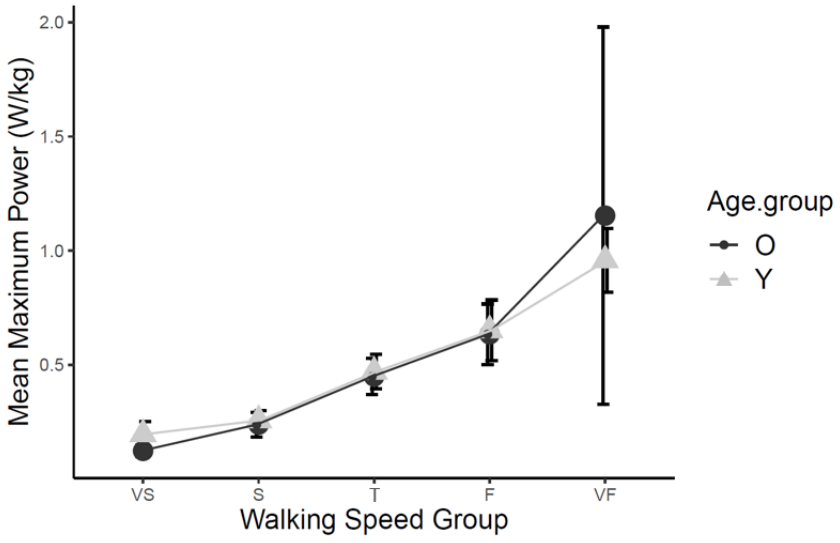


Figure 80. Mean max CNC power of the knee during swing phase for the YG and OG across walking speeds at the 95% confidence interval (VS: Very Slow, S: Slow, T: Typical, F: Fast, VF: Very Fast).

The YG had a significantly ($p<.05$) increased mean max CNC power during swing phase (i.e., significantly higher peak power) at the VS speed only (VS: 0.19±0.14 $\frac{W}{Kg}$) compared to the OG (VS: 0.12±0.07 $\frac{W}{Kg}$), as shown in Table 39.

Significant differences in time to mean max CNC power ($p<.05$) during swing phase were found between YA and OA as WS increased from VS to slow speed (Figure 77, Table 39). The YG had a significantly shorter time to mean max CNC power ($p<.05$) for the VS and slow WSs. For the YG, the max CNC power occurred at 75.90±14.09 percent GC at the VS speed, increasing to 91.71±12.58 percent GC at the slow speed. Whereas the OG demonstrated max CNC power at 87.51±12.11 percent GC at the VS speed, increasing to 97.67±7.54 percent GC at the slow speed.

4.1.13.3 Age-related Differences in Knee Angles

The mean relative angle for the knee segment in the sagittal plane is presented in Figure 81. This is the knee flexion-extension (FLEX/EXT) angle defined by the relative orientation between the thigh and the shank (tibia) segments. The following section focuses on between-group differences. Table 40 presents the significant age-related differences in the mean max and min FLEXT/EXT angles in stance and swing phase as well as their respective time of occurrence as a percentage of GC.

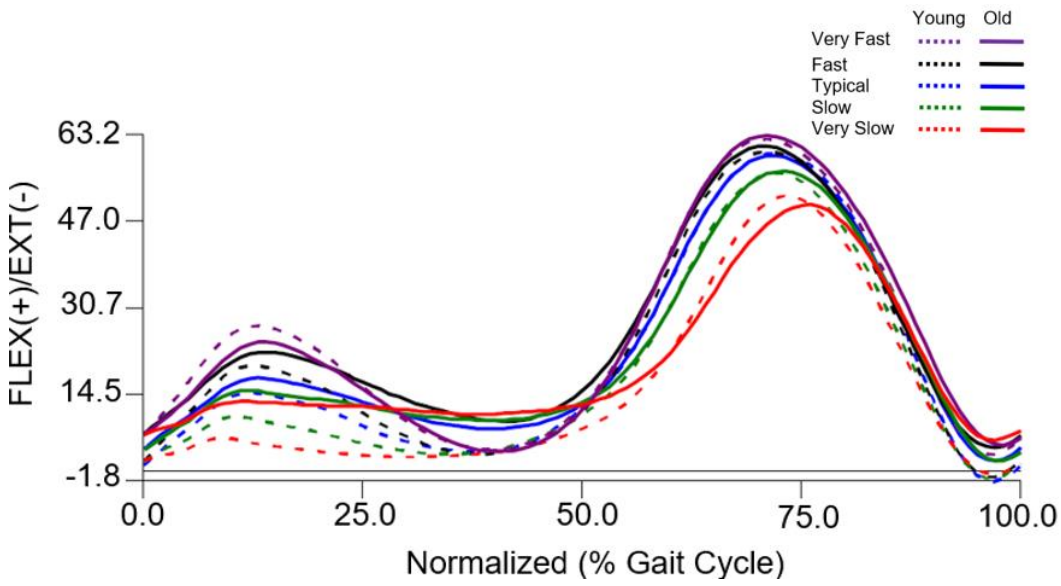


Figure 81. Mean flexion-extension for the knee of the OG versus the YG at each walking speed.

Table 40. Significant p-values of the mean min and max FLEX/EXT angles (∠) of the knee during stance and swing phase, as well as their respective time of occurrence in the gait cycle across five walking speeds.

Walking speed group	Min flexion ∠ in stance p-value	Time to min flexion ∠ in stance p-value	Min flexion ∠ in swing p-value	Time to min flexion ∠ in swing p-value	Max flexion ∠ in stance p-value	Time to max flexion ∠ in stance p-value	Max flexion ∠ in swing p-value	Time to max flexion ∠ in swing p-value
VS	<.01	-	.02	-	.01	<.00001	-	.04
S	-	-	-	-	-	<.0001	-	-
T	-	-	.04	-	.01	<.01	-	-
F	<.01	-	<.001	-	.02	<.01	-	-
VF	-	-	-	<.01	-	<.001	-	-

Note: VS: Very Slow, S: Slow, T: Typical, F: Fast, VF: Very Fast.; '-' indicates no significant difference.

The mean min FLEX angle across WSs during stance, with error bars (95% confidence interval), is presented in Figure 82. Descriptive results for the OG showed that the mean min FLEX angle during stance decreased from VS to typical speed only, after which point, the mean min FLEX angle increased for the fast speed, and then decreased again for the VF speed. The mean min FLEX angle for the YG was relatively consistent

across all speeds. In addition, the OG demonstrated greater mean min FLEX angles across speeds compared to the YG, with a larger associated marginal error (Figure 82).

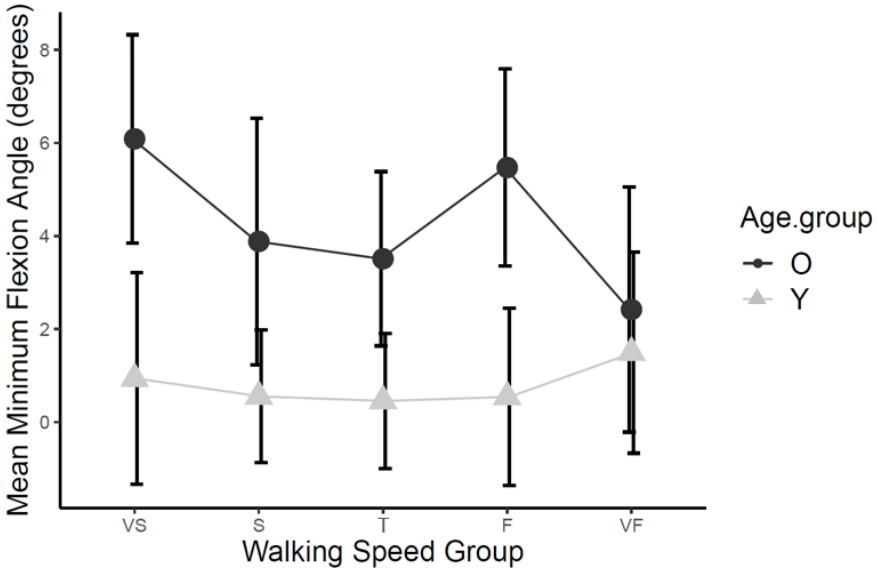


Figure 82. Mean min FLEX angle of the knee during stance phase for the YG and OG across walking speeds at the 95% confidence interval (VS: Very Slow, S: Slow, T: Typical, F: Fast, VF: Very Fast).

The YG had a significantly ($p<.05$) decreased mean min FLEX angle during stance at the VS and fast WSs (VS: 0.93°±6.08°; fast: 0.54°±4.18°) compared to the OG (VS: 6.08°±6.40°; fast: 5.46°±5.66°), as shown in Table 40.

The mean min FLEX angle across WSs during swing, with error bars (95% confidence interval), is presented in Figure 83. Descriptive results for the OG showed that the mean min FLEX angle during swing decreased from VS to typical speed only, after which point, the mean min FLEX angle increased for the fast speed, and then decreased again for the VF speed. The OG displayed a larger associated marginal error. The mean min FLEX angle for the YG decreased from VS to typical speed, after which point, the mean min FLEX angle began to increase. In addition, the OG demonstrated greater mean min FLEX angles across speeds, except for the VF speed, compared to the YG.

Additionally, at the VF WS, the OG exhibited a larger marginal error for the mean min FLEX knee angle during swing (Figure 83). This is due to the variations in sample size between YA and OA. As expected, the OG had a smaller sample size for the VF speed group and therefore a larger marginal error.

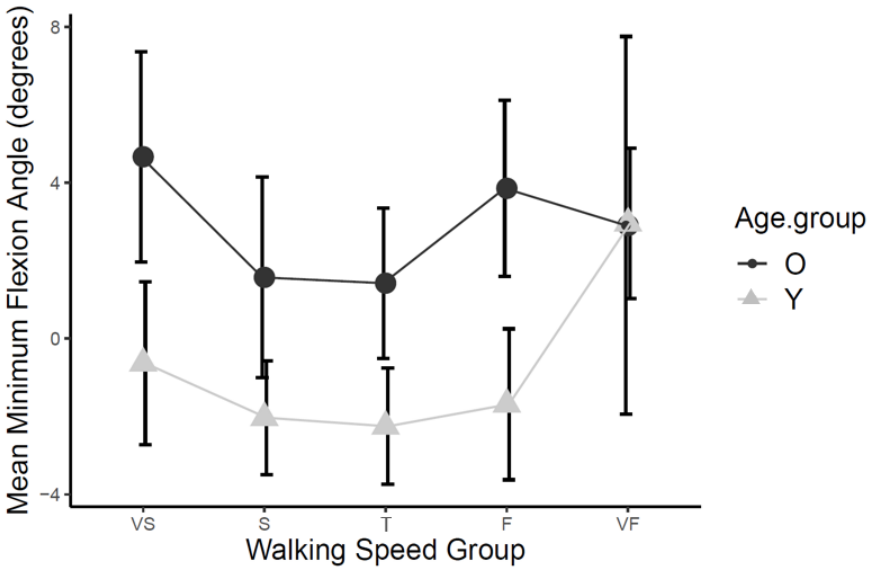


Figure 83. Mean min FLEX angle of the knee during swing phase for the YG and OG across walking speeds at the 95% confidence interval (VS: Very Slow, S: Slow, T: Typical, F: Fast, VF: Very Fast).

The YG had a significantly ($p<.05$) decreased mean min FLEX angle during swing as WS increased from VS to fast WSs, except for the slow WS (VS: -0.63°±5.59°; fast: -1.68°±4.25°) compared to the OG (VS: 4.66°±7.73°; fast: 3.85°±6.04°).

Significant differences in time to mean min FLEX angle ($p<.05$) during swing phase were found between YA and OA at the VF speed only (Figure 80, Table 40). The YG had a significantly shorter time to mean min FLEX angle ($p<.05$) for the VF WS. For the YG, the mean min FLEX angle occurred at 96.76±1.33 percent GC at the VF speed, whereas the OG demonstrated mean min FLEX angle at 97.36±2.73 percent GC at the VF speed (Figure 80).

The mean max FLEX angle across WSs during stance, with error bars (95% confidence interval), is presented in Figure 84. Descriptive results for the OG showed that the mean max FLEX angle (peak) during stance was relatively consistent at each WS. However, the OG displayed a larger associated marginal error. The mean max FLEX angle for the YG increased as WS increased. In addition, the OG showed greater mean max FLEX angles across speeds compared to the YG (Figure 84). The YG had a significantly ($p<.05$) decreased mean max FLEX angle during stance as WS increased from VS to fast WS, except for the slow WS (VS: 36.14°±5.24°; fast: 38.96°±4.32°) compared to the OG (VS: 43.31°±10.50°; fast: 43.56°±6.49°), as shown in Table 40.

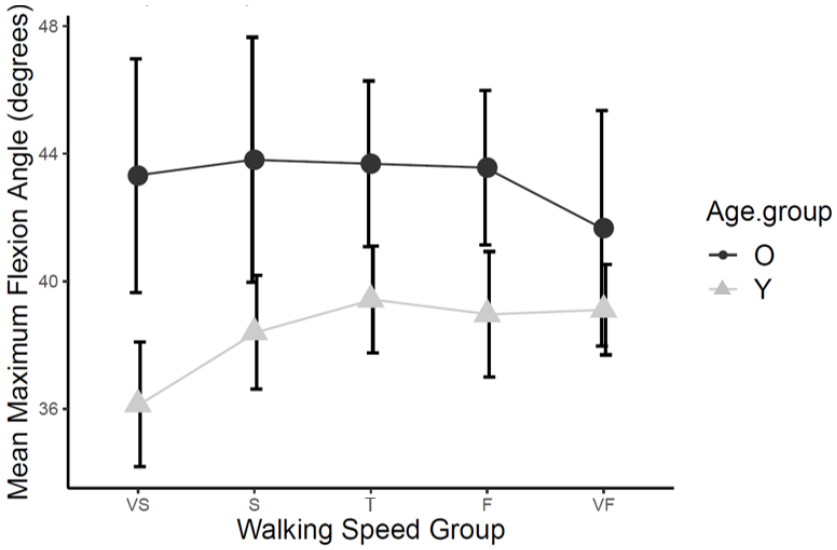


Figure 84. Mean max FLEX angle of the knee during stance phase for the YG and OG across walking speeds at the 95% confidence interval (VS: Very Slow, S: Slow, T: Typical, F: Fast, VF: Very Fast).

Significant differences in time to mean max FLEX angle ($p<.05$) during stance phase were found between YA and OA as WS increased (Figure 81, Table 40). The YG had a significantly shorter time to mean max FLEX angle ($p<.05$) across all speeds. For the YG, the mean max FLEX occurred at 62.06±7.07 percent GC at the VS speed,

decreasing to 52.63±15.74 percent GC at the VF speed. Whereas the OG demonstrated mean max FLEX at 69.32±4.81 percent GC at the VS speed, decreasing to 60.47±1.77 percent GC at the VF speed.

Significant differences in time to mean max FLEX angle ($p<.05$) during swing phase were found between YA and OA at the VS speed only (Figure 81, Table 40). The YG had a significantly shorter time to mean max FLEX angle ($p<.05$) for the VS WS. For the YG, the mean max FLEX angle occurred at 70.79±1.65 percent GC at the VF speed, whereas the OG demonstrated mean max FLEX angle at 75.32±4.04 percent GC at the VS speed (Figure 81).

Table 41 presents the significant ($p<.05$) age-related differences in the FLEX/EXT range of motion (ROM) data for the knee. In addition, relative FLEX/EXT ROM data for the knee are provided in Table 41. The OG showed the greatest FLEX/EXT ROM (Figure 81) across all speeds during stance compared to the YG, except for the fast WS during stance. However, the YG displayed the greatest FLEX/EXT ROM (Figure 81) across all speeds during swing compared to the OG, except for the VF WS during swing. Table 41 presents the between-group differences found for the FLEX/EXT ROM during stance and swing phase. There were no significant ($p<.05$) age-related differences in the FLEX/EXT ROM for the knee during stance. However, during typical speed walking, the FLEX/EXT ROM for the YA and OA increased most in the knee in stance. During swing phase, the YG exhibited a significantly ($p<.05$) greater FLEX/EXT ROM for the VS, typical, and fast WSs (VS: 54.70°±0.34°; typical: 63.26°±0.42°; fast: 63.00°±0.24°) compared to the OG (VS: 48.84°±1.49°; typical: 58.67°±0.33°; fast: 57.69°±1.01°).

Table 41. Significant FLEX/EXT ROM data for the knee during stance and swing phase across five walking speeds.

FLEX/EXT ROM Knee			
	Mean	± Std	P-value
Very Slow Young Stance	35.20°	0.83°	-
Very Slow Old Stance	37.22°	4.09°	
Slow Young Stance	37.84°	1.08°	-
Slow Old Stance	39.92°	2.82°	
Typical Young Stance	38.96°	0.62°	-
Typical Old Stance	40.17°	2.13°	
Fast Young Stance	38.41°	0.13°	-
Fast Old Stance	38.09°	0.83°	
Very Fast Young Stance	37.61°	2.23°	-
Very Fast Old Stance	39.24°	2.38°	
Very Slow Young Swing	54.70°	0.34°	<.05
Very Slow Old Swing	48.84°	1.49°	
Slow Young Swing	58.97°	0.58°	-
Slow Old Swing	55.69°	1.81°	
Typical Young Swing	63.26°	0.42°	<.01
Typical Old Swing	58.67°	0.33°	
Fast Young Swing	63.00°	0.24°	<.01
Fast Old Swing	57.69°	1.01°	
Very Fast Young Swing	59.97°	0.34°	-
Very Fast Old Swing	60.76°	3.82°	

Note: Std: Standard deviation.; '-' indicates no significant difference.

The mean relative angle for the knee segment in the transverse plane is presented in Figure 85. This is the knee internal-external rotation (INT/EXTL) angle defined by the relative orientation between the thigh and the shank (tibia) segments. The following section focuses on between-group differences. Table 42 presents the significant age-related differences in the mean max and min INT/EXTL angles in stance and swing phase as well as their respective time of occurrence as a percentage of GC.

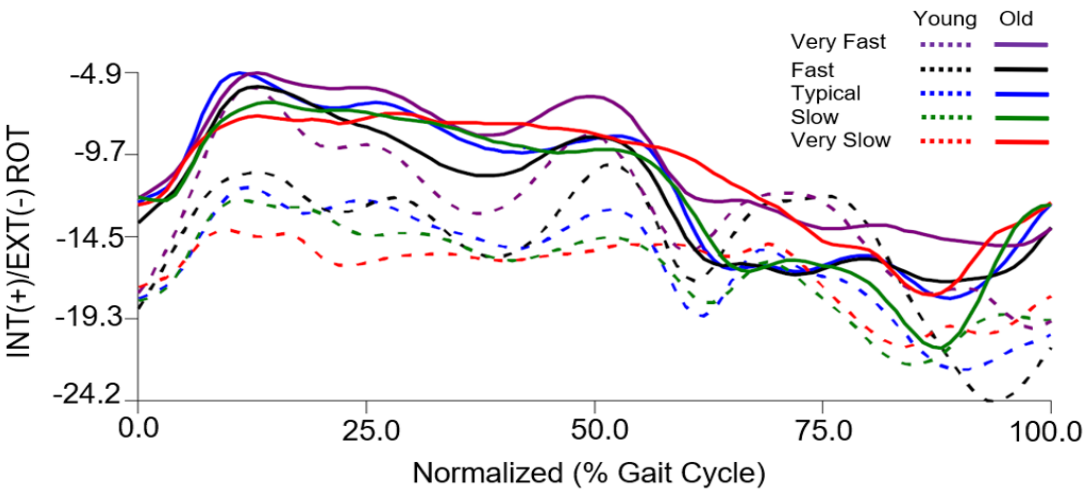


Figure 85. Mean internal-external rotation for the knee of the OG versus the YG at each walking speed.

Table 42. Significant p-values of the mean min and max INT/EXTL rotation angles (∠) of the knee during stance and swing phase, as well as their respective time of occurrence in the gait cycle across five walking speeds.

Walking speed group	Max external rotation ∠ in stance p-value	Time to max external rotation ∠ in stance p-value	Max external rotation ∠ in swing p-value	Time to max external rotation ∠ in swing p-value	Min external rotation ∠ in stance p-value	Time to min external rotation ∠ in stance p-value	Min external rotation ∠ in swing p-value	Time to min external rotation ∠ in swing p-value
VS	-	-	-	-	.03	-	-	<.001
S	-	.01	-	-	-	-	-	<.001
T	-	-	-	.04	-	-	-	<.01
F	-	.04	-	<.01	-	-	-	<.01
VF	-	-	-	-	-	-	-	-

Note: VS: Very Slow, S: Slow, T: Typical, F: Fast, VF: Very Fast.; '-' indicates no significant difference.

The mean min external rotation (ER) angle across WSs during stance, with error bars (95% confidence interval), is presented in Figure 86. Descriptive results for the OG showed that the mean min ER angle showed a consistent pattern for the OG at each speed, whereas the mean min ER angle for the YG increased as WS increased. In addition, the OG demonstrated greater mean min flexion angles across speeds compared to the YG. The latter displayed a larger associated marginal error (Figure 86). The YG had a significantly

(p<.05) increased mean min ER angle during stance at the VS speed only (VS: -10.42°±10.17°) compared to the OG (VS: -3.65°±9.70°), as shown in Table 42.

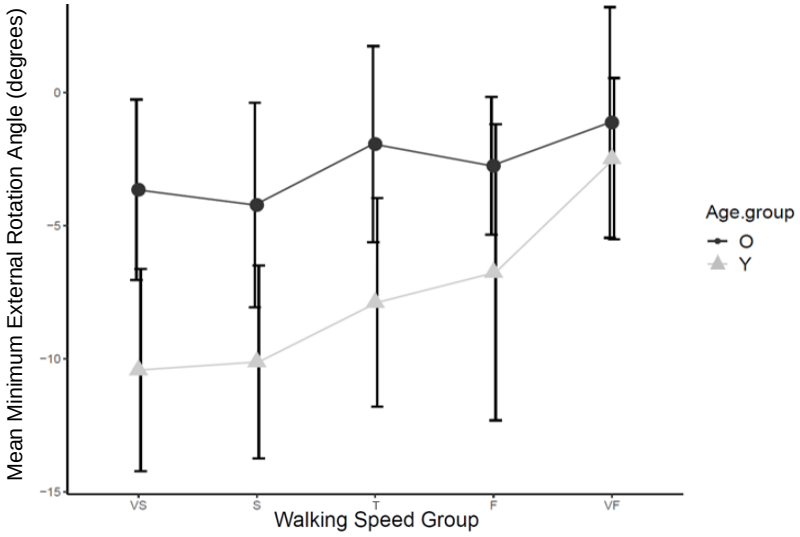


Figure 86. Mean min ER angle of the knee during stance phase for the YG and OG across walking speeds at the 95% confidence interval (VS: Very Slow, S: Slow, T: Typical, F: Fast, VF: Very Fast).

Significant differences in time to mean min ER angle (p<.05) during swing phase were found between YA and OA as WS increased from VS to fast speed (Figure 85, Table 42). The YG had a significantly shorter time to mean min ER angle (p<.05) for the VS, slow, typical, and fast WS. For the YG, the mean min ER occurred at 72.34±6.17 percent GC at the VS speed, decreasing to 70.99±1.52 percent GC at the fast speed. Whereas the OG demonstrated mean min ER at 75.32±6.17 percent GC at the VS speed, decreasing to 71.00±1.65 percent GC at the fast speed.

Significant differences in time to mean max ER angle (p<.05) during stance phase were found between YA and OA at the slow and fast speed (Figure 85, Table 42). The YG had a significantly greater time to mean max ER angle (p<.05) for the slow WS. However, the YG had a significantly shorter time to mean max ER angle (p<.05) for the fast WS. For

the YG, the mean max ER occurred at 14.07±17.31 percent GC at the slow speed, increasing to 17.29±19.05 percent GC at the fast speed. Whereas the OG demonstrated mean max ER at 10.14±16.65 percent GC at the slow speed, increasing to 18.52±19.75 percent GC at the fast speed.

Significant differences in time to mean max ER angle ($p<.05$) during swing phase were found between YA and OA as WS increased from typical to fast WS (Figure 85, Table 42). The YG had a significantly shorter time to mean max ER angle ($p<.05$) for the typical and fast WS. For the YG, the mean max ER occurred at 96.73±1.21 percent GC at the typical speed, decreasing to 96.66±1.48 percent GC at the fast WS. Whereas the OG showed mean max ER at 96.88±1.40 percent GC at the typical WS, decreasing to 96.82±1.76 percent GC at the fast WS.

Table 43 presents the significant ($p<.05$) age-related differences in the internal/ER range of motion (ROM) data for the knee. In addition, relative internal/ER ROM data for the knee are provided in Table 43. The YG displayed the greatest internal/ER ROM (Figure 85) across all speeds during stance and swing compared to the OG, except for the VS and typical speeds during stance and the VF WS during swing. Table 43 presents the between-group differences found for the internal/ER ROM during stance and swing phase. The YG exhibited a significantly ($p<.05$) greater internal/ER ROM during stance for the VF WS only (VF: 19.23°±0.39°) compared to the OG (VF: 14.65°±0.24°) as shown in Table 43. During swing phase, the YG exhibited a significantly ($p<.05$) greater internal/ER ROM as WS increased from typical to fast WS (typical: 15.34°±0.48°; fast: 20.52°±2.54°) compared to the OG (typical: 12.53°±0.32°; fast: 12.66°±0.83°).

Table 43. Significant internal/ER ROM data for the knee during stance and swing phase across five walking speeds.

Internal/External Rotation ROM Knee			
	Mean	± Std	P-value
Very Slow Young Stance	10.78°	0.79°	-
Very Slow Old Stance	11.64°	1.02°	
Slow Young Stance	13.40°	0.57°	-
Slow Old Stance	13.21°	0.32°	
Typical Young Stance	14.70°	0.17°	-
Typical Old Stance	16.78°	1.65°	
Fast Young Stance	16.98°	0.36°	-
Fast Old Stance	14.79°	1.28°	
Very Fast Young Stance	19.23°	0.39°	<.01
Very Fast Old Stance	14.65°	0.24°	
Very Slow Young Swing	14.30°	1.12°	-
Very Slow Old Swing	12.56°	1.45°	
Slow Young Swing	13.37°	1.18°	-
Slow Old Swing	13.18°	0.60°	
Typical Young Swing	15.34°	0.48°	<.01
Typical Old Swing	12.53°	0.32°	
Fast Young Swing	20.52°	2.54°	<.001
Fast Old Swing	12.66°	0.83°	
Very Fast Young Swing	16.58°	0.22°	-
Very Fast Old Swing	20.19°	3.78°	

Note: Std: Standard deviation.; '-' indicates no significant difference.

4.1.14 Summary of Knee Kinetics and Kinematics Results

When the speed effect is being considered, there are significant differences in knee kinetics and kinematics between YA and OA. The key findings of the present study are as follows:

- The mean min flexion moment in stance was significantly increased for the YG for the VS speed only compared to the OG. Conversely, the mean max EXT moment in stance and swing were significantly decreased for the YG as WS increased from typical to VF speed compared to the OG.
- The mean max ECC power of the knee in swing phase was significantly decreased for the YA for the VF speed compared to the OA. Conversely, the mean max CNC

power of the knee (i.e., the knee joint generated energy) in stance and swing phase were significantly increased for the YG for the VS speed only compared to the OG.

- Significant differences for the knee joint angle between age groups as a function of speed were found only in the sagittal and transverse plane.
- In the sagittal plane, the mean min FLEX angle of the knee in stance was significantly increased for the YG for the VS and fast WSs compared to the OG. Further, the mean min FLEX of the knee in swing, and the mean max FLEX of the knee in stance were significantly decreased for the YG for the VS, typical, and fast WSs compared to the OG.
- In the transverse plane, the mean max ER of the knee in swing was significantly increased for the YG for the VS speed only compared to the OG.

4.1.15 Age-related Differences in Hip Kinetics and Kinematics

4.1.15.1 Age-related Differences in Hip Moment

The mean moment for the hip in the sagittal plane is presented in Figure 87. This is the hip flexion-extension (FLEX/EXT) moment defined by the net muscle forces acting to modify the angular rotation of the hip joint. The following section focuses on between-group differences. Table 44 presents the significant age-related differences in the mean max and min FLEX/EXT moments in stance and swing phase as well as their respective time of occurrence as a percentage of GC.

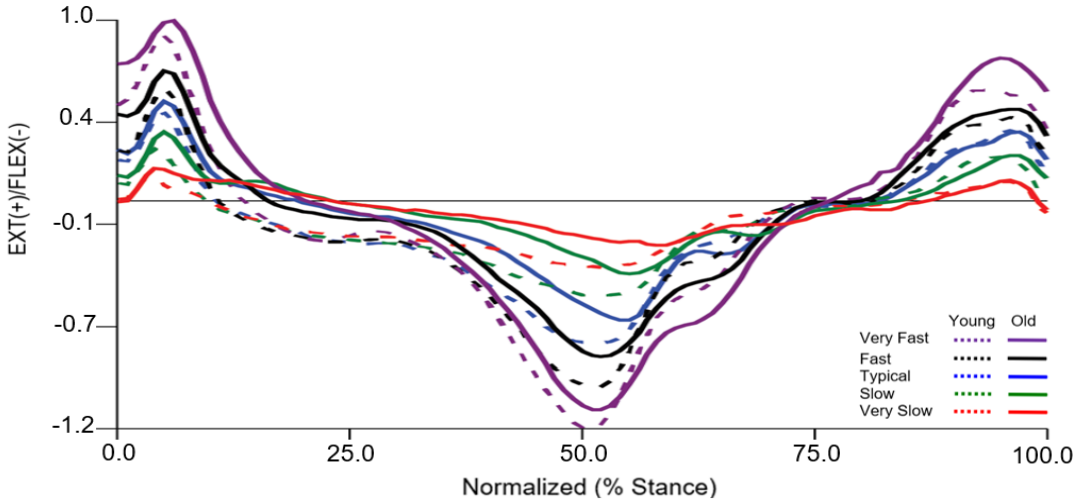


Figure 87. Mean flexion-extension moment for the hip of the OG versus the YG at each WS.

Table 44. Significant p-values of the mean max FLEX/EXT moments ((N·m)/kg) of the hip during stance and swing phase, as well as their respective time of occurrence in the gait cycle across five walking speeds.

Walking speed group	Max flexion moment in stance p-value	Time to max flexion moment in stance p-value	Max flexion moment in swing p-value	Time to max flexion moment in swing p-value	Max extension moment in stance p-value	Time to max extension moment in stance p-value	Max extension moment in swing p-value	Time to max extension moment in swing p-value
VS	.02	<.001	-	-	-	-	-	<.01
S	.01	<.0001	-	.01	.04	.03	-	.04
T	-	<.00001	-	<.001	-	.01	-	-
F	-	<.01	<.01	<.001	-	-	-	.03
VF	-	.02	<.01	<.001	-	-	<.01	-

Note: VS: Very Slow, S: Slow, T: Typical, F: Fast, VF: Very Fast.; '-' indicates no significant difference.

The mean max flexion (FLEX) moment across WSs during stance, with error bars (95% confidence interval), is presented in Figure 88. Descriptive results for both groups showed similar trends but at different magnitudes, where the mean max FLEX moment during stance decreased as WS increased. In addition, the OG demonstrated lower mean max FLEX moments across speeds, with the smallest associated marginal error, compared to the YG (Figure 88). Additionally, at the slow speed, the YG exhibited a similar mean as the OG for the mean max ER angle of the hip (Figure 103). This is due to the pattern

showed in Figure 102, which exhibited a smaller offset between YA and OA for the VF speed at heel strike. The YG had a significantly ($p<.05$) increased mean max FLEX moment during stance phase as WS increased from VS to slow speed (VS: -0.39 ±0.17 $\frac{N \cdot m}{kg}$; slow: -0.71±0.85 $\frac{N \cdot m}{kg}$) compared to the OG (VS: -0.30±0.13 $\frac{N \cdot m}{kg}$; slow: -0.45±0.13 $\frac{N \cdot m}{kg}$), as shown in Table 44.

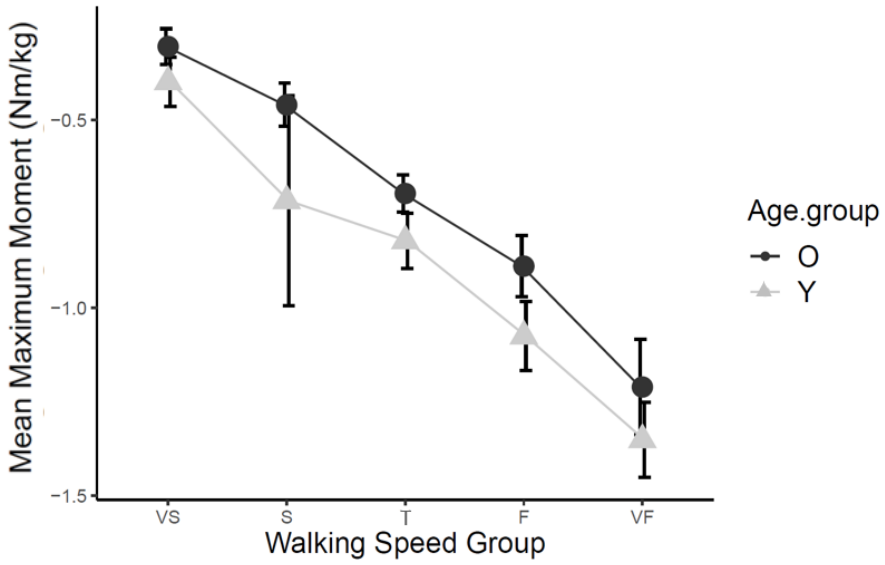


Figure 88. Mean max FLEX moment of the hip during stance phase for the YG and OG across walking speeds at the 95% confidence interval (VS: Very Slow, S: Slow, T: Typical, F: Fast, VF: Very Fast).

Significant differences in time to mean max FLEX moment ($p<.05$) during stance phase were found between YA and OA as WS increased (Figure 87, Table 44). The YG had a significantly shorter time to mean max FLEX moment ($p<.05$) across all WSs. For the YG, the max FLEX moment occurred at 47.03±12.16 percent GC at the VS speed, increasing to 50.09±3.28 percent GC at the VF speed. Whereas the OG demonstrated max FLEX moments at 57.83±6.76 percent GC at the VS speed, decreasing to 52.19±3.18 percent GC at the VF speed.

The mean max FLEX (FLEX) moment across WSs during swing, with error bars (95% confidence interval), is presented in Figure 89. Descriptive results for the OG showed that the mean max FLEX moment during swing decreased as WS increased, with a larger associated marginal error. The mean max FLEX moment during swing for the YG increased from VS to slow WS, after which point, the angle began to decrease. In addition, the OG showed greater mean max FLEX moments across speeds, except for the VS WS, compared to the YG. Additionally, at the VF speed, the OG showed a larger marginal error for the mean max hip FLEX moment during swing. Similarly, at the VS speed, the YG showed a larger marginal error for the mean max hip FLEX moment during swing (Figure 89). This is due to the variations in sample size between YA and OA. As expected, the OG had a smaller sample size for the VF speed group and the YG had a smaller sample size for the VS speed group. In both cases, a small sample size caused a larger marginal error.

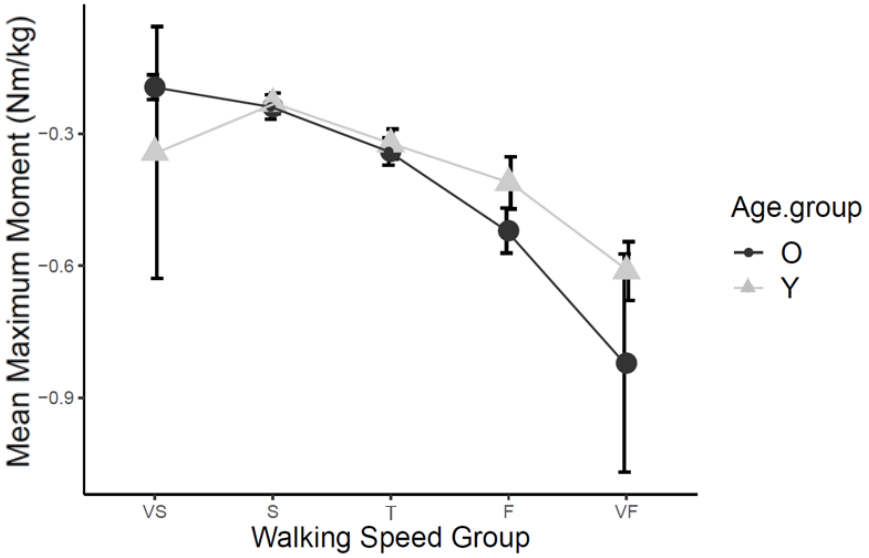


Figure 89. Mean max FLEX moment of the hip during swing phase for the YG and OG across walking speeds at the 95% confidence interval (VS: Very Slow, S: Slow, T: Typical, F: Fast, VF: Very Fast).

The YG had a significantly ($p<.05$) reduced mean max FLEX moment during swing phase as WS increased from fast to VF speed (fast: -0.41 ±0.12 $\frac{N \cdot m}{kg}$; VF: -0.61±0.19 $\frac{N \cdot m}{kg}$) compared to the OG (fast: -0.52±0.13 $\frac{N \cdot m}{kg}$; VF: -0.82±0.55 $\frac{N \cdot m}{kg}$), as shown in Table 44.

Significant differences in time to mean max FLEX moment ($p<.05$) during swing phase were found between YA and OA at the slow speed only (Figure 87, Table 44). The YG had a significantly shorter time to mean max FLEX moment ($p<.05$) as WS increased from slow to VF speed. For the YG, the max FLEX moment occurred at 66.02±4.84 percent GC at the slow speed, decreasing to 60.18±2.04 percent GC at the VF speed. Whereas the OG demonstrated max FLEX moments at 67.76±4.81 percent GC at the slow speed, decreasing to 62.46±1.80 percent GC at the VF speed.

The mean max EXT moment across WSs during stance, with error bars (95% confidence interval), is presented in Figure 90. Descriptive results for both groups showed the mean max EXT moment during stance increased as WS increased. In addition, the OG demonstrated greater mean max EXT moments across speeds compared to the YG. Both groups displayed similar trends with a small associated marginal error (Figure 90). The YG had a significantly ($p<.05$) decreased mean max EXT moment during stance phase at the slow speed only (slow: 0.34±0.21 $\frac{N \cdot m}{kg}$) compared to the OG (slow: 0.39±0.13 $\frac{N \cdot m}{kg}$), as shown in Table 44.

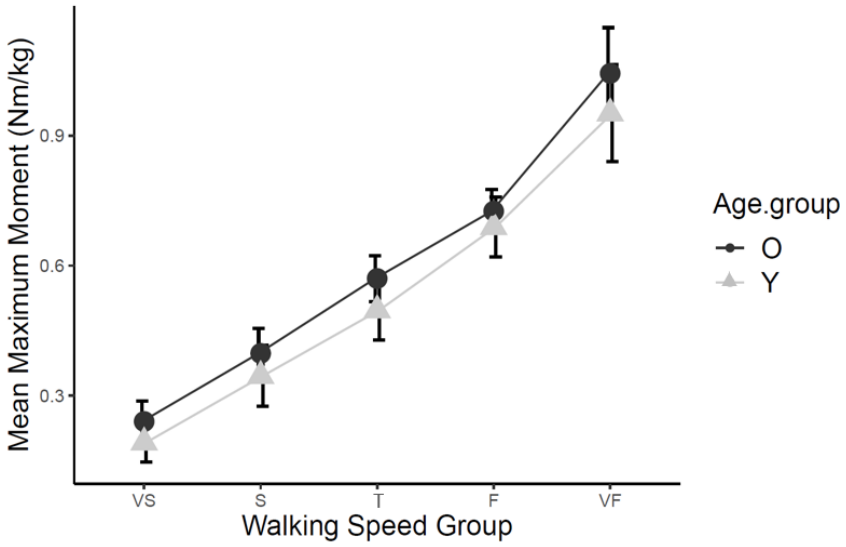


Figure 90. Mean max EXT moment of the hip during stance phase for the YG and OG across walking speeds at the 95% confidence interval (VS: Very Slow, S: Slow, T: Typical, F: Fast, VF: Very Fast).

Significant differences in time to mean max EXT moment ($p<.05$) during stance phase were found between YA and OA as WS increased from slow to typical WS (Figure 87, Table 44). The YG had a longer time to mean max EXT moment ($p<.05$) for the slow WS. However, the YG had a significantly shorter time to mean max EXT moment ($p<.05$) for the typical WS. For the YG, the max EXT moment occurred at 7.72±9.15 percent GC at the slow WS, decreasing to 4.56±1.56 percent GC at the typical WS. Whereas the OG demonstrated max EXT moments at 5.38±1.88 percent GC at the slow WS, increasing to 6.26±4.83 percent GC at the typical WS.

The mean max EXT moment across WSs during swing, with error bars (95% confidence interval), is presented in Figure 91. Descriptive results showed that the mean max EXT moment (peak) during swing increased as WS increased for both groups. However, the OG displayed a larger associated marginal error. In addition, the OG

demonstrated greater mean max EXT moment for the fast and VF speeds compared to the YG (Figure 91). Additionally, at the VF speed, the OG exhibited a larger marginal error for the mean max hip EXT moment during swing (Figure 91). Similarly, at the VS speed, the YG exhibited a larger marginal error for the mean max hip EXT moment during swing (Figure 91). This is due to the variations in sample size between YA and OA. As expected, the OG had a smaller sample size for the VF speed group and the YG had a smaller sample size for the VS speed group. In both cases, a small sample size caused a larger marginal error.

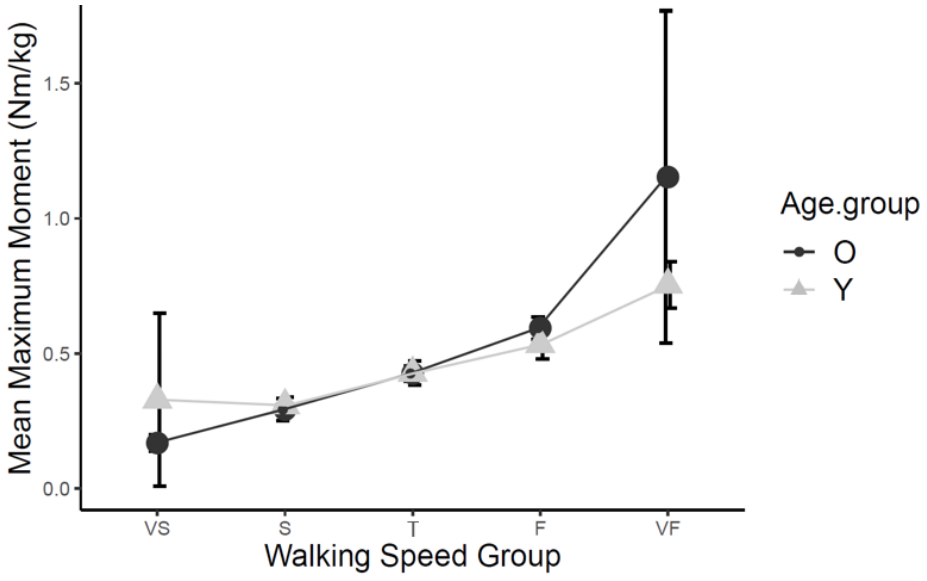


Figure 91. Mean max EXT moment of the hip during swing phase for the YG and OG across walking speeds at the 95% confidence interval (VS: Very Slow, S: Slow, T: Typical, F: Fast, VF: Very Fast).

The YG had a significantly ($p<.05$) decreased mean max EXT moment during swing phase (i.e., significantly lower peak PF) at the VF WS only (VF: 0.75±0.25 $\frac{N \cdot m}{kg}$) compared to the OG (VF: 1.15±1.38 $\frac{N \cdot m}{kg}$).

Significant differences in time to mean max EXT moment ($p<.05$) during swing phase were found between YA and OA as WS increased from VS to fast speed, except for the typical speed (Figure 87, Table 44). The YG had a significantly shorter time to mean max EXT moment ($p<.05$) for the VS, slow, and fast WSs. For the YG, the max EXT moment occurred at 89.31±11.00 percent GC at the VS speed, increasing to 93.18±4.34 percent GC at the fast speed. Whereas the OG showed max EXT moments at 94.62±4.54 percent GC at the VS speed, increasing to 95.28±2.84 percent GC at the fast WS.

4.1.15.2 Age-related Differences in Hip Power

The mean power for the hip in the sagittal plane is presented in Figure 92. This is the hip concentric-eccentric flexion-extension (FLEX/EXT) power by the joint moment of force and joint angular velocity acting at the hip joint. The following section focuses on between-group differences. Table 45 presents the significant age-related differences in the mean max and min flexion-extension powers in stance and swing phase as well as their respective time of occurrence as a percentage of GC.

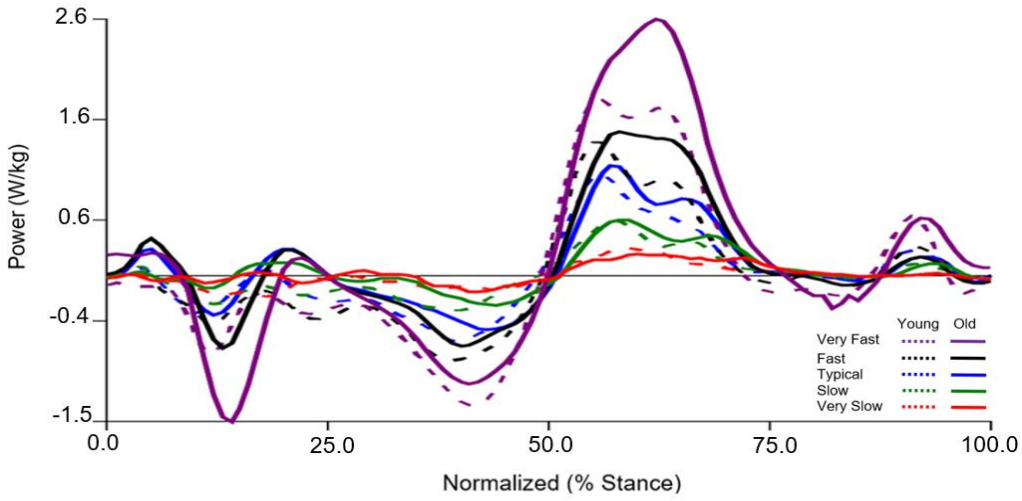


Figure 92. Mean flexion-extension power for the hip of the OG versus the YG at each walking speed.

Table 45. Significant p-values of the mean min and max eccentric and concentric power (W/Kg) of the hip during stance and swing phase, as well as their respective time of occurrence in the gait cycle across five walking speeds.

Walking speed group	Min ECC power in stance p-value	Time to min ECC power in stance p-value	Min ECC power in swing p-value	Time to min ECC power in swing p-value	Max CNC power in stance p-value	Time to max CNC power in stance p-value	Max CNC power in swing p-value	Time to max CNC power in swing p-value
VS	.01	-	-	<.01	-	-	-	.01
S	-	-	-	.03	-	-	-	-
T	-	-	-	-	-	-	-	-
F	-	-	-	-	-	.04	-	<.01
VF	-	-	-	-	-	<.001	-	-

Note: VS: Very Slow, S: Slow, T: Typical, F: Fast, VF: Very Fast.; '-' indicates no significant difference.

The mean min ECC power of the hip across WSs during stance, with error bars (95% confidence interval), is presented in Figure 93. Descriptive results for both groups showed that the mean min ECC power during stance decreased as WS increased. In addition, the OG showed greater mean min ECC power across speeds compared to the OG. Both groups displayed a similar trend of variability with a small associated marginal error.

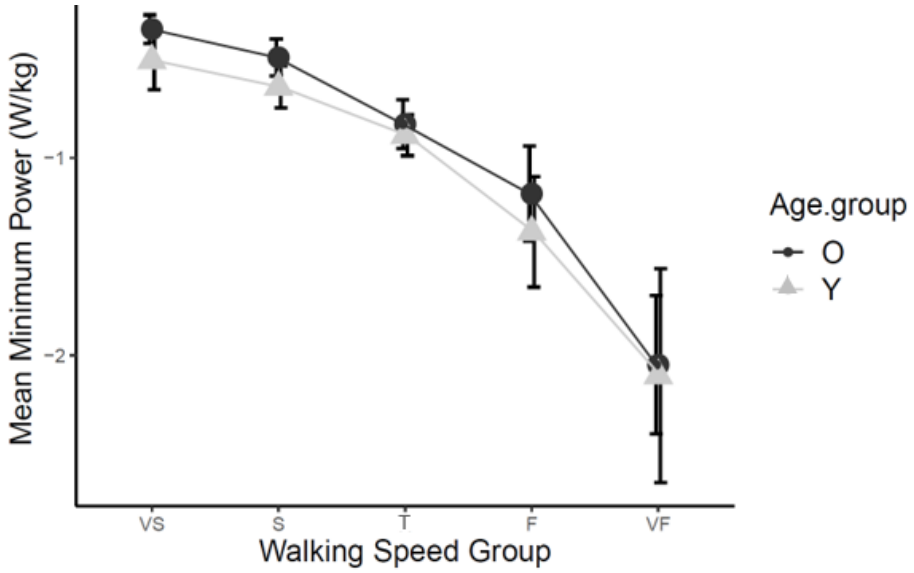


Figure 93. Mean min ECC power of the hip during stance phase for the YG and OG across walking speeds at the 95% confidence interval (VS: Very Slow, S: Slow, T: Typical, F: Fast, VF: Very Fast).

The YG had a significantly ($p<.05$) increased mean min ECC power during stance phase at the VS speed only (VS: -0.50±0.39 $\frac{W}{Kg}$) compared to the OG (VS: -0.34±0.20 $\frac{W}{Kg}$), as shown in Table 45.

Significant differences in time to mean min ECC power ($p<.05$) during swing phase were found between YA and OA as WS increased from VS to slow speed (Figure 92, Table 45). The YG had a significantly shorter time to mean min ECC power ($p<.05$) for the VS and slow speed. For the YG, the min ECC power occurred at 84.37±12.15 percent GC at the VS speed, increasing to 87.05±10.56 percent GC at the slow speed. Whereas the OG demonstrated min ECC power at 93.60±6.79 percent GC at the VS speed, decreasing to 92.12±8.37 percent GC at the slow speed.

4.1.15.3 Age-related Differences in Hip Angles

The mean relative angle for the hip segment in the sagittal plane is presented in Figure 94. This is the hip flexion-extension (FLEX/EXT) angle defined by the relative orientation of the pelvic coordinate system. The following section focuses on between-group differences. Table 46 presents the significant age-related differences in the mean max and min FLEXT/EXT angles in stance and swing phase as well as their respective time of occurrence as a percentage of GC.

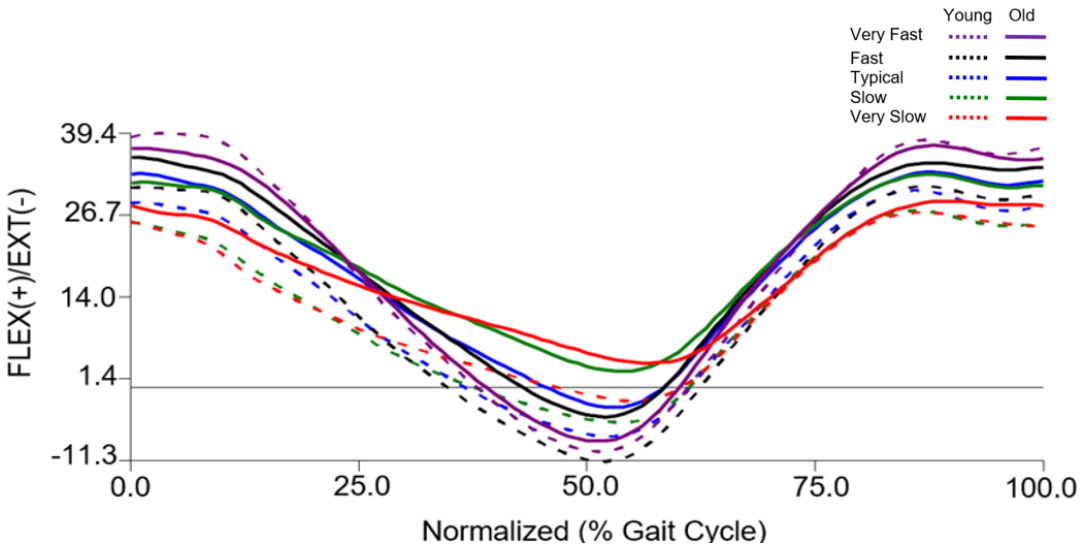


Figure 94. Mean flexion-extension for the hip of the OG versus the YG at each walking speed.

Table 46. Significant p-values of the mean min and max FLEX/EXT angles (∠) of the hip during stance and swing phase, as well as their respective time of occurrence in the gait cycle across five walking speeds.

Walking speed group	Max extension ∠ in stance p-value	Time to max extension ∠ in stance p-value	Min flexion ∠ in swing p-value	Time to min flexion ∠ in swing p-value	Max flexion ∠ in stance p-value	Time to max flexion ∠ in stance p-value	Max flexion ∠ in swing p-value	Time to max flexion ∠ in swing p-value
VS	-	<.01	.03	<.00001	-	-	-	-
S	.01	-	<.01	<.001	.01	.02	.04	-
T	-	-	.03	<.01	-	-	-	<.001
F	.03	-	.01	<.01	-	-	-	-
VF	-	-	-	<.01	-	-	-	-

Note: VS: Very Slow, S: Slow, T: Typical, F: Fast, VF: Very Fast.; '-' indicates no significant difference.

The mean max EXT angle across WSs during stance, with error bars (95% confidence interval), is presented in Figure 95. Descriptive results showed that the mean max EXT angle during stance decreased as WS increased for both groups, except for the VF speed for the YG. In addition, the OG demonstrated greater mean max EXT angles across speeds, with a larger associated marginal error, compared to the YG (Figure 95). The YG had a significantly ($p<.05$) increased mean max EXT angle during stance at the

slow and fast WSs (slow: -5.75°±6.26°; fast: -11.78°±5.39°) compared to the OG (slow: 2.29°±9.55°; fast: -4.27°±8.00°), as shown in Table 46.

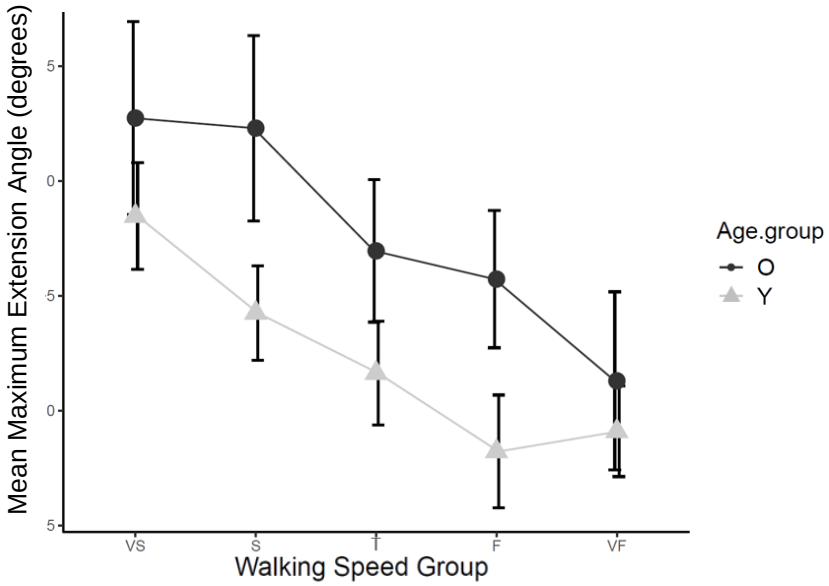


Figure 95. Mean max EXT angle of the hip during stance phase for the YG and OG across walking speeds at the 95% confidence interval (VS: Very Slow, S: Slow, T: Typical, F: Fast, VF: Very Fast).

Significant differences in time to mean max EXT angle ($p<.05$) during stance phase were found between YA and OA at the VS speed only (Figure 94, Table 46). The YG had a significantly shorter time to mean max EXT angle ($p<.05$) for the VS WS. For the YG, the mean max EXT angle occurred at 53.61±6.48 percent GC at the VS speed, whereas the OG demonstrated mean max EXT angle at 58.36±5.24 percent GC at the VS speed.

The mean min FLEX angle across WSs during swing, with error bars (95% confidence interval), is presented in Figure 96. Descriptive results showed that the mean min FLEX angle during swing decreased as WS increased for both groups, except for the VF speed for the YG. In addition, the OG demonstrated greater mean min FLEX angles across speeds, with a larger associated marginal error, compared to the YG (Figure 96).

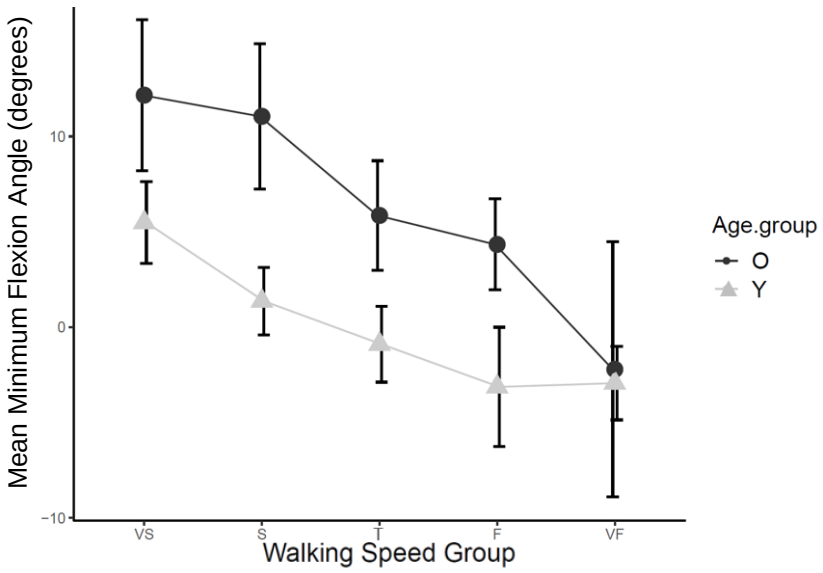


Figure 96. Mean min FLEX angle of the hip during swing phase for the YG and OG across walking speeds at the 95% confidence interval (VS: Very Slow, S: Slow, T: Typical, F: Fast, VF: Very Fast).

The YG had a significantly ($p<.05$) decreased mean min FLEX angle during swing as WS increased from VS to fast WSs (VS: 5.48°±5.74°; fast: -3.13°±6.87°) compared to the OG (VS: 12.16°±11.34°; fast: 4.33°±6.38°), as shown in Table 46.

Significant differences in time to mean min FLEX angle ($p<.05$) during swing phase were found between YA and OA across all speeds (Figure 94, Table 46). The YG had a significantly shorter time to mean min FLEX angle ($p<.05$) for the VS, slow, typical, fast, and VF WS. For the YG, the mean min FLEX occurred at 64.67±2.76 percent GC at the VS speed, decreasing to 59.15±1.51 percent GC at the VF speed. Whereas the OG demonstrated mean min FLEX at 69.32±4.81 percent GC at the VS speed, decreasing to 60.47±1.77 percent GC at the VF speed.

The mean max FLEX angle across WSs during stance, with error bars (95% confidence interval), is presented in Figure 97. Descriptive results for the OG showed that

the mean max FLEX angle (peak) during stance increased as WS increased. The mean max FLEX angle for the YG decreased from VS to slow speed, after which point, the mean max FLEX angle began to increase. Overall, both age groups displayed similar trends and similar associated marginal error. In addition, the OG demonstrated greater mean max FLEX angles across speeds, except for the VF speed, compared to the YG (Figure 97). The YG had a significantly ($p<.05$) decreased mean max FLEX angle during stance at the slow speed only (slow: 25.05°±6.92°) compared to the OG (slow: 32.32°±7.05°), as shown in Table 46.

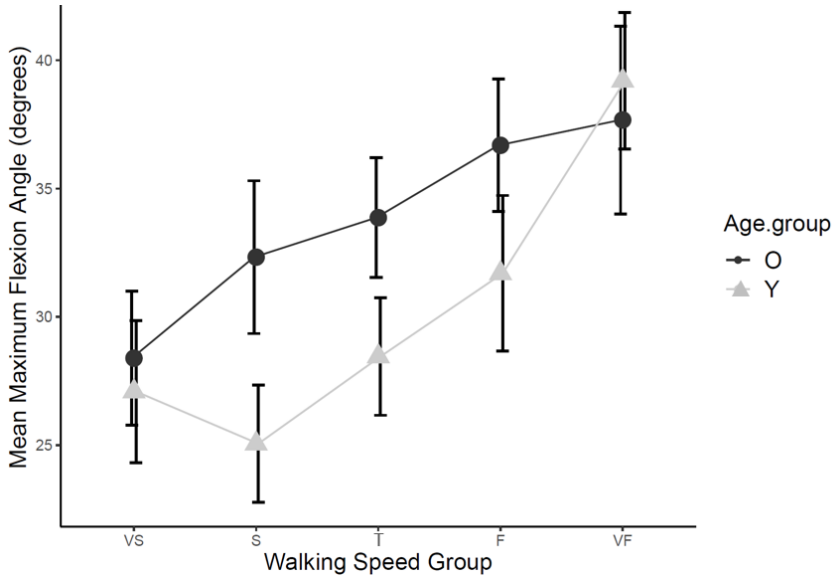


Figure 97. Mean max FLEX angle of the hip during stance phase for the YG and OG across walking speeds at the 95% confidence interval (VS: Very Slow, S: Slow, T: Typical, F: Fast, VF: Very Fast).

Significant differences in time to mean max FLEX angle ($p<.05$) during stance phase were found between YA and OA at the slow WS only (Figure 94, Table 46). The YG had a significantly shorter time to mean max FLEX angle ($p<.05$) for the slow WS. For the YG, the mean max FLEX angle occurred at 1.52±3.73 percent GC at the slow WS, whereas the OG showed mean max FLEX angle at 2.93±3.26 percent GC at the slow WS.

The mean max FLEX angle across WSs during swing, with error bars (95% confidence interval), is presented in Figure 98. Descriptive results for the OG showed that the mean max FLEX angle (peak) during stance increased as WS increased. The mean max FLEX angle for the YG decreased from VS to slow speed, after which point, the mean max FLEX angle began to increase. Overall, both age groups displayed similar trends and similar associated marginal error. In addition, the OG demonstrated greater mean max FLEX angles across speeds, except for the VF speed, compared to the YG (Figure 98).

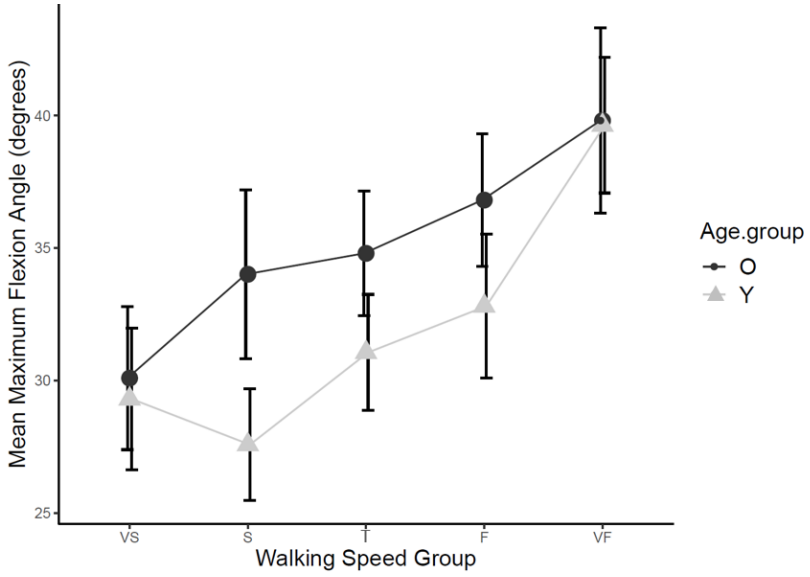


Figure 98. Mean max FLEX angle of the hip during swing phase for the YG and OG across walking speeds at the 95% confidence interval (VS: Very Slow, S: Slow, T: Typical, F: Fast, VF: Very Fast).

The YG had a significantly ($p<.05$) decreased mean max FLEX angle during swing at the slow speed only (slow: 27.58°±6.40°) compared to the OG (slow: 34.01°±7.55°), as shown in Table 46.

Significant differences in time to mean max FLEX angle ($p<.05$) during swing phase were found between YA and OA at the typical speed only (Figure 94, Table 46). The

YG had a significantly shorter time to mean max FLEX angle ($p<.05$) for the typical WS. For the YG, the mean max FLEX angle occurred at 88.36±5.38 percent GC at the typical speed, whereas the OG demonstrated mean max FLEX angle at 91.79±5.68 percent GC at the typical speed (Figure 94).

Table 47 presents the significant ($p<.05$) age-related differences in the FLEX/EXT range of motion (ROM) data for the hip. Relative FLEX/EXT ROM data for the hip are provided in Table 47. The YG displayed the greatest FLEX/EXT ROM (Figure 89) across all speeds during stance and swing compared to the OG. Table 47 presents the between-group differences found for the FLEX/EXT ROM during stance and swing phase.

Table 47. Significant FLEX/EXT ROM data for the hip during stance and swing phase across five walking speeds.

FLEX/EXT ROM Hip			
	Mean	± Std	P-value
Very Slow Young Stance	28.62°	1.19°	-
Very Slow Old Stance	25.65°	4.53°	
Slow Young Stance	30.81°	0.66°	-
Slow Old Stance	30.03°	2.49°	
Typical Young Stance	36.83°	0.06°	-
Typical Old Stance	36.91°	2.28°	
Fast Young Stance	43.47°	1.27°	-
Fast Old Stance	40.96°	1.09°	
Very Fast Young Stance	50.10°	2.05°	<.05
Very Fast Old Stance	46.38°	0.48°	
Very Slow Young Swing	23.82°	1.40°	<.001
Very Slow Old Swing	17.93°	3.59°	
Slow Young Swing	26.21°	1.04°	<.05
Slow Old Swing	22.95°	1.45°	
Typical Young Swing	31.95°	0.57°	<.01
Typical Old Swing	28.94°	1.53°	
Fast Young Swing	35.94°	0.89°	<.05
Fast Old Swing	32.47°	0.31°	
Very Fast Young Swing	42.56°	1.88°	-
Very Fast Old Swing	42.02°	7.18°	

Note: Std: Standard deviation.; '-' indicates no significant difference.

The YG exhibited a significantly ($p<.05$) greater FLEX/EXT ROM during stance for the VF speed only (VF: 50.10°±2.05°) compared to the OG (VF: 46.38°±0.48°) as shown in Table 47. During swing phase, the YG exhibited a significantly ($p<.05$) greater FLEX/EXT ROM as WS increased speed from VS to fast WS (VS: 23.82°±1.40°; fast: 35.94°±0.89°) compared to the OG (VS: 17.93°±3.59°; fast: 32.47°±0.31°) as shown in Table 47. During VF speed walking, the FLEX/EXT ROM for the YA and OA increased most in the hip during stance and swing.

The mean relative angle for the hip segment in the frontal plane is presented in Figure 99. This is the hip adduction-abduction (ADD/ABD) angle defined by the relative orientation of the pelvic coordinate system. The following section focuses on between-group differences. Table 48 presents the significant age-related differences in the mean max and min ADD/ABD angles in stance and swing phase as well as their respective time of occurrence as a percentage of GC.

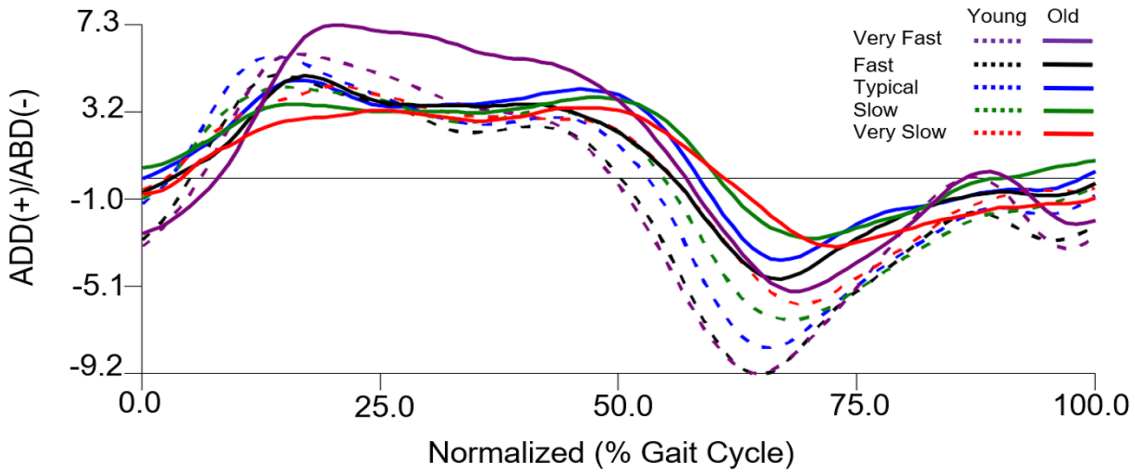


Figure 99. Mean adduction-abduction for the hip of the OG versus the YG at each walking speed.

Table 48. Significant p-values of the mean max ADD/ABD angles (∠) of the hip during stance and swing phase, as well as their respective time of occurrence in the gait cycle across five walking speeds.

Walking speed group	Max ABD ∠ in stance p-value	Time to max ABD ∠ in stance p-value	Max ABD ∠ in swing p-value	Time to max ABD ∠ in swing p-value	Max ADD ∠ in stance p-value	Time to max ADD ∠ in stance p-value	Max ADD ∠ in swing p-value	Time to max ADD ∠ in swing p-value
VS	-	<.01	.03	<.01	-	-	-	-
S	.01	.04	<.001	.01	-	-	-	-
T	.02	-	<.001	<.001	-	.01	-	-
F	<.01	-	<.01	.01	-	.02	-	-
VF	.01	-	<.01	<.0001	-	.03	-	-

Note: VS: Very Slow, S: Slow, T: Typical, F: Fast, VF: Very Fast.; '-' indicates no significant difference.

The mean max ABD angle across WSs during stance, with error bars (95% confidence interval), is presented in Figure 100. Descriptive results showed that the mean max ABD angle during stance decreased as WS increased for the YG. The mean max ABD angle for the OG increased from VS to slow WS, after which point, began to decrease. Overall, both age groups displayed similar trends and similar associated marginal error. Further, the OG showed greater mean max ABD angles across speeds compared to the YG.

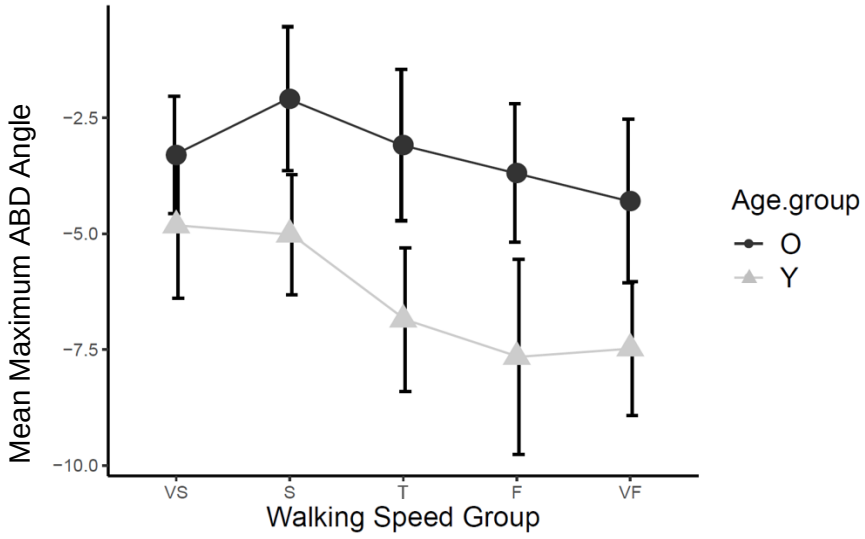


Figure 100. Mean max ABD angle of the hip during stance phase for the YG and OG across walking speeds at the 95% confidence interval (VS: Very Slow, S: Slow, T: Typical, F: Fast, VF: Very Fast).

The YG had a significantly ($p<.05$) increased mean max ABD angle during stance as WS increased from slow to VF speed (slow: -5.01°±3.94°; VF: -7.47°±4.32°) compared to the OG (slow: -2.09°±3.68°; VF: -4.29°±3.98°), as shown in Table 48.

Significant differences in time to mean max ABD angle ($p<.05$) during stance phase were found between YA and OA as WS increased form VS to slow speed (Figure 99, Table 48). The YG had a significantly longer time to mean max ABD angle ($p<.05$) for the slow and VS WS. For the YG, the mean max ABD occurred at 56.48±19.27 percent GC at the VS speed, increasing to 57.72±14.64 percent GC at the slow speed. Whereas the OG demonstrated mean max ABD at 54.62±27.86 percent GC at the VS speed, decreasing to 52.99±23.91 percent GC at the slow speed (Figure 99).

The mean max ABD angle across WSs during swing, with error bars (95% confidence interval), is presented in Figure 101. Descriptive results showed that the mean max ABD angle during swing decreased as WS increased for the YG. The mean max ABD angle for the OG increased from VS to slow speed, after which point, began to decrease. Overall, both age groups displayed similar trends as WS increased from slow to VF speed and showed similar associated marginal error. In addition, the OG demonstrated greater mean max ABD angles across speeds compared to the YG (Figure 101). The YG had a significantly ($p<.05$) increased mean max ABD angle during swing as WS increased (VS: -6.67°±3.94°; VF: -9.76°±3.50°) compared to the OG (VS: -4.26°±3.71°; VF: -6.41°±3.80°), as shown in Table 48.

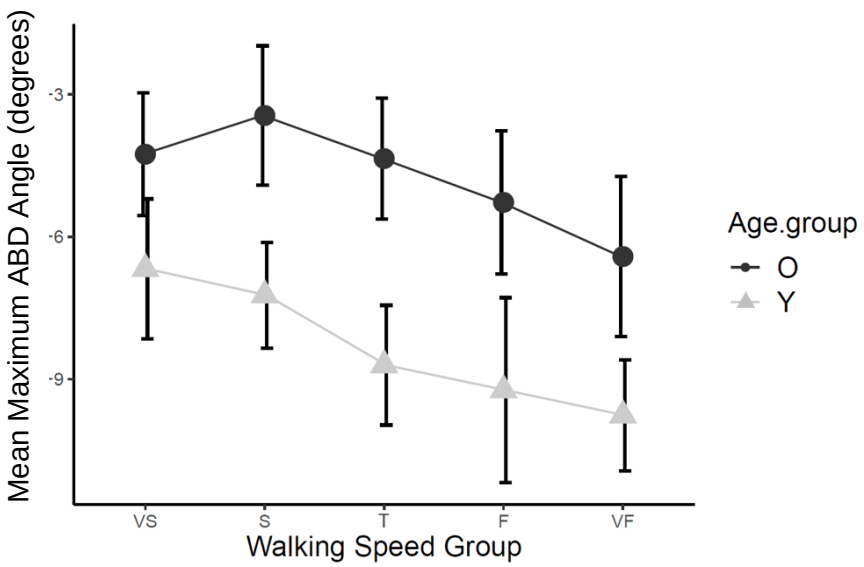


Figure 101. Mean max ABD angle of the hip during swing phase for the YG and OG across walking speeds at the 95% confidence interval (VS: Very Slow, S: Slow, T: Typical, F: Fast, VF: Very Fast).

Significant differences in time to mean max ABD angle ($p<.05$) during swing phase were found between YA and OA across all speeds (Figure 99, Table 48). The YG had a significantly shorter time to mean max ABD angle ($p<.05$) for the VS, slow, typical, fast, and VF WS. For the YG, the mean max ABD occurred at 69.20±7.55 percent GC at the VS speed, decreasing to 67.58±8.05 percent GC at the VF speed. Whereas the OG demonstrated mean max ABD at 76.31±9.18 percent GC at the VS speed, decreasing to 76.00±11.86 percent GC at the VF speed (Figure 99).

Table 49 presents the significant ($p<.05$) age-related differences in the ADD/ABD range of motion (ROM) data for the hip. In addition, relative ADD/ABD ROM data for the hip are provided in Table 49. The YG displayed the greatest ADD/ABD ROM (Figure 101) across all speeds during stance and swing compared to the OG. Table 49 presents the between-group differences found for the ADD/ABD ROM during stance and swing phase.

The YG exhibited a significantly (p<.05) greater ADD/ABD ROM during stance as WS increased from VS to fast WS (VS: 9.92°±0.89°; fast: 13.42°±1.02°) compared to the OG (VS: 7.89°±0.12°; fast: 10.29°±0.01°) as shown in Table 49. During swing phase, the YG exhibited a significantly (p<.05) greater ADD/ABD ROM as WS increased from VS to fast WS (VS: 7.36°±0.69°; fast: 8.70°±0.96°) compared to the OG (VS: 4.21°±0.51°; fast: 6.76°±0.07°) as shown in Table 49. During VF speed walking, the ADD/ABD ROM for the YA and OA increased most in the hip during stance and swing.

Table 49. Significant ADD/ABD ROM data for the hip during stance and swing phase across five walking speeds and their respective significant p-values.

ADD/ABD ROM Hip			
	Mean	± Std	P-value
Very Slow Young Stance	9.92°	0.89°	<.01
Very Slow Old Stance	7.89°	0.12°	
Slow Young Stance	10.54°	0.46°	<.001
Slow Old Stance	7.37°	0.33°	
Typical Young Stance	13.10°	0.58°	<.01
Typical Old Stance	9.70°	0.38°	
Fast Young Stance	13.42°	1.02°	<.01
Fast Old Stance	10.29°	0.01°	
Very Fast Young Stance	14.78°	1.01°	-
Very Fast Old Stance	13.31°	0.41°	
Very Slow Young Swing	7.36°	0.69°	<.001
Very Slow Old Swing	4.21°	0.51°	
Slow Young Swing	7.16°	0.06°	<.001
Slow Old Swing	4.68°	0.24°	
Typical Young Swing	8.41°	0.27°	<.001
Typical Old Swing	5.55°	0.12°	
Fast Young Swing	8.70°	0.96°	<.05
Fast Old Swing	6.76°	0.07°	
Very Fast Young Swing	10.51°	0.12°	-
Very Fast Old Swing	9.14°	3.04°	

Note: Std: Standard deviation.; '-' indicates no significant difference.

The mean relative angle for the hip segment in the transverse plane is presented in Figure 102. This is the hip internal-ER (INT/EXTL) angle defined by the relative orientation of the pelvic coordinate system. The following section focuses on between-

group differences. Table 50 presents the significant age-related differences in the mean max and min INT/EXTL rotation angles in stance and swing phase as well as their respective time of occurrence as a percentage of GC.

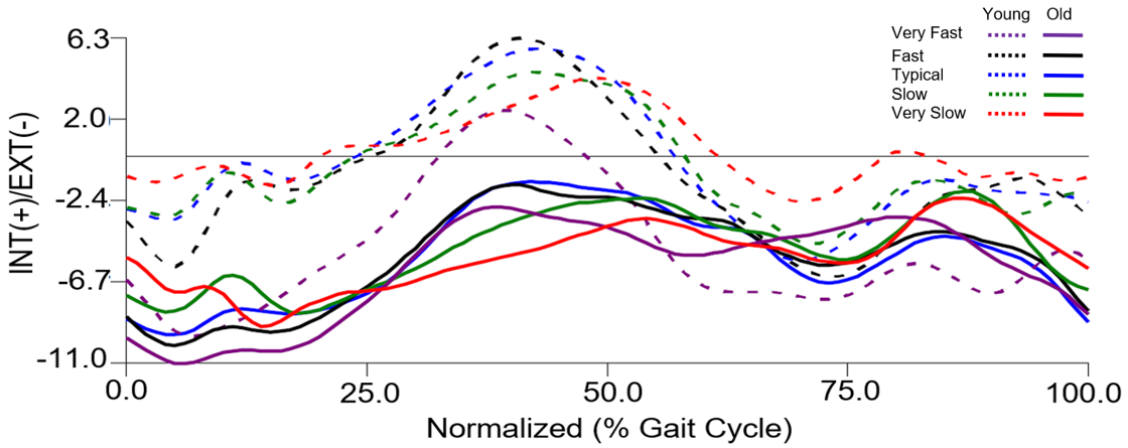


Figure 102. Mean internal-external rotation for the hip of the OG versus the YG at each walking speed.

Table 50. Significant p-values of the mean max INT/EXTL rotation angles (∠) of the hip during stance and swing phase, as well as their respective time of occurrence in the gait cycle across five walking speeds.

Walking speed group	Max external rotation ∠ in stance p-value	Time to max external rotation ∠ in stance p-value	Max external rotation ∠ in swing p-value	Time to max external rotation ∠ in swing p-value	Max internal rotation ∠ in stance p-value	Time to max internal rotation ∠ in stance p-value	Max internal rotation ∠ in swing p-value	Time to max internal rotation ∠ in swing p-value
VS	.01	-	-	-	<.01	-	-	-
S	-	-	-	<.001	.04	-	-	-
T	.02	-	-	<.00001	.02	-	-	.02
F	-	.04	-	<.01	<.01	-	-	-
VF	-	-	-	-	.03	-	-	-

Note: VS: Very Slow, S: Slow, T: Typical, F: Fast, VF: Very Fast.; '-' indicates no significant difference.

The mean max ER angle across WSs during stance, with error bars (95% confidence interval), is presented in Figure 103. Descriptive results showed that the mean max ER angle during stance decreased as WS increased for the YG. The mean max ER angle for the OG increased from VS to slow speed, after which point, began to decrease.

Overall, the OG demonstrated relatively consistent patterns of variability for the mean max ER angle. In addition, the YG demonstrated greater mean max ER angles across speeds compared to the OG. Both age groups showed a similar associated marginal error (Figure 103). Additionally, at the VF speed, the YG exhibited a similar mean as the OG for the mean max ER angle of the hip (Figure 103). This is due to the pattern showed in Figure 104, which exhibited a smaller offset between YA and OA for the VF speed at heel strike.

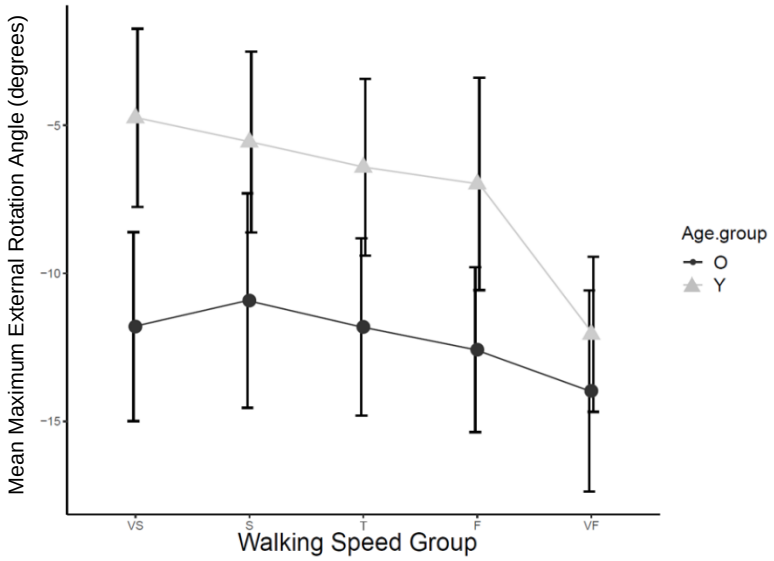


Figure 103. Mean max ER angle of the hip during stance phase for the YG and OG across walking speeds at the 95% confidence interval (VS: Very Slow, S: Slow, T: Typical, F: Fast, VF: Very Fast).

The YG had a significantly ($p<.05$) decreased mean max ER angle during stance as WS at the VS and typical WSs (VS: -4.74°±8.06°; typical: -6.41°±8.56°) compared to the OG (VS: -11.79°±9.14°; typical: -11.80°±8.85°), as shown in Table 50.

Significant differences in time to mean max ER angle ($p<.05$) during stance phase were found between YA and OA at the fast speed only (Figure 102, Table 50). The YG had a significantly shorter time to mean max ER angle ($p<.05$) for fast WS. For the YG,

the mean max ER occurred at 8.65±12.47 percent GC at the fast WS, whereas the OG demonstrated mean max ER at 13.71±14.75 percent GC at the fast WS (Figure 102).

The mean max internal rotation (IR) angle across WSs during stance, with error bars (95% confidence interval), is presented in Figure 104. Descriptive results showed that the mean max IR angle during stance for the YG increased from VS to fast speed, after which point, the angle began to decrease. The mean max IR angle for the OG increased from VS to typical speed, after which point, the angle began to decrease. Overall, both age groups demonstrated relatively consistent patterns of variability for the max IR angles at each speed. In addition, the YG demonstrated greater mean max IR angles across speeds, with a larger associated marginal error, compared to the OG (Figure 104).

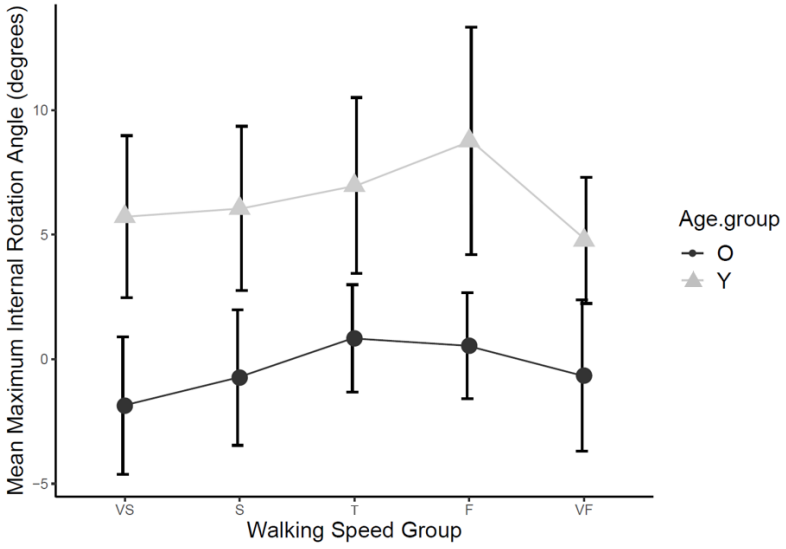


Figure 104. Mean max IR angle of the hip during stance phase for the YG and OG across walking speeds at the 95% confidence interval (VS: Very Slow, S: Slow, T: Typical, F: Fast, VF: Very Fast).

The YG had a significantly ($p<.05$) increased mean max IR angle during stance as WS increased from VS to fast speed (slow: 6.04°±10.04°; fast: 8.76°±10.04°) compared to the OG (slow: -0.74°±6.43°; fast: 0.53°±5.68°), as shown in Table 50.

Significant differences in time to mean max IR angle ($p<.05$) during swing phase were found between YA and OA at the typical speed only (Figure 102, Table 50). The YG had a significantly longer time to mean max IR angle ($p<.05$) for the typical WS. For the YG, the mean max IR occurred at 83.73±11.50 percent GC at the typical speed, whereas the OG demonstrated mean max IR at 77.10±11.94 percent GC at the typical speed (Figure 102).

Table 51 presents the significant ($p<.05$) age-related differences in the internal/ER range of motion (ROM) data for the hip. Relative internal/external ROM data for the hip are provided in Table 51. The YG displayed the greatest internal/ER ROM (Figure 102) across all speeds during stance compared to the OG. However, the OG displayed the greatest internal/ER ROM across all speeds during swing compared to the YG, except for the slow speed (Figure 102). Table 51 presents the between-group differences found for the internal/ER ROM during stance and swing phase. The YG exhibited a significantly ($p<.05$) greater internal/ER ROM during stance as WS increased from fast to VF speed (fast: 15.74°±2.16°; VF: 16.83°±0.24°) compared to the OG (fast: 13.11°±1.75°; VF: 13.30°±0.81°) as shown in Table 51. There were no significant ($p<.05$) age-related differences in the internal/ER ROM for the hip during swing (Table 51). During VF speed walking, the internal/external ROM for the YA and OA increased most in the hip during stance.

Table 51. Significant internal/ER ROM data for the hip during stance and swing phase across five walking speeds and their respective significant p-values.

INT/EXTL Rotation ROM Hip			
	Mean	± Std	P-value
Very Slow Young Stance	10.46°	0.63°	-
Very Slow Old Stance	9.92°	1.22°	
Slow Young Stance	11.61°	0.74°	-
Slow Old Stance	10.17°	2.13°	
Typical Young Stance	13.38°	1.56°	-
Typical Old Stance	12.64°	2.48°	
Fast Young Stance	15.74°	2.16°	<.05
Fast Old Stance	13.11°	1.75°	
Very Fast Young Stance	16.83°	0.24°	<.01
Very Fast Old Stance	13.30°	0.81°	
Very Slow Young Swing	8.34°	1.03°	-
Very Slow Old Swing	8.54°	0.17°	
Slow Young Swing	9.61°	0.31°	-
Slow Old Swing	9.30°	0.04°	
Typical Young Swing	8.92°	0.23°	-
Typical Old Swing	10.06°	0.32°	
Fast Young Swing	10.10°	1.88°	-
Fast Old Swing	10.35°	0.19°	
Very Fast Young Swing	9.72°	0.08°	-
Very Fast Old Swing	17.47°	1.09°	

Note: Std: Standard deviation.; '-' indicates no significant difference.

4.1.16 Summary of Hip Kinetics and Kinematics Results

When the speed effect is being considered, there are significant differences in the hip kinetics and kinematics between YA and OA. The key findings of the present study are as follows:

- The mean min FLEX moment in stance was significantly increased for the YG for the slow and VS speed compared to the OG. Similarly, the mean max EXT moment in stance was significantly increased for the YA for the slow speed only compared to the OA.
- The mean min FLEX moment in swing was significantly decreased for the YG for the fast and VF speed compared to the OG. Similarly, the mean max EXT

moment in swing was significantly decreased for the YA for the VF speed only compared to the OA.

- The mean min ECC power of the hip in stance phase was significantly decreased for the YG for the VS speed only compared to the OG.
- Significant differences for the hip joint angle in the sagittal, frontal, and transverse plane were found between age groups as a function of speed.
- In the sagittal plane, the mean max EXT angle of the hip in stance phase was significantly increased for the YG for the slow and fast WSs compared to the OG. Similarly, the mean max FLEX angle in stance was significantly increased for the YG for the slow speed only compared to the OA. Conversely, the mean min FLEX angle in swing phase was significantly decreased for the YG as WS decreased from VS to fast WS compared to the OG. Similarly, the mean max FLEX angle in swing was significantly decreased for the YG for the slow speed only compared to the OG.
- In the frontal plane, the mean max ABD angle of the hip in stance phase was significantly increased for the YG as WS increased from slow to VF WSs compared to the OG. Similarly, the mean max ABD angle of the hip in swing phase was significantly increased for the YA across all speeds compared to the OA.
- In the transverse plane, the mean max ER of the hip in stance phase was significantly decreased for the YG for the VS and typical WSs compared to the OG. Conversely, the mean max IR of the hip in stance phase was significantly increased for the YG across all WSs compared to the OG.

4.1.17 Age-related Differences in Pelvic Kinematics

The mean relative angle for the pelvic segment in the sagittal plane is presented in Figure 105. This is the pelvic anterior-posterior (ANT/POST) tilt angle defined by the relative orientation of the sacrum and the left and right anterior superior iliac spine. The following section focuses on between-group differences. Table 52 presents the significant age-related differences in the mean max and min ANT/POST tilt angles in stance and swing phase as well as their respective time of occurrence as a percentage of GC.

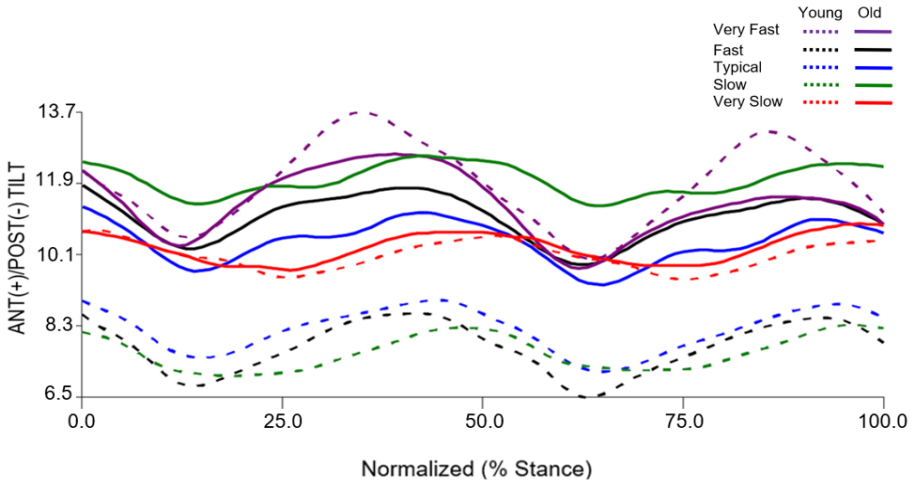


Figure 105. Mean anterior-posterior tilt for the pelvis of the OG versus the YG at each walking speed.

Table 52. Significant p-values of the mean min and max ANT/POST tilt angles (∠) of the pelvis during stance and swing phase, as well as their respective time of occurrence in the gait cycle across five walking speeds.

Walking speed group	Min anterior tilt ∠ in stance p-value	Time to min anterior tilt ∠ in stance p-value	Min anterior tilt ∠ in swing p-value	Time to min anterior tilt ∠ in swing p-value	Max anterior tilt ∠ in stance p-value	Time to max anterior tilt ∠ in stance p-value	Max anterior tilt ∠ in swing p-value	Time to max anterior tilt ∠ in swing p-value
VS	-	-	-	-	-	.04	-	-
S	<.001	-	<.01	-	.02	-	.03	-
T	.02	-	.01	-	.01	-	.02	-
F	-	-	-	-	-	-	-	-
VF	-	-	-	-	-	-	-	-

Note: VS: Very Slow, S: Slow, T: Typical, F: Fast, VF: Very Fast.; '-' indicates no significant difference.

The mean min anterior (ANT) tilt angle across WSs during stance, with error bars (95% confidence interval), is presented in Figure 106. Descriptive results showed that the mean min ANT tilt angle during stance decreased from VS to slow speed, after which point, the mean min ANT tilt angle was relatively consistent until the fast speed, where it increased again. The mean min ANT tilt angle for the OG increased from VS to slow speed, after which point, the mean min ANT tilt angle was relatively consistent. In addition, the OG demonstrated greater mean min ANT tilt angles across speeds, except for the VS speed, compared to the YG. Both age groups showed a similar associated marginal error (Figure 106).

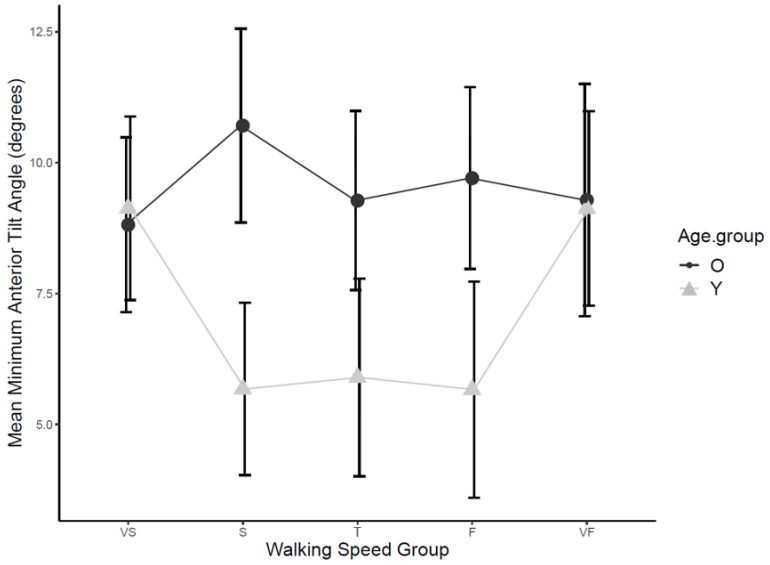


Figure 106. Mean min ANT tilt angle of the pelvis during stance phase for the YG and OG across walking speeds at the 95% confidence interval (VS: Very Slow, S: Slow, T: Typical, F: Fast, VF: Very Fast).

The YG had a significantly ($p<.05$) decreased mean min ANT tilt angle during stance as WS increased from slow to typical WS (slow: 5.67°±5.01°; typical: 5.89°±5.40°) compared to the OG (slow: 10.70°±4.38°; typical: 9.27°±5.05°), as shown in Table 52.

The mean min ANT tilt angle across WSs during swing, with error bars (95% confidence interval), is presented in Figure 107. Descriptive results showed that the mean min ANT tilt angle during stance decreased from VS to slow speed, after which point, the mean min ANT tilt angle was relatively consistent until the fast speed, where it increased again. The mean min ANT tilt angle for the OG increased from VS to slow speed, after which point, the mean min ANT tilt angle was relatively consistent. Both age groups demonstrated similar associated marginal error. In addition, the OG demonstrated greater mean min ANT tilt angles across speeds compared to the YG (Figure 107).

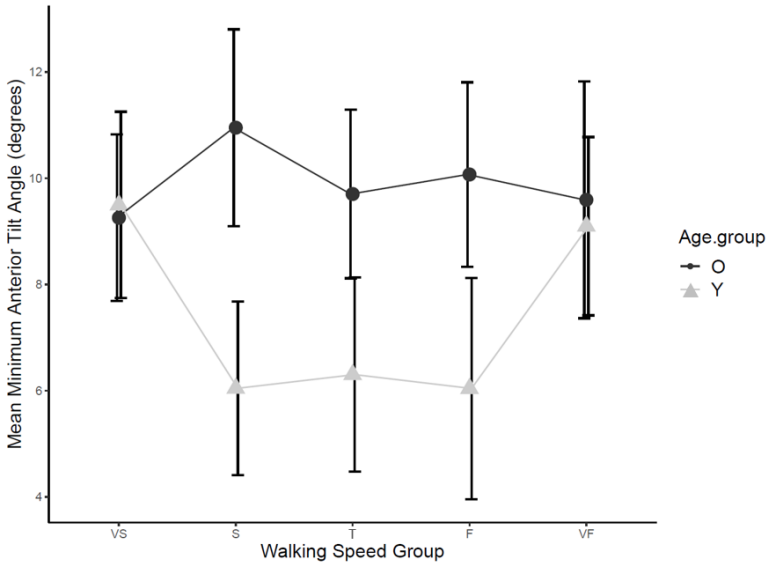


Figure 107. Mean min ANT tilt angle of the pelvis during swing phase for the YG and OG across walking speeds at the 95% confidence interval (VS: Very Slow, S: Slow, T: Typical, F: Fast, VF: Very Fast).

The YG had a significantly ($p<.05$) decreased mean min ANT tilt angle during swing as WS increased from slow to typical WS (slow: 6.04°±4.96°; typical: 6.30°±5.24°) compared to the OG (slow: 10.95°±4.39°; typical: 9.70°±4.69°), as shown in Table 52.

The mean max ANT tilt angle across WSs during stance, with error bars (95% confidence interval), is presented in Figure 108. Descriptive results showed that the mean max ANT tilt angle (peak) during stance decreased from VS to slow speed, after which point, the mean max ANT tilt angle was relatively consistent until the fast speed, where it increased again. The mean max ANT tilt angle for the OG increased from VS to slow speed, after which point, the mean max ANT tilt angle was relatively consistent. Both age groups demonstrated similar associated marginal error. In addition, the OG demonstrated greater mean max ANT tilt angles across speeds, except for the VS and VF speeds, compared to the YG (Figure 108).

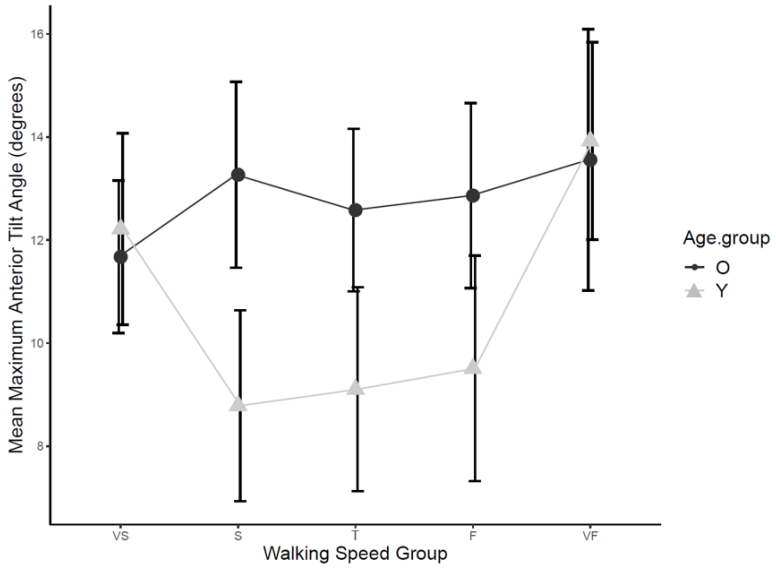


Figure 108. Mean max ANT tilt angle of the pelvis during stance phase for the YG and OG across walking speeds at the 95% confidence interval (VS: Very Slow, S: Slow, T: Typical, F: Fast, VF: Very Fast).

The YG had a significantly ($p<.05$) decreased mean max ANT tilt angle during stance as WS increased from slow to typical speed (slow: 8.78°±5.62°; typical: 9.10°±5.67°) compared to the OG (slow: 13.26°±4.26°; typical: 12.58°±4.65°), as shown in Table 52.

Significant differences in time to mean max ANT tilt angle ($p<.05$) during stance phase were found between YA and OA at the VS speed only (Figure 105, Table 52). The YG had a significantly longer time to mean max ANT tilt angle ($p<.05$) for the VS WS. For the YG, the mean max ANT tilt angle occurred at 30.08±23.20 percent GC at the VS speed, whereas the OG demonstrated mean max ANT tilt angle at 22.80±25.09 percent GC at the VS speed (Figure 105).

The mean max ANT tilt angle across WSs during swing, with error bars (95% confidence interval), is presented in Figure 109. Descriptive results showed that the mean max ANT tilt angle (peak) during swing decreased from VS to slow speed, after which point, the mean max ANT tilt angle was relatively consistent until the fast speed, where it increased again. The mean max ANT tilt angle for the OG increased from VS to slow speed, after which point, the mean max ANT tilt angle was relatively consistent. Both age groups demonstrated similar associated marginal error. In addition, the OG demonstrated greater mean max ANT tilt angles across speeds, except for the VS and VF speeds, compared to the YG (Figure 109). The YG had a significantly ($p<.05$) decreased mean max ANT tilt angle during swing as WS increased from slow to typical speed (slow: 8.56°±5.47°; typical: 8.91°±5.44°) compared to the OG (slow: 12.88°±4.33°; typical: 11.88°±4.80°), as shown in Table 54.

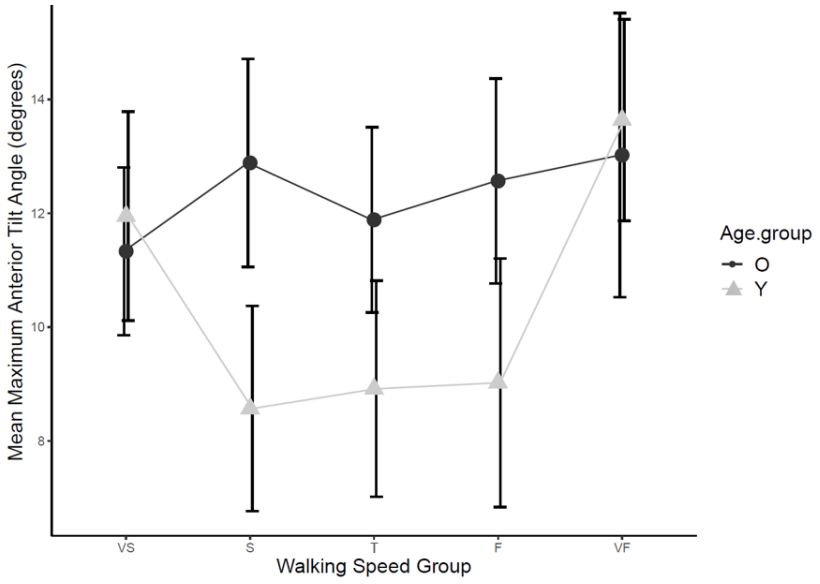


Figure 109. Mean max ANT tilt angle of the pelvis during swing phase for the YG and OG across walking speeds at the 95% confidence interval (VS: Very Slow, S: Slow, T: Typical, F: Fast, VF: Very Fast).

Table 53 presents the significant ($p<.05$) age-related differences in the anterior/posterior tilt range of motion (ROM) data for the pelvis. In addition, relative anterior/posterior tilt ROM data for the pelvis are provided in Table 53. The YG displayed the greatest anterior/posterior tilt ROM (Figure 105) across all speeds during stance and swing compared to the OG, except for the typical speed during stance. Table 53 presents the between-group differences found for the anterior/posterior tilt ROM during stance and swing phase. There were no significant ($p<.05$) age-related differences in the anterior/posterior tilt ROM for the pelvis during stance (Table 53). During swing phase, the YG exhibited a significantly ($p<.05$) greater anterior/posterior tilt ROM for the slow and VF WSs (slow: 2.52°±0.50°; VF: 4.54°±0.27°) compared to the OG (slow: 1.93°±0.05°; VF: 3.42°±0.60°) as shown in Table 53. During VF speed walking, the anterior/posterior tilt ROM for the YA and OA increased most in the pelvis during stance and swing.

Table 53. Significant anterior/posterior tilt ROM data for the pelvis during stance and swing phase across five walking speeds and their respective significant p-values.

ANT/POST Tilt ROM Hip			
	Mean	± Std	P-value
Very Slow Young Stance	3.08°	0.27°	-
Very Slow Old Stance	2.86°	0.54°	
Slow Young Stance	3.10°	0.61°	-
Slow Old Stance	2.55°	0.11°	
Typical Young Stance	3.20°	0.26°	-
Typical Old Stance	3.30°	0.39°	
Fast Young Stance	3.84°	0.27°	-
Fast Old Stance	3.15°	0.15°	
Very Fast Young Stance	4.79°	0.18°	-
Very Fast Old Stance	4.27°	0.71°	
Very Slow Young Swing	2.45°	0.21°	-
Very Slow Old Swing	2.07°	0.26°	
Slow Young Swing	2.52°	0.50°	<.05
Slow Old Swing	1.93°	0.05°	
Typical Young Swing	2.61°	0.20°	-
Typical Old Swing	2.18°	0.11°	
Fast Young Swing	2.98°	0.21°	-
Fast Old Swing	2.49°	0.16°	
Very Fast Young Swing	4.54°	0.27°	<.01
Very Fast Old Swing	3.42°	0.60°	

Note: Std: Standard deviation.; '-' indicates no significant difference.

The mean relative angle for the pelvic segment in the frontal plane is presented in Figure 110. This is the pelvic upward-downward obliquity (UP/DOWN) angle defined by the relative orientation of the sacrum and the left and right anterior superior iliac spine. The following section focuses on between-group differences. Table 54 presents the significant age-related differences in the mean max and min UP/DOWN tilt angles in stance and swing phase as well as their respective time of occurrence as a percentage of GC.

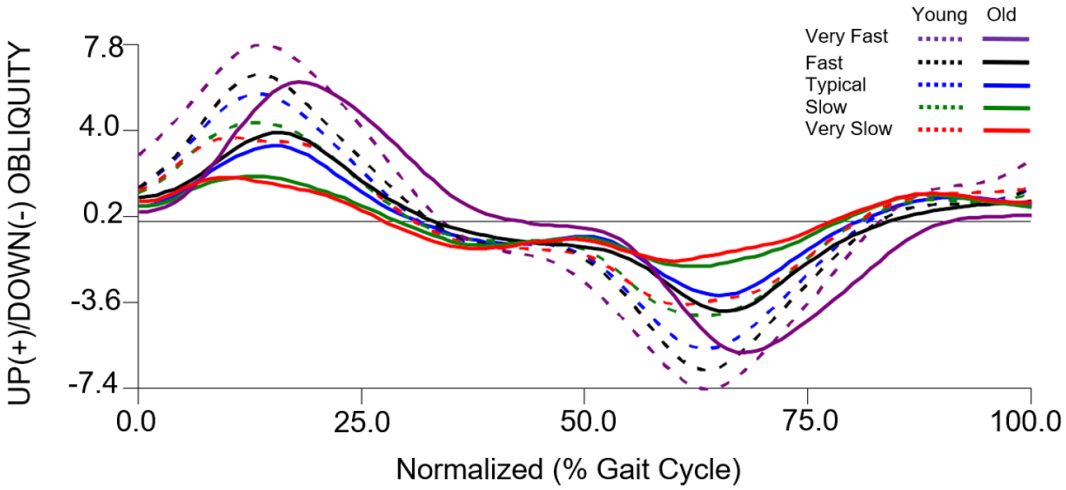


Figure 110. Mean upward-downward obliquity for the pelvis of the OG versus the YG at each walking speed.

Table 54. Significant p-values of the mean max UP/DOWN obliquity angles (∠) of the pelvis during stance and swing phase, as well as their respective time of occurrence in the gait cycle across five walking speeds.

Walking speed group	Max DOWN obliquity ∠ in stance p-value	Time to max DOWN obliquity ∠ in stance p-value	Max DOWN obliquity ∠ in swing p-value	Time to max DOWN obliquity ∠ in swing p-value	Max UP obliquity ∠ in stance p-value	Time to max UP obliquity ∠ in stance p-value	Max UP obliquity ∠ in swing p-value	Time to max UP obliquity ∠ in swing p-value
VS	.03	-	<.01	<.001	.02	-	-	-
S	.01	-	<.01	<.01	<.01	-	-	.03
T	<.01	-	<.01	<.001	<.01	-	-	.04
F	.02	-	.01	<.01	<.01	<.01	-	-
VF	<.01	-	-	<.00001	-	<.00001	<.001	-

Note: VS: Very Slow, S: Slow, T: Typical, F: Fast, VF: Very Fast.; '-' indicates no significant difference.

The mean max downward (DOWN) obliquity angle across WSs during stance, with error bars (95% confidence interval), is presented in Figure 111. Descriptive results showed that the mean max DOWN obliquity angle during stance increased from VS to slow speed, after which point, the mean max DOWN obliquity angle decreased for both groups, except for the VF speed for the OG. Overall, both age groups demonstrated similar trends and similar associated marginal error. In addition, the OG demonstrated greater mean max DOWN obliquity angles across speeds compared to the YG (Figure 111).

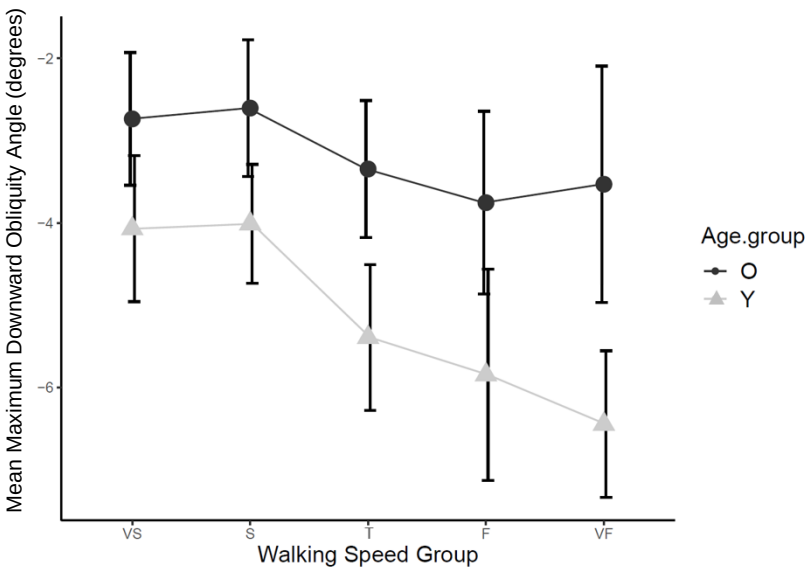


Figure 111. Mean max DOWN obliquity angle of the pelvis during stance phase for the YG and OG across walking speeds at the 95% confidence interval (VS: Very Slow, S: Slow, T: Typical, F: Fast, VF: Very Fast).

The YG had a significantly ($p<.05$) increased mean max DOWN obliquity angle during stance as WS increased (VS: -4.07°±2.37°; VF: -6.44°±2.67°) compared to the OG (VS: -2.73°±2.31°; VF: -3.53°±3.24°), as shown in Table 54.

The mean max DOWN obliquity angle across WSs during swing, with error bars (95% confidence interval), is presented in Figure 112. Descriptive results showed that the mean max DOWN obliquity angle during swing decreased as WS increased for both groups. Overall, both age groups displayed similar trends but at different magnitudes. In addition, the OG demonstrated greater mean max DOWN obliquity angles across speeds compared to the YG. Both age groups showed similar associated marginal error (Figure 112). The YG had a significantly ($p<.05$) increased mean max DOWN obliquity angle during swing as WS increased from VS to fast speed (VS: -3.79°±2.59°; fast: -6.61°±2.80°) compared to the OG (VS: -1.23°±2.87°; fast: -4.48°±2.76°), as shown in Table 54.

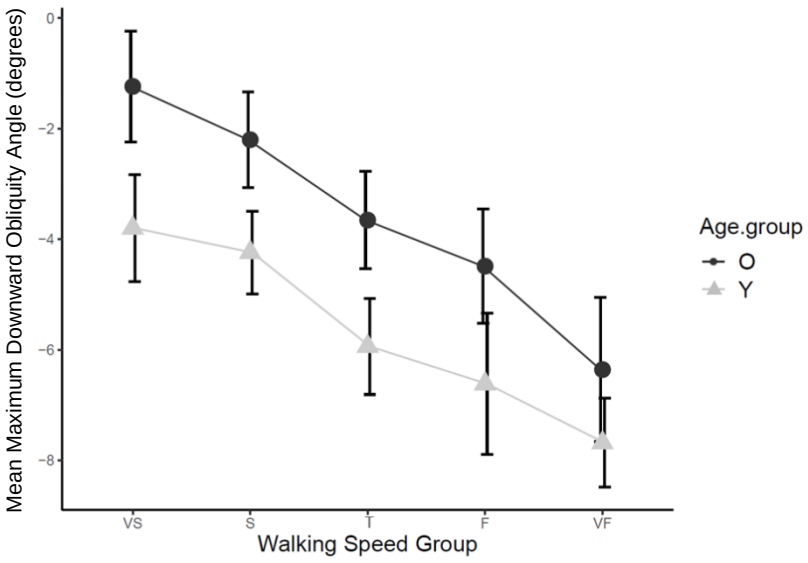


Figure 112. Mean max DOWN obliquity angle of the pelvis during swing phase for the YG and OG across walking speeds at the 95% confidence interval (VS: Very Slow, S: Slow, T: Typical, F: Fast, VF: Very Fast).

Significant differences in time to mean max DOWN obliquity angle ($p<.05$) during swing phase were found between YA and OA across all speeds (Figure 110, Table 54). The YG had a significantly shorter time to mean max DOWN obliquity angle ($p<.05$) for the VS, slow, typical, fast, and VF WSs. For the YG, the mean max DOWN obliquity angle occurred at 66.40±3.42 percent GC at the VS speed, decreasing to 64.26±2.16 percent GC at the VF speed. Whereas the OG demonstrated mean max DOWN obliquity angle at 72.86±9.73 percent GC at the VS speed, decreasing to 68.78±2.90 percent GC at the VF speed (Figure 110).

The mean max upward (UP) obliquity angle across WSs during stance, with error bars (95% confidence interval), is presented in Figure 113. Descriptive results for the YG showed that the mean max UP obliquity angle (peak) during stance increased as WS increased. The mean max UP obliquity angle for the OG increased as speed increased from

VS to typical speed, where the angle began to decrease for the fast speed and then increased for the VF speed. Further, the OG showed a larger associated marginal error. Overall, both age groups displayed similar trends but at different magnitudes. In addition, the YG demonstrated greater mean max UP obliquity angles across speeds compared to the YG. Moreover, at typical speed, both groups show less variability between them for the mean max UP obliquity angle. However, when speed changed to a slower or faster speed, the variability between groups increased (Figure 113).

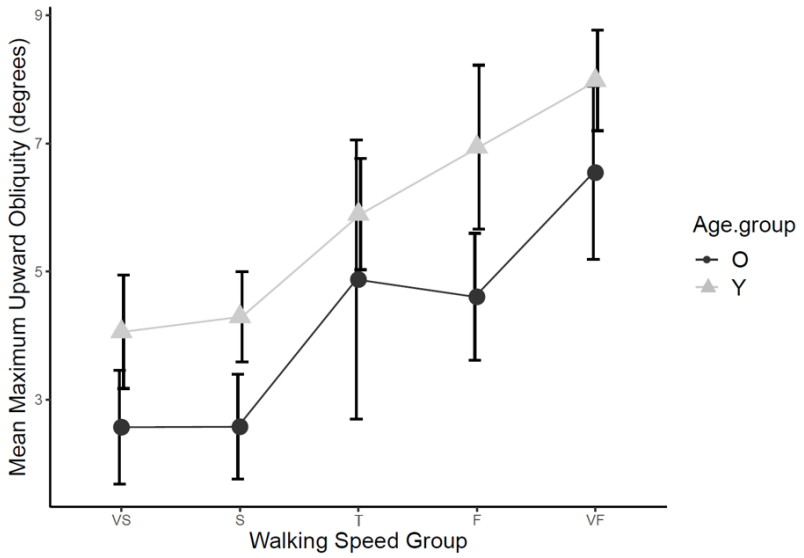


Figure 113. Mean max UP obliquity angle of the pelvis during stance phase for the YG and OG across walking speeds at the 95% confidence interval (VS: Very Slow, S: Slow, T: Typical, F: Fast, VF: Very Fast).

The YG had a significantly ($p<.05$) increased mean max UP obliquity angle during stance as WS increased from slow to fast speed (slow: 4.29°±2.14°; fast: 6.94°±2.80°) compared to the OG (slow: 2.57°±1.93°; fast: 4.60°±2.65°), as shown in Table 54.

Significant differences in time to mean max UP obliquity angle ($p<.05$) during stance phase were found between YA and OA as WS increased from fast to VF (Figure

110, Table 54). The YG had a significantly shorter time to mean max UP obliquity angle ($p<.05$) for the fast and VF WSs. For the YG, the mean max UP obliquity angle occurred at 13.94±1.62 percent GC at the fast speed, decreasing to 13.77±3.14 percent GC at the VF speed. Whereas the OG demonstrated mean max UP obliquity angle at 15.72±7.89 percent GC at the fast speed, increasing to 19.25±3.46 percent GC at the VF speed (Figure 110).

The mean max UP obliquity angle across WSs during swing, with error bars (95% confidence interval), is presented in Figure 114. Descriptive results showed that the mean max UP obliquity (peak) during swing for the OG decreased from VS to slow speed, after which point, the mean max UP obliquity angle was relatively consistent until the fast speed, where it decreased again. The mean max UP obliquity angle for the OG decreased from VS to slow speed, after which point, the mean max UP obliquity angle increased. Overall, both age groups demonstrated relatively consistent patterns of variability for the mean max UP obliquity angle as speed increased from VS to fast WS. In addition, the YG demonstrated greater mean max UP obliquity angles across speeds compared to the OG. The latter displayed a larger associated marginal error (Figure 114). Additionally, at the VF speed, the YG exhibited a spike in the mean max UP obliquity pelvic angle, whereas the mean max UP obliquity pelvic angle decreased for the OG. This is due to the pattern showed in Figure 110, which exhibited an offset between YA and OA for the VF speed at terminal swing, whereas the WSs from VS to fast have a decreased offset between them. More specifically, at terminal swing, the younger group's pattern shows a spike at the end toward a more positive angle, whereas the older group's pattern showed a decline at terminal swing towards a more negative angle value.

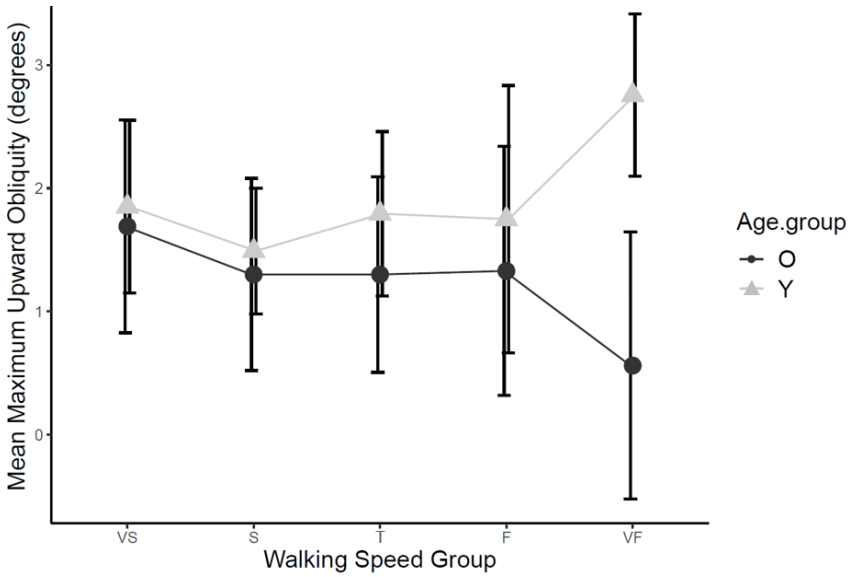


Figure 114. Mean max UP obliquity angle of the pelvis during swing phase for the YG and OG across walking speeds at the 95% confidence interval (VS: Very Slow, S: Slow, T: Typical, F: Fast, VF: Very Fast).

The YG had a significantly ($p<.05$) increased mean max UP obliquity angle during swing at the VF speed only (VF: 2.75°±1.97°) compared to the OG (VF: 0.56°±2.44°), as shown in Table 56.

Significant differences in time to mean max UP obliquity angle ($p<.05$) during stance phase were found between YA and OA as WS increased from slow to typical speed (Figure 110, Table 54). The YG had a significantly longer time to mean max UP obliquity angle ($p<.05$) for the slow and typical WSs. For the YG, the mean max UP obliquity angle occurred at 93.59±6.39 percent GC at the slow speed, decreasing to 94.43±5.81 percent GC at the typical speed. Whereas the OG demonstrated mean max UP obliquity angle at 88.87±6.97 percent GC at the slow speed, increasing to 91.10±7.23 percent GC at the typical speed (Figure 110).

Table 55 presents the significant (p<.05) age-related differences in the UP/DOWN obliquity range of motion (ROM) data for the pelvis. In addition, relative UP/DOWN obliquity ROM data for the pelvis are provided in Table 55. The YG displayed the greatest UP/DOWN obliquity ROM (Figure 110) across all speeds during stance and swing compared to the OG. Table 55 presents the between-group differences found for the UP/DOWN obliquity ROM during stance and swing phase.

Table 55. Significant UP/DOWN obliquity ROM data for the pelvis during stance and swing phase across five walking speeds and their respective significant p-values.

UP/DOWN Obliquity ROM Pelvis			
	Mean	± Std	P-value
Very Slow Young Stance	8.13°	0.01°	<.001
Very Slow Old Stance	5.30°	0.23°	
Slow Young Stance	8.30°	0.05°	<.001
Slow Old Stance	5.18°	0.03°	
Typical Young Stance	11.28°	0.05°	<.05
Typical Old Stance	8.22°	3.97°	
Fast Young Stance	12.78°	0.01°	<.001
Fast Old Stance	8.36°	0.32°	
Very Fast Young Stance	14.43°	0.31°	<.001
Very Fast Old Stance	10.07°	0.19°	
Very Slow Young Swing	5.64°	0.71°	<.001
Very Slow Old Swing	2.92°	0.39°	
Slow Young Swing	5.73°	0.72°	<.001
Slow Old Swing	3.49°	0.19°	
Typical Young Swing	7.73°	0.58°	<.001
Typical Old Swing	4.95°	0.26°	
Fast Young Swing	8.36°	0.42°	<.01
Fast Old Swing	5.81°	0.05°	
Very Fast Young Swing	10.43°	0.43°	<.001
Very Fast Old Swing	6.92°	0.50°	

Note: Std: Standard deviation.; '-' indicates no significant difference.

The YG exhibited a significantly (p<.05) greater UP/DOWN obliquity ROM during stance as WS increased (VS: 8.13°±0.01°; VF: 14.43°±0.31°) compared to the OG (VS: 5.30°±0.23°; VF: 10.07°±0.19°) as shown in Table 55. During swing phase, the YG exhibited a significantly (p<.05) greater UP/DOWN obliquity ROM as WS increased (VS:

5.64°±0.71°; VF: 10.43°±0.43°) compared to the OG (VS: 2.92°±0.39°; VF: 6.92°±0.50°) as shown in Table 55. During VF speed walking, the UP/DOWN obliquity ROM for the YA and OA increased most in the pelvis during stance and swing.

4.1.18 Summary of Pelvic Kinematics Results

When the speed effect is being considered, there are significant differences in the pelvic kinematics between YA and OA . The key findings of the present study are as follows:

- Significant differences for the hip joint angle in the sagittal and frontal plane were found between age groups as a function of speed.
- In the sagittal plane, the mean min ANT tilt of the pelvis in stance and swing phase, as well as the mean max ANT tilt of the pelvis in stance and swing phase, were significantly decreased for the YG for the slow and typical WSs compared to the OG.
- In the frontal plane, the mean max DOWN obliquity angle of the pelvis in stance phase was significantly increased for the YG across all speeds compared to the OG. Similarly, the mean max DOWN obliquity of the pelvis in swing and the mean max UP obliquity of the pelvis in stance were significantly increased for the YG as WS increased from VS to fast WS compared to the OG. Further, the mean max UP obliquity of the pelvis in swing phase was significantly increased for the VF speed only compared to the OG.

4.1.19 Age-related Differences in Torso Kinematics

The mean relative angle for the torso segment in the sagittal plane is presented in Figure 115. This is the torso anterior-posterior tilt (ANT/POST) angle defined by the

relative orientation of the shoulders and C7 vertebra. The following section focuses on between-group differences. Table 56 presents the significant age-related differences in the mean max and min ANT/POST tilt angles in stance and swing phase as well as their respective time of occurrence as a percentage of GC.

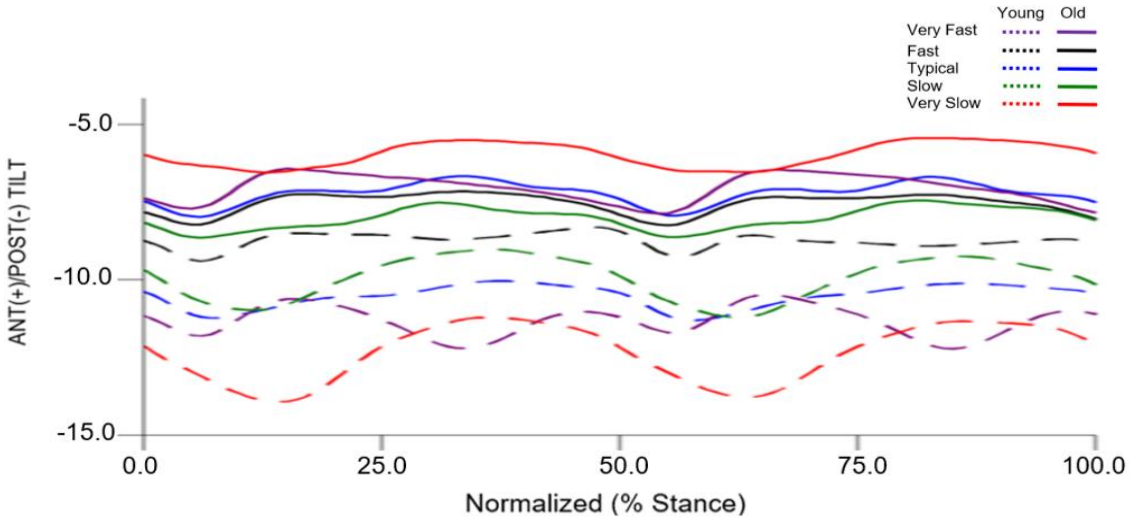


Figure 115. Mean anterior-posterior tilt for the torso of the OG versus the YG at each walking speed.

Table 56. Significant p-values of the mean min and max ANT/POST tilt angles (∠) of the torso during stance and swing phase, as well as their respective time of occurrence in the gait cycle across five walking speeds.

Walking speed group	Max POST tilt ∠ in stance p-value	Time to max POST tilt ∠ in stance p-value	Max POST tilt ∠ in swing p-value	Time to max POST tilt ∠ in swing p-value	Min POST tilt ∠ in stance p-value	Time to min POST tilt ∠ in stance p-value	Min POST tilt ∠ in swing p-value	Time to min POST tilt ∠ in swing p-value
VS	.02	-	.01	<.0001	<.0001	-	<.0001	-
S	-	-	-	<.01	-	-	-	-
T	-	-	-	-	-	-	-	-
F	-	-	-	-	-	-	-	-
VF	-	-	-	<.01	-	-	-	-

Note: VS: Very Slow, S: Slow, T: Typical, F: Fast, VF: Very Fast.; '-' indicates no significant difference.

The mean max posterior (POST) tilt angle across WSs during stance, with error bars (95% confidence interval), is presented in Figure 116. Descriptive results for the OG showed that the mean max POST tilt angle during stance decreased from VS to typical

speed, after which point, the mean max POST tilt angle began to increase. Overall, the OG demonstrated relatively consistent patterns of variability for the mean max POST tilt angle. The mean max POST tilt angle for the YG increased from VS to slow speed, after which point, the mean max POST tilt angle was relatively consistent, except for the VF speed. Both age groups showed similar associated marginal error. In addition, the OG demonstrated greater mean max POST tilt angles across speeds compared to the YG.

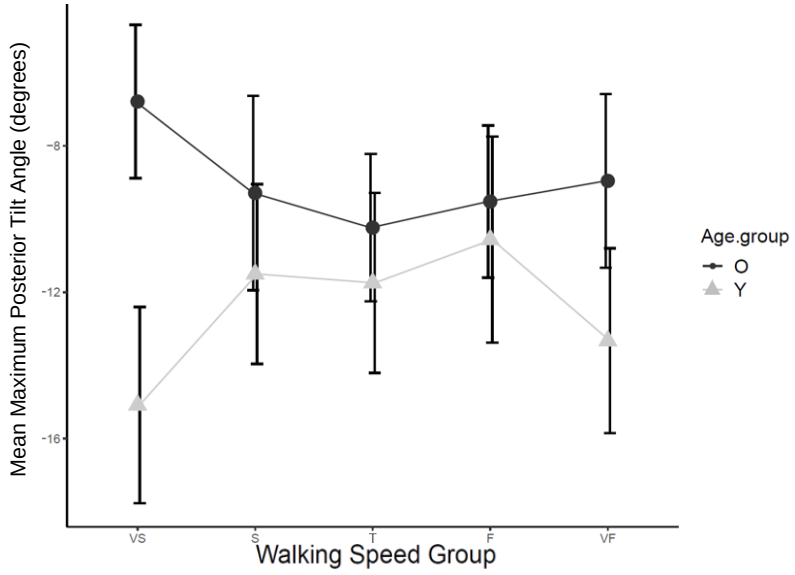


Figure 116. Mean max POST tilt angle of the torso during stance phase for the YG and OG across walking speeds at the 95% confidence interval (VS: Very Slow, S: Slow, T: Typical, F: Fast, VF: Very Fast).

The YG had a significantly ($p<.05$) increased mean max POST tilt angle during stance at the VS speed only (VS: -15.08°±7.18°) compared to the OG (VS: -6.78°±6.01°), as shown in Table 56.

The mean max POST tilt angle across WSs during swing, with error bars (95% confidence interval), is presented in Figure 117. Descriptive results for the OG showed that the mean max POST tilt angle during swing decreased from VS to typical speed, after

which point, the mean max POST tilt angle began to increase. Overall, the OG demonstrated relatively consistent patterns of variability for the mean max POST tilt angle. The mean max POST tilt angle for the YG increased from VS to slow speed, after which point, the mean max POST tilt angle was relatively consistent, except for the VF speed. In addition, the OG demonstrated greater mean max POST tilt angles across speeds compared to the YG (Figure 117).

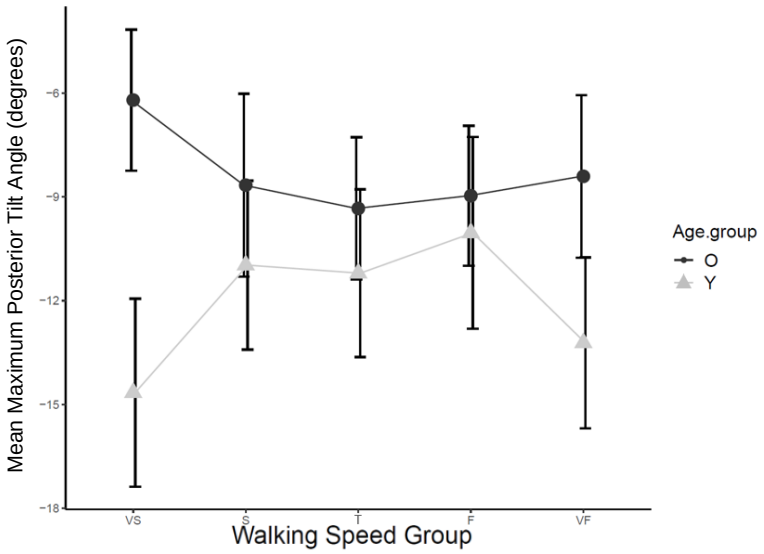


Figure 117. Mean max POST tilt angle of the torso during swing phase for the YG and OG across walking speeds at the 95% confidence interval (VS: Very Slow, S: Slow, T: Typical, F: Fast, VF: Very Fast).

The YG had a significantly ($p<.05$) increased mean max POST tilt angle during swing at the VS speed only (VS: -14.65°±7.27°) compared to the OG (VS: -6.20°±5.48°), as shown in Table 56.

Significant differences in time to mean max POST tilt angle ($p<.05$) during swing phase were found between YA and OA at the VS, slow, and VF WSs (Figure 115, Table 56). The YG had a significantly shorter time to mean max POST tilt angle ($p<.05$) for the

VS, slow, and VF WS. For the YG, the mean max POST tilt angle occurred at 69.87±9.84 percent GC at the VS speed, increasing to 79.61±11.43 percent GC at the VF WS. Whereas the OG demonstrated mean max POST tilt angle at 81.93±14.04 percent GC at the VS speed, increasing to 88.92±13.02 percent GC at the VF WS (Figure 115).

The mean min POST tilt angle across WSs during stance, with error bars (95% confidence interval), is presented in Figure 118. Descriptive results for the OG showed that the mean min POST tilt angle during stance decreased from VS to typical speed, after which point, the mean min POST tilt angle began to increase. Overall, the OG demonstrated relatively consistent patterns of variability for the mean min POST tilt angle. The mean min POST tilt angle for the YG increased from VS to slow speed, after which point, the mean min POST tilt angle was relatively consistent, except for the VF speed. Both age groups showed similar associated marginal error. In addition, the OG demonstrated greater mean min POST tilt angles across speeds compared to the YG (Figure 118). The YG had a significantly ($p<.05$) increased mean min POST tilt angle during stance at the VS speed only (VS: -11.05°±6.36°) compared to the OG (VS: -4.55°±5.80°), as shown in Table 56. No significant differences in time to mean min POST tilt angle during stance were found between YA and OA (Table 56).

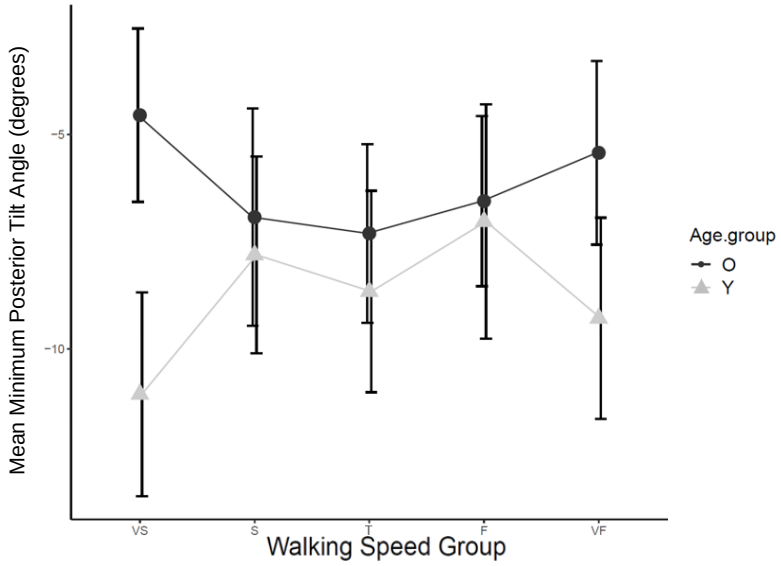


Figure 118. Mean min POST tilt angle of the torso during stance phase for the YG and OG across walking speeds at the 95% confidence interval (VS: Very Slow, S: Slow, T: Typical, F: Fast, VF: Very Fast).

The mean min POST tilt angle across WSs during swing, with error bars (95% confidence interval), is presented in Figure 119. Descriptive results for the OG showed that the mean min POST tilt angle during swing decreased from VS to typical speed, after which point, the mean min POST tilt angle began to increase. Overall, the OG demonstrated relatively consistent patterns of variability for the mean min POST tilt angle. The mean min POST tilt angle for the YG increased from VS to slow speed, after which point, the mean min POST tilt angle was relatively consistent, except for the VF speed. Both age groups showed a similar associated marginal error. In addition, the OG demonstrated greater mean min POST tilt angles across speeds compared to the YG (Figure 119).

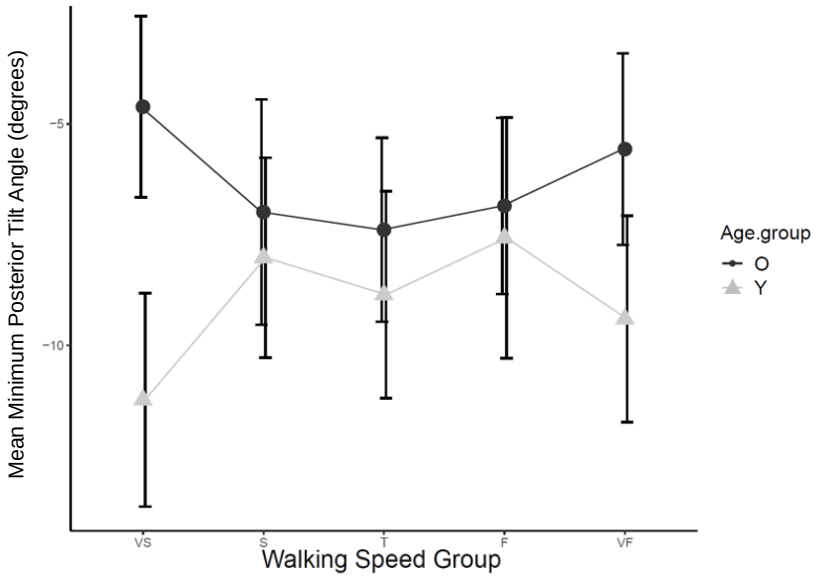


Figure 119. Mean min POST tilt angle of the torso during swing phase for the YG and OG across walking speeds at the 95% confidence interval (VS: Very Slow, S: Slow, T: Typical, F: Fast, VF: Very Fast).

The YG had a significantly ($p<.05$) increased mean min POST tilt angle during swing at the VS speed only (VS: -11.23°±6.44°) compared to the OG (VS: -4.61°±5.86°), as shown in Table 56.

Table 57 presents the significant ($p<.05$) age-related differences in the anterior/POST tilt range of motion (ROM) data for the torso. Relative anterior/POST tilt ROM data for the torso are provided in Table 57. The YG displayed the greatest UP/DOWN obliquity ROM (Figure 117) across all speeds during stance and swing compared to the OG. Table 57 presents the between-group differences found for the anterior/POST tilt ROM during stance and swing phase. The YG exhibited a significantly ($p<.05$) greater anterior/POST tilt ROM during stance as WS increased from VS to slow WSs (VS: 4.02°±0.81°; slow: 3.68°±0.49°) compared to the OG (VS: 2.23°±0.21°; slow: 2.35°±0.29°) as shown in Table 57. During swing phase, the YG exhibited a significantly ($p<.05$) greater anterior/POST tilt ROM for the VS, slow, and VF WSs (VS: 3.42°±0.82°;

slow: 2.95°±0.55°; VF: 3.81°±0.40°) compared to the OG (VS: 1.58°±0.02°; slow: 1.67°±0.22°; VF: 2.83°±0.41°) as shown in Table 57. During VF speed walking, the anterior/POST tilt ROM for the YA and OA increased most in the torso during stance and swing.

Table 57. Significant anterior/POST tilt ROM data for the torso during stance and swing phase across five walking speeds and their respective significant p-values.

ANT/POST Tilt ROM Torso			
	Mean	± Std	P-value
Very Slow Young Stance	4.02°	0.81°	<.001
Very Slow Old Stance	2.23°	0.21°	
Slow Young Stance	3.68°	0.49°	<.01
Slow Old Stance	2.35°	0.29°	
Typical Young Stance	3.07°	0.32°	-
Typical Old Stance	2.92°	0.20°	
Fast Young Stance	3.52°	0.17°	-
Fast Old Stance	2.96°	0.25°	
Very Fast Young Stance	4.03°	0.53°	-
Very Fast Old Stance	3.52°	0.52°	
Very Slow Young Swing	3.42°	0.82°	<.001
Very Slow Old Swing	1.58°	0.02°	
Slow Young Swing	2.95°	0.55°	<.01
Slow Old Swing	1.67°	0.22°	
Typical Young Swing	2.34°	0.24°	-
Typical Old Swing	1.94°	0.05°	
Fast Young Swing	2.46°	0.12°	-
Fast Old Swing	2.11°	0.07°	
Very Fast Young Swing	3.81°	0.40°	<.05
Very Fast Old Swing	2.83°	0.41°	

Note: Std: Standard deviation.; '-' indicates no significant difference.

The mean relative angle for the torso segment in the frontal plane is presented in Figure 120. This is the torso ipsilateral-contralateral lean (IPSI/CONTRA) angle defined by the relative orientation of the shoulders and C7 vertebra. The following section focuses on between-group differences. Table 58 presents the significant age-related differences in the mean max and min IPSI/CONTRA lean angles in stance and swing phase as well as their respective time of occurrence as a percentage of GC.

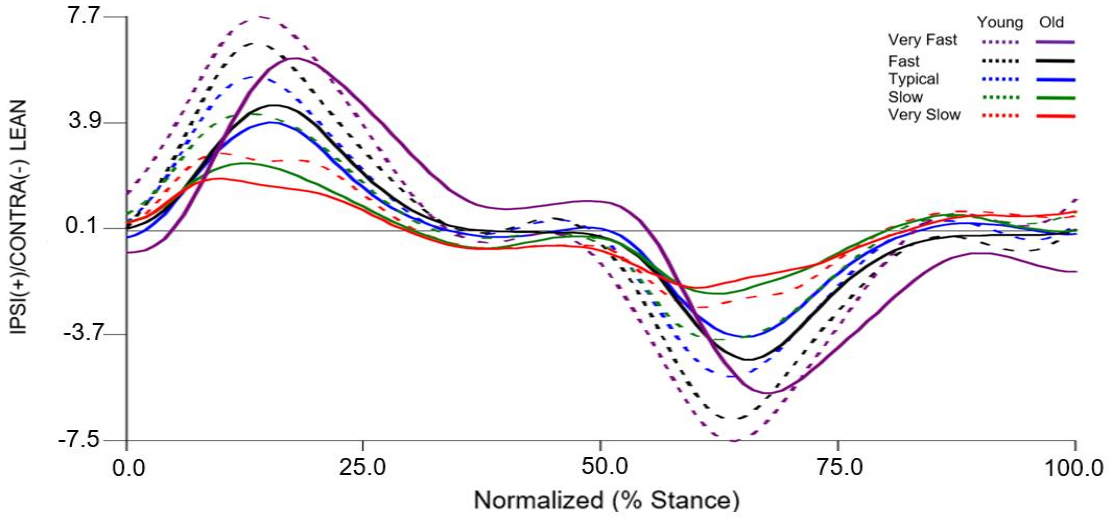


Figure 120. Mean ipsilateral-contralateral lean for the torso of the OG versus the YG at each walking speed.

Table 58. Significant p-values of the mean max IPSI/CONTRA lean angles (∠) of the torso during stance and swing phase, as well as their respective time of occurrence in the gait cycle across five walking speeds.

Walking speed group	Max CONTRA torso lean ∠ in stance p-value	Time to max CONTRA torso lean ∠ in stance p-value	Max CONTRA torso lean ∠ in swing p-value	Time to max CONTRA torso lean ∠ in swing p-value	Max IPSI torso lean ∠ in stance p-value	Time to max IPSI torso lean ∠ in stance p-value	Max IPSI torso lean ∠ in swing p-value	Time to max IPSI torso lean ∠ in swing p-value
VS	-	-	.02	.02	-	-	-	.02
S	<.01	-	<.01	.03	<.01	-	-	.01
T	.02	-	<.01	<.01	-	-	-	-
F	.03	.01	.01	<.01	.03	<.01	-	-
VF	.01	-	-	<.001	.04	<.0001	<.01	-

Note: VS: Very Slow, S: Slow, T: Typical, F: Fast, VF: Very Fast.; '-' indicates no significant difference.

The mean max contralateral (CONTRA) lean angle across WSs during stance, with error bars (95% confidence interval), is presented in Figure 121. Descriptive results showed that the mean max CONTRA lean angle for the OG during stance increased from VS to slow speed, after which point, the mean max CONTRA lean angle began to decrease. Whereas the mean max CONTRA lean angle for the YG decreased as WS increased. Overall, both age groups displayed a similar trend but at different magnitudes. The OG

showed a larger associated marginal error. In addition, the OG demonstrated greater mean max CONTRA lean angles across speeds compared to the YG (Figure 121).

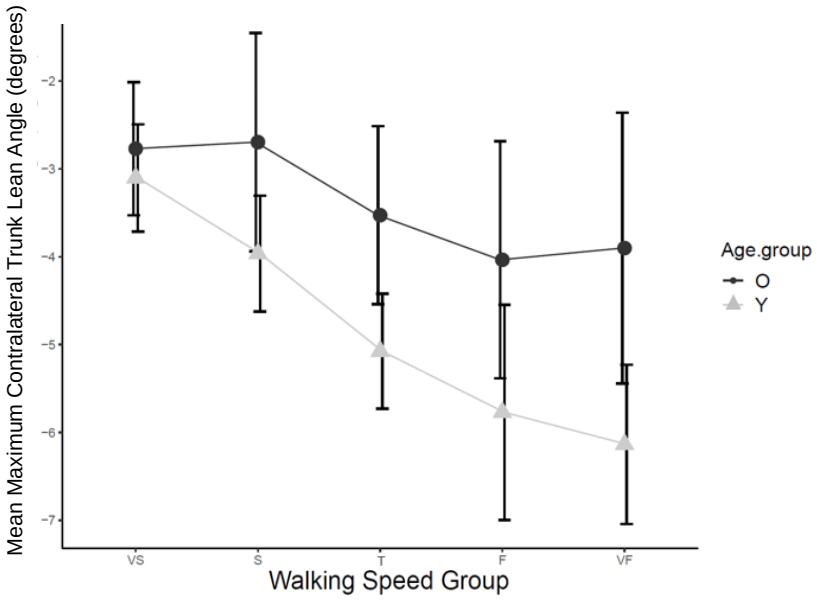


Figure 121. Mean max CONTRA lean angle of the torso during stance phase for the YG and OG across walking speeds at the 95% confidence interval (VS: Very Slow, S: Slow, T: Typical, F: Fast, VF: Very Fast).

The YG had a significantly ($p<.05$) increased mean max CONTRA lean angle during stance as WS increased from slow to VF speed (slow: -3.96°±3.47°; VF: -6.13°±2.71°) compared to the OG (slow: -2.69°±2.94°; VF: -3.90°±3.47°), as shown in Table 58.

Significant differences in time to mean max CONTRA lean angle ($p<.05$) during stance phase were found between YA and OA at the fast speed only (Figure 120, Table 58). The YG had a significantly longer time to mean max CONTRA lean angle ($p<.05$) for the fast WS. For the YG, the mean max CONTRA lean angle occurred at 52.64±18.65 percent GC at the fast speed, whereas the OG demonstrated mean max CONTRA lean angle at 52.04±19.32 percent GC at the fast speed (Figure 120).

The mean max CONTRA lean angle across WSs during swing, with error bars (95% confidence interval), is presented in Figure 122. Descriptive results showed that the mean max CONTRA lean angle during swing decreased as WS increased for the YA and OA. Overall, both age groups displayed a similar trend but at different magnitudes. In addition, the OG demonstrated greater mean max CONTRA lean angles across speeds compared to the YG. The OG showed a larger associated marginal error (Figure 122). The YG had a significantly ($p<.05$) increased mean max CONTRA lean angle during swing as WS increased from VS to fast speed (VS: -2.82° ±1.87°; fast: -6.96°±2.58°) compared to the OG (VS: -1.85°±2.13°; fast: -5.18 °±3.42°).

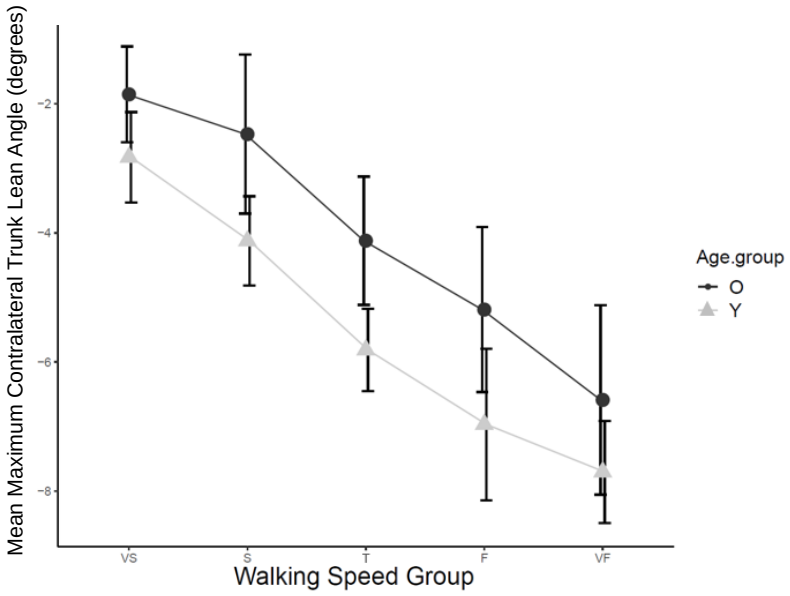


Figure 122. Mean max CONTRA lean angle of the torso during swing phase for the YG and OG across walking speeds at the 95% confidence interval (VS: Very Slow, S: Slow, T: Typical, F: Fast, VF: Very Fast).

Significant differences in time to mean max CONTRA lean angle ($p<.05$) during swing phase were found between YA and OA as WS increased (Figure 120, Table 58). The YG had a significantly shorter time to mean max CONTRA lean angle ($p<.05$) for the VS,

slow, typical, fast, and VF WSs. For the YG, the mean max CONTRA lean angle occurred at 69.61±10.39 percent GC at the VS speed, decreasing to 65.25±6.20 percent GC at the VF speed. Whereas the OG showed mean max CONTRA lean angle at 73.79±9.75 percent GC at the VS speed, decreasing to 68.45±4.64 percent GC at the VF speed (Figure 120).

The mean max ipsilateral (IPSI) lean angle across WSs during stance, with error bars (95% confidence interval), is presented in Figure 123. Descriptive results showed that the mean max IPSI lean angle (peak) during stance increased as WS increased for both groups. Overall, both age groups displayed a similar trend, with the OG showing a larger associated marginal error. In addition, the YG demonstrated greater mean max IPSI lean angles across speeds compared to the OG (Figure 123).

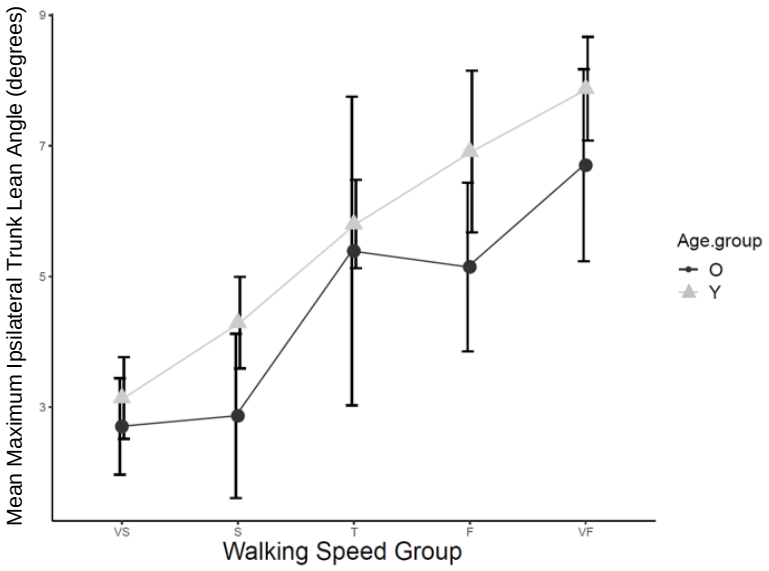


Figure 123. Mean max IPSI lean angle of the torso during stance phase for the YG and OG across walking speeds at the 95% confidence interval (VS: Very Slow, S: Slow, T: Typical, F: Fast, VF: Very Fast).

The YG had a significantly ($p<.05$) increased mean max IPSI lean angle during stance as WS increased from slow to VF speed, except for the typical speed (slow:

4.29°±2.13°; VF: 7.87°±2.38°) compared to the OG (slow: 2.86°±2.97°; VF: 6.70°±3.31°), as shown in Table 58.

Significant differences in time to mean max IPSI lean angle ($p<.05$) during stance phase were found between YA and OA as WS increased from fast to VF (Figure 120, Table 58). The YG had a significantly shorter time to mean max IPSI lean angle ($p<.05$) for the fast and VF WSs. For the YG, the mean max IPSI lean angle occurred at 14.05±1.51 percent GC at the fast WS, increasing to 14.43±2.36 percent GC at the VF WS. Whereas the OG demonstrated mean max IPSI lean angle at 15.36±3.99 percent GC at the fast WS, increasing to 18.02±3.61 percent GC at the VF speed (Figure 120).

The mean max IPSI (IPSI) lean angle across WSs during swing, with error bars (95% confidence interval), is presented in Figure 124. Descriptive results for the YG showed that the mean max IPSI lean angle during swing decreased as WS increased, except for the VF speed. Whereas the mean max IPSI lean angle during swing decreased as WS increased, except for the fast speed. The OG displayed a larger associated marginal error. In addition, the YG demonstrated greater mean max IPSI lean angles as WS increased, except for the fast speed, compared to the OG (Figure 124). Additionally, at the VF speed, the YG exhibited a spike in the mean max IPSI lean angle. This is due to the pattern showed in Figure 120 at terminal swing, where the younger group's pattern shows a spike at the end, whereas the older group's pattern showed a decline at terminal swing. The YG had a significantly ($p<.05$) increased mean max IPSI lean angle during swing at the VF speed only (VF: 1.45°±1.64°) compared to the OG (VF: -0.05°±3.07°), as shown in Table 58.

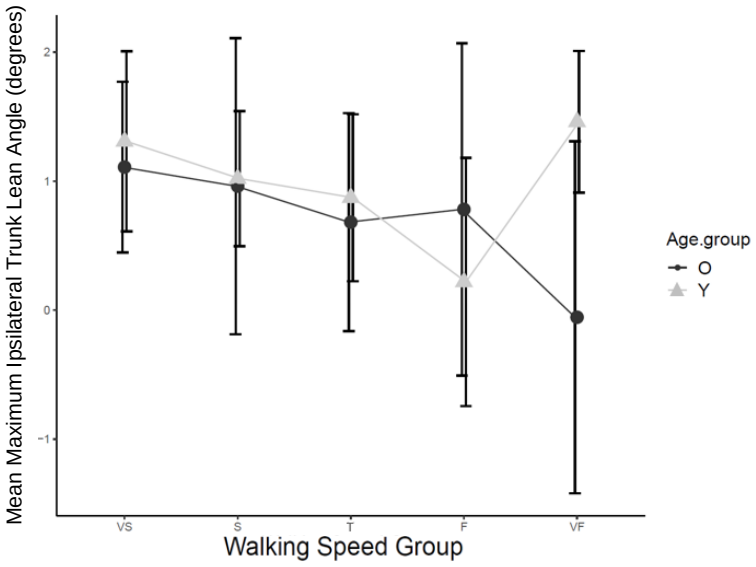


Figure 124. Mean max IPSI lean angle of the pelvis during swing phase for the YG and OG across walking speeds at the 95% confidence interval (VS: Very Slow, S: Slow, T: Typical, F: Fast, VF: Very Fast).

Significant differences in time to mean max IPSI lean angle ($p<.05$) during swing phase were found between YA and OA as WS increased from VS to slow speed (Figure 120, Table 58). The YG had a significantly shorter time to mean max IPSI lean angle ($p<.05$) for the VS and slow WSs. For the YG, the mean max IPSI lean angle occurred at 88.59±8.83 percent GC at the VS speed, increasing to 92.76±6.82 percent GC at the slow speed. Whereas the OG demonstrated mean max IPSI lean angle at 93.03±7.31 percent GC at the VS speed, decreasing to 86.98±8.92 percent GC at the slow speed (Figure 120).

Table 59 presents the significant ($p<.05$) age-related differences in the IPSI/CONTRA lean range of motion (ROM) data for the torso. In addition, relative IPSI/CONTRA lean ROM data for the torso are provided in Table 59. The YG displayed the greatest UP/DOWN obliquity ROM (Figure 120) across all speeds during stance and swing compared to the OG. Table 59 presents the between-group differences found for the

IPSI/CONTRA lean ROM during stance and swing phase. The YG exhibited a significantly ($p<.05$) greater IPSI/CONTRA lean ROM during stance for the slow, fast, and VF WSs (slow: 8.25°±0.12°; fast: 12.68°±0.02°; VF: 14.00°±0.33°) compared to the OG (slow: 5.56°±0.03°; fast: 9.18°±0.15°; VF: 10.60°±0.15°) as shown in Table 59. During swing phase, the YG exhibited a significantly ($p<.05$) greater IPSI/CONTRA lean ROM as WS increased (VS: 4.13°±0.01°; VF: 9.16°±0.72°) compared to the OG (VS: 2.96°±0.23°; VF: 6.53°±0.23°), except for the fast WS, as shown in Table 59. During VF speed walking, the IPSI/CONTRA lean ROM for the YA and OA increased most in the torso during stance and swing.

Table 59. Significant IPSI/CONTRA lean ROM data for the torso during stance and swing phase across five walking speeds and their respective significant p-values.

IPSI/CONTRA Lean ROM Torso			
	Mean	± Std	P-value
Very Slow Young Stance	6.24°	0.03°	-
Very Slow Old Stance	5.47°	0.04°	
Slow Young Stance	8.25°	0.12°	<.001
Slow Old Stance	5.56°	0.03°	
Typical Young Stance	10.87°	0.06°	-
Typical Old Stance	8.91°	3.98°	
Fast Young Stance	12.68°	0.02°	<.01
Fast Old Stance	9.18°	0.15°	
Very Fast Young Stance	14.00°	0.33°	<.01
Very Fast Old Stance	10.60°	0.15°	
Very Slow Young Swing	4.13°	0.01°	<.01
Very Slow Old Swing	2.96°	0.23°	
Slow Young Swing	5.14°	0.50°	<.01
Slow Old Swing	3.43°	0.20°	
Typical Young Swing	6.68°	0.02°	<.01
Typical Old Swing	4.80°	0.44°	
Fast Young Swing	7.18°	0.46°	-
Fast Old Swing	5.96°	0.02°	
Very Fast Young Swing	9.16°	0.72°	<.001
Very Fast Old Swing	6.53°	0.23°	

Note: Std: Standard deviation.; '-' indicates no significant difference.

4.1.20 Summary of Torso Kinematics Results

When the speed effect is being considered, there are significant differences in torso kinematics between YA and OA . The key findings of the present study are as follows:

- Significant differences for the torso joint angle in the sagittal and frontal plane were found between age groups as a function of speed.
- In the sagittal plane, the mean min POST tilt of the torso in stance and swing, as well as the mean max POST tilt of the torso in stance and swing, were significantly increased for the YG for the VS speed only compared to the OG.
- In the frontal plane, the mean max CONTRA lean angle of the torso in stance phase was significantly increased for the YG as WS increased from slow to VF WS compared to the OG. Similarly, the mean max CONTRA lean angle of the torso in swing phase was significantly increased for the YA as WS increased from VS to fast WS compared to the OA. Likewise, the mean max IPSI lean angle of the torso in stance phase was significantly increased for the YG for the slow, fast, and VF WSs. Further, the mean max IPSI lean angle of the torso in swing phase was significantly greater for the YG for the VF WS only compared to the OG.
- The OG had similar results as the pelvic angles, with an overall decreased motion of the torso.

4.1.21 Age-related Differences in Ground Reaction Forces

The mean ground reaction force (GRF) in the sagittal plane is presented in Figure 125. This is the antero-posterior (A/P) force defined by the shear force exerted from the ground in the X-axis direction. The following section focuses on between-group differences. Table 60 presents the significant age-related differences in the mean max and

min A/P forces in stance and swing phase as well as their respective time of occurrence as a percentage of GC.

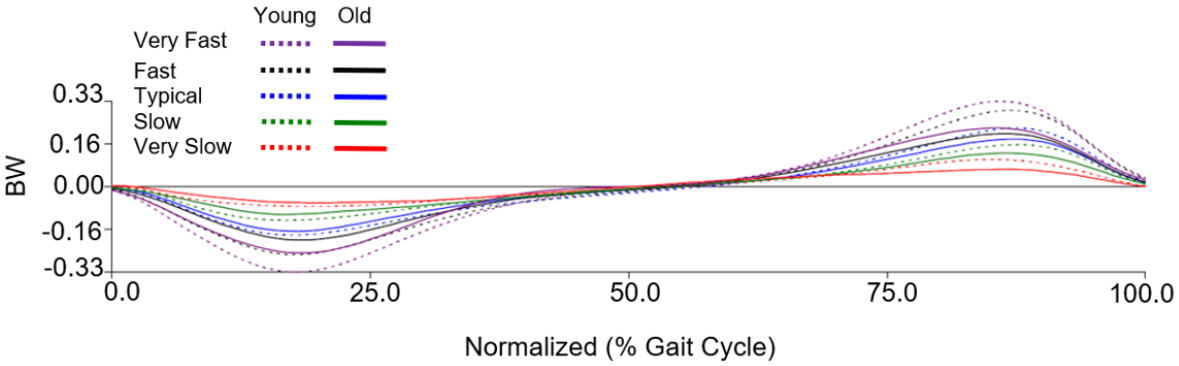


Figure 125. Mean antero-posterior ground reaction force of the OG versus the YG at each walking speed.

Table 60. Significant p-values of the mean min and max antero-posterior ground reaction forces (%Body Weight) during stance and swing phase, as well as their respective time of occurrence in the gait cycle across five walking speeds.

Walking speed group	Min A/P GRF p-value	Time to min A/P GRF p-value	Max A/P GRF p-value	Time to max A/P GRF p-value
VS	-	.01	-	-
S	-	.03	-	-
T	-	-	-	-
F	-	-	.02	-
VF	-	-	.01	-

Note: VS: Very Slow, S: Slow, T: Typical, F: Fast, VF: Very Fast.; '-' indicates no significant difference.

The mean max A/P GRF across WSs during stance, with error bars (95% confidence interval), is presented in Figure 126. Descriptive results showed that the mean max A/P GRF (peak) during stance increased from VS to fast speed, after which point, the mean max A/P GRF began to decrease for both groups. Overall, both age groups demonstrated relatively consistent patterns of variability for the mean max A/P GRF as WS increased from VS to fast speed. In addition, the OG demonstrated greater mean max A/P GRF across speeds compared to the YG (Figure 126).

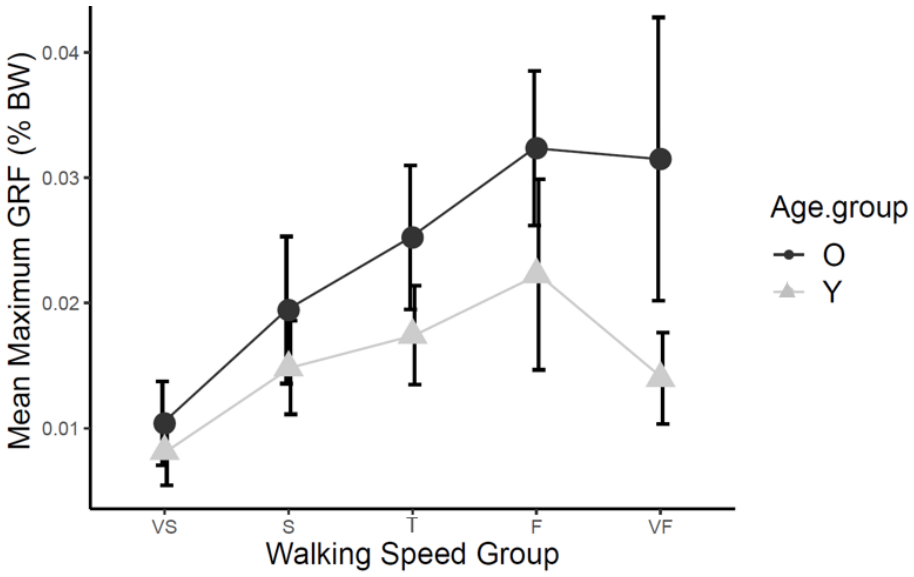


Figure 126. Mean max A/P GRF during stance phase for the YG and OG across walking speeds at the 95% confidence interval (VS: Very Slow, S: Slow, T: Typical, F: Fast, VF: Very Fast).

The YG had a significantly ($p<.05$) decreased mean max A/P GRF during stance as WS increased from fast to VF speed (fast: 0.02±0.01 %BW; VF: 0.01±0.01 %BW) compared to the OG (fast: 0.03±0.01 %BW; VF: 0.03±0.02 %BW), as shown in Table 60.

Significant differences in time to mean min A/P GRF ($p<.05$) during stance phase were found between YA and OA as WS increased from VS to slow speed (Figure 125, Table 60). The YG had a significantly shorter time to mean min A/P GRF ($p<.05$) for the VS and slow WS. For the YG, the mean min A/P GRF occurred at 33.08±16.02 percent GC at the VS speed, decreasing to 30.25±13.58 percent GC at the slow speed. Whereas the OG demonstrated mean min A/P GRF at 43.47±12.07 percent GC at the VS speed, increasing to 36.75±13.17 percent GC at the slow speed (Figure 125).

The mean ground reaction force (GRF) in the transverse plane is presented in Figure 127. This is the vertical force defined by the vertical force exerted from the ground in the Z-axis direction. The following section focuses on between-group differences. Table 64

presents the significant age-related differences in the mean max and min vertical forces in stance and swing phase as well as their respective time of occurrence as a percentage of GC.

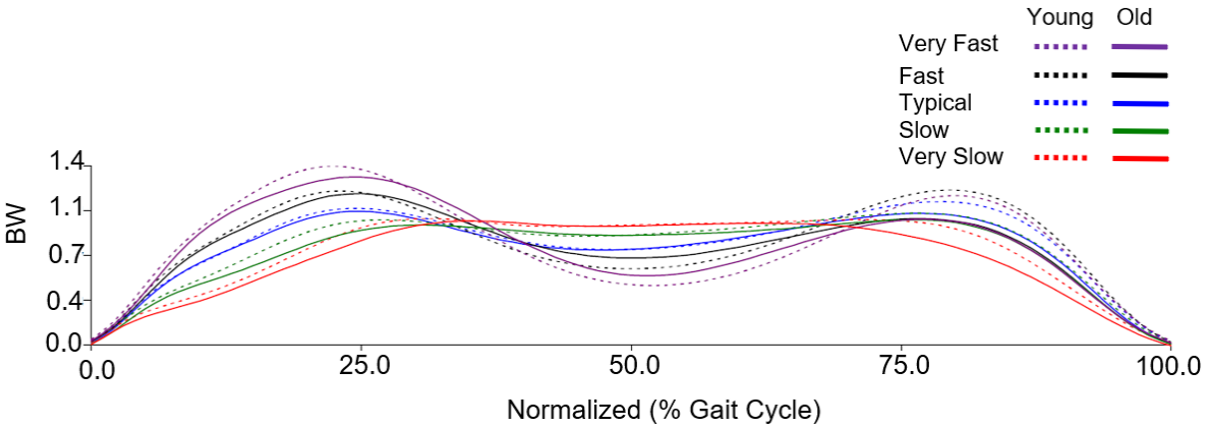


Figure 127. Mean vertical ground reaction force of the OG versus the YG at each walking speed.

Table 61. Significant p-values of the mean min and max vertical ground reaction forces (%Body Weight) during stance and swing phase, as well as their respective time of occurrence in the gait cycle across five walking speeds.

Walking speed group	Min Vertical GRF p-value	Time to min Vertical GRF p-value	Max Vertical GRF p-value	Time to max Vertical GRF p-value
VS	.03	<.0001	-	.04
S	-	-	-	.03
T	-	.02	<.01	-
F	.01	-	.02	-
VF	.04	.02	-	-

Note: VS: Very Slow, S: Slow, T: Typical, F: Fast, VF: Very Fast.; '-' indicates no significant difference.

The mean min vertical GRF across WSs during stance, with error bars (95% confidence interval), is presented in Figure 128. Descriptive results showed that the mean min vertical GRF during stance increased as WS increased for the YG and OG. Overall, both age groups displayed a similar trend but at different magnitudes. In addition, the YG demonstrated greater mean min vertical GRF across speeds compared to the YG (Figure 128). Both groups showed similar trends at different magnitudes, however, the OG had the

smallest associated marginal error (Figure 128). The YG had a significantly ($p<.05$) increased mean min vertical GRF during stance at the VS, fast and VF WSs (VS: 0.05±0.02 %BW; fast: 0.05±0.01 %BW; VF: 0.06±0.02 %BW) compared to the OG (VS: 0.03±0.01 %BW fast: 0.04±0.01 %BW; VF: 0.04±0.02 %BW), as shown in Table 64.

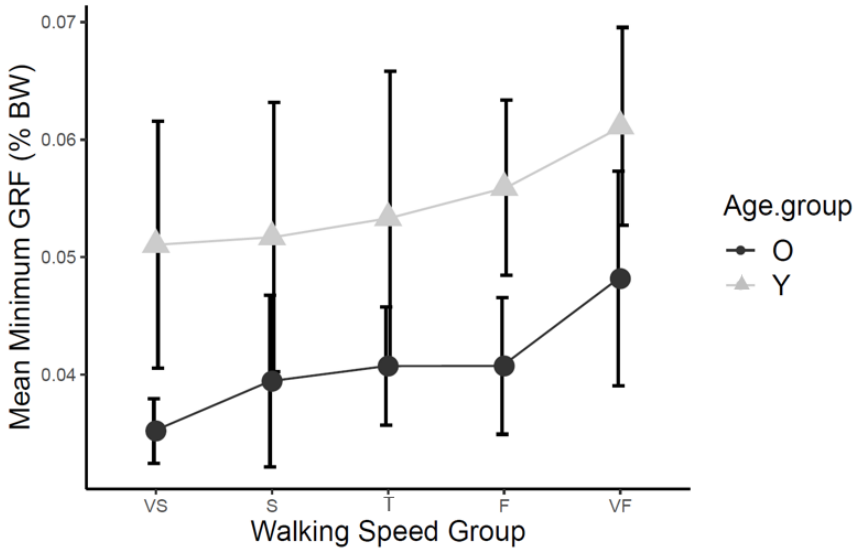


Figure 128. Mean min vertical GRF during stance phase for the YG and OG across walking speeds at the 95% confidence interval (VS: Very Slow, S: Slow, T: Typical, F: Fast, VF: Very Fast).

Significant differences in time to mean min vertical GRF ($p<.05$) during stance phase were found between YA and OA at the VS, typical, and VF speed (Figure 127, Table 64). The YG had a significantly shorter time to mean min vertical GRF ($p<.05$) for the VS, typical, and VF WS. For the YG, the mean min vertical GRF occurred at 40.74±28.93 percent GC at the VS WS, increasing to 41.36±25.64 percent GC at the VF WS. Whereas the OG demonstrated mean min vertical GRF at 57.05±27.13 percent GC at the VS speed, decreasing to 45.01±26.52 percent GC at the VF WS (Figure 127).

The mean max vertical GRF across WSs during stance, with error bars (95% confidence interval), is presented in Figure 129. Descriptive results showed that the mean max vertical GRF during stance increased as WS increased for both groups. Further, the YG showed a greater mean min vertical GRF as WS increased, except for the VS and slow speeds, compared to the OG (Figure 129). Both groups showed similar trends at different magnitudes, however, the YG had the smallest associated marginal error (Figure 129).

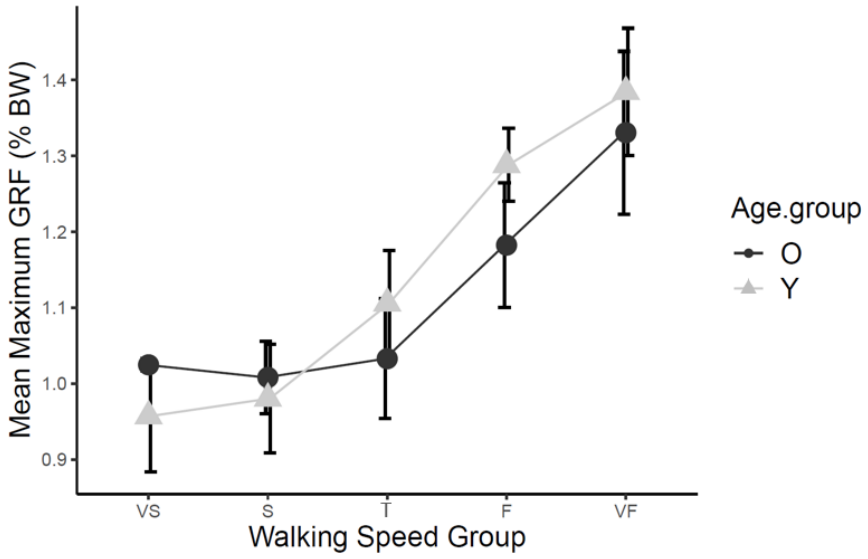


Figure 129. Mean max vertical GRF during stance phase for the YG and OG across walking speeds at the 95% confidence interval (VS: Very Slow, S: Slow, T: Typical, F: Fast, VF: Very Fast).

The YG had a significantly ($p<.05$) increased mean max vertical GRF during stance as WS increased from typical to fast WS (typical: 1.10±0.19 %BW; fast: 1.28±0.10 %BW) compared to the OG (typical: 1.03±0.23 %BW fast: 1.18±0.21 %BW), as shown in Table 64.

Significant differences in time to mean max vertical GRF ($p<.05$) during stance phase were found between YA and OA as WS increased from VS to slow speed (Figure 127, Table 64). The YG had a significantly shorter time to mean max vertical GRF ($p<.05$)

for the VS and slow WS. For the YG, the mean max vertical GRF occurred at 26.89±13.33 percent GC at the VS speed, increasing to 35.68±13.95 percent GC at the slow WS. Whereas the OG demonstrated mean max vertical GRF at 30.55±11.22 percent GC at the VS speed, increasing to 40.16±13.03 percent GC at the slow WS (Figure 127).

4.1.22 Summary of Ground Reaction Forces Results

When the WS effect is being considered, there are significant differences in the GRFs between YA and OA. The key findings of the present study are as follows:

- Significant differences for the GRFs in the antero-posterior (A/P) and vertical directions were found between age groups as a function of speed.
- The mean max A/P force was significantly decreased for the YG for the fast and VF WSs compared to the OG.
- The mean min vertical force was significantly increased for the YG for the VS, fast, and VF speeds compared to the OG. Similarly, the mean max vertical force was significantly increased for the YA for the typical and fast WSs compared to the OA.

4.2 Age-related Differences in MSF and Lower Extremity Kinematic and Kinetic Variables Independent of Speed

The second purpose of the study was to investigate differences in MSF kinematics and lower extremity kinematics and kinetics between young and OA during walking independent of WS. Therefore, it was hypothesized that, independent of WS, there would be significant differences in MSF and lower limb kinematic and kinetic variables (e.g., max foot-tibia angle, calcaneus-tibia, mid-cal, and planar angles of the foot, as well as time to max angle, ankle plantarflexor moment, etc.) between the YA and OA.

4.2.1 Age-related Differences in Temporospatial Variables Independent of Speed

Table 62 presents the significant age-related differences in the mean temporospatial variables independent of WS. The following section focuses on between-group differences. Table 63 presents the significant age-related differences in the temporospatial variables independent of WS that were found in comparison to the findings in the first hypothesis, where the speed effect was tested. A different finding means that the same result was not found when both groups were walking at different speeds.

Table 62. Significant p-values of the mean temporospatial variables independent of WS.

Cadence p-value	Stride Length p-value	Single Leg Support Time p-value	Double Leg Support Time p-value	Time to Toe-off p-value	Cycle Time p-value	Step Length p-value	Speed p-value
<.001	<.001	<.001	<.01	<.001	<.01	<.01	-

Table 63. Temporospatial variables, independent of WS, found similar/different to the first hypothesis.

	Similar	Different
Cadence	✓	
Stride Length	✓	
Single Leg Support Time	✓	
Double Leg Support Time	✓	
Time to Toe-off	✓	
Cycle Time	✓	
Step Length	✓	

4.2.2 Summary of Temporospatial Results

The present study found significant differences for the mean temporospatial variables between YA and OA independent of WS, including the cadence, stride length, singe leg support time, double leg support time, time to toe off, cycle time and step length. Thus, when the speed effect is being controlled, there are still significant differences in temporospatial variables between YA and OA.

4.2.3 Age-related Differences in Relative Angles Between the Foot and Shank Independent of Speed

The mean relative angle for the foot-shank segment in the sagittal plane was presented in Figure 1 (see Section 4.1.3). The following section focuses on between-group differences. Table 64 presents the significant age-related differences in the mean max DF/PF angles in stance and swing phase as well as their respective time of occurrence as a percentage of GC, independent of WS. Table 65 presents the significant age-related differences in the foot-shank DF/PF angles independent of WS that were found in comparison to the findings in the first hypothesis, where the speed effect was tested.

Table 64. Significant p-values of the mean max DF/PF angles (∠) of the foot-shank during stance and swing phase, as well as their respective time of occurrence in the gait cycle independent of WS.

Max PF ∠ in stance p-value	Time to max PF ∠ in stance p-value	Max PF ∠ in swing p-value	Time to max PF ∠ in swing p-value	Max DF ∠ in stance p-value	Time to max DF ∠ in stance p-value	Max DF ∠ in swing p-value	Time to max DF ∠ in swing p-value
<.001	<.001	<.001	<.001	<.001	<.001	<.001	<.01

Table 65. Foot-shank DF/PF angles, independent of WS, found similar/different to the first hypothesis.

	Similar	Different
Max PF in stance	✓	X
Time to max PF in stance		
Max PF in swing	✓	
Time to max PF in swing	✓	
Max DF in stance	✓	
Time to max DF in stance	✓	
Max DF in swing	✓	
Time to max DF in swing	✓	

Significant differences in time to mean max PF ($p<.05$) during stance phase were found between YA and OA independent of WS (Figure 1, Table 64). The YG had a significantly longer time to mean max PF angle ($p<.05$) compared to the OG. For the YG, the max PF occurred at 57.67±1.36 percent GC, whereas the OG demonstrated max PF

angles at 56.44±1.30 percent GC. This result was found different as the previous hypothesis, where the speed effect was tested (Table 65), since the YG had exhibited a shorter time to mean max PF across speeds.

Significant differences for the mean relative angle for the foot-shank in the frontal plane were found between YA and OA independent of WS. This is the ankle eversion-inversion (EVE/INV) angle defined by the relative orientation between the foot and the shank (tibia) segments, which will be hereon referred to as the foot-shank. It should be noted that for the previous hypothesis, where the speed effect was tested, there were no significant differences found for the mean relative angles for the foot-shank in the frontal plane. The following section focuses on between-group differences. Table 66 presents the significant age-related differences in the mean max EVE/INV angles in stance and swing phase as well as their respective time of occurrence as a percentage of GC, independent of WS. Table 67 presents the significant age-related differences in the foot-shank EVE/INV angles independent of WS that were found in comparison to the findings in the first hypothesis, where the speed effect was tested.

Table 66. Significant p-values of the mean min and max EVE/INV angles (∠) of the foot-shank during stance and swing phase, as well as their respective time of occurrence in the gait cycle independent of WS.

Min EVE ∠ in stance p-value	Time to min EVE ∠ in stance p-value	Min EVE ∠ in swing p-value	Time to min EVE ∠ in swing p-value	Max EVE ∠ in stance p-value	Time to max EVE ∠ in stance p-value	Max EVE ∠ in swing p-value	Time to max EVE ∠ in swing p-value
-	-	<.01	<.001	<.05	<.05	<.05	-

Table 67. Foot-shank EVE/INV angles, independent of WS, found similar/different to the first hypothesis.

	Similar	Different
Max EVE in stance	✓	
Time to max EVE in stance	✓	
Max EVE in swing		X
Time to max EVE in swing		X
Max EVE in stance		X
Time to max EVE in stance		X
Max EVE in swing		X
Time to max EVE in swing	✓	X

Independent of speed, the YG had a significantly ($p<.05$) decreased mean min EVE angle during swing (-0.18° ±0.41°) compared to the OG (2.30°±0.43°), as shown in Table 66. Significant differences in time to mean min EVE ($p<.05$) during swing phase were found between YA and OA independent of WS (Table 66). The YG had a significantly shorter time to mean min EVE angle ($p<.05$) compared to the OG. For the YG, the min EVE occurred at 65.63±0.61 percent GC, whereas the OG demonstrated min EVE angles at 70.81±0.64 percent GC.

Independent of speed, the YG had a significantly ($p<.05$) increased mean max EVE angle during stance (12.74°±0.33°) compared to the OG (12.04°±0.34°), as shown in Table 66. Significant differences in time to mean max EVE ($p<.05$) during stance phase were found between YA and OA independent of WS (Table 66). The YG had a significantly shorter time to mean max EVE angle ($p<.05$) compared to the OG. For the YG, the max EVE occurred at 33.47±2.01 percent GC, whereas the OG demonstrated max EVE angles at 38.02±2.10 percent GC.

Independent of WS, the YG had a significantly ($p<.05$) increased mean max EVE angle during swing (11.93°±0.33°) compared to the OG (10.98°±0.35°), as shown in Table 66.

The mean relative angle for the foot-shank segment in the transverse plane was presented in Figure 6 (see Section 4.1.3). The following section focuses on between-group differences. Table 68 presents the significant age-related differences in the mean max ADD/ABD angles in stance and swing phase as well as their respective time of occurrence as a percentage of GC, independent of WS. Table 69 presents the significant age-related differences in the foot-shank ADD/ABD angles independent of WS that were found in comparison to the findings in the first hypothesis, where the WS effect was tested.

Table 68. Significant p-values of the mean min and max ADD/ABD angles (∠) of the foot-shank during stance and swing phase, as well as their respective time of occurrence in the gait cycle independent of WS.

Min ADD ∠ in stance p-value	Time to min ADD ∠ in stance p-value	Min ADD ∠ in swing p-value	Time to min ADD ∠ in swing p-value	Max ADD ∠ in stance p-value	Time to max ADD ∠ in stance p-value	Max ADD ∠ in swing p-value	Time to max ADD ∠ in swing p-value
<.001	<.05	<.001	-	<.001	<.001	<.001	<.001

Table 69. Foot-shank ADD/ABD angles, independent of WS, found similar/different to the first hypothesis.

	Similar	Different
Min ADD in stance	✓	
Time to min ADD in stance	✓	
Min ADD in swing	✓	
Time to min ADD in swing	✓	
Max ADD in stance	✓	
Time to max ADD in stance		X
Max ADD in swing	✓	
Time to max ADD in swing	✓	

Significant differences in time to mean max ADD ($p<.05$) during stance phase were found between YA and OA independent of WS (Figure 6, Table 68). The YG had a significantly shorter time to mean max ADD angle ($p<.05$) compared to the OG. For the YG, the max ADD occurred at 55.14±1.30 percent GC, whereas the OG demonstrated max ADD angles at 56.96±1.37 percent GC. This result was found different as the previous

hypothesis, where the speed effect was tested (Table 69), since the YG had exhibited a longer time to mean max ADD for the VS speed.

4.2.4 Age-related Differences in Relative Angles Between the Midfoot and Calcaneus Independent of Speed

The mean relative angle gait curve for the mid-cal segment in the sagittal plane was presented in Figure 11 (see Section 4.1.4). The following section focuses on between-group differences. Table 70 presents the significant age-related differences in the mean max and min DF/PF angles in stance and swing phase as well as their respective time of occurrence as a percentage of GC, independent of WS. Table 71 presents the significant age-related differences in the mid-cal DF/PF angles independent of WS that were found in comparison to the findings in the first hypothesis, where the speed effect was tested.

Table 70. Significant p-values of the mean min and max DF/PF angles (∠) of the mid-cal during stance and swing phase, as well as their respective time of occurrence in the gait cycle independent of WS.

Min DF ∠ in stance p-value	Time to min DF ∠ in stance p-value	Min DF ∠ in swing p-value	Time to min DF ∠ in swing p-value	Max DF ∠ in stance p-value	Time to max DF ∠ in stance p-value	Max DF ∠ in swing p-value	Time to max DF ∠ in swing p-value
-	<.01	-	<.001	<.05	<.001	<.05	<.01

Table 71. Midfoot-calcaneus DF/PF angles, independent of WS, found similar/different to the first hypothesis.

	Similar	Different
Min DF in stance	✓	
Time to min DF in stance	✓	
Min DF in swing	✓	
Time to min DF in swing	✓	
Max DF in stance		X
Time to max DF in stance	✓	
Max DF in swing	✓	
Time to max DF in swing	✓	

Independent of speed, the YG had a significantly ($p<.05$) increased mean max DF angle during stance (35.23°±0.56°) compared to the OG (33.53°±0.58°), as shown in Table 70. When the WS effect was tested, there were no significant differences ($p<.05$) for the mean max DF angle during stance between YA and OA (Table 71).

The mean relative angle gait curve for the mid-cal segment in the frontal plane was presented in Figure 13 (see Section 4.1.4). The following section focuses on between-group differences. Table 72 presents the significant age-related differences in the mean max and min EVE/INV angles in stance and swing phase as well as their respective time of occurrence as a percentage of GC, independent of WS. Table 73 presents the significant age-related differences in the mid-cal EVE/INV angles independent of WS that were found in comparison to the findings in the first hypothesis, where the speed effect was tested.

Table 72. Significant p-values of the mean min and max EVE/INV angles (∠) of the mid-cal during stance and swing phase, as well as their respective time of occurrence in the gait cycle independent of WS.

Min EVE ∠ in stance p-value	Time to min EVE ∠ in stance p-value	Min EVE ∠ in swing p-value	Time to min EVE ∠ in swing p-value	Max EVE ∠ in stance p-value	Time to max EVE ∠ in stance p-value	Max EVE ∠ in swing p-value	Time to max EVE ∠ in swing p-value
<.001	<.001	<.001	-	<.001	<.05	<.001	<.001

Table 73. Midfoot-calcaneus EVE/INV angles, independent of WS, found similar/different to the first hypothesis.

	Similar	Different
Min EVE in stance	✓	
Time to min EVE in stance	✓	
Min EVE in swing	✓	
Time to min EVE in swing	✓	
Max EVE in stance	✓	
Time to max EVE in stance		X
Max EVE in swing	✓	
Time to max EVE in swing	✓	

Significant differences in time to mean max EVE ($p<.05$) during stance phase were found between YA and OA independent of WS (Figure 13, Table 72). The YG had a significantly longer time to mean max EVE angle ($p<.05$) compared to the OG. For the YG, the max EVE occurred at 39.76±2.16 percent GC, whereas the OG demonstrated max EVE angles at 23.58±2.26 percent GC. In the previous hypothesis, where the speed effect was tested, there were no significant differences ($p<.05$) for the time to mean max EVE angle during stance between YA and OA (Table 73).

The mean relative angle gait curve for the mid-cal segment in the transverse plane was presented in Figure 18 (see Section 4.1.4). The following section focuses on between-group differences. Table 74 presents the significant age-related differences in the mean max and min ADD/ABD angles in stance and swing phase as well as their respective time of occurrence as a percentage of GC, independent of WS. Table 75 presents the significant age-related differences in the mid-cal ADD/ABD angles independent of WS that were found in comparison to the findings in the first hypothesis, where the WS effect was tested.

Table 74. Significant p-values of the mean min and max ADD/ABD angles (∠) of the mid-cal during stance and swing phase, as well as their respective time of occurrence in the gait cycle independent of WS.

Min ADD ∠ in stance p-value	Time to min ADD ∠ in stance p-value	Min ADD ∠ in swing p-value	Time to min ADD ∠ in swing p-value	Max ADD ∠ in stance p-value	Time to max ADD ∠ in stance p-value	Max ADD ∠ in swing p-value	Time to max ADD ∠ in swing p-value
<.001	-	<.001	<.05	<.001	<.001	<.001	<.001

Table 75. Midfoot-calcaneus ADD/ABD angles, independent of WS, found similar/different to the first hypothesis.

	Similar	Different
Min ADD in stance	✓	
Time to min ADD in stance	✓	
Min ADD in swing	✓	
Time to min ADD in swing	✓	
Max ADD in stance	✓	X
Time to max ADD in stance		
Max ADD in swing	✓	
Time to max ADD in swing	✓	

Significant differences in time to mean max ADD ($p<.05$) during stance phase were found between YA and OA independent of WS (Figure 18, Table 74). The YG had a significantly longer time to mean max ADD angle ($p<.05$) compared to the OG. For the YG, the max ADD occurred at 58.20±1.08 percent GC, whereas the OG demonstrated max ADD angles at 57.97±1.13 percent GC. This result was found different as the previous hypothesis, since the YG had showed a shorter time to mean max ADD angle as WS increased from VS to typical WS.

4.2.5 Age-related Differences in Relative Angles Between the Shank and Calcaneus Independent of Speed

The mean relative angle gait curve for the sha-cal segment in the sagittal plane was presented in Figure 23 (see Section 4.1.5). The following section focuses on between-group differences. Table 76 presents the significant age-related differences in the mean max and min DF/PF angles in stance and swing phase as well as their respective time of occurrence as a percentage of GC, independent of WS. Table 77 presents the significant age-related differences in the sha-cal DF/PF angles independent of WS that were found in comparison to the findings in the first hypothesis, where the speed effect was tested.

Table 76. Significant p-values of the mean min and max DF/PF angles (∠) of the sha-cal during stance and swing phase, as well as their respective time of occurrence in the gait cycle independent of WS.

Min PF ∠ in stance p-value	Time to min PF ∠ in stance p-value	Min PF ∠ in swing p-value	Time to min PF ∠ in swing p-value	Max DF ∠ in stance p-value	Time to max DF ∠ in stance p-value	Max DF ∠ in swing p-value	Time to max DF ∠ in swing p-value
<.001	<.01	<.001	<.001	<.001	<.01	<.001	<.01

Table 77. Shank-calcaneus DF/PF angles, independent of WS, found similar/different to the first hypothesis.

	Similar	Different
Min PF in stance	✓	X
Time to min PF in stance		
Min PF in swing	✓	
Time to min PF in swing	✓	
Max DF in stance	✓	
Time to max DF in stance	✓	
Max DF in swing	✓	
Time to max DF in swing	✓	

Significant differences in time to mean min PF ($p<.05$) during stance phase were found between YA and OA independent of WS (Figure 23, Table 76). The YG had a significantly longer time to mean min PF angle ($p<.05$) compared to the OG. For the YG, the min PF occurred at 54.94±1.53 percent GC, whereas the OG demonstrated min PF angles at 53.08±1.60 percent GC. This result was found different as the previous hypothesis, where the speed effect was tested (Table 77).

Significant differences for the mean relative angle for the sha-cal in the frontal plane were found between YA and OA independent of WS. This is the sha-cal eversion-inversion (EVE/INV) angle defined by the relative orientation between the shank (tibia) and the calcaneus segments. It should be noted that for the previous hypothesis, where the speed effect was tested, there were no significant differences found for the mean relative angles for the sha-cal in the frontal plane. The following section focuses on between-group differences. Table 78 presents the significant age-related differences in the mean max and

min EVE/INV angles in stance and swing phase as well as their respective time of occurrence as a percentage of GC, independent of WS. Table 79 presents the significant age-related differences in the sha-cal EVE/INV angles independent of WS that were found in comparison to the findings in the first hypothesis, where the speed effect was tested.

Table 78. Significant p-values of the mean min and max EVE/INV angles (∠) of the sha-cal during stance and swing phase, as well as their respective time of occurrence in the gait cycle independent of WS.

Min EVE ∠ in stance p-value	Time to min EVE ∠ in stance p-value	Min EVE ∠ in swing p-value	Time to min EVE ∠ in swing p-value	Max EVE ∠ in stance p-value	Time to max EVE ∠ in stance p-value	Max EVE ∠ in swing p-value	Time to max EVE ∠ in swing p-value
-	-	<.01	<.001	-	<.001	-	-

Table 79. Shank-calcaneus EVE/INV angles, independent of WS, found similar/different to the first hypothesis.

	Similar	Different
Min EVE in stance	✓	
Time to min EVE in stance	✓	
Min EVE in swing		X
Time to min EVE in swing		X
Max EVE in stance	✓	
Time to max EVE in stance		X
Max EVE in swing	✓	
Time to max EVE in swing	✓	

Independent of speed, the YG had a significantly ($p<.05$) decreased mean min EVE angle during swing (4.01°±0.35°) compared to the OG (5.75°±0.37°), as shown in Table 78. Significant differences in time to mean min EVE ($p<.05$) during swing phase were found between YA and OA independent of WS (Table 78). The YG had a significantly shorter time to mean min EVE angle ($p<.05$) compared to the OG. For the YG, the min EVE occurred at 71.62±0.85 percent GC, whereas the OG demonstrated min EVE angles at 77.80±0.89 percent GC.

Significant differences in time to mean max EVE ($p<.05$) during stance phase were found between YA and OA independent of WS (Table 78). The YG had a significantly shorter time to mean max EVE angle ($p<.05$) compared to the OG. For the YG, the max EVE occurred at 41.83±1.91 percent GC, whereas the OG demonstrated max EVE angles at 50.13±1.82 percent GC.

The mean relative angle gait curve for the sha-cal segment in the transverse plane was presented in Figure 28 (see Section 4.1.5). The following section focuses on between-group differences. Table 80 presents the significant age-related differences in the mean max and min ADD/ABD angles in stance and swing phase as well as their respective time of occurrence as a percentage of GC, independent of WS. Table 81 presents the significant age-related differences in the sha-cal ADD/ABD angles independent of WS that were found in comparison to the findings in the first hypothesis, where the speed effect was tested.

Table 80. Significant p-values of the mean min and max ADD/ABD angles (∠) of the sha-cal during stance and swing phase, as well as their respective time of occurrence in the gait cycle independent of WS.

Min ADD ∠ in stance p-value	Time to min ADD ∠ in stance p-value	Min ADD ∠ in swing p-value	Time to min ADD ∠ in swing p-value	Max ADD ∠ in stance p-value	Time to max ADD ∠ in stance p-value	Max ADD ∠ in swing p-value	Time to max ADD ∠ in swing p-value
<.001	-	<.001	-	<.001	-	<.001	<.001

Table 81. Shank-calcaneus ADD/ABD angles, independent of WS, found similar/different to the first hypothesis.

	Similar	Different
Min ADD in stance		X
Time to min ADD in stance		X
Min ADD in swing		X
Time to min ADD in swing	✓	
Max ADD in stance		X
Time to max ADD in stance		X
Max ADD in swing		X
Time to max ADD in swing	✓	

Independent of speed, the YG had a significantly ($p<.05$) increased mean min ADD angle during stance (4.68°±0.43°) compared to the OG (1.43°±0.45°), as shown in Table 80. This result was found different as the previous hypothesis, where the speed effect was tested (Table 81), since the YG had exhibited a decreased mean min ADD angle during stance at the VS speed.

Similar to the results of the stance phase, independent of WS, the YG had a significantly ($p<.05$) increased mean min ADD angle during swing (7.30°±0.43°) compared to the OG (2.99°±0.45°), as shown in Table 80. This result was found different as the previous hypothesis, where the speed effect was tested (Table 81), since the YG had exhibited a decreased mean min ADD angle during swing across all speeds.

Independent of speed, the YG had a significantly ($p<.05$) increased mean max ADD angle during stance (17.56°±0.41°) compared to the OG (12.25°±0.43°), as shown in Table 80. This result was found different as the previous hypothesis, where the speed effect was tested (Table 81), since the YG had exhibited an increased mean max ADD angle during stance at the VS and fast speeds.

Similar to the results of the stance phase, independent of WS, the YG had a significantly ($p<.05$) increased mean max ADD angle during swing (17.77°±0.44°) compared to the OG (12.27°±0.47°), as shown in Table 80. This result was found different as the previous hypothesis, since the YG had exhibited a decreased mean max ADD angle during swing as WS increased from VS to fast WS.

4.2.6 Age-related Differences in Relative Angles Between the Midfoot and Forefoot Independent of Speed

The mean relative angle gait curve for the mid-met segment in the sagittal plane was presented in Figure 33 (see Section 4.1.6). The following section focuses on between-group differences. Table 82 presents the significant age-related differences in the mean max and min DF/PF angles in stance and swing phase as well as their respective time of occurrence as a percentage of GC, independent of WS. Table 83 presents the significant age-related differences in the mid-met DF/PF angles independent of WS that were found in comparison to the findings in the first hypothesis, where the speed effect was tested. It should be noted that the significant results for the mean max and min mid-met DF/PF angles angle as well as their respective time of occurrence in the gait cycle as a function of speed were also found when controlling for speed (Table 83).

Table 82. Significant p-values of the mean min and max DF/PF angles (∠) of the mid-met during stance and swing phase, as well as their respective time of occurrence in the gait cycle independent of WS.

Min PF ∠ in stance p-value	Time to min PF ∠ in stance p-value	Min PF ∠ in swing p-value	Time to min PF ∠ in swing p-value	Max PF ∠ in stance p-value	Time to max PF ∠ in stance p-value	Max PF ∠ in swing p-value	Time to max PF ∠ in swing p-value
<.001	-	<.001	<.001	<.001	<.001	<.001	-

Table 83. Midfoot-forefoot DF/PF angles, independent of WS, found similar/different to the first hypothesis.

	Similar	Different
Min PF in stance	✓	
Time to min PF in stance	✓	
Min PF in swing	✓	
Time to min PF in swing	✓	
Max PF in stance	✓	
Time to max PF in stance	✓	
Max PF in swing	✓	
Time to max PF in swing	✓	

Significant differences for the mean relative angle for the mid-met in the frontal plane were found between YA and OA independent of WS. This is the mid-met eversion-inversion (EVE/INV) angle defined by the relative orientation between the midfoot and the forefoot (metatarsus) segments. It should be noted that for the previous hypothesis, where the speed effect was tested, there were no significant differences found for the mean relative angles for the mid-met in the frontal plane. The following section focuses on between-group differences. Table 84 presents the significant age-related differences in the mean max and min EVE/INV angles in stance and swing phase as well as their respective time of occurrence as a percentage of GC, independent of WS. Table 85 presents the significant age-related differences in the mid-met EVE/INV angles independent of WS that were found in comparison to the findings in the first hypothesis, where the WS effect was tested.

Table 84. Significant p-values of the mean min and max EVE/INV angles (∠) of the mid-met during stance and swing phase, as well as their respective time of occurrence in the gait cycle independent of WS.

Min EVE ∠ in stance p-value	Time to min EVE ∠ in stance p-value	Min EVE ∠ in swing p-value	Time to min EVE ∠ in swing p-value	Max EVE ∠ in stance p-value	Time to max EVE ∠ in stance p-value	Max EVE ∠ in swing p-value	Time to max EVE ∠ in swing p-value
<.01	<.001	<.01	<.01	<.05	-	-	<.01

Table 85. Midfoot-forefoot EVE/INV angles, independent of WS, found similar/different to the first hypothesis.

	Similar	Different
Min EVE in stance		X
Time to min EVE in stance		X
Min EVE in swing		X
Time to min EVE in swing		X
Max EVE in stance		X
Time to max EVE in stance	✓	
Max EVE in swing	✓	
Time to max EVE in swing		X

Independent of speed, the YG had a significantly ($p<.05$) decreased mean min EVE angle during stance (8.79°±0.49°) compared to the OG (9.47°±0.52°), as shown in Table 84. Significant differences in time to mean min EVE ($p<.05$) during stance phase were found between YA and OA independent of WS (Table 84). The YG had a significantly shorter time to mean min EVE angle ($p<.05$) compared to the OG. For the YG, the min EVE occurred at 55.62±0.91 percent GC, whereas the OG demonstrated min EVE angles at 58.94±0.95 percent GC.

Similar to the results of the stance phase, independent of WS, the YG had a significantly ($p<.05$) decreased mean min EVE angle during swing (9.07°±0.50°) compared to the OG (9.78°±0.53°), as shown in Table 84. Significant differences in time to mean min EVE ($p<.05$) during swing phase were found between YA and OA independent of WS (Table 84). The YG had a shorter time to mean min EVE angle ($p<.05$) compared to the OG. For the YG, the min EVE occurred at 64.60±0.61 percent GC, whereas the OG demonstrated min EVE angles at 66.17±0.64 percent GC.

Independent of WS, the YG had a significantly ($p<.05$) decreased mean max EVE angle during stance (13.31°±0.48°) compared to the OG (14.04°±0.51°), as shown in Table 84.

Significant differences in time to mean max EVE ($p<.05$) during swing phase were found between YA and OA independent of WS (Table 84). The YG had a significantly shorter time to mean max EVE angle ($p<.05$) compared to the OG. For the YG, the max EVE occurred at 90.70±0.72 percent GC, whereas the OG demonstrated max EVE angles at 93.39±0.76 percent GC.

The mean relative angle gait curve for the mid-met segment in the transverse plane was presented in Figure 38 (see Section 4.1.6). The following section focuses on between-group differences. Table 86 presents the significant age-related differences in the mean max and min ADD/ABD angles in stance and swing phase as well as their respective time of occurrence as a percentage of GC, independent of WS. Table 87 presents the significant age-related differences in the mid-met ADD/ABD angles independent of WS that were found in comparison to the findings in the first hypothesis, where the speed effect was tested.

Table 86. Significant p-values of the mean min and max ADD/ABD angles (∠) of the mid-met during stance and swing phase, as well as their respective time of occurrence in the gait cycle independent of WS.

Max ABD ∠ in stance p-value	Time to max ABD ∠ in stance p-value	Max ABD ∠ in swing p-value	Time to max ABD ∠ in swing p-value	Min ABD ∠ in stance p-value	Time to min ABD ∠ in stance p-value	Min ABD ∠ in swing p-value	Time to min ABD ∠ in swing p-value
<.001	<.01	<.001	-	<.001	<.001	<.001	-

Table 87. Midfoot-forefoot ADD/ABD angles, independent of WS, found similar/different to the first hypothesis.

	Similar	Different
Max ABD in stance	✓	
Time to max ABD in stance		X
Max ABD in swing	✓	
Time to max ABD in swing	✓	
Min ABD in stance	✓	
Time to min ABD in stance	✓	
Min ABD in swing	✓	
Time to min ABD in swing	✓	

Significant differences in time to mean max ABD ($p<.05$) during stance phase were found between YA and OA independent of WS (Table 86). The YG had a significantly shorter time to mean max ABD angle ($p<.05$) compared to the OG. For the YG, the max ABD occurred at 33.75±2.26 percent GC, whereas the OG demonstrated max ABD angles at 38.23±2.37 percent GC. In the previous hypothesis, where the speed effect was tested,

there were no significant differences ($p<.05$) for the time to mean max ABD during stance between YA and OA (Table 87).

4.2.7 Age-related Differences in Relative Angles Between the Calcaneus and Forefoot Independent of Speed

The mean relative angle gait curve for the cal-met segment in the sagittal plane was presented in Figure 43 (see Section 4.1.7). The following section focuses on between-group differences. Table 88 presents the significant age-related differences in the mean max and min DF/PF angles in stance and swing phase as well as their respective time of occurrence as a percentage of GC, independent of WS. Table 89 presents the significant age-related differences in the cal-met DF/PF angles independent of WS that were found in comparison to the findings in the first hypothesis, where the speed effect was tested.

Table 88. Significant p-values of the mean max DF/PF angles (∠) of the cal-met during stance and swing phase, as well as their respective time of occurrence in the gait cycle independent of WS.

Max PF ∠ in stance p-value	Time to max PF ∠ in stance p-value	Max PF ∠ in swing p-value	Time to max PF ∠ in swing p-value	Max PF ∠ in stance p-value	Time to max PF ∠ in stance p-value	Max PF ∠ in swing p-value	Time to max PF ∠ in swing p-value
<.001	<.01	<.001	<.001	<.001	<.001	<.001	-

Table 89. Calcaneus-forefoot DF/PF angles, independent of WS, found similar/different to the first hypothesis.

	Similar	Different
Max PF in stance	✓	
Time to max PF in stance		X
Max PF in swing	✓	
Time to max PF in swing	✓	
Min PF in stance	✓	
Time to min PF in stance	✓	
Min PF in swing	✓	
Time to min PF in swing		X

Significant differences in time to mean max PF ($p<.05$) during stance phase were found between YA and OA independent of WS (Figure 43, Table 88). The YG had a

significantly longer time to mean max PF angle ($p<.05$) compared to the OG. For the YG, the max PF occurred at 57.54±1.35 percent GC, whereas the OG demonstrated max PF angles at 54.15±1.42 percent GC. These results were found different as the previous hypothesis (Table 89), since the YG had exhibited a shorter time to mean max PF angle as WS increased from typical to fast WS.

Opposite to the previous hypothesis, where the speed was tested, no significant differences in time to mean min PF ($p<.05$) during swing phase were found between YA and OA independent of WS (Table 88).

The mean relative angle gait curve for the cal-met segment in the frontal plane was presented in Figure 48 (see Section 4.1.7). The following section focuses on between-group differences. Table 90 presents the significant age-related differences in the mean max and min EVE/INV angles in stance and swing phase as well as their respective time of occurrence as a percentage of GC, independent of WS. Table 91 presents the significant age-related differences in the cal-met EVE/INV angles independent of WS that were found in comparison to the findings in the first hypothesis, where the speed effect was tested.

Table 90. Significant p-values of the mean min and max EVE/INV angles (∠) of the cal-met during stance and swing phase, as well as their respective time of occurrence in the gait cycle independent of WS.

Min EVE ∠ in stance p-value	Time to min EVE ∠ in stance p-value	Min EVE ∠ in swing p-value	Time to min EVE ∠ in swing p-value	Max EVE ∠ in stance p-value	Time to max EVE ∠ in stance p-value	Max EVE ∠ in swing p-value	Time to max EVE ∠ in swing p-value
<.001	<.001	<.001	<.001	<.001	-	<.001	-

Table 91. Calcaneus-forefoot EVE/INV angles, independent of WS, found similar/different to the first hypothesis.

	Similar	Different
Min EVE in stance	✓	
Time to min EVE in stance	✓	
Min EVE in swing	✓	
Time to min EVE in swing	✓	
Max EVE in stance	✓	
Time to max EVE in stance		X
Max EVE in swing	✓	
Time to max EVE in swing		X

No significant differences in time to mean max EVE ($p<.05$) during stance phase were found between YA and OA independent of WS (Table 90). No significant differences in time to mean max EVE ($p<.05$) during swing phase were found between YA and OA independent of WS (Table 90). These results were found different as the previous hypothesis, where the speed effect was tested (Table 91), since there were significant differences between age groups in the time to mean max EVE angle during stance and swing.

The mean relative angle gait curve for the cal-met segment in the transverse plane was presented in Figure 53 (see Section 4.1.7). The following section focuses on between-group differences. Table 92 presents the significant age-related differences in the mean max and min ADD/ABD angles in stance and swing phase as well as their respective time of occurrence as a percentage of GC, independent of WS. Table 93 presents the significant age-related differences in the cal-met ADD/ABD angles independent of WS that were found in comparison to the findings in the first hypothesis, where the WS effect was tested.

Table 92. Significant p-values of the mean min and max ADD/ABD angles (∠) of the cal-met during stance and swing phase, as well as their respective time of occurrence in the gait cycle independent of WS.

Min ADD ∠ in stance p-value	Time to min ADD ∠ in stance p-value	Min ADD ∠ in swing p-value	Time to min ADD ∠ in swing p-value	Max ADD ∠ in stance p-value	Time to max ADD ∠ in stance p-value	Max ADD ∠ in swing p-value	Time to max ADD ∠ in swing p-value
<.001	<.05	<.001	-	<.001	-	<.001	<.001

Table 93. Calcaneus-forefoot ADD/ABD angles, independent of WS, found similar/different to the first hypothesis.

	Similar	Different
Min ADD in stance	✓	
Time to min ADD in stance	✓	
Min ADD in swing	✓	
Time to min ADD in swing	✓	
Max ADD in stance	✓	
Time to max ADD in stance	✓	
Max ADD in swing	✓	
Time to max ADD in swing	✓	

4.2.8 Summary of MSF Kinematics Results

The present study found significant differences for MSF angles between YA and OA independent of WS. The results found for this second hypothesis, where the speed effect was being controlled, slightly varied compared to when analyses examined the age-related differences between YA and OA as a function of speed (Section 4.1). In the sagittal plane, the mean max shank-foot PF and DF angle in stance and swing were found significantly different between YA and OA independent of WS. The mean max mid-cal DF angle in stance and swing was significantly different between age groups when the speed was controlled. The mean min and max PF sha-cal angle in both stance and swing were found significantly different between YA and OA independent of WS. These latter results were similar to the shank-foot angles in the sagittal plane. The mean min and max mid-met PF angle in stance and swing were found significantly different between YA and OA independent of WS. Further, the mean min and max cal-met DF angle in stance and

swing were found significantly different between age groups when speed was controlled. Further, in this comparison where the speed effect was controlled, there were more findings for the MSF angles in the frontal plane. In the frontal plane, the mean min EVE angle in swing and the max shank-foot EVE angles in both stance and swing were found significantly different between YA and OA independent of WS. The mean min and max EVE mid-cal angle in stance and swing were found significantly different between YA and OA when speed was controlled. The mean min sha-cal EVE angle in swing phase was also found significantly different between age groups independent of WS. In addition, the mean min mid-met EVE angle in stance and swing phase, and the mean max mid-met EVE angle in stance were found significantly different between YA and OA independent of WS. Further, the mean min and max EVE cal-met angle in stance and swing phase were found significantly different between age groups independent of WS. In the transverse plane, the mean min and max shank-foot ADD angles in stance and swing were found significantly different between YA and OA independent of WS. The mean min and max mid-cal ADD angles in stance and swing phase were found significantly different between age groups when controlling for speed. Further, the mean min and max mid-met ABD angles in stance and swing were also found significantly different between YA and OA independent of WS. The mean min and max cal-met ADD angles in stance and swing were found significantly different between age groups independent of WS. Thus, when the speed effect is being controlled, there are significant differences in MSF kinematics between YA and OA.

4.2.9 Age-related Differences in Planar Angles of the Foot Independent of Speed

4.2.9.1 Age-related Differences in the F2Pt Planar Angle of the Foot Independent of Speed

The mean relative angle gait curve for the F2Pt planar angle was presented in Figure 58 (see Section 4.1.9.1). The following section focuses on between-group differences. Table 94 presents the significant age-related differences in the mean max and min F2Pt angles in stance phase as well as their respective time of occurrence as a percentage of GC, independent of WS. Table 95 presents the significant age-related differences in the F2Pt planar angle independent of WS that were found in comparison to the findings in the first hypothesis, where the speed effect was tested.

Table 94. Significant p-values of the mean min and max F2Pt angles (∠) during stance phase, as well as their respective time of occurrence in the gait cycle independent of WS.

Min F2Pt ∠ p-value	Time to min F2Pt ∠ p-value	Max F2Pt ∠ p-value	Time to max F2Pt ∠ p-value
-	-	<.01	<.001

Table 95. F2Pt angles, independent of WS, found similar/different to the first hypothesis.

	Similar	Different
Min F2Pt in stance	✓	
Time to min F2Pt in stance		X
Max F2Pt in stance	✓	
Time to max F2Pt in stance	✓	

Significant differences in time to mean max F2Pt ($p<.05$) during stance phase were found between YA and OA independent of WS (Figure 58, Table 94). The YG had a significantly shorter time to mean max F2Pt angle ($p<.05$) compared to the OG. For the YG, the max F2Pt occurred at 25.43±1.35 percent GC, whereas the OG demonstrated max F2Pt angles at 36.40±1.42 percent GC. This result was found different as the previous

hypothesis, where the speed effect was tested (Table 95), as the YG had exhibited a longer time to mean max F2Pt angle as WS increased.

4.2.9.2 Age-related Differences in the V2G Planar Angle of the Foot Independent of Speed

The mean relative angle gait curve for the V2G planar angle was presented in Figure 60 (see Section 4.1.9.2). The following section focuses on between-group differences. Table 96 presents the significant age-related differences in the mean max and min V2G angles in stance phase as well as their respective time of occurrence as a percentage of GC, independent of WS. Table 97 presents the significant age-related differences in the V2G planar angle independent of WS that were found in comparison to the findings in the first hypothesis, where the speed effect was tested.

Table 96. Significant p-values of the mean min and max V2G angles (∠) during stance phase, as well as their respective time of occurrence in the gait cycle independent of WS.

Max V2G ∠ p-value	Time to max V2G ∠ p-value	Min V2G ∠ p-value	Time to min V2G ∠ p-value
<.001	-	-	<.001

Table 97. V2G angles, independent of WS, found similar/different to the first hypothesis.

	Similar	Different
Max V2G in stance		X
Time to max V2G in stance	✓	
Min V2G in stance	✓	
Time to min V2G in stance	✓	

Independent of speed, the YG had a significantly ($p<.05$) increased mean max V2G angle during stance (-18.80°±0.69°) compared to the OG (-16.29°±0.72°), as shown in Table 96. It should be noted that there were no significant differences between age groups for the mean max V2G angle during stance as a function of WS.

4.2.9.3 Age-related Differences in the S2F Planar Angle of the Foot Independent of Speed

The mean relative angle gait curve for the S2F planar angle was presented in Figure 62 (see Section 4.1.9.3). The following section focuses on between-group differences. Table 98 presents the significant age-related differences in the mean max and min S2F angles in stance phase as well as their respective time of occurrence as a percentage of GC, independent of WS. Table 99 presents the significant age-related differences in the mean S2F planar angles independent of WS that were found in comparison to the findings in the first hypothesis, where the speed effect was tested. It should be noted that the significant results for the mean max and min S2F planar angle as well as their respective time of occurrence in the gait cycle as a function of speed were also found when controlling for speed (Table 98).

Table 98. Significant p-values of the mean min and max S2F angles (∠) during stance phase, as well as their respective time of occurrence in the gait cycle independent of WS.

Min S2F ∠ p-value	Time to min S2F ∠ p-value	Max S2F ∠ p-value	Time to max S2F ∠ p-value
-	<.05	-	-

Table 99. S2F angles, independent of WS, found similar/different to the first hypothesis.

	Similar	Different
Min S2F in stance	✓	
Time to min S2F in stance	✓	
Max S2F in stance	✓	
Time to max S2F in stance	✓	

4.2.9.4 Age-related Differences in the S2V Planar Angle of the Foot Independent of Speed

The mean relative angle gait curve for the S2V planar angle was presented in Figure 63 (see Section 4.1.9.4). The following section focuses on between-group differences. Table 100 presents the significant age-related differences in the mean max and min S2V angles in stance phase as well as their respective time of occurrence as a percentage of GC, independent of WS. Table 101 presents the significant age-related differences in the S2V planar angle independent of WS that were found in comparison to the findings in the first hypothesis, where the speed effect was tested.

Table 100. Significant p-values of the mean min and max S2V angles (∠) during stance phase, as well as their respective time of occurrence in the gait cycle independent of WS.

Min S2V ∠ p-value	Time to min S2V ∠ p-value	Max S2V ∠ p-value	Time to max S2V ∠ p-value
-	<.01	-	-

Table 101. S2V angles, independent of WS, found similar/different to the first hypothesis.

	Similar	Different
Min S2V in stance	✓	
Time to min S2V in stance		X
Max S2V in stance	✓	
Time to max S2V in stance	✓	

Significant differences in time to mean min S2V ($p<.05$) during stance phase were found between YA and OA independent of WS (Figure 63, Table 100). The YG had a significantly shorter time to mean min S2V angle ($p<.05$) compared to the OG. For the YG, the min S2V occurred at 3.21±1.23 percent GC, whereas the OG demonstrated min S2V angles at 9.82±1.28 percent GC. Similarly, significant differences in time to mean max S2V ($p<.05$) during stance phase were found between YA and OA independent of WS (Figure 63, Table 100). This result was found different as the previous hypothesis (Table

101), as there were no significant differences between age groups for the time to mean min S2V angle as a function of speed.

4.2.9.5 Age-related Differences in the F2G Planar Angle of the Foot Independent of Speed

The mean relative angle gait curve for the F2G planar angle was presented in Figure 64 (see Section 4.1.9.5). The following section focuses on between-group differences. Table 102 presents the significant age-related differences in the mean max and min F2G angles in stance phase as well as their respective time of occurrence as a percentage of GC, independent of WS. Table 103 presents the significant age-related differences in the F2G planar angle independent of WS that were found in comparison to the findings in the first hypothesis, where the speed effect was tested.

Table 102. Significant p-values of the mean min and max F2G angles (∠) during stance phase, as well as their respective time of occurrence in the gait cycle independent of WS.

Min F2G ∠ p-value	Time to min F2G ∠ p-value	Max F2G ∠ p-value	Time to max F2G ∠ p-value
<.01	<.01	-	<.001

Table 103. F2G angles, independent of WS, found similar/different to the first hypothesis.

	Similar	Different
Min F2G in stance		X
Time to min F2G in stance		X
Max F2G in stance	✓	
Time to max F2G in stance	✓	

Independent of speed, the YG had a significantly ($p<.05$) increased mean min F2G angle during stance (2.77°±0.22°) compared to the OG (2.07°±0.23°), as shown in Table 102. Significant differences in time to mean min F2G ($p<.05$) during stance phase were found between YA and OA independent of WS (Figure 64, Table 102). The YG had a significantly shorter time to mean min F2G angle ($p<.05$) compared to the OG. For the YG,

the min F2G occurred at 1.21±0.25 percent GC, whereas the OG demonstrated min F2G angles at 2.19±0.26 percent GC. In the previous hypothesis, where the speed effect was tested, there were no significant differences ($p<.05$) for the mean min F2G angle nor the time to mean min F2G angle during stance between YA and OA (Table 103).

4.2.9.6 Age-related Differences in the S2G Planar Angle of the Foot Independent of Speed

The mean relative angle gait curve for the S2G planar angle was presented in Figure 65 (see Section 4.1.9.6). The following section focuses on between-group differences. Table 104 presents the significant age-related differences in the mean max and min S2G angles in stance phase as well as their respective time of occurrence as a percentage of GC, independent of WS. Table 105 presents the significant age-related differences in the mean S2G planar angle independent of WS that were found in comparison to the findings in the first hypothesis, where the speed effect was tested. It should be noted that the significant results for the mean max and min S2G planar angle as well as their respective time of occurrence in the gait cycle as a function of speed were also found when controlling for speed (Table 104).

Table 104. Significant p-values of the mean min and max S2G angles (∠) during stance phase, as well as their respective time of occurrence in the gait cycle independent of WS.

Min S2G ∠ p-value	Time to min S2G ∠ p-value	Max S2G ∠ p-value	Time to max S2G ∠ p-value
-	-	-	<.001

Table 105. S2G angles, independent of WS, found similar/different to the first hypothesis.

	Similar	Different
Min S2G in stance	✓	
Time to min S2G in stance	✓	
Max S2G in stance	✓	
Time to max S2G in stance	✓	

4.2.9.7 Age-related Differences in the F2Ps Planar Angle of the Foot Independent of Speed

The mean relative angle gait curve for the F2Ps planar angle was presented in Figure 66 (see Section 4.1.9.7). The following section focuses on between-group differences. Table 106 presents the significant age-related differences in the mean max and min F2Ps angles in stance phase as well as their respective time of occurrence as a percentage of GC, independent of WS. Table 107 presents the significant age-related differences in the mean F2Ps planar angle independent of WS that were found in comparison to the findings in the first hypothesis, where the speed effect was tested. It should be noted that the significant results for the mean max and min F2Ps planar angle as well as their respective time of occurrence in the gait cycle as a function of speed were also found when controlling for speed (Table 107).

Table 106. Significant p-values of the mean min and max F2Ps angles (∠) during stance phase, as well as their respective time of occurrence in the gait cycle independent of WS.

Min F2Ps ∠ p-value	Time to min F2Ps ∠ p-value	Max F2Ps ∠ p-value	Time to max F2Ps ∠ p-value
-	<.001	-	<.001

Table 107. F2Ps angles, independent of WS, found similar/different to the first hypothesis.

	Similar	Different
Min F2Ps in stance	✓	
Time to min F2Ps in stance	✓	
Max F2Ps in stance	✓	
Time to max F2Ps in stance	✓	

4.2.9.8 Age-related Differences in the MLA Planar Angle of the Foot Independent of Speed

The mean relative angle gait curve for the MLA planar angle was presented in Figure 67 (see Section 4.1.9.8). The following section focuses on between-group

differences. Table 108 presents the significant age-related differences in the mean max and min MLA angles in stance phase as well as their respective time of occurrence as a percentage of GC, independent of WS. Table 109 presents the significant age-related differences in the MLA planar angle independent of WS that were found in comparison to the findings in the first hypothesis, where the WS effect was tested.

Table 108. Significant p-values of the mean min and max MLA angles (∠) during stance phase, as well as their respective time of occurrence in the gait cycle independent of WS.

Min MLA ∠ p-value	Time to min MLA ∠ p-value	Max MLA ∠ p-value	Time to max MLA ∠ p-value
<.01	<.001	<.01	<.01

Table 109. MLA angles, independent of WS, found similar/different to the first hypothesis.

	Similar	Different
Min MLA in stance		X
Time to min MLA in stance	✓	
Max MLA in stance		X
Time to max MLA in stance	✓	

Independent of speed, the YG had a significantly ($p<.05$) decreased mean min MLA angle during stance (169.89°±0.66°) compared to the OG (173.05°±0.70°). Similarly, independent of WS, the YG had a significantly ($p<.05$) decreased mean max MLA angle during stance (187.68°±0.57°) compared to the OG (190.28°±0.59°), as shown in Table 108. In the previous hypothesis, where the WS effect was tested, there were no significant differences ($p<.05$) for the mean max and min MLA angles during stance between YA and OA.

4.2.10 Summary of Planar Angles Results

The present study found significant differences for the mean planar angles between YA and OA independent of WS. Differences in F2Pt and V2G angles were also found between age-groups, as in the previous hypothesis where the speed effect was tested.

However, when controlling for speed, significant differences for the mean min and max Medial Longitudinal Arch (MLA) angles were also found between YA and OA. It should be noted that this angle was not found significantly different between age groups as a function of speed. In addition, the mean min F2G angle was found significantly different between YA and OA, independent of WS. Thus, when the speed effect is being controlled, there are more significant differences in planar angles between YA and OA.

4.2.11 Age-related Differences in Ankle Kinetics Independent of Speed

4.2.11.1 Age-related Differences in Ankle Moment Independent of Speed

The mean moment for the foot-shank in the sagittal plane was presented in Figure 68 (see Section 4.1.11.1). The following section focuses on between-group differences. Table 110 presents the significant age-related differences in the mean max and min DF/PF moments in stance and swing phase as well as their respective time of occurrence as a percentage of GC, independent of WS. Table 111 presents the significant age-related differences in the mean ankle moment independent of WS that were found in comparison to the findings in the first hypothesis, where the speed effect was tested. It should be noted that the significant results for the mean max and min DF/PF ankle moments as well as their respective time of occurrence in the gait cycle as a function of speed were also found when controlling for speed (Table 111).

Table 110. Significant p-values of the mean min and max DF/PF ankle moments ((N·m)/kg) during stance and swing phase, as well as their respective time of occurrence in the gait cycle independent of WS.

Min DF moment in stance p-value	Time to min DF moment in stance p-value	Min DF moment in swing p-value	Time to min DF moment in swing p-value	Max PF moment in stance p-value	Time to max PF moment in stance p-value	Max PF moment in swing p-value	Time to max PF moment in swing p-value
-	<.001	-	-	<.001	<.01	<.001	<.01

Table 111. Ankle moment, independent of WS, found similar/different to the first hypothesis.

	Similar	Different
Min DF moment in stance	✓	
Time to min DF moment in stance	✓	
Min DF moment in swing	✓	
Time to min DF moment in swing	✓	
Max PF moment in stance	✓	
Time to max PF moment in stance	✓	
Max PF moment in swing	✓	
Time to max PF moment in swing		

4.2.11.2 Age-related Differences in Ankle Power Independent of Speed

The mean power for the foot-shank in the sagittal plane was presented in Figure 71 (see Section 4.1.11.2). The following section focuses on between-group differences. Table 112 presents the significant age-related differences in the mean max and min DF/PF powers in stance and swing phase as well as their respective time of occurrence as a percentage of GC, independent of WS. Table 113 presents the significant age-related differences in the mean ankle power independent of WS that were found in comparison to the findings in the first hypothesis, where the WS effect was tested. It should be noted that the significant results for the mean max and min concentric-eccentric DF/PF ankle power as well as their respective time of occurrence in the gait cycle as a function of speed were also found when controlling for speed (Table 113).

Table 112. Significant p-values of the mean max eccentric and concentric power (W/Kg) of the ankle during stance and swing phase, as well as their respective time of occurrence in the gait cycle independent of WS.

Max ECC power in stance p-value	Time to max ECC power in stance p-value	Max ECC power in swing p-value	Time to max ECC power in swing p-value	Max CNC power in stance p-value	Time to max CNC power in stance p-value	Max CNC power in swing p-value	Time to max CNC power in swing p-value
-	-	<.001	<.001	<.05	<.001	<.001	<.001

Table 113. Ankle power, independent of WS, found similar/different to the first hypothesis.

	Similar	Different
Max ECC power in stance	✓	
Time to max ECC power in stance	✓	
Max ECC power in swing	✓	
Time to max ECC power in swing	✓	
Max CNC power in stance	✓	
Time to max CNC power in stance	✓	
Max CNC power in swing	✓	
Time to max CNC power in swing	✓	

4.2.12 Summary of Ankle Kinetics Results

The present study found significant differences for ankle moment and ankle power between YA and OA independent of WS. The results found for this second hypothesis, where the speed effect was being controlled, did not vary compared to when analyses examined the age-related differences between YA and OA as a function of speed (Section 4.1). Independent of speed, the mean max PF moment in stance and swing phase were still found significantly different between YA and OA. The mean min ECC power in swing phase was also found significantly different between age groups when controlling for speed. Further, the mean max CNC power in stance and swing phase were also found significantly different between YA and OA independent of WS. Thus, when the speed effect is being controlled, significant differences in ankle kinetics are still being found between YA and OA.

4.2.13 Age-related Differences in Knee Kinetics and Kinematics Independent of Speed

4.2.13.1 Age-related Differences in Knee Moment Independent of Speed

The mean moment for the knee in the sagittal plane was presented in Figure 75 (see Section 4.1.13.1). The following section focuses on between-group differences. Table 114 presents the significant age-related differences in the mean max and min FLEX/EXT

moments in stance and swing phase as well as their respective time of occurrence as a percentage of GC, independent of WS. Table 115 presents the significant age-related differences in the knee moment independent of WS that were found in comparison to the findings in the first hypothesis, where the WS effect was tested.

Table 114. Significant p-values of the mean min and max FLEX/EXT moments ((N·m)/kg) of the knee during stance and swing phase, as well as their respective time of occurrence in the gait cycle independent of WS.

Min FLEX moment in stance p-value	Time to min FLEX moment in stance p-value	Min FLEX moment in swing p-value	Time to min FLEX moment in swing p-value	Max EXT moment in stance p-value	Time to max EXT in stance p-value	Max EXT moment in swing p-value	Time to max EXT moment in swing p-value
<.01	<.001	<.05	<.01	<.05	<.001	<.001	<.001

Table 115. Knee moment, independent of WS, found similar/different to the first hypothesis.

	Similar	Different
Min FLEX moment in stance	✓	
Time to min FLEX moment in stance	✓	
Min FLEX moment in swing		X
Time to min FLEX moment in swing	✓	
Max EXT moment in stance		X
Time to max EXT moment in stance		X
Max EXT moment in swing	✓	
Time to max EXT moment in swing	✓	

Independent of speed, the YG had a significantly (p<.05) decreased mean min FLEX moment during swing (-0.31±0.01 $\frac{N \cdot m}{kg}$) compared to the OG (-0.32 ±0.01$\frac{N \cdot m}{kg}$), as shown in Table 114. In the previous hypothesis, where the speed effect was tested, there were no significant differences (p<.05) for the min FLEX moment during swing between YA and OA (Table 115).

Independent of speed, the YG had a significantly (p<.05) greater mean max EXT moment during stance (0.75±0.02 $\frac{N \cdot m}{kg}$) compared to the OG (0.72±0.02$\frac{N \cdot m}{kg}$), as shown in Table 114. Significant differences in time to mean max EXT moment (p<.05) during stance

phase were found between YA and OA independent of WS (Figure 75, Table 114). The YG had a significantly longer time to mean max EXT moment ($p<.05$) compared to the OG. For the YG, the max EXT moment occurred at 19.26±1.02 percent GC, whereas the OG demonstrated max EXT moment at 17.94±1.07 percent GC.

4.2.13.2 Age-related Differences in Knee Power Independent of Speed

The mean power for the knee in the sagittal plane was presented in Figure 79 (see Section 4.1.13.2). The following section focuses on between-group differences. Table 116 presents the significant age-related differences in the mean max and min flexion-extension powers in stance and swing phase as well as their respective time of occurrence as a percentage of GC, independent of WS. Table 117 presents the significant age-related differences in the knee power independent of WS that were found in comparison to the findings in the first hypothesis, where the speed effect was tested.

Table 116. Significant p-values of the mean max eccentric and concentric power (W/Kg) of the knee during stance and swing phase, as well as their respective time of occurrence in the gait cycle independent of WS.

Max ECC power in stance p-value	Time to max ECC power in stance p-value	Max ECC power in swing p-value	Time to max ECC power in swing p-value	Max CNC power in stance p-value	Time to max CNC power in stance p-value	Max CNC power in swing p-value	Time to max CNC power in swing p-value
-	<.001	-	<.05	<.05	-	-	<.001

Table 117. Knee power, independent of WS, found similar/different to the first hypothesis.

	Similar	Different
Max ECC power in stance	✓	
Time to max ECC power in stance	✓	
Max ECC power in swing	✓	
Time to max ECC power in swing	✓	
Max CNC power in stance	✓	
Time to max CNC power in stance	✓	
Max CNC power in swing		X
Time to max CNC power in swing	✓	

There were no significant differences found for the mean max concentric knee power in stance between YA and OA independent of WS. It should be noted that in the previous hypothesis, there were significant differences for the mean max concentric knee power in stance between age groups (Table 117).

4.2.13.3 Age-related Differences in Knee Angles Independent of Speed

The mean relative angle for the knee segment in the sagittal plane was presented in Figure 83 (see Section 4.1.13.3). The following section focuses on between-group differences. Table 118 presents the significant age-related differences in the mean max and min FLEXT/EXT angles in stance and swing phase as well as their respective time of occurrence as a percentage of GC, independent of WS. Table 119 presents the significant age-related differences in the knee FLEX/EXT angles independent of WS that were found in comparison to the findings in the first hypothesis, where the speed effect was tested.

Table 118. Significant p-values of the mean min and max FLEX/EXT angles (∠) of the knee during stance and swing phase, as well as their respective time of occurrence in the gait cycle independent of WS.

Min flexion ∠ in stance p-value	Time to min flexion ∠ in stance p-value	Min flexion ∠ in swing p-value	Time to min flexion ∠ in swing p-value	Max flexion ∠ in stance p-value	Time to max flexion ∠ in stance p-value	Max flexion ∠ in swing p-value	Time to max flexion ∠ in swing p-value
<.001	<.05	<.001	<.001	<.001	<.001	-	<.05

Table 119. Knee FLEX/EXT angles, independent of WS, found similar/different to the first hypothesis.

	Similar	Different
Min flexion in stance	✓	
Time to min flexion in stance		X
Min flexion in swing	✓	
Time to min flexion in swing	✓	
Max flexion in stance	✓	
Time to max flexion in stance	✓	
Max flexion in swing	✓	
Time to max flexion in swing	✓	

Significant differences in time to mean min FLEX ($p<.05$) during stance phase were found between YA and OA independent of WS (Figure 83, Table 118). The YG had a significantly longer time to mean min FLEX angle ($p<.05$) compared to the OG. For the YG, the min FLEX occurred at 19.45±1.44 percent GC, whereas the OG demonstrated min FLEX angles at 14.59±1.51 percent GC. In the previous hypothesis, where the speed effect was tested, there were no significant differences in time to mean min FLEX during stance between age groups (Table 119).

Similar to the previous hypothesis, where the speed effect was tested, there were no significant differences found in the frontal plane for the mean min and max varus/valgus angles between YA and OA, independent of WS.

The mean relative angle for the knee segment in the transverse plane was presented in Figure 87 (see Section 4.1.13.3). The following section focuses on between-group differences. Table 120 presents the significant age-related differences in the mean max and min INT/EXTL angles in stance and swing phase as well as their respective time of occurrence as a percentage of GC, independent of WS. Table 121 presents the significant age-related differences in the knee INT/EXTL rotation angles independent of WS that were found in comparison to the findings in the first hypothesis, where the speed effect was tested.

Table 120. Significant p-values of the mean min and max INT/EXTL rotation angles (∠) of the knee during stance and swing phase, as well as their respective time of occurrence in the gait cycle independent of WS.

Max ER ∠ in stance p-value	Time to max ER ∠ in stance p-value	Max ER ∠ in swing p-value	Time to max ER ∠ in swing p-value	Min ER ∠ in stance p-value	Time to min ER ∠ in stance p-value	Min ER ∠ in swing p-value	Time to min ER ∠ in swing p-value
<.001	<.01	<.01	<.01	<.01	-	-	<.001

Table 121. Knee INT/EXTL rotation angles, independent of WS, found similar/different to the first hypothesis.

	Similar	Different
Max ER in stance		X
Time to max ER in stance	✓	
Max ER in swing		X
Time to max ER in swing		X
Min ER in stance	✓	
Time to min ER in stance	✓	
Min ER in swing	✓	
Time to min ER in swing	✓	

Independent of speed, the YG had a significantly ($p<.05$) increased mean max ER angle during stance (-22.52°±0.77°) compared to the OG (-17.01°±0.81°), as shown in Table 120. In the previous hypothesis, where the WS effect was tested, there were no significant differences ($p<.05$) for the mean max ER angle during stance between YA and OA (Table 121).

Similar to the results of the stance phase, independent of WS, the YG had a significantly ($p<.05$) increased mean max ER angle during swing (-26.23° ±0.84°) compared to the OG (-22.22°±0.88°), as shown in Table 120. In the previous hypothesis, where the speed effect was tested, there were no significant differences ($p<.05$) for the mean max ER angle during swing between YA and OA (Table 121).

Significant differences in time to mean max ER ($p<.05$) during swing phase were found between YA and OA independent of WS (Figure 87, Table 120). The YG had a significantly longer time to mean max ER angle ($p<.05$) compared to the OG. For the YG, the max ER occurred at 86.15±0.88 percent GC, whereas the OG demonstrated max ER angles at 82.78±0.92 percent GC. This result was found different as the previous hypothesis, where the speed effect was tested (Table 121), as the YG had exhibited a shorter time to mean max ER during swing as WS increased from typical to fast speed.

4.2.14 Summary of Knee Kinetics and Kinematics Results

The present study found significant differences for knee moment and knee power between YA and OA independent of WS. The results found for this second hypothesis, where the WS effect was being controlled, did vary compared to when analyses examined the age-related differences between YA and OA as a function of speed (Section 4.1). Independent of speed, the mean min FLEX moment in stance and swing phase were found significantly different between YA and OA. The significant differences for the mean min FLEX moment in swing were not found in the previous hypothesis, where the speed effect was tested. The mean max EXT moment in stance and swing were also found significantly different between YA and OA. Further, the mean max CNC power of the knee in stance was found significantly different between age groups. These two different results mentioned above were also found for the previous hypothesis, where the WS effect was tested. Thus, when the WS effect is being controlled, significant differences in knee kinetics are still being found between YA and OA.

Significant differences for the knee joint angle in the sagittal and transverse plane were also found between age groups independent of WS. Similar to the previous hypothesis, where the speed effect was tested, the mean min FLEX angle of the knee in stance and swing were found significantly different between YA and OA. In addition, the mean max FLEX angle of the knee in stance was also found significantly different between age groups. For the transverse plane, more results were found when the speed was controlled. The mean min ER of the knee in stance and swing were found significantly different between YA and OA. Further, the mean max ER of the knee in stance was found

significantly different between age groups. Thus, when the speed effect is being controlled, significant differences in knee kinematics are still being found between YA and OA.

4.2.15 Age-related Differences in Hip Kinetics and Kinematics Independent of Speed

4.2.15.1 Age-related Differences in Hip Moment Independent of Speed

The mean moment for the hip in the sagittal plane was presented in Figure 89 (see Section 4.1.15.1). The following section focuses on between-group differences. Table 122 presents the significant age-related differences in the mean max and min FLEX/EXT moments in stance and swing phase as well as their respective time of occurrence as a percentage of GC, independent of WS. Table 123 presents the significant age-related differences in the hip moment independent of WS that were found in comparison to the findings in the first hypothesis, where the speed effect was tested.

Table 122. Significant p-values of the mean max FLEX/EXT moments ((N·m)/kg) of the hip during stance and swing phase, as well as their respective time of occurrence in the gait cycle independent of WS.

Max flexion moment in stance p-value	Time to max flexion moment in stance p-value	Max flexion moment in swing p-value	Time to max flexion moment in swing p-value	Max extension moment in stance p-value	Time to max extension moment in stance p-value	Max extension moment in swing p-value	Time to max extension moment in swing p-value
<.001	<.001	<.01	<.001	<.001	<.01	<.05	<.001

Table 123. Hip FLEX/EXT moments, independent of WS, found similar/different to the first hypothesis.

	Similar	Different
Max flexion moment in stance	✓	
Time to max flexion moment in stance	✓	
Max flexion moment in swing	✓	
Time to max flexion moment in swing	✓	
Max extension moment in stance	✓	
Time to max extension moment in stance	✓	
Max extension moment in swing	✓	
Time to max extension moment in swing	✓	

4.2.15.2 Age-related Differences in Hip Power Independent of Speed

The mean power for the hip in the sagittal plane was presented in Figure 94 (see Section 4.1.15.2). The following section focuses on between-group differences. Table 124 presents the significant age-related differences in the mean max and min flexion-extension powers in stance and swing phase as well as their respective time of occurrence as a percentage of GC. Table 125 presents the significant age-related differences in the hip power independent of WS that were found in comparison to the findings in the first hypothesis, where the speed effect was tested.

Table 124. Significant p-values of the mean min and max eccentric and concentric power (W/Kg) of the hip during stance and swing phase, as well as their respective time of occurrence in the gait cycle independent of WS.

Min ECC power in stance p-value	Time to min ECC power in stance p-value	Min ECC power in swing p-value	Time to min ECC power in swing p-value	Max CNC power in stance p-value	Time to max CNC power in stance p-value	Max CNC power in swing p-value	Time to max CNC power in swing p-value
<.01	-	-	<.001	<.01	<.01	<.001	<.001

Table 125. Hip concentric-eccentric FLEX/EXT power, independent of WS, found similar/different to the first hypothesis.

	Similar	Different
Min ECC power in stance	✓	
Time to min ECC power in stance		X
Min ECC power in swing	✓	
Time to min ECC power in swing	✓	
Max CNC power in stance		X
Time to max CNC power in stance	✓	
Max CNC power in swing		X
Time to max CNC power in swing	✓	

Significant differences in time to mean min ECC power ($p<.05$) during stance phase were found between YA and OA independent of WS (Figure 94, Table 124). The YG had a significantly shorter time to mean min ECC power ($p<.05$) compared to the OG. For the YG, the min ECC power occurred at 28.44±1.14 percent GC, whereas the OG

demonstrated min ECC power at 29.51±1.19 percent GC. In the previous hypothesis, where the speed effect was tested, there were no significant differences ($p<.05$) for the time to mean min ECC power of the hip during stance between YA and OA (Table 125).

Independent of speed, the YG had a significantly ($p<.05$) decreased mean max CNC power during stance (1.22±0.08 $\frac{W}{Kg}$) compared to the OG (1.41±0.08$\frac{W}{Kg}$), as shown in Table 124. In the previous hypothesis, where the speed effect was tested, there were no significant differences ($p<.05$) for the mean max CNC power during stance between YA and OA (Table 128). Similarly, independent of WS, the YG had a significantly ($p<.05$) decreased mean max CNC power during swing (-0.12±8.12 $\frac{W}{Kg}$) compared to the OG (14.91±8.51$\frac{W}{Kg}$), as shown in Table 124. In the previous hypothesis, where the speed effect was tested, there were no significant differences ($p<.05$) for the mean max CNC power during swing between YA and OA (Table 125).

4.2.15.3 Age-related Differences in Hip Angles Independent of Speed

The mean relative angle for the hip segment in the sagittal plane was presented in Figure 96 (see Section 4.1.15.3). The following section focuses on between-group differences. Table 126 presents the significant age-related differences in the mean max and min FLEXT/EXT angles in stance and swing phase as well as their respective time of occurrence as a percentage of GC. Table 127 presents the significant age-related differences in the hip FLEX/EXT angles independent of WS that were found in comparison to the findings in the first hypothesis, where the WS effect was tested.

Table 126. Significant p-values of the mean min and max FLEX/EXT angles (∠) of the hip during stance and swing phase, as well as their respective time of occurrence in the gait cycle independent of WS.

Max extension ∠ in stance p-value	Time to max extension ∠ in stance p-value	Min flexion ∠ in swing p-value	Time to min flexion ∠ in swing p-value	Max flexion ∠ in stance p-value	Time to max flexion ∠ in stance p-value	Max flexion ∠ in swing p-value	Time to max flexion ∠ in swing p-value
<.001	<.001	<.001	<.001	<.001	-	<.001	<.001

Table 127. Hip FLEX/EXT angles, independent of WS, found similar/different to the first hypothesis.

	Similar	Different
Max extension in stance	✓	
Time to max extension in stance	✓	
Min flexion in swing	✓	
Time to min flexion in swing	✓	
Max flexion in stance	✓	
Time to max flexion in stance		X
Max flexion in swing	✓	
Time to max flexion in swing	✓	

No significant differences in time to mean max FLEX ($p<.05$) during stance phase were found between YA and OA independent of WS (Figure 96, Table 126). In the previous hypothesis, there were significant differences ($p<.05$) for the time to mean max hip FLEX during stance between YA and OA (Table 127).

The mean relative angle for the hip segment in the frontal plane was presented in Figure 101 (see Section 4.1.15.3). The following section focuses on between-group differences. Table 128 presents the significant age-related differences in the mean max and min ADD/ABD angles in stance and swing phase as well as their respective time of occurrence as a percentage of GC, independent of WS. Table 129 presents the significant age-related differences in the hip ADD/ABD angles independent of WS that were found in comparison to the findings in the first hypothesis, where the speed effect was tested.

Table 128. Significant p-values of the mean max ADD/ABD angles (∠) of the hip during stance and swing phase, as well as their respective time of occurrence in the gait cycle independent of WS.

Max ABD ∠ in stance p-value	Time to max ABD ∠ in stance p-value	Max ABD ∠ in swing p-value	Time to max ABD ∠ in swing p-value	Max ADD ∠ in stance p-value	Time to max ADD ∠ in stance p-value	Max ADD ∠ in swing p-value	Time to max ADD ∠ in swing p-value
<.001	-	<.001	<.001	-	<.001	-	-

Table 129. Hip ADD/ABD angles, independent of WS, found similar/different to the first hypothesis.

	Similar	Different
Max ABD in stance	✓	
Time to max ABD in stance		X
Max ABD in swing	✓	
Time to max ABD in swing	✓	
Max ADD in stance	✓	
Time to max ADD in stance	✓	
Max ADD in swing	✓	
Time to max ADD in swing	✓	

No significant differences in time to mean min ABD ($p<.05$) during stance phase were found between YA and OA independent of WS (Figure 101, Table 128). In the previous hypothesis, where the speed effect was tested, there were significant differences ($p<.05$) for the time to mean max hip ABD during stance between YA and OA (Table 129).

The mean relative angle for the hip segment in the transverse plane was presented in Figure 104 (see Section 4.1.15.3). The following section focuses on between-group differences. Table 130 presents the significant age-related differences in the mean max and min INT/EXTL rotation angles in stance and swing phase as well as their respective time of occurrence as a percentage of GC, independent of WS. Table 131 presents the significant age-related differences in the hip INT/EXTL rotation angles independent of WS that were found in comparison to the findings in the first hypothesis, where the speed effect was tested.

Table 130. Significant p-values of the mean max INT/EXTL rotation angles (∠) of the hip during stance and swing phase, as well as their respective time of occurrence in the gait cycle independent of WS.

Max ER ∠ in stance p-value	Time to max ER ∠ in stance p-value	Max ER ∠ in swing p-value	Time to max ER ∠ in swing p-value	Max internal rotation ∠ in stance p-value	Time to max internal rotation ∠ in stance p-value	Max internal rotation ∠ in swing p-value	Time to max internal rotation ∠ in swing p-value
<.001	-	-	<.001	<.001	<.05	-	-

Table 131. Hip INT/EXTL rotation angles, independent of WS, found similar/different to the first hypothesis.

	Similar	Different
Max ER in stance	✓	
Time to max ER in stance		X
Max ER in swing	✓	
Time to max ER in swing	✓	
Max internal rotation in stance	✓	
Time to max internal rotation in stance		X
Max internal rotation in swing	✓	
Time to max internal rotation in swing		X

No significant differences in time to mean max ER ($p<.05$) during stance phase were found between YA and OA independent of WS (Figure 104, Table 130). In the previous hypothesis, where the speed effect was tested, there were significant differences ($p<.05$) for the time to mean max hip ER during stance between YA and OA (Table 131).

Significant differences in time to mean max IR ($p<.05$) during stance phase were found between YA and OA independent of WS (Figure 104, Table 130). The YG had a significantly shorter time to mean max IR angle ($p<.05$) compared to the OG. For the YG, the max IR occurred at 39.08±1.30 percent GC, whereas the OG demonstrated max IR angles at 40.13±1.36 percent GC. In the previous hypothesis, where the speed effect was tested, there were no significant differences ($p<.05$) for the time to mean max IR during stance between YA and OA (Table 131).

No significant differences in time to mean max IR ($p<.05$) during swing phase were found between YA and OA independent of WS (Figure 104, Table 130). In the previous hypothesis, where the speed effect was tested, there were significant differences ($p<.05$) for the time to mean max IR during swing between YA and OA (Table 131).

4.2.16 Summary of Hip Kinetics and Kinematics Results

The present study found significant differences for hip moment and hip power between YA and OA independent of WS. The results found for this second hypothesis, were similar compared to when analyses examined the age-related differences between YA and OA as a function of speed (Section 4.1). The only exception was for the mean max CNC power of the hip in stance and swing that was found significantly different between age groups when controlling for speed. A similar result was for the significant difference of the mean max FLEX moment in stance and swing, as well as the mean max EXT moment in stance and swing, between YA and OA. In addition, the mean max CNC power of the hip in stance and swing was found significantly different between age groups independent of WS. Thus, when the WS effect is being controlled, significant differences in hip kinetics are still being found between YA and OA.

Significant differences for the hip joint angle in the sagittal, frontal, and transverse plane were also found between age groups independent of WS. The results found in this second hypothesis, where the speed effect was being controlled, did not vary compared to the previous hypothesis where the speed effect was tested. Independent of speed, the mean min EXT angle of the hip in stance and swing phase were found significantly different between YA and OA. The mean max FLEX hip angle was also found significantly different in stance and swing phase between age groups when controlling for speed. Independent of

speed, the mean min ABD hip angle was found significantly different in stance and swing phase between YA and OA. Further, the mean min and max ER angles in stance phase were found significantly different between age groups when controlling for speed. Thus, when the speed effect is being controlled, significant differences in hip kinematics are still being found between YA and OA.

4.2.17 Age-related Differences in Pelvic Kinematics Independent of Speed

The mean relative angle for the pelvic segment in the sagittal plane was presented in Figure 107 (see Section 4.1.17). The following section focuses on between-group differences. Table 132 presents the significant age-related differences in the mean max and min ANT/POST tilt angles in stance and swing phase as well as their respective time of occurrence as a percentage of GC, independent of WS. Table 133 presents the significant age-related differences in the pelvic ANT/POST tilt angles independent of WS that were found in comparison to the findings in the first hypothesis, where the WS effect was tested. No significant differences in time to mean max ANT tilt ($p<.05$) during stance phase were found between YA and OA independent of WS (Table 132). In the previous hypothesis, where the speed effect was tested, there were significant differences ($p<.05$) for the time to mean max ANT tilt during stance between YA and OA (Table 133).

Table 132. Significant p-values of the mean min and max ANT/POST tilt angles (∠) of the pelvis during stance and swing phase, as well as their respective time of occurrence in the gait cycle independent of WS.

Min anterior tilt ∠ in stance p-value	Time to min anterior tilt ∠ in stance p-value	Min anterior tilt ∠ in swing p-value	Time to min anterior tilt ∠ in swing p-value	Max anterior tilt ∠ in stance p-value	Time to max anterior tilt ∠ in stance p-value	Max anterior tilt ∠ in swing p-value	Time to max anterior tilt ∠ in swing p-value
<.001	-	<.001	-	<.01	-	<.05	-

Table 133. Pelvic ANT/POST tilt angles, independent of WS, found similar/different to the first hypothesis.

	Similar	Different
Min anterior tilt in stance	✓	
Time to min anterior tilt in stance	✓	
Min anterior tilt in swing	✓	
Time to min anterior tilt in swing	✓	
Max anterior tilt in stance	✓	
Time to max anterior tilt in stance		X
Max anterior tilt in swing	✓	
Time to max anterior tilt in swing	✓	

The mean relative angle for the pelvic segment in the frontal plane was presented in Figure 112 (see Section 4.1.17). The following section focuses on between-group differences. Table 134 presents the significant age-related differences in the mean max and min UP/DOWN tilt angles in stance and swing phase as well as their respective time of occurrence as a percentage of GC. Table 135 presents the significant age-related differences in the mean UP/DOWN pelvic angles independent of WS that were found in comparison to the findings in the first hypothesis, where the speed effect was tested. It should be noted that the significant results for the mean max and min pelvic UP-DOWN obliquity angle as well as their respective time of occurrence in the gait cycle as a function of speed were also found when controlling for speed (Table 135).

Table 134. Significant p-values of the mean max UP/DOWN obliquity angles (∠) of the pelvis during stance and swing phase, as well as their respective time of occurrence in the gait cycle independent of WS.

Max DOWN obliquity ∠ in stance p-value	Time to max DOWN obliquity ∠ in stance p-value	Max DOWN obliquity ∠ in swing p-value	Time to max DOWN obliquity ∠ in swing p-value	Max UP obliquity ∠ in stance p-value	Time to max UP obliquity ∠ in stance p-value	Max UP obliquity ∠ in swing p-value	Time to max UP obliquity ∠ in swing p-value
<.001	-	<.001	<.001	<.001	<.001	<.01	<.001

Table 135. Pelvic UP/DOWN obliquity angles, independent of WS, found similar/different to the first hypothesis.

	Similar	Different
Max DOWN obliquity in stance	✓	
Time to max DOWN obliquity in stance	✓	
Max DOWN obliquity in swing	✓	
Time to max DOWN obliquity in swing	✓	
Max UP obliquity in stance	✓	
Time to max UP obliquity in stance	✓	
Max UP obliquity in swing	✓	
Time to max UP obliquity in swing	✓	

4.2.18 Summary of Pelvic Kinematics Results

Significant differences for the pelvic joint angle in the sagittal and frontal plane were also found between age groups independent of WS. The results found for this second hypothesis, where the speed effect was being controlled, were similar compared to when analyses examined the age-related differences between YA and OA as a function of speed (Section 4.1). The only exception was for the mean max UP obliquity pelvic angle in stance that was found significantly different between age groups when controlling for speed. Similar to the previous hypothesis, independent of WS, the mean min and max ANT tilt of the pelvis in stance and swing were found significantly different between YA and OA. The mean min DOWN obliquity pelvic angle in stance and swing were also found significantly different between age groups when controlling for speed. Further, the mean max UP obliquity pelvic angle in swing was found significantly different between YA and OA independent of WS. Thus, when the speed effect is being controlled, significant differences in pelvic kinematics are still being found between YA and OA.

4.2.19 Age-related Differences in Torso Kinematics Independent of Speed

The mean relative angle for the torso segment in the sagittal plane was presented in Figure 117 (see Section 4.1.19). The following section focuses on between-group

differences. Table 136 presents the significant age-related differences in the mean max and min ANT/POST tilt angles in stance and swing phase as well as their respective time of occurrence as a percentage of GC.

Table 136. Significant p-values of the mean min and max ANT/POST tilt angles (∠) of the torso during stance and swing phase, as well as their respective time of occurrence in the gait cycle independent of WS.

Max POST tilt ∠ in stance p-value	Time to max POST tilt ∠ in stance p-value	Max POST tilt ∠ in swing p-value	Time to max POST tilt ∠ in swing p-value	Min POST tilt ∠ in stance p-value	Time to min POST tilt ∠ in stance p-value	Min POST tilt ∠ in swing p-value	Time to min POST tilt ∠ in swing p-value
<.001	-	<.001	<.001	<.001	-	<.001	-

Table 137 presents the significant age-related differences in the mean pelvic ANT/POST tilt angles independent of WS that were found in comparison to the findings in the first hypothesis, where the speed effect was tested. It should be noted that the significant results for the mean max and min anterior-POST tilt angles of the torso as well as their respective time of occurrence in the gait cycle as a function of speed were also found when controlling for speed (Table 137).

Table 137. Torso ANT/POST tilt angles, independent of WS, found similar/different to the first hypothesis.

	Similar	Different
Max POST tilt in stance	✓	
Time to max POST tilt in stance	✓	
Max POST tilt in swing	✓	
Time to max POST tilt in swing	✓	
Min POST tilt in stance	✓	
Time to min POST tilt in stance	✓	
Min POST tilt in swing	✓	
Time to min POST tilt in swing	✓	

The mean relative angle for the torso segment in the frontal plane was presented in Figure 122 (see Section 4.1.19). The following section focuses on between-group differences. Table 138 presents the significant age-related differences in the mean max and

min IPSI/CONTRA lean angles in stance and swing phase as well as their respective time of occurrence as a percentage of GC. Table 139 presents the significant age-related differences in the mean torso IPSI/CONTRA lean angles independent of WS that were found in comparison to the findings in the first hypothesis, where the speed effect was tested. It should be noted that the significant results for the mean max and min ipsilateral-contralateral lean angles of the torso as well as their respective time of occurrence in the gait cycle as a function of speed were also found when controlling for speed (Table 139).

Table 138. Significant p-values of the mean max IPSI/CONTRA lean angles (∠) of the torso during stance and swing phase, as well as their respective time of occurrence in the gait cycle independent of WS.

Max CONTRA torso lean ∠ in stance p-value	Time to max CONTRA torso lean ∠ in stance p-value	Max CONTRA torso lean ∠ in swing p-value	Time to max CONTRA torso lean ∠ in swing p-value	Max IPSI torso lean ∠ in stance p-value	Time to max IPSI torso lean ∠ in stance p-value	Max IPSI torso lean ∠ in swing p-value	Time to max IPSI torso lean ∠ in swing p-value
<.001	-	<.001	<.001	<.001	<.05	<.05	-

Table 139. Torso IPSI/CONTRA lean angles, independent of WS, found similar/different to the first hypothesis.

	Similar	Different
Max CONTRA torso lean in stance	✓	
Time to max CONTRA torso lean in stance		X
Max CONTRA torso lean in swing	✓	
Time to max CONTRA torso lean in swing	✓	
Max IPSI torso lean in stance	✓	
Time to max IPSI torso lean in stance	✓	
Max IPSI torso lean in swing	✓	
Time to max IPSI torso lean in swing		X

4.2.20 Summary of Torso Kinematics Results

Significant differences for the torso joint angle in the sagittal and frontal plane were also found between age groups independent of WS. The results found for this second hypothesis, where the speed effect was being controlled, did not vary compared to when analyses examined the age-related differences between YA and OA as a function of speed

(Section 4.1). Independent of speed, the mean min and max POST tilt of the pelvis in stance and swing were found significantly different between YA and OA. The mean min contralateral lean angle of the torso in stance and swing were also found significantly different between age groups when controlling for speed. Further, the mean max ipsilateral lean angle of the torso in stance and swing were found significantly different between YA and OA independent of WS. Thus, when the speed effect is being controlled, significant differences in torso kinematics are still being found between YA and OA.

4.2.21 Age-related Differences in Ground Reaction Forces Independent of Speed

The mean ground reaction force (GRF) in the sagittal plane was presented in Figure 127 (see Section 4.1.21). The following section focuses on between-group differences. Table 140 presents the significant age-related differences in the mean max and min A/P forces in stance and swing phase as well as their respective time of occurrence as a percentage of GC, independent of WS. Table 141 presents the significant age-related differences in the antero-posterior GRFs independent of WS that were found in comparison to the findings in the first hypothesis.

Table 140. Significant p-values of the mean min and max antero-posterior ground reaction forces (%Body Weight) during stance and swing phase, as well as their respective time of occurrence in the gait cycle independent of WS.

Min A/P GRF p-value	Time to min A/P GRF p-value	Max A/P GRF p-value	Time to max A/P GRF p-value
-	<.01	<.001	<.05

Table 141. Antero-posterior GRFs, independent of WS, found similar/different to the first hypothesis.

	Similar	Different
Min A/P GRF	✓	
Time to min A/P GRF	✓	
Max A/P GRF	✓	
Time to max A/P GRF		X

Significant differences in time to mean max A/P GRF ($p<.05$) during stance phase were found between YA and OA independent of WS (Figure 127, Table 140). The YG had a significantly longer time to mean max A/P GRF angle ($p<.05$) compared to the OG. For the YG, the max A/P GRF occurred at 14.24±1.68 percent GC, whereas the OG demonstrated max A/P GRF angles at 11.00±1.76 percent GC. In the previous hypothesis, where the speed effect was tested, there were no significant differences ($p<.05$) for the time to mean max A/P GRF during stance between YA and OA (Table 141).

Significant differences for the mean ground reaction force (GRF) in the frontal plane were found between YA and OA independent of WS. This is the medial-lateral (M/L) force defined by the shear force exerted from the ground in the Y-axis direction. It should be noted that for the previous hypothesis, where the speed effect was tested, there were no significant differences found for the mean GRF in the frontal plane. The following section focuses on between-group differences. Table 142 presents the significant age-related differences in the mean max and min M/L forces in stance and swing phase as well as their respective time of occurrence as a percentage of GC, independent of WS. Table 143 presents the significant age-related differences in the medial-lateral GRFs independent of WS that were found in comparison to the findings in the first hypothesis, where the speed effect was tested.

Table 142. Significant p-values of the mean min and max medial-lateral ground reaction forces (%Body Weight) during stance and swing phase, as well as their respective time of occurrence in the gait cycle independent of WS.

Min M/L GRF p-value	Time to min M/L GRF p-value	Max M/L GRF p-value	Time to max M/L GRF p-value
<.001	<.001	<.001	<.001

Table 143. Medial-lateral GRFs, independent of WS, found similar/different to the first hypothesis.

	Similar	Different
Min M/L GRF		X
Time to min M/L GRF		X
Max M/L GRF		X
Time to max M/L GRF		X

Independent of speed, the YG had a significantly ($p<.05$) increased mean min M/L GRF during stance (-0.18°±0.01°) compared to the OG (-0.15°±0.01°), as shown in Table 142. Significant differences in time to mean min M/L GRF ($p<.05$) during stance phase were found between YA and OA independent of WS (Table 142). The YG had a significantly shorter time to mean min M/L GRF force ($p<.05$) compared to the OG. For the YG, the min M/L GRF occurred at 10.23±0.32 percent GC, whereas the OG demonstrated min M/L GRF force at 11.83±0.34 percent GC.

Independent of speed, the YG had a significantly ($p<.05$) increased mean max M/L GRF during stance (0.20°±0.52°) compared to the OG (0.15°±0.55°), as shown in Table 142. Significant differences in time to mean max M/L GRF ($p<.05$) during stance phase were found between YA and OA independent of WS (Table 142). The YG had a significantly shorter time to mean max M/L GRF force ($p<.05$) compared to the OG. For the YG, the max M/L GRF occurred at 49.56±0.68 percent GC, whereas the OG demonstrated max M/L GRF force at 52.63±0.72 percent GC.

The mean ground reaction force (GRF) in the transverse plane was presented in Figure 129 (see Section 4.1.21). The following section focuses on between-group differences. Table 144 presents the significant age-related differences in the mean max and min vertical forces in stance and swing phase as well as their respective time of occurrence as a percentage of GC, independent of WS. Table 145 presents the significant age-related

differences in the vertical GRFs independent of WS that were found in comparison to the findings in the first hypothesis.

Table 144. Significant p-values of the mean min and max vertical ground reaction forces (%Body Weight) during stance and swing phase, as well as their respective time of occurrence in the gait cycle independent of WS.

Min Vertical GRF p-value	Time to min Vertical GRF p-value	Max Vertical GRF p-value	Time to max Vertical GRF p-value
<.001	<.001	<.05	-

Table 145. Vertical GRFs, independent of WS, found similar/different to the first hypothesis.

	Similar	Different
Min Vertical GRF	✓	
Time to min Vertical GRF	✓	
Max Vertical GRF	✓	
Time to max Vertical GRF		X

Opposite to the previous hypothesis, no significant differences in time to mean max vertical GRF ($p<.05$) during stance phase were found between YA and OA independent of WS (Table 144).

4.2.22 Summary of Ground Reaction Forces Results

Significant differences for the ground reaction forces (GRFs) in the three planes were found between age groups independent of WS. The results from the A/P GRF found for this second hypothesis, where the speed effect was being controlled, did not vary compared to when analyses examined the age-related differences between YA and OA as a function of speed (Section 4.1), except for the time to mean max A/P GRF. Further, significant differences in the M/L GRFs were found between YA and OA independent of WS. This result was found different as the first hypothesis where the speed effect was tested, as there were no significant differences found in the M/L GRFs between age groups. Another different result was found in the vertical GRFs, where no significant differences

in time to mean max vertical GRF during stance phase were found between YA and OA independent of WS. Thus, when the speed effect is being controlled, significant differences in GRFs are still being found between YA and OA.

4.3 Age-related Differences in MSF and Lower Extremity Kinematic and Kinetic Variables as a Function of Foot Structure and Mobility Independent of Speed

The third purpose of the study was to investigate the relationship between age-related changes in foot kinematics/kinetics and foot structure and mobility. Therefore, it was hypothesized that, independent of WS, there would be significant differences in MSF and lower extremity kinematic and kinetic variables (e.g. ROM of the ankle joint, midfoot and metatarsophalangeal joints, vertical ground reaction force, step length, etc.) between age groups as a function of foot structure and mobility.

4.3.1 Age, Foot Type and Foot Mobility Differences in Relative Angles Between the Foot and Shank Independent of Speed

Independent of speed, significant age-related differences in the mean relative angle for the foot-shank in the frontal plane were found between YA and OA as a function of foot structure and mobility. It should be noted that for the previous hypothesis, where the age differences independent of WS were tested, there were significant differences found for the mean relative angles for the foot-shank in the frontal plane as well. The following section focuses on between-group differences.

Independent of speed, the YG, with mobile feet and rectus foot (RF) type, had a significantly ($p<.05$) decreased mean min EVE angle during stance (-8.82°±1.60°) compared to the OG with mobile feet and RF type (1.33°±2.80°). Similarly, independent of WS, the YG with mobile feet and RF type, had a significantly ($p<.05$) decreased mean

min EVE angle during swing (4.42°±3.99°) compared to the OG with mobile feet and RF type (-10.16°±1.80°).

4.3.2 Age, Foot Type and Foot Mobility Differences in Relative Angles Between the Calcaneus and Forefoot Independent of Speed

Independent of speed, significant age-related differences in the mean relative angle for the cal-met in the sagittal plane were found between YA and OA as a function of foot structure and mobility. It should be noted that for the previous hypothesis, where the age differences independent of WS were tested, there were significant differences found for the mean relative angles for the cal-met in the frontal plane as well. The following section focuses on between-group differences.

Independent of speed, the YG, with mobile feet and planus foot (PLF) type, had a significantly ($p<.05$) decreased mean max cal-met PF angle during stance (-47.50°±6.97°) compared to the OG with mobile feet and PLF type (-61.62°±5.69°). Similarly, independent of WS, the YG with mobile feet and PLF type, had a significantly ($p<.05$) decreased mean max cal-met PF angle during swing (-48.53°±6.71°) compared to the OG with mobile feet and PLF type (-62.40°±6.63°). Significant differences in time to mean max PF angle ($p<.05$) during swing phase were found between YA and OA independent of WS, as a function of foot structure and mobility. The YG had a shorter time to mean max PF angle ($p<.05$) compared to the OG. For the YG, the max PF angle occurred at 61.93±0.82 percent GC, whereas the OG showed max PF angle at 94.84±2.42 percent GC.

Independent of speed, significant differences for the mean relative angle for the cal-met in the frontal plane were found between YA and OA as a function of foot structure and mobility. It should be noted that for the previous hypothesis, where the age differences

independent of WS were tested, there were significant differences found for the mean relative angles for the cal-met in the transverse plane as well. The following section focuses on between-group differences.

Independent of speed, the YG, with mobile feet and RF type, had a significantly ($p<.05$) decreased mean min ADD angle during stance (-7.59°±2.33°) compared to the OG with mobile feet and RF type (9.21°±4.58°).

4.3.3 Age, Foot Type and Foot Mobility Differences in Planar Angles of the Foot Independent of Speed

4.3.3.1 Age, Foot Type and Foot Mobility Differences in the F2Pt Planar Angle of the Foot Independent of Speed

Independent of speed, significant differences for the mean relative F2Pt planar angle were found between younger and older adult as a function of foot structure and mobility. It should be noted that for the previous hypothesis, where the age differences independent of WS were tested, there were significant differences found for the mean relative angles for the F2Pt planar angle as well. The following section focuses on between-group differences.

Independent of speed, the YG, with mobile feet and RF type, had a significantly ($p<.05$) increased mean min F2Pt angle (-109.95°±75.47°) compared to the OG with mobile feet and RF type (-30.81°±31.74°). Significant differences in time to mean min F2Pt angle ($p<.05$) were found between YA and OA independent of WS, as a function of foot structure and mobility. The YG had a significantly longer time to mean min F2Pt angle ($p<.05$) compared to the OG. For the YG, the min F2Pt angle occurred at 59.04±1.33 percent GC, whereas the OG demonstrated min F2Pt angle at 46.49±26.29 percent GC.

4.3.3.2 Age, Foot Type and Foot Mobility Differences in the MLA Planar Angle of the Foot Independent of Speed

Independent of speed, significant differences for the mean relative MLA planar angle were found between YA and OA as a function of foot structure and mobility. It should be noted that for the previous hypothesis, where the age differences independent of WS were tested, there were significant differences found for the mean relative angles for the MLA planar angle as well. The following section focuses on between-group differences.

Independent of speed, the YG, with mobile feet and RF type, had a significantly ($p<.05$) decreased mean min MLA angle (153.70°±0.97°) compared to the OG with mobile feet and RF type (171.97°±3.37°). Similarly, independent of WS, the YG with mobile feet and RF type, had a significantly ($p<.05$) decreased mean max MLA angle (176.01°±2.32°) compared to the OG with mobile feet and RF type (191.47°±3.32°).

4.4 Summary of MSF Kinematics and Planar Angles Results

Independent of speed, the present study found significant differences for MSF angles between YA and OA as a function of foot structure and mobility. The results found for this third hypothesis varied compared to when analyses examined the age-related differences between YA and OA as a function of speed and independent of WS (Section 4.1 and 4.2). The differences found between YA and OA as a function of foot structure and mobility were only for the MSF kinematics and planar angles of the foot. The main differences were between YA and OA, with mobile feet and RF type. Thus, when the foot structure and mobility effect are being considered, there are only a few significant differences in MSF kinematics and planar angles between YA and OA independent of WS.

5.0 Discussion

The present study aimed to examine the differences in MSF and lower extremity kinematic and kinetic variables between YA and OA: (1) as a function of speed, (2) independent of WS, and (3) as a function of foot structure and mobility. The results for the first hypothesis showed significant ($p<.05$) age-related differences in MSF and lower extremity kinematic and kinetic variables between YA and OA, especially for the midfoot segment, suggesting that speed significantly influences foot and lower limb kinematics and kinetics. However, when controlling for speed, significant ($p<.05$) age-related differences in MSF kinematics and lower limb kinetics and kinematics were still found. These differences, independent of WS, suggest that OA exhibit unique characteristics of MSF and lower limb biomechanics. The results of the third hypothesis showed only a few significant ($p<.05$) age-related differences in MSF kinematics as a function of foot structure and mobility and independent of WS. Findings in the present study indicated that planus and RF type have a distinct pattern of motion and that age-related differences exist.

5.1 Differences in MSF and Lower Extremity Kinematic and Kinetic Variables Between Age Groups as a Function of Speed

5.1.1 Temporospatial Variables

In the present study, the OG had a significantly ($p<.05$) increased cadence compared to YA, as WS increased from slow to VF speed. Previous research has observed increased cadence in OA compared to YA as WS increased (DeVita & Hortobagyi, 2000; Hollman et al., 2011). It has been previously suggested that increased cadence is directly associated with increased joint torque and power (DeVita & Hortobagyi, 2000; Winter, 1983a; Winter, 1983b). Winter (1983) showed that an increased cadence seems to be the

result from increased power levels. However, although cadence, power and torque increase simultaneously, cadence appeared to be an effect, not the cause. Thus, the increased cadence in the present study may be related to the significant increases in hip and knee joint moment and power for the OG (see Section 5.1.4 and 5.1.5).

In the present study, the OG showed a significantly ($p<.05$) decreased mean stride length across all speeds similar to previous research (Arnold et al., 2014; DeVita & Hortobagyi, 2000; Hollman et al., 2011; Lee et al., 2007; Lockhart et al., 2003; Menz et al., 2003; Nagano et al., 2013; Samson et al., 2001; Schrager et al., 2008). A reduction in mean stride length is strongly associated with a slower WS in OA (Alcock et al., 2013; DeVita & Hortobagyi, 2000). Possible mechanisms that may explain a reduced stride length include muscle weakness (McGibbon et al., 2001), balance impairments (Wolfson et al., 1995), and reduction of energy cost (Holt et al., 1995). Further, it has been observed that OA control the vertical center of mass (COM) movement during gait by using shorter strides (Malatesta et al., 2003). However, the main reason for a reduced stride length in the OG may be related to the reduced hip extension (Kerrigan et al., 2001) that was found in the present study. In addition, the shorter stride itself may be performed as a compensation for poor balance (See Section 5.1.5). Moreover, in 2015, Gimmon et al. suggested that shorter strides reduce shock attenuation and energy absorbed at the ankle, knee, and hip joint. In the present study, only a reduction in energy absorption in stance phase at the hip joint was found (See Section 5.1.5).

The mean single leg support time was significantly ($p<.05$) decreased for the OG compared to the YG across all speeds in the present study. Likewise, Arnold et al. (2014) reported that OA had decreased single leg support time at a slow speed walking compared

to YA. However, discrepancies with other previous research exist. Herssens et al. (2018) and Begg and Sparrow (2006) found that OA had a greater single support time compared to YA. Further, McGibbon et al. (1999) did not observe significant differences in single leg support time, however, researchers were controlling for height and weight. Throughout single leg support (i.e., approximately 40% of gait cycle) the body is known to be in a state of "instability" (Francois et al., 1997). A reduction in single leg support time may represent an age-induced gait adaptation, where the OA increase stability by reducing the amount of time spent on one limb only (Alcock et al., 2013) as WS increases.

The reduction in mean single leg support time is related to the significant ($p<.05$) increase in mean double leg support time and significant ($p<.05$) increased time to toe off (i.e., stance time) found for the OG across speeds in the present study. Similarly, previous research has reported increased double leg support time and time to toe off (Aboutorabi et al., 2016; Arnold et al., 2014; Begg & Sparrow, 2006; Herssens et al., 2018; Winter, 1991). Double leg support time is known as the period of stability (Prince et al., 1997) during gait as both limbs are weightbearing. An increased time to toe off suggests that OA tried to have both feet in contact with the ground for a longer time than the YA before swing phase started. Therefore, a significant increased double leg support time and time to toe off in the OG indicate that they are adapting their gait pattern, increasing stability, and avoiding the risk of fall while speed increases. Further, muscle weakness has also been associated with increased cadence and increased double leg support time (Aboutorabi et al., 2016).

The OG also showed a significantly ($p<.05$) shorter mean step length for the VS, slow, and fast WSs in the present study. It has been previously reported that OA have a reduced step length compared to YA (Kirkwood et al., 2011). However, Silder et al. (2008)

did not find significant differences in step length between YA and OA. A reduced mean step length is related to the increased mean double leg support time as it also suggests the adoption of a more stabilized gait pattern. The increased time spent in mean double support time and shorter mean step length for the OG could be considered as influencing factors for the OA to walk slower (Menz et al., 2003). Loss of muscle strength and associated force production are reflected in changes such as reduced step length (Kirkwood et al., 2011). Furthermore, white matter atrophy and hippocampal atrophy has been associated with a decline in step length (Callisaya et al., 2013).

In the present study, the OG showed a significantly ($p<.05$) increased mean cycle time for the fast and VF speeds compared to YA, indicating that when WS increased to fast and VF, they were walking slower than the YG. In fact, for the fast speed, the OG walked at 1.58 $\frac{m}{s}$ whereas the YG walked at 1.59 $\frac{m}{s}$. For the VF speed, the OG walked at 1.99 $\frac{m}{s}$ whereas the YG walked at 2.01 $\frac{m}{s}$. It has been previously reported that WS declines with age (Aboutorabi et al., 2016). However, Van Hoeve et al. (2017) reported a mean fast WS of 1.57 $\frac{m}{s}$ for the YG and 1.63 $\frac{m}{s}$ for the OG, indicating that the OG was walking faster. Changes in WS with aging may be explained by a compensation for muscle weakness and balance impairments (Aboutorabi et al., 2016). In summary, the OG displayed a tendency to walk slower, with a longer stance time and keeping both feet in contact with the ground for a longer period than the YG.

5.1.2 Ankle Kinetics and Kinematics

In the present study, the OG showed significantly ($p<.05$) decreased mean maximum ankle PF moment in the sagittal plane in stance when compared to YA for the

VS, typical, fast, and VF WS. Further, the OG showed significantly ($p<.05$) decreased mean maximum concentric ankle power during stance for the fast and VF speeds.

Previous research has reported decreased peak ankle PF moments in OA (Alcock et al., 2013; DeVita & Hortobagyi, 2000; Judge et al., 1996). Studies varied in terms of age and sex of participants, range of WSs tested and mechanical models of foot. Alcock et al. (2013) studied MSF kinematics during walking at a self-selected speed in healthy female OA only (60-83 years old, 71.5±7 years old). Furthermore, DeVita and Hortobagyi (2000) studied older female and male participants with different age ranges (young: 21.6±2.7 years old; old: 69±6.5 years old), walking at a fast and self-selected speed only and using a more simplistic single foot model. In addition, Judge et al. (1996) also used a single foot model and collected data from older female and male participants with different age ranges (young: 18-42 years, 26±3.7 years old; old: 70-90 years, 79±6 years old. They asked their participants to walk at a typical and fast speed only. In the present study, there were two age groups with different age ranges (young: 18-35 years, 23.6±3.7 years old; old: 65-87 years, 71.6±6 years old), and a broader range of speeds was studied. Examining a broader range of WSs helps identify age-related changes from speed-mediated effects thus slower speeds should also be examined. Moreover, a broader range of WS is needed to provide speed-matched data when evaluating a patient (Grant & Chester, 2015).

Previous research has also reported decreased mean maximum concentric ankle power during stance. Studies varied in terms of mechanical model (Cofré et al., 2011; Judge et al., 1996; Kerrigan et al., 1998; Monaco et al., 2009) and method (Lanza et al., 2003). Interestingly, McGibbon and Krebs (1999) did not find significant differences in concentric ankle power between YA and OA, however, they controlled for center of gravity velocity.

McGibbon and Krebs (1999) also suggested that decreased ankle plantarflexor power in stance is a factor associated with functional limitations beyond those of normal aging and stated that their lack of significance was probably due to their participants being more fit than participants in past research studies besides controlling for center of gravity velocity.

In Figure 71 (See Section 4.1.11.2), the YA and OA exhibited comparable levels of ankle CNC power at the VS, slow and typical WSs during push-off. However, as speed increased to fast and VF, the gap in power generated at push-off between age groups was significantly different, where the YG demonstrated greater ankle power during push-off (fast: 4.41±1.18 $\frac{W}{Kg}$; VF: 5.10±1.61 $\frac{W}{Kg}$) compared to the OG (fast: 3.41±0.99 $\frac{W}{Kg}$; VF: 3.57±1.17 $\frac{W}{Kg}$). This is in agreement with previous research that have reported that OA may be unable to produce sufficient ankle power during push-off, specifically at faster WS (Judge et al., 1996; Kerrigan et al., 1998). The reduction in power generation for the OG found in the present study indicates a decrease in the energy generated through concentric muscle activity to propel the body forward as WS increases, showing again an impairment of the overall propulsive capacity, especially at faster WSs. Reduced concentric ankle power and reduced PF moment may be a function of dynamic stiffness, as a consequence of intrinsic muscle or soft tissue changes in the ankle plantarflexors, or co-contraction in the antagonistic ankle dorsiflexors, that restrains the development of rapid ankle plantar flexion (Kerrigan et al., 1998). Moreover, it has been recognized that plantar flexors provide crucial propulsive energy during push-off, thus, the significant ($p<.05$) reduction in PF moments found in the present study may impair the overall propulsive capacity of the leg during forward progression in OA (Alcock et al., 2013). In addition, it has been

suggested that a reduced ankle power in OA is correlated to their decline in gait speed (Bassey et al., 1988; Bassey et al., 1992).

Deteriorations in muscle strength could provoke changes in lower extremity joint kinetics and kinematics (Aboutorabi et al., 2016). It has been observed that ankle plantar flexors have greater physiological and biomechanical deficits in contrast with other muscle groups in OA compared with YA (DeVita & Hortobagyi, 2000) due to different reasons such as a decline in maximal voluntary isometric force (Christ et al., 1992), decline in citrate synthase activity in the gastrocnemius (Houmard et al., 1998) and reductions in type IIa and IIb fiber areas and lower mitochondrial enzyme activity in gastrocnemius of OA compared with YA (Coggan et al., 1992). This suggests a functional decline with age that may be compensated by efforts at the hip (See Section 5.1.5).

In the present study, WS significantly affected the ankle joint kinematics in the sagittal and transverse planes similar to previous research (Dubbeldam et al., 2010). In the present study, the OG exhibited a significantly ($p<.05$) decreased mean maximum ankle PF angle and a significantly ($p<.05$) decreased mean maximum ankle DF angle in stance as WS increased from VS to typical speed. In 2006, Begg and Sparrow also showed significant ($p<.05$) decreased ankle PF angle but using a single foot model. It is plausible that ankle PF and DF angles are purposefully decreased to maintain greater foot-floor contact to extend the support base (Kerrigan et al., 1998).

The OG also exhibited a significantly ($p<.05$) decreased mean maximum ankle PF in swing as WS increased from VS to typical speed, as well as a significantly ($p<.05$) decreased mean maximum ankle DF in swing across all speeds. These results suggest a reduced foot clearance as WS increases, (i.e., foot's height from the ground was decreased

during the swing phase). These findings agree with previous studies that have reported a decreased foot clearance due to reduced ankle DF (Alcock et al., 2013). A reduced foot clearance can lead to tripping, causing the person to fall. Both mechanisms in stance and swing indicate a strategy that the OG may adapt to reduce the risk of falling.

In the present study, the OG showed significantly ($p<.05$) less ADD motion of the ankle in the transverse plane during stance and swing across speeds and exhibited a significantly ($p<.05$) smaller ADD/ABD ROM in the transverse plane during stance as WS increased from VS to fast WS. Previous research has not reported information comparing younger and older adult's transverse ankle motion, thus, results in the present study represent a novel contribution to the field. Reporting only sagittal data can be deceiving as it does not reflect the complex multi-segmental motion that occurs in the ankle and foot during walking. Overall, MSF motion data in the frontal and transverse plane is scarce (Pol et al., 2021). In the present study there were no significant differences in the PF/DF ROM in the sagittal plane of the ankle between age groups. Similarly, Legault-Moore et al. (2012) and Van Hoeve et al. (2017) did not find significant differences in the ankle PF/DF ROM between YA and OA. Conversely, previous research using single segment foot models reported reduced ankle PF ROM (Boyer et al., 2012; Judge et al., 1996; Kerrigan et al., 1998).

5.1.3 Multisegment Foot Kinematics

5.1.3.1 Shank-Calcaneus

The relative angles of the foot with respect to the tibia (shank-foot) showed similar results to that of the calcaneus relative to the tibia (sha-cal). This was expected as they share a common articulation with the calcaneus and tibia. The similarities included the

mean minimum and maximum relative angles in the sagittal and transverse plane (i.e. DF/PF and ADD/ABD respectively). However, the OG exhibited a significant ($p<.05$) reduced DF/PF ROM in the sagittal plane for the sha-cal in swing for the slow speed only, whereas no significant differences were found in the DF/PF ROM for the ankle angle. Further, the OG exhibited a significantly ($p<.05$) reduced ADD/ABD ROM in the transverse plane for the sha-cal in stance and swing for the VS speed only. The ADD/ABD ROM of the shank-foot angle was also found significantly ($p<.05$) different between age groups in stance and swing for the VS speed (See Section 5.1.2).

Previous research has not reported information comparing younger and older adult's DF/PF ROM in swing phase thus direct comparison with other studies cannot be made. Nonetheless, Vandervoort et al. (1992) observed a decreased DF/PF ROM at the ankle joint in OA during non-weight bearing tasks. This reduction may occur due to the influence of stiffening of soft tissues that provide passive joint constraint (Prince et al., 1997). The decreased ADD/ABD ROM may contribute to impaired performance in weight-bearing activities such as walking (Menz et al., 2015).

5.1.3.2 Midfoot-Calcaneus

Significant differences ($p<.05$) in the mid-cal segment between YA and OA were found in the sagittal, frontal, and transverse plane as a function of speed. In the sagittal plane, the OG exhibited a significantly ($p<.05$) reduced mean peak DF angle during swing phase for the VS speed only. Further, the OG displayed significantly ($p<.05$) less eversion (EVE) in the frontal plane and significantly ($p<.05$) less adduction (ADD) motion in the transverse plane during stance and swing across speeds. The only study that has previously studied the midfoot angular motion in YA and OA at different WSs was conducted by

Arnold et al. (2014). However, researchers reported that there were no significant ($p<.05$) differences in the angular position of the mid-cal joint in stance in any plane between YA and OA at self-selected and slow WS. Further, in the present study, the OG displayed a significantly ($p<.05$) smaller DF/PF ROM in the sagittal plane of the mid-cal angle during stance and swing across all WSs. This finding is in agreement with previous research that observed a decreased DF/PF ROM of the mid-cal joint in stance at both preferred and slow WSs for OA (Arnold et al., 2014).

In the frontal plane, the EVE/INV ROM of the mid-cal angle was significantly ($p<.05$) smaller during stance across all speeds, and during swing for the VS, slow, and VF WSs. In addition, OA showed smaller ADD/ABD ROM in the transverse plane throughout stance and swing across speeds albeit there was not statistical significance. Arnold et al. (2014) reported no significant differences in the frontal and transverse ROM of the mid-cal angle in stance between YA and OA. The ROM results found in the present study in the three planes exhibit reduced mobility of the mid-cal angle in the OG.

A reduced ROM in the joints of the foot and ankle is strongly associated with impaired balance and functional ability in older people (Menz et al., 2005; Spink et al., 2011). Moreover, reduced ROM in the calcaneus and midfoot may affect the extent to which plantar loads can be attenuated (Menz et al., 2014). A previous study conducted by Giacomozzi et al. (2014) reported that the ROM at the ankle, rearfoot and midfoot when walking was inversely correlated with peak pressure at the corresponding plantar regions i.e., individuals with less foot joint mobility produce significantly greater plantar loads. Therefore, since OA exhibited less foot joint mobility in the present study, it can be suggested that they also generate larger plantar loads.

The reduced DF and reduced EVE of the mid-cal found in the present study could suggest a trend towards a less pronated dynamic foot position for the OA during walking across speeds (See Section 5.1.3.3). This could be linked to the rotation of the hip as it has been observed that the lower limb IR and rearfoot EVE are relatively interdependent and simultaneous (Snyder et al., 2009; Souza et al., 2010), i.e., this link may represent a functional adaptation from the OA. In the present study the OG showed reduced mean maximum hip IR in stance across all speeds (See Section 5.1.5). It has been reported that soft tissues of the hip that resist IR may resist foot pronation indirectly (Souza et al., 2014). Thus, it is possible that the reduced hip IR in the OG across all WSs is associated with the reduced mid-cal EVE angle in the OG across all speeds. Conversely, in 2013, Min-Chi et al. and Hagerdon et al. (2013) stated that OA tend to have a more dynamically pronated foot. However, both studies used a plantar pressure measurement system and participants were asked to walk at their preferred WS only.

It should be noted that most studies using an MSF model did not study the midfoot segment and compared its angular motion between YA and OA at different WSs, thus the age-related changes found in the present study for the midfoot represent an important contribution to the literature. The midfoot segment is often excluded due to a lack of clinical interest, a reduced number, quality and location of available cameras of the stereophotogrammetric system, difficulty of tracking markers (e.g. the navicular and cuboid markers) and probability of marker merging in a relatively small segment (especially in children's feet). Further, some researchers have excluded the midfoot segment as they deteremined it does not play an important role in the overall foot function (Ouzounian & Shereff, 1989), hence, violate the rigid body assumption. This violation may

lead researchers to oversight important biomechanical data between segments or attribute motion to one joint when in fact it is occuring at another (Nester et al., 2010). However, the data presented in our study shows that the midfoot contributes to the mechanics of the foot and should be included in relevant foot kinematic studies.

Currently, the midfoot segment is tracked by only a few mechanical models (Leardini et al., 2007; MacWilliams et al., 2003; Portinaro et al., 2014; Rouhani et al., 2011). Moreover, in vivo and in vitro studies have shown that significant and consistent rotations occur in typical feet at the Chopart and Lisfranc joints (Leardini et al., 2007; Lundgren et al., 2008; Maurer et al., 2013; Ouzounian & Shereff, 1989; Rao et al., 2009). These studies have demonstrated that the motion of the midfoot during gait is significant and should be studied (Leardini & Caravaggi, 2016). In 2015, De Ridder et al. (2015) studied chronic ankle instability and compared results from a single model foot and an MSF model. They showed important deviations in kinematics at the midfoot, which simply could not be detected with a rigid single model of the foot (Leardini & Caravaggi, 2016). Dixon et al. (2012) reported significant differences between two different foot models and exhibited that the model excluding the midfoot segment overestimated the power of the ankle by about 40% and neglected the important midfoot loading (Leardini & Caravaggi, 2016). Including the midfoot segment in mechanical model provides important evidence about its role in overall foot function. Further, there are pathologic conditions and surgical procedures that involve this area, such as midfoot arthritis and midfoot break, yet its effect on foot motion remains unclear (Ouzounian & Shereff, 1989).

5.1.3.3 Midfoot-Forefoot

In the present study, significant ($p<.05$) differences in the mid-met segment between YA and OA were found in the sagittal and transverse plane as a function of speed. In the sagittal plane, the OG displayed significantly ($p<.05$) increased mean minimum and maximum mid-met PF angles in stance and swing across speeds and significantly ($p<.05$) increased DF/PF ROM in the sagittal plane in stance as WS increased from VS to fast speed. However, the OG exhibited a significantly ($p<.05$) decreased DF/PF ROM for the VF speed in stance and across all speeds in swing. Nonetheless, it should be noted that only the difference in DF/PF ROM in the sagittal plane during swing for the VS speed was significant. In the frontal plane, the OG exhibited a significantly ($p<.05$) increased INV of the segment during stance and swing across speeds. However, this difference did not reach statistical significance.

In the transverse plane, the OG exhibited significantly ($p<.05$) reduced mean minimum and maximum mid-met ABD angles during stance and swing across all speeds. However, the OG displayed a significantly ($p<.05$) increased ADD/ABD ROM in the transverse plane for the VS speed in stance. As previously mentioned in Section 5.1.3.2, most studies using an MSF model excluded the midfoot segment, except for Arnold et al. (2014). Thus, direct comparison in the mid-met results with other studies is challenging. Arnold et al. (2014) reported that there were no significant differences in the angular position of the mid-met joint in stance in any plane, as well as no significant differences in the sagittal and transverse ROM between YA and OA at self-selected and slow speed (Arnold et al., 2014). Previous research has observed a decreased EVE/INV ROM in the frontal plane of the mid-met joint in stance at both preferred and slow WSs for OA (Arnold

et al., 2014) whereas in the present study there were no significant differences in the EVE/INV ROM between age groups.

The reduced mid-met ABD, increased INV and increased PF in stance and swing across all speeds for the OG further indicates a less pronated dynamic foot position (See Section 5.1.3.2). When this occurs, the midfoot is considered hypomobile, compromising the ability of the foot to adapt to the terrain and increasing the demand on surrounding structures to retain postural stability and balance (Cote et al., 2005). This suggests a functional decline for the older adults' feet in their ability to adapt to the terrain. Moreover, Marcial et al. (2021) conducted a study comparing the foot mobility magnitude (FMM) between YA and OA using a three-dimensional (3D) scanner. The FMM is a measure of the mobility of the midfoot (McPoil et al., 2009). Although researchers found a lack of statistical significance, OA exhibited a lower FMM, suggesting less mobility of the midfoot. A reduction in midfoot and forefoot mobility suggests increased stiffness for the OG, which may be explained by changes in plantar tissues (Menz et al., 2014). The plantar soft tissues attenuate the shear forces applied when walking. With advancing age, the metatarsal pads maintain their thickness but exhibit greater stiffness, dissipate more energy when compressed and are slower to recover after load is removed (Hsu et al., 2005; Kwan et al., 2010).

5.1.3.4 Calcaneus-Forefoot

In the present study, the OG displayed significantly ($p<.05$) increased mean maximum PF angles in stance and swing for the typical and fast speeds and increased mean minimum PF angle in stance and swing across speeds during push-off. An increase in cal-met PF angle in the sagittal plane was expected as the metatarsals rotate towards PF to

activate the windlass mechanism. This mechanism helps to achieve stronger propulsion to move the body forward during walking, thus it is possible the OG attempted to effectively propel their body forward by achieving greater PF of the cal-met.

The significantly ($p<.05$) increased cal-met PF in the OG may suggest a compensation for the decreased mean ankle PF moments (see Section 5.1.2), decreased mean maximum F2Ps angle and increased mean minimum and maximum MLA angles (see Section 5.1.3.5). However, previous research reported that there were no significant differences in the ROM of the hindfoot-forefoot in stance in any plane between YA and OA at slow and fast speed (Van Hoeve et al., 2017). Study varied in terms of mechanical MSF model, speed, and age of participants. Van Hoeve et al. (2017) used the OFM, thus, used different definitions for the hindfoot (calcaneus) and forefoot segment. "Mechanical models are simple representations of complex systems" (Nordin & Frankel, 2001). These mechanical models are limited by the assumptions that must be made to simplify the system under consideration (Nordin & Frankel, 2001) and by the clinical interest (Leardini & Caravaggi, 2016). Nonetheless, it becomes challenging to compare results when the definitions of each segment vary. Further, Van Hoeve et al. (2017) also collected only typical, slow and fast WSs. In addition, there were two age groups with different age ranges (young: 20-24 years, 22.4±1.3 years old; old: 53-65 years, 57.5±3.9 years old). In the present study, the model used was the RFM. In addition, a broader range of WSs was collected (VS, slow, typical, fast and VF). Moreover, there were two age groups with different age ranges (young: 18-35 years, 23.6±3.7 years old; old: 65-87 years, 71.6±6 years old).

The YG exhibited a greater DF/PF and EVE/INV cal-met ROM, in the sagittal and frontal plane respectively, in stance and swing across all speeds. Further, the OG displayed significantly ($p<.05$) less EVE motion of the cal-met during stance and swing as WS increased from slow to fast speed. Although Van Hoeve et al. (2017) did not find statistical significance, OA in their study also exhibited less EVE motion in the frontal plane of the cal-met. When the calcaneus is everted, there is increased forefoot motion (Blackwood et al., 2005). This occurs when the midtarsal locking mechanism is activated, allowing the foot to be flexible and adjust to the surface during heel strike. Later in the gait cycle, due to this mechanism, the foot acts as a rigid lever to propel the weight of the body forward. Thus, if the OG displayed less EVE motion in the frontal plane during stance, it suggests a lesser activation of the midtarsal locking mechanism. Hence, the foot becomes less flexible, affecting its adjustment to the surface. This again suggests a functional decline for the OA in their ability to adapt to the terrain (See Section 5.1.3.3). As previously mentioned, a reduction in foot mobility suggests increased stiffness for the OG, which may be explained by changes in plantar tissues (Menz et al., 2014). Similar to the metatarsal pads (See Section 5.1.3.3), the heel pad preserves its thickness with age, but becomes stiffer (Hsu et al., 1998; Kwan et al., 2010). An increase in stiffness of the heel pad is usually associated to a decreased echogenicity of the plantar fascia (Menz et al., 2014). This may indicate a physiological aging process of the plantar fascia or a secondary effect of the deficiency of heel-pad elasticity (Cheng et al., 2014). The physiological change of the plantar fascia with age may also affect the windlass mechanism activation on the foot (See Section 5.1.3.5).

Differences in the MSF angles between YA and OA could also be explained by a magnitude offset. The offset observed may have a larger effect in balance problems

compared to the ROM. The ankle DF and PF angles are most likely reduced in the elderly to maintain greater foot-floor contact to broaden the base of support and therefore have more stability and balance. Also the reduction in the mid-cal motion that the OG exhibited might be related to the reduced DF of the 1st MTPJ and a reduced medial longitudinal arch, affecting the windlass mechanism, thus affecting their propulsion during push off. Further, differences in the temporospatial variables could explain the offset in the time to minimum and maximum peak angles such as decreased single leg support, increased time to toe off and increased double support time, indicating that they are adapting their gait pattern to increase stability, hence improve balance.

In the present study, anatomical offsets could explain the differences in the dynamic data. During data collection, an anatomical standing position is usually recorded to provide reference orientations of the lower limb and foot segments. This neutral orientation can be used as offset and it has the advantage of eliminating the bias associated to the anatomical frame definitions. Therefore, it allows to focus the analysis on the dynamic pattern of the joint rotations. However, this approach eliminates any misalignments due to bone and/or joint deformity, which are usually included in the clinical evidence and thus it is not recommended to remove from the analysis (Leardini & Caravaggi, 2016). “The choice of offsetting joint rotations by using a neutral posture is thus related to the specific study and should take into consideration, for example, if there’s any ongoing treatment to correct a foot deformity” (Leardini & Caravaggi, 2016). Although the participants recruited in the present study were healthy adults, the anatomical offsets were not used in the study. Thus, the magnitude differences found in the present study represent extremely valuable information and indicate age-related differences in foot kinematics.

5.1.3.5 Planar Angles

Unlike most studies using an MSF model, planar angles of the foot between YA and OA at different WSs were examined in the present study. Thus, the age-related changes found in the present study for the planar angles represent an important contribution to the literature. Due to the scarcity of bony landmarks and the small size of several foot bones, 2D projection angles are also used to measure relative rotations of a joint, with respect to anatomical planes. This technique is used to track motion of the metatarsal bones, as well as the medial longitudinal arch (MLA), and the varus/valgus inclination of the calcaneus (Leardini & Caravaggi, 2016). However, with this approach, erroneous and misleading values can be obtained in particular conditions, e.g., in case of large ROM and in case of large deviations between the line segment and the projection plane. 2D angles are also prone to noise at key events in the gait cycle (e.g. toe-off).

In the present study, only a few planar angles were found significantly different between YA and OA as a function of speed. The F2Pt angle corresponded to the motion in valgus of the 1st metatarsophalangeal joint (MTPJ), in the transverse plane (Leardini et al., 2007). The OG exhibited a significantly ($p<.05$) greater motion in varus of the mean maximum F2Pt angle throughout most of the stance phase for the VF speed. Moreover, the ROM of the 1st MTPJ in the transverse plane for the OA was significantly ($p<.05$) greater across all speeds.

The OG displayed a significantly ($p<.05$) greater mean minimum V2G angle for the fast WS compared to the YG. However, the YG exhibited greater ROM of the V2G angle across all speeds, but this did not reach statistical significance. A trend towards a greater mean minimum and maximum medial longitudinal arch (MLA) angle (suggesting

a more dynamically PLF posture) in the OG across speeds was observed. However, the differences in the mean minimum and maximum MLA angles between age groups did not reach statistical significance. Previous research (Arnold et al., 2014) has reported similar findings for the MLA angle.

Older adults also showed reduced mean maximum F2Ps (i.e., reduced DF of the 1st MTPJ) angle and reduced ROM of the F2Ps angle across speeds, except for the fast speed. Although these latter results were not statistically significant, it could be postulated that the reduced DF of the 1st MTPJ in the OG emphasizes the greater foot-floor contact previously seen by the decreased ankle PF and DF angles in stance (see Section 5.1.2). Similarly, Arnold et al. (2014) reported a reduced sagittal ROM between YA and OA when walking at a preferred WS. The F2Ps and MLA angles play an important role in the midtarsal locking mechanism as they pull the plantar aponeurosis further during walking (Bolgla & Malone, 2004). Thus, the decreased F2Ps and increased MLA angles found in the OG across speeds could indicate that the plantar aponeurosis is not being pulled further (Bolgla & Malone, 2004), thus suggesting again (see Section 5.1.3.4) a lesser activation of the midtarsal locking mechanism (i.e., less rigidity of the foot). Hence, there is a lesser activation of the windlass mechanism. This mechanism contributes to the stiffening of the foot by pulling on the heel to help have a stronger propulsion. Therefore, it is inferred that the older group's propulsion to walk forward is being affected and thus exhibit less propulsion during push off. This further relates to the reduced mean maximum ankle PF moment in stance found in the OG (see Section 5.1.2).

5.1.4 Knee Kinetics and Kinematics

In the present study, the OG had a significantly ($p<.05$) decreased mean maximum concentric knee power throughout stance phase at the VS speed. Further, OA also exhibited significantly ($p<.05$) reduced mean minimum knee FLEX moment in the sagittal plane in stance but for the VS speed. However, during swing for the fast and VF speeds, OA exhibited significantly ($p<.05$) increased mean maximum knee EXT moment and significantly ($p<.05$) increased mean minimum eccentric knee power. Previous research has showed reduced knee concentric powers in stance phase in OA (Cofré et al., 2011; DeVita & Hortobagyi, 2000; Lanza et al., 2003). Studies varied in terms of range of WSs tested, mechanical models of the foot and methods used. Cofré et al. (2011) reported that OA showed reduced knee concentric powers in early stance when walking at typical and fast speeds only. In addition, Lanza et al. (2003) reported decreased knee CNC power for the OG although they collected knee kinetics data using a dynamometer. DeVita & Hortobagyi (2000) reported decreased knee concentric and eccentric power for the OG when walking at a self-selected speed. Conversely, Monaco et al. (2009) reported increased knee CNC power in OA during stance phase despite decreased ankle PF kinetics. However, they used a single foot model and a treadmill to control the gait speeds. Furthermore, Riley et al. (2001) reported decreased knee moments in OA compared to YA when walking at their normal gait speed. Moreover, Riley et al. (2001) reported that at faster WSs, OA significantly increased their knee moment to levels comparable to those of YA. This could indicate that the OG have equivalent maximal strength in the quadriceps to the YG and are capable to use this strength when walking at faster speeds (Kerrigan et al., 1998).

Current literature does not report large differences in knee kinetics and kinematics in OA and inconsistencies remain (Boyer et al., 2017). In fact, only a few significant ($p<.05$) differences in knee kinematics were found in the present study suggesting that differences between YA and OA are scarce.

As WS increased, OA showed significantly ($p<.05$) increased mean minimum and maximum knee FLEX angles in the sagittal plane throughout stance and mean minimum knee FLEX angle during swing phase (See Section 4.2.13.3, Figure 83). The significant ($p<.05$) increased knee FLEX in the OG may suggest a compensation for the reduced mean minimum hip extension found in the present study during pre-swing (See Section 4.1.15.3, Figure 96). An increase in knee FLEX during swing in OA may also suggest a trend towards increasing the foot-ground clearance, compensating for the reduced ankle DF in swing across all speeds (See Section 4.1.3, Figure 1). Conversely, Begg and Sparrow (2006) reported that OA displayed significantly reduced knee FLEX during stance. However, differences between studies remain. Researchers only compared differences at a comfortable WS and recruited participants with different age ranges (young: 28.1±5.6 years, old; 68.8±4.6 years). Nonetheless, increased knee FLEX in the older group in the present study suggests a compensatory mechanism for the reduced hip extension and ankle DF motion.

5.1.5 Hip Kinetics and Kinematics

The OG had significantly ($p<.05$) increased mean maximum EXT moment in the sagittal plane of the hip during initial contact for the slow speed and significantly ($p<.05$) decreased mean minimum FLEX moment in the sagittal plane of the hip during stance for the slow and VS WSs. The reduced mean minimum hip FLEX moment in the OG may be

interpreted as reduced hip extensor activity. However, without EMG this finding cannot be confirmed. Riley et al. (2001) reported decreased hip moments in the OG but subjects where walking at their typical gait speed. Riley et al. (2001) also noted that OA were capable of significantly increase their hip moments when asked to walk faster to levels comparable to those of YA, similar to the knee moment (See Section 5.1.4). Moreover, in the present study, the OG exhibited significantly ($p<.05$) increased mean maximum hip EXT moment during swing phase at the VF speed. The latter has been reported in previous research (Aboutorabi et al., 2016). Further, the OG in the present study had significant ($p<.05$) reduced mean minimum eccentric power of the hip in stance for the VS WS, which indicates a reduced power energy absorption. This reduction in energy absorption may be related to the reduced stride length found in the OG (See Section 5.1.1).

The OG also had significantly ($p<.05$) increased mean maximum CNC power of the hip during stance as WS increased, i.e., increased power generation, although it was not significantly different from the YG. This finding is in agreement with previous studies that reported greater hip power generation in the OG (Boyer et al., 2017; Monaco et al., 2009). Previous research has also observed a redistribution of joint power contributions to forward progression during walking in OA with decreased ankle power and an increased external hip extensor moment and power generation during terminal stance (Arnold et al., 2014; Boyer et al., 2017; DeVita and Hortobagyi, 2000). The redistribution of joint torques and powers in the OG could be interpreted as an alteration in motor performance, and it could represent an adjustment in the motor pattern used to walk (DeVita & Hortobagyi, 2000). Thus, the decreased ankle power and increased hip extensor moment and power generation in stance found in the present study could indicate a ‘pull-off’ rather than ‘push-

off' strategy for walking propulsion in OA, consistent with the reduced sha-cal PF angle noted in the present study (Arnold et al., 2014). Further, it has been previously observed (Alcock et al., 2013; Lewis & Ferris, 2008) that when the functional demands of locomotion cannot be met at the ankle (see Section 5.1.2), possibly because of a reduced capacity in the OG, they are transferred proximally and counteracted by efforts at the hip. Previous research has observed that this transfer represents a motor control strategy and is due to a neuromuscular adaptation (DeVita & Hortobagyi, 2000; Monaco et al., 2009; Silder et al., 2008).

The OG exhibited a significantly ($p<.05$) decreased FLEX/EXT ROM in the sagittal plane of the hip in stance and swing phase compared to the YG. More specifically, the OG showed a significantly ($p<.05$) increased mean maximum FLEX of the hip in the sagittal plane at initial contact for the slow speed, and as the body was moving forward, they showed a significantly ($p<.05$) decreased mean minimum extension of the hip in the sagittal plane during pre-swing for the slow and fast speeds. Previous research studies (Haight, 2012; Lee et al., 2005; Murray et al., 1984) found similar results to the present work for the hip angles in the sagittal plane. Interestingly, it has been previously reported that a reduction in hip extension in the OG at both comfortable and fast speeds is consistent with the prevalence of hip FLEX contractures in the older population at large, which impede the hip from reaching full hyperextension (Kerrigan et al., 1998*)*.

Hip FLEX contractures may occur in OA for different reasons. For example, when the hip remains flexed for a long period of time such as sitting, it will more likely develop FLEX contracture. The only daily activity performed on a regular basis that hyperextends the hip and consequently stretches the hip flexors is gait (Kottke, 1990). Thus, it is plausible

that an overall decline in gait, persistent reduction in step length, and/or lumbosacral postural changes in the older population will cause less frequent stretching of the hip flexors, eventually producing hip flexor tightness and contracture (Kerrigan et al., 1998). Further, it is known that the body compensates for hip FLEX contractures through increased anterior pelvic tilting, decreased step length, and increased knee FLEX (Lee & Kerrigan, 2004). These compensations were found in the present study in the OG and indicate an alteration in the gait posture of OA.

It has been previously postulated as well that a decrease in hip extension range may be the cause of reduced stride length and WS in the OG. Alternatively, a shorter stride length itself may be the initial cause of reduced hip extension, possibly as a compensation for poor balance (Kerrigan et al., 2001). In any case, walking with a decreased stride length would probably generate a hip contracture, as a hip contracture would likely reduce stride length, therefore generating a continuous DOWN spiral of walking disability (Kerrigan et al., 2001).

5.1.6 Pelvic Kinematics

In the present study the OG showed significantly ($p<.05$) increased mean minimum and maximum ANT tilt of the pelvis in the sagittal plane throughout stance and swing for the slow and typical speed. Similarly, previous research has reported increased anterior pelvic tilt in the OG compared to YA at slow, typical and fast speeds (Lee et al., 2005). An increased mean minimum and maximum ANT tilt of the pelvis is related to the observed reduction in mean minimum hip extension in stance. This relation is made because reduced hip extension range causes a shorter maximal contralateral step length. To keep an appropriate step length with reduced hip extension, the body must compensate with

increased anterior pelvic tilt. The pelvis becomes more anteriorly tilted, especially during terminal stance, possibly to reach a slightly longer contralateral step length.

As previously mentioned, less frequent stretching of the hip flexors, eventually may produce hip flexor tightness and contracture (See Section 5.1.5). Hip flexion contractures restrict hip hyperextension beyond a given range, thus, to take a longer step with increased WS, the pelvis must anteriorly tilt further than normal in terminal stance when the hip is maximally hyperextended (Kerrigan et al., 1998). Therefore, due to a reduced extension of the hip, it is plausible that OA adapt their posture with an increased ANT tilt to compensate for reduced hip flexion. This has been previously reported to also occur in the presence of reduced hip flexion ROM (Kerrigan et al., 1998).

An increased anterior pelvic tilt may also be a compensatory attempt to increase the shortened stride length found in the OA. However, this compensation theoretically predisposes to low back pain and postural or spinal deformity (Kottke, 1990; Lee et al., 1997; Shimada, 1996). In addition, postural changes, arising from weakened abdominal and hip muscles, or as a compensation for instability (Woodhull-McNeal, 1992), may also cause the increased anterior pelvic tilt and flexed hip joint in OA (Lee et al., 2005). Nonetheless, Lee et al. (2005) conducted a study comparing dynamical and statical posture between YA and OA and showed that these age-related changes are a dynamic rather than a postural phenomenon.

In the present study, the OG exhibited a significantly ($p<.05$) reduced FLEX/EXT and UP/DOWN obliquity ROM of the pelvis, in the sagittal and frontal plane respectively, in stance and swing across speeds. The OG displayed significantly ($p<.05$) less up and down obliquity motion of the pelvis during stance and swing across speeds. Similarly, Van

Emmerik et al. (2005) reported decreased ROM in the three planes in the OG. Overall decreased pelvic ROM may suggest a joint stiffening caused by the muscles around the pelvic and trunk, therefore, the ROM needed for walking is limited (Gimmon et al., 2005; Woollacott & Shumway-Cook, 1990).

5.1.7 Torso Kinematics

Overall, in the present study, the OG had similar results for the torso angles as the pelvic angles in the sagittal and frontal planes, with a decreased motion of the torso. It has been shown that trunk rotations help compensate for pelvic angular movements (Gimmon et al. 2015). In the sagittal plane, the OG had a significantly ($p<.05$) decreased mean minimum and maximum POST tilt of the trunk in stance and swing for the VS speed. These findings in the sagittal plane agree with previous research (Van Emmerik et al., 2005).

In the frontal plane, the OA had a significantly ($p<.05$) decreased mean minimum contralateral lean angle in stance for the slow, normal, fast, and VF WSs. They also had a significantly ($p<.05$) decreased mean maximum ipsilateral lean angle in the frontal plane in stance for the VS, slow, fast, and VF speeds. In addition, the OG had a significantly ($p<.05$) decreased mean minimum contralateral lean angle for the VS, slow, normal, and fast WSs in swing. Lastly, they also had a significantly ($p<.05$) decreased ipsilateral lean angle in swing for the VF speed only. Similarly, Gimmon et al. (2015) found a decrease in trunk and pelvic motion in OA. More specifically, Gimmon et al. (2015) found a smaller trunk transverse rotation in the OG across different speeds. They suggested that the decreased pelvic rotation found in OA was likely affected by the natural reduction of the lumbar spine mobility that occurs with age and caused a reduction in stride length. Conversely, in the present study there were no significant ($p>.05$) differences between YA

and OA for the transverse trunk rotation. This would indicate that trunk transverse rotation in the OG was similar to the YG, thus there was no reduction of the lumbar spine mobility present in our OG as Gimmon et al. (2015) reported in their study. However, differences between studies should be considered. Gimmon et al. (2015) participant's mean age was different (young: 26.4±0.9 years old; old: +70 years, 80±5.3 years old) compared to the present study, and researchers used a treadmill to control the speed. Thus, comparison between studies is challenging.

Decreased trunk and pelvic motion may alter gait posture and reduce stability in OA. Both mechanisms may represent an adaptation for reduced hip extension ROM and consequently reduced stride length.

5.1.8 Ground Reaction Forces

Significant differences ($p<.05$) in ground reaction forces (GRFs) between age groups as a function of speed were found in the study. The mean minimum and maximum vertical GRFs were found significantly ($p<.05$) decreased in the OG as WS increased. These results were expected as decreased peak vertical forces are related to the tendency of OA to walk slower than YA (Alcock et al., 2013). Previous research has reported that vertical and horizontal GRF are significantly affected by WS (White et al., 1996). Further, in the present study, OA showed significant ($p<.05$) increased mean maximum A/P GRF for the fast and VF speeds. This might suggest that OA attempted to compensate for the decreased ankle PF moment by exerting more A/P force to walk forward as WS increased, thus, showing a more vigorous push-off. Therefore, it is suggested that in the present study WS affected both vertical and A/P GRFs. To our knowledge, previous studies comparing lower limb biomechanics between YA and OA walking at different WSs did not report

GRF data, thus the age-related changes found in the present study for the A/P and vertical GRFs represent an important contribution to the literature.

5.2 Differences in MSF and Lower Extremity Kinematic and Kinetic Variables Between Age Groups Independent of Speed

Most temporospatial, kinematic and kinetic results found in the first hypothesis where the speed effect was tested were also found after controlling for speed (See Section 4.2). However, there were additional results discovered, and they are mentioned below.

5.2.1 Temporospatial Variables Independent of Speed

Independent of speed, there were still significant ($p<.05$) differences in the temporospatial variables between YA and OA. This suggests that the differences in cadence, stride length, double and single support limb, time to toe off, step length and cycle time are not only because of speed but due to age.

5.2.2 MSF Kinematics and Planar Angles Independent of Speed

Regarding the MSF kinematics, differences in the frontal plane of the foot-shank (ankle), sha-cal and mid-met were found. It should be noted that in the first hypothesis, where the speed effect was tested, there were no significant ($p<.05$) differences in the frontal plane for the previously mentioned angles. Further differences found for the OG when controlling for speed include a significantly ($p<.05$) reduced maximum DF of the mid-cal angle in stance and significantly ($p<.05$) reduced minimum and maximum ADD of the sha-cal angle in stance and swing. The OG displayed a similar outcome as the first hypothesis for the rest of the MSF angles. Further, the OG exhibited a significantly ($p<.05$) decreased mean minimum F2G planar angle, suggesting a less DOWN rotation of the first

metatarsal at heel strike. Moreover, the OG displayed a significantly ($p<.05$) increased mean minimum and maximum MLA planar angle in stance.

These aforementioned differences in planar angles were not statically significant when groups walked at five different speeds, suggesting an age rather than speed-related change. Similarly, Arnold et al. (2014) found that OA exhibited reduced mobility of the forefoot, midfoot and calcaneus, suggesting a less propulsive gait pattern. In contrast, Van Hoeve et al. (2017) and Legault-Moore et al. (2012) reported that there was no significant effect of age on foot and ankle kinematics. However, differences between these studies exist. Van Hoeve et al. (2017) used a 4-segment foot model and eliminated the effect of speed by using equal WSs for both groups, whereas we controlled for the speed using the feedback control method and then divided the groups using the percentage method following the Grant and Chester (2015) protocol (See Section 3.4.17). In addition, researchers recruited participants with a different age range (young: 20-24 years, 22.4±1.3 years old; old: 53-65 years, 57.5±3.9 years old), whereas the OG in our study was older. Further, Legault-Moore et al. (2012) only recruited male participants, with different age ranges (young: 18-30 years, 24.6±3 years old; old: +55 years, 65±4.2 years old), and all participants had a minimum shoe size of nine to facilitate marker tracking and autolabeling. Additionally, Legault-Moore et al. (2012) excluded the midfoot segment.

The significant ($p<.05$) differences found between YA and OA (see Section 4.2) in the present study after controlling for speed indicate the existence of unique characteristics of foot kinematics in OA. Most studies using an MSF model did not compare the differences in ankle and MSF between YA and OA while controlling for speed, thus the age-related changes found in the present study for the ankle and MSF biomechanics

represent an important contribution to the literature. It can be difficult to determine whether differences in walking patterns are age-related or simply due to the speed at which the person was walking. Therefore, it is important to control the speed to be able to separate speed-mediated effects from those due to age. The appreciation of age-related effects is critical for increasing our understanding of foot mechanics in YA and OA.

5.2.3 Knee Kinetics and Kinematics Independent of Speed

Independent of speed, the OG also displayed significant ($p<.05$) differences in the sagittal and transverse plane of the knee. These included a significantly ($p<.05$) increased mean minimum FLEX moment in swing, as well as a significantly ($p<.05$) decreased mean maximum EXT moment in stance. A reduction in knee extensor function with age has been previously reported (Abe et al., 2011; Boyer et al., 2017; Lindle et al., 1997) and it has been related with joint degeneration (Segal et al., 2012). In addition, in the present study, the OG exhibited a significantly ($p<.05$) increased mean minimum FLEX angle of the knee in stance and significantly ($p<.05$) reduced mean maximum ER in stance and swing. These findings further support the compensation for reduced hip FLEX and possible contractures (see Section 5.1.5). Thus, it could be inferred that independent of WS, reduced hip motion is an age-related change.

5.2.4 Hip Kinetics and Kinematics Independent of Speed

Independent of speed, we found that OA continued to show a significantly ($p<.05$) increased mean maximum EXT moment of the hip in the sagittal plane in stance as well as a significantly ($p<.05$) reduced mean minimum eccentric hip power and significantly ($p<.05$) increased mean maximum concentric hip power in stance. These changes in hip kinetics after controlling for speed suggest an age-related change and represents a motor

control strategy in OA due to a neuromuscular adaptation (DeVita & Hortobagyi, 2000; Monaco et al., 2009; Silder et al., 2008). In terms of kinematics, the OG displayed a significantly ($p<.05$) increased mean maximum hip flexion in the sagittal plane in stance. The increased mean maximum hip flexion and mean minimum and maximum knee flexion in stance after controlling for speed strongly supports the possibility of hip flexion contractures (Kerrigan et al., 1998) in the OG as previously mentioned in Section 5.1.5. This indicates that the body compensation for hip flexion contractures through increased anterior pelvic tilting, decreased step length, and increased knee flexion occurs because of an age rather than speed-related change, altering the gait pattern of OA.

5.2.5 Ground Reaction Forces

After controlling for speed, the OG exhibited significantly ($p<.05$) reduced mean minimum and maximum M/L GRFs in addition to the significantly ($p<.05$) increased A/P and significantly ($p<.05$) reduced vertical GRFs. In the literature, the medial-lateral (M/L) GRF has been characterized by extreme variability (Munro et al., 1987). It should be noted that in the first hypothesis, where the speed effect was tested, there were no significant differences in the medial-lateral (M/L) GRFs between YA and OA. Further, it is known that vertical forces from the body weight travel DOWN via the tibia and tend to flatten the MLA. Additionally, GRFs travel UP on the metatarsal and the calcaneus bones, which can further reduce the flattening of the MLA because both forces fall posterior and anterior to the tibia (Bolgla and Malone, 2004). In the present study, since the mean minimum and maximum vertical GRFs were found decreased for the OG, it could indicate a flattening of the MLA in OA. This would be consistent with the greater MLA angle (see Section 5.1.3.5) found in the OG. In addition, it has been previously reported that the OA tend to have flatter

feet compared to YA (Frey, 2000; Scott et al., 2007). Thus, it can be inferred that the flattening of the foot arises due to age.

5.3 Differences in MSF and Lower Extremity Kinematic and Kinetic Variables Between Age Groups as a Function of Foot Structure and Mobility and Independent of Speed

The present study provides a novel comparison of MSF and lower extremity biomechanics between YA and OA considering the structure and mobility of the foot. To our knowledge, no single study has examined differences in MSF and lower limb joint kinematics and kinetics as a function of age, speed, and foot. A specific foot type was not targeted for the present study. Nonetheless, static foot structure measurements were used to classify the foot into three different postures (rectus, planus and cavus). After classifying the posture of the foot for both age groups, it was found that differences between YA and OA that exhibited a cavus foot posture did not reach statistical significance. An explanation for the lack of significance could be that most participants were classified either in the rectus or PLF posture. In addition, the mobility of the foot was also classified using static foot measurements into two categories (mobile and rigid foot). It was found that differences between YA and OA that exhibited a rigid foot did not reach statistical significance. Therefore, the results discussed below will correspond to the mobile feet group only.

In the present study, the OG with static PLF posture exhibited a significantly ($p<.05$) greater mean maximum cal-met PF angle in the sagittal plane during stance and swing compared to YA with static PLF posture. In addition, albeit there was not statistical significance, the OG showed greater mean minimum and maximum cal-met ADD angle in the transverse plane in stance. The increased PF and ADD angles of the cal-met could

suggest a more dynamically supinated position during propulsion for the OG. Similarly, Buldt et al. (2015) reported an association between PLF posture and a more supinated position. Conversely, Hillstrom et al. (2013) reported that planus feet generally over-pronate and cavus feet over-supinates.

In the present study, the OG with static RF posture showed a significantly ($p<.05$) increased mean minimum EVE foot-shank angle in the frontal plane during stance and swing compared to YA with static RF posture. This finding may suggest a more dynamically pronated position of the foot for the OG with RF. Moreover, OA with static RF posture displayed a significantly ($p<.05$) increased mean minimum ADD cal-met angle in the transverse plane during stance. In addition, although there was not statistical significance, OA had decreased mean minimum and maximum cal-met PF angle in the sagittal plane in stance and increased mean minimum and maximum cal-met EVE in the frontal plane during stance, suggesting a more pronated position for the OG. Moreover, OA with RF posture exhibited a significantly ($p<.05$) decreased valgus motion of the 1st MTPJ and significantly ($p<.05$) increased mean minimum and maximum MLA angle, indicating that within the RF posture, the OG had a flatter feet compared to YA. The findings mentioned above indicate that planus and rectus feet have a distinct pattern of motion and that age-related differences exist. The lack of statistical significance in the midfoot angle was unexpected since the Foot Mobility Measure (FMM) used to classify the mobility of the foot focuses on changes in midfoot position with and without load applied (weightbearing vs non-weight bearing). Further, to our knowledge, no studies have compared differences in lower limb and MSF biomechanics between YA and OA as a function of foot structure and mobility, thus comparisons are challenging.

A separate research study conducted by Marcial et al. (2021) analyzed anatomical foot structure differences between YA and OA using a 3D foot scanner. The database used was the same as the one presented in this thesis. Static foot measurements were taken while standing (weight bearing) and sitting (non-weight bearing). Results included significantly ($p<.05$) wider rearfoot width for the OG in both weight bearing and non-weight bearing conditions. In addition, albeit there was not statistical significance, OA exhibited longer feet when standing and wider midfoot width when sitting. A secondary test was conducted by Marcial et al. (2021) using the TFL as a covariate. This was done to address reduced foot length, that may result as a function of toe deformities. The results of this second test showed that OA had significantly ($p<.05$) wider forefoot width and midfoot width. Preliminary results based on the sample size of the study provided evidence of anatomical foot differences between YA and OA, more specifically differences in foot size (width and length).

Due to the results mentioned in this section, it can be stated that static and dynamic foot measures are different between age groups. Thus, the magnitude differences found in the present study between YA and OA in MSF kinematics may be due to the anatomical differences mentioned above and represent an age-related change. Further research is needed to analyze differences in static measures obtained from the motion capture system images. In this manner, correlations between static and dynamic anatomical offsets can be determined.

5.4 Limitations of the study

Limitations of the study should be considered. A specific foot type (e.g. planus and cavus feet) was not targeted in the present study, thus, the sample size in each foot type

group was relatively small. This might explain the lack of significant age-related differences in the lower limb kinematics and kinetics as a function of foot structure and mobility. Further, the mechanical model implemented in the study is limited by the defined number of segments and degrees of freedom. In addition, joint kinematics could have been affected by the soft tissue artifact (STA) error caused by the skin mounted markers. Moreover, MSF models using surface mounted markers may not detect subtle changes in MSF kinematics, especially if the motions are small. Furthermore, findings of the study could have been further supported by examining lower limb muscle activity during walking, however, EMG data was not analyzed. Additionally, only minimum and maximum peaks of the waveforms were examined in the present study, thus, it may be likely that some relevant data were neglected.

5.5 Future recommendations

Future studies should examine the effects of static posture on MSF kinematics with an increased sample size of each posture group. Further, changes in MSF kinematics and lower limb biomechanics in YA and OA may be further understood through the examination of EMG data. This would also provide more information about the muscle activity during walking and may further support the findings presented in the study. Thus, research into the walking mechanism in OA is warranted. In addition, the analysis of the entire waveform data is suggested as it may provide more information about the MSF and lower limb biomechanical differences between YA and OA during walking. Moreover, MSF kinematic differences observed between YA and OA could have been affected by the magnitude offset. These offsets were outside the scope of the study but warrant further investigation. Foot modelling analysis is also recommended as it would allow the

implementation of a more complex mechanical model with more and smaller foot segments and more degrees of freedom. This would allow the study of more complex foot motion (e.g. individual tarsometatarsal joint motion) in YA and OA as well as the study of MSF kinetics (e.g. Chopart and Lisfranc joint power). Thus, it may provide a more in depth understanding of the intrinsic motion of the foot.

6.0 Conclusion

This study examined age-related changes in MSF kinematics and lower limb biomechanics in YA and OA (1) as a function of WS, (2) independent of WS and (3) as a function of foot structure and mobility. Findings of the study were mainly an age-related change, altering the gait pattern of OA. Regarding temporospatial variables, OA displayed a tendency to walk slower, with a longer stance time and keeping both feet in contact with the ground for a longer period than the YG in order to improve balance and stability when walking.

Older adults showed reduced foot mobility, particularly in the midfoot. A reduction in midfoot and forefoot mobility suggested increased stiffness for the OG. Further, the midfoot kinematics in the OG indicated a less pronated dynamic foot position. In addition, the reduced hip IR may be linked to the reduced mid-cal eversion angle as soft tissues of the hip that resist IR may resist foot pronation indirectly. A less pronated dynamic foot position may compromise the ability of the foot to adapt to the terrain and increase the demand on surrounding structures to retain postural stability and balance. This is further supported by the lesser activation of the midtarsal locking mechanism found in the OG since the foot becomes less flexible and thus affects its adjustment to the surface.

Consequently, OA showed a lesser activation of the windlass mechanism, affecting their propulsive capacity. Further, decreased ROM in the foot may cause impaired balance and functional ability in OA. Overall, differences in MSF were still found after controlling for speed, demonstrating the existence of unique characteristics of foot kinematics in OA.

Decreased ankle moment and decreased ankle power in the OG may indicate a functional decline, possibly due to muscle weakness from the ankle plantarflexors. However, without EMG or strength testing this finding cannot be confirmed. This functional decline in OA was compensated by efforts at the hip, indicating a motor control strategy due to a neuromuscular adaptation. Further, the reduced ankle kinetics indicated an impaired propulsive capacity during push-off in OA. Results suggest that OA were compensating for the reduced hip ROM by increased knee flexion. They also exhibited a trend towards increasing the foot clearance by increasing knee flexion in swing, compensating for the reduced ankle DF. Nonetheless, age-related changes in knee biomechanics does not seem well understood as inconsistencies between studies remained.

An alteration in the gait posture of OA was also noted by increased anterior pelvic tilting and decreased step length. These adaptations may be a compensation for the reduced hip ROM and consequently reduced stride length. However, this adapted posture may reduce stability in OA. Further, ROM of the pelvis and trunk in the OG was reduced, suggesting joint stiffening and thus limiting the ROM needed for gait.

The inclusion and study of the relationship between age-related changes in foot biomechanics and foot structure and mobility, independent of WS, represents a novel contribution to the field. The findings in the present study indicate that planus and rectus feet have a distinct pattern of motion and that age-related differences exist. Moreover, the

anatomical differences of the foot between YA and OA (e.g. rearfoot and forefoot width) may result in an angular difference between both groups. Thus, the anatomical differences of the foot may explain the angle offsets observed in MSF kinematics. Therefore, the magnitude differences observed represent age-related differences in foot kinematics.

7.0 Significance and Impact of the Study

Despite the important function of the ankle during gait, the mechanics of the foot are poorly understood. This research has improved our understanding of MSF mechanics in YA and OA. Further, by examining a broad range of WSs, age-related and speed-mediated effects were differentiated. The inclusion and study of the relationship between age-related changes in foot biomechanics and foot structure and mobility represents a novel contribution to the field. To our knowledge, no single study has examined MSF and lower limb joint kinematics and kinetics across age, speed and foot structure and mobility. Age-related differences in foot mobility are strongly associated with impaired balance and functional ability in older people (Menz et al., 2005; Spink et al., 2011). Such age-related changes may lead to alterations in foot mechanics, locomotion, and quality of life and warrant further investigation. Other potential benefits of this work include improved design of wearable device technology, including customized footwear, sensor-based insoles, prostheses, orthoses and exoskeletons. Additionally, the data provided can be used as a reference of typical gait parameters to identify atypical gait patterns, e.g., patients with planus and cavus feet, diabetic foot, or after stroke. Hence, the findings may provide guidance to improve gait performance.

Bibliography

Abe, T., Sakamaki, M., Yasuda, T., Bemben, M., Kondo, M., Kawakami, Y., & Fukunaga, T. (2011). Age-related, site-specific muscle loss in 1507 Japanese men and women aged 20 to 95 years. *J Sports Sci Med*, 145-150.

Aboutorabi, A., Arazpour, M., Bahramizadeh, M., Hutchins, S., & Fadayevatan, R. (2016). The effect of aging on gait parameters in able-bodied older subjects: a literature review. *Aging Clinical and Experimental Research*, 393-405.

Amorim, P., Hills, A., & Byrne, N. (2009). Treadmill adaptation and verification of self-selected walking speed: A protocol for children. *Research Quarterly for Exercise and Sport*, 380-385.

Andrews, A., Folger, S., Norbert, S., & Swift, L. (2008). Tests and measures used by specialist physical therapists when examining patients with stroke. *J Neurol Phys Ther*, 122-128.

Arangio, G., Chen, C., & Salathe, E. (1998). Effect of varying arch height with and without the plantar fascia on the mechanical properties of the foot. *Foot Ankle Int.*, 705-709.

Ardestani, M., Ferrigno, C., Moazen, M., & Wimmer, M. (2016). From normal to fast walking: Impact of cadence and stride length on lower extremity joint moments. *Gait & Posture*, 118-125.

Arnold, J., Mackintosh, S., Jones, S., & Thewlis, D. (2014). Differences in foot kinematics between young and older adults during walking. *Gait & Posture*, 689-694.

B, H., J, H., & van Emmerik, R. (2002). Variability of stride characteristics and joint coordination among individuals with unilateral patellofemoral pain. *J Appl Biomech* , 110-121.

Baer, G., & Smith, M. (2001). The recovery of walking ability and subclassification of stroke. *Physiotherapy Research International*, 135-144.

Bassey, E., Bendall, M., & Pearson, M. (1988). Muscle strength in the triceps surae and objectively measured customary walking activity in men and women over 65 years of age. *Clin Sci*, 85-89.

Begg, R., & Sparrow, W. (2006). Ageing effects on knee and ankle joint angles at key events and phases of the gait cycle. *Journal of Medical Engineering & Technology*, 382-389.

Bejek, Z., Paroczai, R., Illyes, A., & Kiss, R. (2006). The influence of walking speed on gait parameters in healthy people and in patients with osteoarthritis. . *Knee Surgery, Sports Traumatology, Arthroscopy*, 612-622.

Bertram, J., & Ruina, A. (2001). Multiple walking speed-frequency relations are predicted by constrained optimization. . *Journal of Theoretical Biology*, 445-453.

Blackwood, C., Yuen, T., Sangeorzan, B., & Ledoux, W. (2005). The midtarsal joint locking mechanism. *Foot Ankle Int.*, 1074-1080.

Bohannon, R. (1997). Comfortable and maximum walking speed of adults aged 20-79 years: reference values and determinants. *Age and Ageing*.

Bohannon, R., & Williams, A. (2011). Normal walking speed: a descriptive meta-analysis. *Physiotherapy*, 182-189.

Bolgla, L., & Malone, T. (2004). Plantar Fasciitis and the Windlass Mechanism: A Biomechanical Link to Clinical Practice. *Journal of Athletic Training*, 77-82.

Boyer, E., Stout, J., Laine, J., Gutknecht, S., Oliveira, L., Munger, M., . . . Novacheck, T. (2017). Evidence of knee extensor dysfunction during sit-to-stand following distal femoral extension osteotomy and patellar tendon advancement in young adults with cerebral palsy: A pilot study. *Gait & Posture*, 527-532.

Boyer, K., Andriacchi, T., & Beaupre, G. (2012). The role of physical activity in changes in walking mechanics with age. *Gait & Posture*, 149-153.

Briggs, P., & Tansey, P. (2001). Active and passive mechanisms in the control of heel supination. *Foot Ankle Surg*, 131-136.

Brown, M., Sinacore, D., & Host, H. (1995). The relationship of strength to function in the older adult. *J Gerontol Med Sci*, 55-59.

Browne, M., & Franz, J. (2017). The independent effects of speed and propulsive force on joint power generation in walking. *Journal of Biomechanics*, 48-55.

Bruening, D., & Takahashi, K. (2018). Partitioning ground reaction forces for multi-segment foot joint kinetics. *Gait & Posture*, 111-116.

Bruening, D., Cooney, K., & Buczek, F. (2012a). Analysis of a kinetic multi-segment foot model. Part I: Model repeatability and kinematic validity. *Gait & Posture*, 529-534.

Bruening, D., Cooney, K., & Buczek, F. (2012b). Analysis of a kinetic multi-segment foot model part II: Kinetics and clinical implications. *Gait & Posture*, 535-540.

Buldt, A., Murley, G., Levinger, P., Menz, H., Nester, C., & Landorf, K. (2015). Are clinical measures of foot posture and mobility associated with foot kinematics when walking? *Journal of Foot and Ankle Research* , 1-12.

Callisaya, M., Beare, R., Phan, T., Blizzard, L., Thrift, A., Chen, J., & Srikanth, V. (2013). Longitudinal associations of white matter lesions, brain infarcts and brain atrophy on gait decline–a population-based study. *International Journal of Stroke*.

Cappozzo, A., Della Croce, U., Leardini, A., & Chiari, L. (2005). Human movement analysis using stereophotogrammetry:Part 1: theoretical background. . *Gait & Posture*, 186-196.

Caravaggi, P., Giazomozzi, C., Lullini, G., Marchesini, G., Baccolini, L., Ortolani, M., . . . Leardini, A. (2021). The Effect of Neuropathy and Diabetes Type on Multisegment Foot Kinematics: A Cohort Study on 70 Participants with Diabetes. *Applied Sciences*, 1-15.

Caravaggi, P., Leardini, A., & Crompton, R. (2010). Kinematic correlates of walking cadence in the foot. *Journal of Biomechanics*, 2425-2433.

Caravaggi, P., Pataky, T., Goulermas, J., Savage, R., & Crompton, R. (2009). A dynamic model of the windlass mechanism of the foot: evidence for early stance phase preloading of the plantar aponeurosis. *The Journal of Experimental Biology*, 2491-2499.

Carson, M., Harrington, M., Thompson, N., O'Connor, J., & Theologis, T. (2001). Kinematic analysis of a multi-segment foot model for research and clinical applications: a repeatability analysis. *Journal of Biomechanics*, 1299-1307.

Cesari, M., Kritchevsky, S., Penninx, B., Nicklas, B., Simonsick, E., Newman, A., . . . Pahor, M. (2005). Prognostic Value of Usual Gait Speed in Well-Functioning Older People. Results from the Health, Aging and Body Composition Study. *Journal of the American Geriatrics Society*, 1675-1680.

Chang, M., Shaikh, S., & Chau, T. (2009). Effect of treadmill walking on the stride interval dynamics of human gait. *Gait & Posture*, 431-435.

Chang, R., Van Emmerik, R., & Hamill, J. (2008). Quantifying rearfoot–forefoot coordination in human walking. *Journal of Biomechanics*, 3101-3105.

Chehab, E., Andriacchi, T., & Favre, J. (2017). Speed, age, sex, and body mass index provide a rigorous basis for comparing the kinematic and kinetic profiles of the lower extremity during walking. *Journal of Biomechanics*, 11-20.

Chen, I., Kuo, K., & Andriacchi, T. (1997). The influence of walking speed on mechanical joint power during gait. *Gait & Posture*, 171-176.

Cheng, J., Tsai, W., & Yu, T. (2014). Gender-Related Effect of Aging on the Sonographic Appearance of Plantar Fascia. *Journal of Musculoskeletal Pain*, 33-37.

Christ, C., Boileau, R., Slaughter, M., Stillman, R., Cameron, J., & Massey, B. (1992). Maximal voluntary isometric force production characteristics ofsix muscle groups in women aged 25 to 74 years. *Am J Hum Biol*, 537-545.

Coggan, A., Spina, R., King, D., Rogers, M., Brown, M., Nemeth, P., & Holloszy, J. (1992). Histochemical and enzymatic comparison of the gastrocnemius muscle of young and elderly men and women. *J Gerontol*, B71–B76.

Cornwall, M., & McPoil, T. (2011). Relationship between static foot posture and foot mobility. *Journal of Foot and Ankle Research*, 1-9.

Cote, K., Brunet, M., Gansneder, B., & Shultz, S. (2005). Effects of Pronated and Supinated Foot Postures on Static and Dynamic Postural Stability. *Journal of Athletic Training*, 41-46.

Crenna, P., & Frigo, C. (2011). Dynamics of the ankle joint analyzed through moment-angle loops during human walking: gender and age effects. *Human Mov Sci*, 1185-1198.

Davis, R., Õunpuu, S., Tyburski, D., & Gage, J. (1991). A gait analysis data collection and reduction technique. *Human Movement Science*, 575-587.

De Ridder, R., Willems, T., Vanrenterghem, J., Robinson, M., Palmans, T., & Roosen, P. (2015). Multi-segment foot landing kinematics in subjects with chronic ankle instability. *Clinical Biomechanics*, 585-592.

DeLeo, A., Dierks, T., Ferber, R., & Davis, I. (2004). Lower extremity joint coupling during running: a current update. *Clinical Biomechanics*, 983-991.

Den Otter, A., Geurts, A., Mulder, T., & Duysens, J. (2004). Speed related changes in muscle activity from normal to very slow walking speeds. *Gait & Posture*, 270-278.

Deschamps, K., Eerdekens, M., Desmet, D., Matricali, G. A., Wuite, S., & Staes, F. (2017). Estimation of foot joint kinetics in three and four segment foot models using an existing proportionality scheme: Application in paediatric barefoot walking. *Journal of Biomechanics*, 168-175.

DeVita, P., & Hortobagyi, T. (2000). Age causes a redistribution of joint torques and powers during gait. *J Appl Physiol*, 1804-1811.

DiMarco, R., Rossi, S., Racic, V., Cappa, P., & Mazzà, C. (2015a). A comparison between four foot model protocols: the effect of walking on a treadmill. *XXV congress of the international society of biomechanics.* Glasgow.

DiMarco, R., Rossi, S., Racic, V., Cappa, P., & Mazzà, C. (2015b). Concurrent reliability assessment of four foot models for gait analysis. *XVI congress od the Società Italiana di Analisi del Movimiento in Clinica.* Padova.

Diop, M., Rahmani, A., Belli, A., Gautheron, V., Geyssant, A., & Cottalorda, J. (2005). Influence of Speed Variation and Age on Ground Reaction Forces and Stride Parameters of Children's Normal Gait. *International Journal of Sports Medicine*, 682-687.

Dixon, P., Böhm, H., & Döderlein, L. (2012). Ankle and midfoot kinetics during normal gait: A multi-segment approach. *Journal of Biomechanics*, 1011-1016.

Dobkin, B. (2006). Short-distance walking speed and timed walking distance: Redundant measures for clinical trials? *Neurology*, 584-586.

Dubbeldam, R., Buurke, J., Simons, C., Groothuis-Oudshoorn, C., Baan, H., Nene, A., & Hermens, H. (2010). The effects of walking speed on forefoot, hindfoot and ankle joint motion. *Clinical Biomechanics*, 796-801.

Ebrahimi, A., Goldberg, S., & Stanhope, S. (2017). Changes in relative work of the lower extremity joints and distal foot with walking speed. *Journal of Biomechanics*, 212-216.

EBSCOHealth. (2012, October 29). *Medial View of the Foot.* Retrieved from SMARTImagebase. Scientific and medical ART.:

https://ebsco.smartimagebase.com/search?q=bones+of+the+foot%3A+medial+view&invert=1

Edelstein, J. (1988). Foot care for the aging. *Phys Ther.*, 1882-1886.

Eerdekens, M., Deschamps, K., & Staes, F. (2019). The impact of walking speed on the kinetic behaviour of different foot joints. *Gait & Posture*, 375-381.

Elftman, H. (1960). The transverse tarsal joint and its control. *Clin Orthop.*, 41-46.

Endo, M., Ashton-Miller, J., & Alexander, N. (2002). Effects of age and gender on toe flexor muscle strength. *J Gerontol A Biol Sci Med Sci*, 392-397.

England, S., & Granata, K. (2007). The influence of gait speed on local dynamic stability of walking Scott. *Gait & Posture*, 172-178.

Eslami, M., Begon, M., Farahpour, N., & Allard, P. (2007). Forefoot–rearfoot coupling patterns and tibial internal rotation during stance phase of barefoot versus shod running. *Clinical Biomechanics*, 74-80.

Frey, C. (2000). Foot health and shoewear for women. *Clin Orthop Relat Res*, 32-44.

Fritz, J., Canseco, K., Konop, K., Kruger, K., Tarima, S., Long, J., . . . Harris, G. (2021). Multi-segment foot kinematics during gait following ankle arthroplasty. *Journal of Orthopaedic Research*, 1-10.

G, M., C, P., Labs, K., & Duda, G. (2003). The influence of walking speed on kinetic and kinematic parameters in patients with osteoarthritis of the hip using a force-instrumented treadmill and standardised gait speeds. . *Archives of Orthopaedic and Trauma Surgery*, 278-282.

Giacomozzi, C., & Macellari, V. (1997). Piezo-dynamometric platform for a more complete analysis of foot-to-floor interaction. *IEEE Trans Rehabil Eng*, 322-330.

Giacomozzi, C., Leardini, A., & Caravaggi, P. (2014). Correlates between kinematics and baropodometric measurements for an integrated in-vivo assessment of the segmental foot function in gait. *Journal of Biomechanics*, 2654-2659.

Goldie, P., Matyas, T., & Evans, O. (1996). Deficit and change in gait velocity during rehabilitation after stroke. *Archives of Physical Medicine and Rehabilitation*, 1074-1082.

Graham, J., Ostir, G., Fisher, S., & Ottenbacher, K. (2008). Assessing walking speed in clinical research: a systematic review. *Journal of Evaluation in Clinical Practice*, 552-562.

Grant, J., & Chester, V. (2015). The Effects of Walking Speed on Adult Multi-segment Foot Kinematics. *Bioengineering & Biomedical Science*.

Green, J., Forster, A., & Young, J. (2002). Reliability of gait speed measured by a timed walking test in patients one year after stroke. *Clinical Rehabilitation*, 306-314.

Guralnik, J., Ferucci, L., Pieper, C., Leveille, S., Markides, K., Ostir, G., . . . Wallace, R. (2000). Lower extremity function and subsequent disability: consistency across studies, predictive models, and value of gait speed alone compared with the short

physical performance battery. *Journals of Gerontology Series A Biological Sciences and Medical Sciences*, 221-231.

Hagerdon, T., Dufour, A., Golightly, Y., Riskowski, J., Hillstrom, H., Casey, V., & Hannan, M. (2013). Factors affecting center of pressure in older adults: the Framingham Foot Study. *Journal of Foot and Ankle Research*.

Haight, D. (2012). The effects of walking speed on knee joint loading estimated via musculoskeletal modeling.

Haight, D. (2012). *THE EFFECTS OF WALKING SPEED ON KNEE JOINT LOADING ESTIMATED VIA MUSCULOSKELETAL MODELING*. Colorado: Colorado State University.

Hawes, M., Nachbauer, W., Sovak, D., & Nigg, B. (1992). Footprint parameters as a measure of arch height. *Foot Ankle*, 22-26.

Henley, J., Hudson, D., Church, C., Coleman, S., Kerstetter, L., & Miller, F. (2008). Reliability of a clinically practical multisegment foot marker set/model. In G. Harris, & P. Smith, *Foot and ankle motion analysis clinical treatment and technology* (pp. 445-463). CRC Press.

Herman, S., Kiely, D., Leveille, S., O'Neill, E., Cyberey, S., & Bean, J. (2005). Upper and Lower Limb Muscle Power Relationships in Mobility-Limited Older Adults. *Journal of Gerontoly*, 476-480.

Herssens, N., Verbecque, E., Hallemans, A., Vereeck, L., Van Rompaey, V., & Saeys, W. (2018). Do spatiotemporal parameters and gait variability differ across the lifespan of healthy adults? A systematic review. *Gait & Posture*, 181-190.

Hesse, S., Werner, C., Paul, T., Bardeleben, A., & Chaler, J. (2001). Influence of walking speed on lower limb muscle activity and energy consumption during treadmill walking of hemiparetic patients. *Archives of Physical Medicine and Rehabilitation*, 1547-1550.

Hicks, J. (1954). The mechanics of the foot. II. The plantar aponeurosis and the arch. *J. Anat.*, 25-30.

Hill, M., Naemi, R., Branthwaite, H., & Chockalingam, N. (2017). The relationship between arch height and foot length: Implications for size grading. *Applied Ergonomics*, 243-250.

Hillstrom, H., Song, J., & Kraszewski, A. (2013). Foot type biomechanics part 1: structure and function of the asymptomatic foot. . *Gait & Posture*, 445-451.

Hoeymans, N., Wouters, E., Feskens, E., van den Bos, G., & Kromhout, D. (1997). Reproducibility of Performance-Based and Self-Reported Measures of Functional Status. *Journal of Gerontology*, 363-368.

Hof, A., Elzinga, H., Grimmius, W., & Halbertsma, J. (2002). Speed dependence of averaged EMG profiles in walking. *Gait and Posture*, 78-86.

Hollman, J., McDade, E., & Petersen, R. (2011). Normative spatiotemporal gait parameters in older adults. *Gait & Posture*, 111-118.

Holt, K., Jeng, S., Ratcliffe, R., & Hamill, J. (1995). Energetic Cost and Stability during Human Walking at the Preferred Stride Frequency. *Journal of Motor Behavior*, 164-178.

Houmard, J., Weidner, M., Gavigan, K., Tyndall, G., Hickey, M., & Alshami, A. (1998). Fiber type and citrate synthase activity in the human gastrocnemius and vastus lateralis with aging. . *J Appl Physiol*, 1337-1341.

Howard, L., Doherty, P., & Boyes, C. (2008). A survey of outcome measurement of balance, walking and gait amongst physiotherapists working in neurology in the UK. *Physiotherapy*, 125-132.

Hsu, C., Tsai, W., Chen, C., Shau, Y., Wang, C., & Chen, M. (2005). Effects of aging on the plantar soft tissues properties under the metatarsal heads at different impact velocities. *Ultrasound in Medicine Biology*, 1423-1429.

Hsu, J. (1971). Foot problems in the elderly patient. *J Am Geriatr Soc*, 880-886.

Hsu, T., Wang, C., Tsai, W., Kuo, J., & Tang, K. (1998). Comparison of the mechanical properties of the heel pad between young and elderly adults. *Archives of Physical Medicine Rehabilitation*, 1101-1104.

James, B., & Parker, A. (1989). Active and passive mobility of lower limb joints in elderly men and women. *Am J Phys Med Rehabil*, 162-167.

Jenkyn, T., Anas, K., & Nichol, A. (2009). Foot segment kinematics during normal walking using a multisegment model of the foot and ankle complex. *Journal of Biomechanics*, 3271-3278.

Judge, J., Davis, R., & Ounpuu, S. (1996). Step length reductions in advanced age: the role of ankle and hip kinetics. *Journals of Georontology Series A Biological Sciences and Medical Sciences*, 303-312.

Kadaba, M., Ramakrishnan, H., & Wootten, M. (1990). Measurement of Lower Extremity Kinematics During Level Walking. *Journal of Orthopaedic Research*, 383-392.

Kang, H., & Dingwell, J. (2008). Separating the effects of age and walking speed on gait variability. *Gait & Posture*, 572-577.

Kerrigan, D., Todd, M., Della Croce, U., Lipsitz, L., & Collins, J. (1998). Biomechanical gait alterations independent of speed in the healthy elderly: evidence for specific limiting impairments. *Archives of Physical Medicine and Rehabilitation*, 317-322.

Kim, E., Shin, H., Takatori, N., Yoo, H., Cho, Y., Yoo, W., & Lee, D. (2020). Inter-segmental foot kinematics during gait in elderly females according to the severity of hallux valgus. *Journal of Orthopaedic Research*, 2409-2418.

Kirkwood, R., de Souza, B., Vallone, M., Mingoti, S., Correa, R., & Ferreira, R. (2011). Step length appears to be a strong discriminant gait parameter for elderly females

highly concerned about falls: a cross-sectional observational study. *Physiotherapy*, 126-131.

Kirtley, C. (2006). Observational gait analysis . *Clinical Gait Analysis: Theory and Practice*, 267-278.

Kirtley, C., Whittle, M., & Jefferson, R. (1985). Influence of walking speed on gait parameters. *Journal of Biomedical Engineering*, 282-288.

Kottke, F. (1990). Therapeutic exercise to maintain mobility. *Krusen's handbook of physical medicine*, 436-451.

Kouchi, M. (1998). Foot dimensions and foot shape: differences due to growth, generation and ethnic origin. *Anthropol Sci*, 161-188.

Krauss, I., & Mauch, M. (2013). Foot Morphology. In R. Goonetilleke, *The Science of Footwear* (pp. 19-45). Florida: CRC Press.

Krauss, I., Grau, S., Mauch, M., Maiwald, C., & Horstmann, T. (2008). Sex-related differences in foot shape. *Ergonomics*, 1693-1709.

Krauss, I., Langbein, C., Horstmann, T., & Grau, S. (2011). Sex-related differences in foot shape of adult Caucasians - A follow up study focusing on long and short feet. *Ergonomics*, 294-300.

Kuo, H., Leveille, S., Yen, C., Chai, H., Chang, C., Yeh, Y., . . . Bean, J. (2006). Exploring How Peak Leg Power and Usual Gait Speed Are Linked to Late-Life Disability: Data from the National Health and Nutrition Examination Survey (NHANES), 1999–2002. *Am J Phys Med Rehabil*, 650-658.

Kwan, R., Zheng, Y., & Cheing, G. (2010). The effect of aging on the biomechanical properties of plantar soft tissues. *Clinical Biomechanics*, 601-605.

Kyung, M., Cho, Y., Hwang, S. L., Lee, M., & Lee, D. (2020). Change in intersegmental foot and ankle motion after a high tibial osteotomy in genu varum patients. *Journal of Orthopaedic Research*, 86-93.

Lanza, I., Towse, T., Caldwell, G., Wigmore, D., & Kent-Braun, J. (2003). Effects of age on human muscle torque, velocity, and power in two muscle groups. *Journal of Applied Physiology*, 2361-2369.

Lavcanska, V., Taylor, N., & Schache, A. (2005). Familiarization to treadmill running in young unimpaired adults. *Human Movement Science*, 544-557.

Leardini, A., & Caravaggi, P. (2016). Kinematic Foot Models for Instrumented Gait Analysis. In B. Müller, & S. Wolf, *Handbook of Human Motion* (pp. 1-24). Springer International Publishing.

Leardini, A., Benedetti, M., Berti, L., Bettinelli, D., Nativo, R., & Giannini, S. (2007). Rear-foot, mid-foot and fore-foot motion during the stance phase of gait. *Gait & Posture*, 453-462.

Lee, D., Seo, S., Lee, D., Bae, K., Lee, K., & Choi, H. (2007). Inter-segmental motions of the foot: differences between younger and older healthy adult females. *Journal of Foot and Ankle Research*, 1-9.

Lee, L., & Kerrigan, C. (2004). Dynamic Hip Flexion Contractures. *American Journal of Physical Medicine & Rehabilitation*.

Lee, L., Kerrigan, D., & Della Croce, U. (1997). Dynamic implications of hip flexion contractures. *Am J Phys Med Rehabil*, 502-508.

Lee, L., Zavarei, K., Evans, J., Lelas, J., Riley, P., & Kerrigan, C. (2005). Reduced Hip Extension in the Elderly: Dynamic or Postural? *Archives of Physical Medicine and Rehabilitation*, 1851-1854.

Lee, Y., Lin, G., & Wang, M. (2014). Comparing 3D foot scanning with conventional measurement methods. *Journal of Foot and Ankle Research*.

Legault-Moore, D., Chester, V., & de Vries, G. (2012). Multisegment Foot Kinematics During Walking in Younger and Older Adults. *J Clin Med Res*, 259-266.

Lelas, J., Merriman, G., Riley, P., & Kerrigan, C. (2003). Predicting peak kinematic and kinetic parameters from gait speed. *Gait & Posture*, 106-112.

Li, L., & Caldwell, G. (1999). Coefficient of cross correlation and the time domain correspondence. *J Electromyogr Kinesiol*, 385-389.

Lindle, R., Metter, E., Lynch, N., Fleg, J., Fozard, J., Tobin, J., . . . Hurley, B. (1997). Age and gender comparisons of muscle strength in 654 women and men aged 20–93 yr. *Journal of Applied Physiology*.

Lockhart, T., Woldstad, J., & Smith, J. (2003). Effects of age-related gait changes on the biomechanics of slips and falls. *Ergonomics*, 1136-1160.

Lundgren, P., Nester, C., Liu, A., Jones, R., Stacoff, A., Wolf, P., & Lundberg, A. (2008). Invasive in vivo measurement of rear-, mid- and forefoot motion during walking. *Gait & Posture*, 93-100.

MacWilliams, B., Cowley, M., & Nicholson, D. (2003). Foot kinematics and kinetics during adolescent gait. *Gait & Posture*, 214-224.

Mahaffey, R., Morrison, S., Drechsler, W., & Cramp, M. (2013). Evaluation of multi-segmental kinematic modelling in the paediatric foot using three concurrent foot models. *Journal of Foot and Ankle Research*.

Malatesta, D., Simar, D., Dauvilliers, Y., Candau, R., Borrani, F., Prefaut, C., & Caillaud, C. (2003). Energy cost of walking and gait instability in healthy 65-and 80-yr-olds. *Journal of Applied Physiology*.

Marcial, N., Kieley, M., Sembinelli, D., & Chester, V. (2021). Inter- and Intra-rater reliability and validity of real-time 3D foot scanner in non-weight bearing and weight bearing conditions. *Canadian Socierty for Biomechanics.* Montreal.

Marcial, N., Kuruganti, U., & Chester, V. (2021). Age-related differences in foot structure and mobility. *The 42nd Conference of The Canadian Medical and Biological Engineering Society/La Société Canadienne de Génie Biomédical.* Montreal.

Mauch, M., Grau, S. K., Maiwald, C., & Horstmann, T. (2009). A new approach to children's footwear based on foot type classification. *Ergonomics*, 999-1008.

Mauch, M., Mickle, K., Munro, B., Dowling, A., Grau, S., & Steele, J. (2008). Do the feet of German and Australian children differ in structure? Implications for children's shoe design. *Ergonomics*, 527-539.

Maurer, J., Ward, V., Mayson, T., Davies, K., Alvarez, C., Beauchamp, R., & Black, A. (2013). A kinematic description of dynamic midfoot break in children using a multi-segment foot model. *Gait & Posture*, 287-292.

McGibbon, C., & Krebs, D. (1999). Effects of age and functional limitation on leg joint power and work during stance phase of gait. *Journal of Rehabilitation Research & Development*.

McKeon, P., Hertel, J., Bramble, D., & Davis, I. (2015). The foot core system: a new paradigm for understanding intrinsic foot muscle function. *British Journal of Sports Medicine*, 1-9.

McPoil, T., Cornwall, M., Medoff, L., Vicenzino, B., Forsberg, K., & Hilz, D. (2008b). Arch height change during sit-to-stand: an alternative for the navicular drop test. *Journal of Foot and Ankle Research*.

McPoil, T., Cornwall, M., Vicenzino, B., Teyhen, D., Molloy, J., Christie, D., & Collins, N. (2008a). Effects of using truncated versus total foot length to calculate the arch height ratio. *The Foot*, 220-227.

McPoil, T., Vicenzino, B., Cornwall, M., Collins, N., & Warren, M. (2009). Reliability and normative values for the foot mobility magnitude: a composite measure of vertical and medial-lateral mobility of the midfoot. *Journal of Foot and Ankle Research*.

Menz, H. (2003). Alternative techniques for the clinical assessment of foot pronation. *J Am Podiatr Med Assoc*, 203-213.

Menz, H. (2014). Biomechanics of the Ageing Foot and Ankle: A Mini-Review. *Gerontology*, 381-388.

Menz, H., & Munteanu, S. (2006). Validity of 3 clinical techniques for the measurement of static foot posture in older people. *J Orthop Sports Phys Ther*, 479-486.

Menz, H., Lord, S., & Fitzpatrick, R. (2003). Age-related differences in walking stability. *Age and Ageing*, 137-142.

Menz, H., Morris, M., & Lord, S. (2005). Foot and Ankle Characteristics Associated With Impaired Balance and Functional Ability in Older People. *Journal of Gerontology*, 1546-1552.

Mickle, K., Steele, J., & Munro, B. (2006). Does excess mass affect plantar pressure in young children? *Int. J. Pediatr. Obes.*, 183-188.

Middleton, A., Fritz, S., & Lusardi, M. (2015). Walking Speed: The Functional Vital Sign. *Human Kinetics Journal*, 314-322.

Min-Chi, C., Hsin-Chieh, W., Li-Yu, C., & Min-Huan, W. (2013). Center of pressure progression characteristics under the plantar region for elderly adults. *Gait & Posture*, 408-412.

Monaco, V., Rinaldi, L., Macri, G., & Micera, S. (2009). During walking elders increase efforts at proximal joints and keep low kinetics at the ankle. *Clinical Biomechanics*, 493-498.

Moretto, P., Bisiaux, M., & Lafortune, M. (2007). Froude number fractions to increase walking pattern dynamic similarities: Application to plantar pressure study in healthy subjects. *Gait & Posture*, 40-48.

Munro, C., Miller, D., & Fuglevand, A. (1987). Ground reaction forces in running: A reexamination. *Journal of Biomechanics*, 147-155.

Murray, M., Mollinger, L., G, G., & Sepic, S. (1984). Kinematic and EMG patterns during slow, free, and fast walking. *J Orthop Res*, 272-280.

Murray, M., Spurr, G., Sepic, S., Gardner, G., & Mollinger, L. (1985). Treadmill vs. floor walking: kinematics, electromyogram, and heart rate. *Journal of applied physiology*, 87-91.

Nácher, B., Alemany, S., Gonzáles, J., Alcántara, E., Garcia-Hernández, J., Heras, S., & Juan, A. (2006). A footwear fit classification model based on anthropometric data. *2006 Digital Human Modeling for Design and Engineering Conference.* Lyon.

Nagano, H., Begg, R., Sparrow, W., & Taylor, S. (2013). A Comparison of Treadmill and Overground Walking Effects on Step Cycle Asymmetry in Young and Older Individuals. *Journal of Applied Biomechanics*, 188-193.

Nawoczenski, D., Saltzman, C., & Cook, T. (1998). The effect of foot structure on the three-dimensional kinematic coupling behavior of the leg and rear foot. *Phys. Ter.*, 404-416.

Nester, C., Liu, A., Ward, E., Howard, D., Cocheba, J., & Derrick, T. (2010). Error in the description of foot kinematics due to violation of rigid body assumptions. *Journal of Biomechanics*, 666-672.

Nigg, B., Cole, G., & Nachbauer, W. (1993). Effects of arch height of the foot on angular motion of the lower extremities in running. *Journal of Biomechanics*, 909-916.

Nigg, B., Fisher, V., Allinger, T., Ronsky, J., & Engsberg, J. (1992). Range of motion of the foot as a function of age. *Foot Ankle*, 336-343.

Okita, N., Meyers, S., Challis, J., & Sharkey, N. (2013). Midtarsal Joint Locking: New Perspectives on an Old Paradigm. *Journal of Orthopaedic Research*, 110-115.

Orendurff, M., Segal, A., Klute, G., Berge, J., Rohr, E., & Kadel, N. (2004). The effect of walking speed on center of mass displacement. *Journal of Rehabilitation Research & Development*, 829-834.

Ouzounian, T., & Shereff, M. (1989). In Vitro Determination of Midfoot Motion. *Foot & Ankle*, 140-146.

Pearson Education Inc. (2016). *Dorsal view of the bones of the right foot.* Retrieved from PurposeGames: https://www.purposegames.com/game/dorsal-view-of-the-bones-of-the-right-foot

Pol, F., Baharlouei, H., Taheri, A., Menz, H., & Forghany, S. (2021). Foot and ankle biomechanics during walking in older adults: A systematic review and meta-analysis of observational studies. *Gait & Posture*, 14-24.

Portinaro, N., Leardini, A., Panou, A., Monzani, V., & Caravaggi, P. (2014). Modifying the Rizzoli Foot Model to improve the diagnosis of pes-planus: application to kinematics of feet in teenagers. *Journal of Foot and Ankle Research*.

Prince, F., Corriveau, H., Hebert, R., & Winter, D. (1997). Gait in the elderly. *Gait & Posture*, 128-135.

Purser, J., Weinberger, M., Cohen, H., Pieper, C., Morey, M., Li, T., . . . Lapuerta, P. (2005). Walking speed predicts health status and hospital costs for frail elderly male veterans. *Journal of Rehabilitation Research & Development*, 535-546.

R, F., IM, D., & DS, W. (2005). Effect of foot orthotics on rearfoot and tibia joint coupling patterns and variability. *J Biomech*, 477-483.

Rabadi, M., & Blau, A. (2005). Admission ambulation velocity predicts length of stay and discharge disposition following stroke in an acute rehabilitation hospital. *Neurorehabil Neural Repair*, 20-26.

Rao, S., Baumhauer, J., Tome, J., & Nawoczenski, D. (2009). Comparison of in vivo segmental foot motion during walking and step descent in patients with midfoot arthritis and matched asymptomatic control subjects. *Journal of Biomechanics*, 1054-1060.

Riddiford-Harland, D., Steele, J., & Storlien, L. (2000). Does obesity influence foot structure in prepubescent children? *Int. J. Obes. Relat. Metab. Disord.*, 541-544.

Riley, P., Della Croce, U., & Kerrigan, C. (2001). Effect of age on lower extremity joint moment contributions to gait speed. *Gait & Posture*, 264-270.

Riley, P., Paolini, G., Della Croce, U., Paylo, K., & Kerrigan, C. (2007). A kinematic and kinetic comparison of overground and treadmill walking in healthy subjects. *Gait & Posture*, 17-24.

Robertson, D., Caldwell, G., Hamill, J., Kamen, G., & Whittlesey, S. (2014). *Research Methods in Biomechanics.* Champaign, IL: Human Kinetics.

Rodgers, M. (1995). Dynamic Foot Biomechanics. *Journal of Orthopaedic & Sports Physical Therapy*, 306-316.

Roislien, J., Skare, O., Gustavsen, M., Broch, N., Rennie, L., & Opheim, A. (2009). Simultaneous estimation of effects of gender, age and walking speed on kinematic gait data. *Gait & Posture* , 441-445.

Rothstein, J., & Echternach, J. (1993). Primer on measurement: an introductory guide to measurement issues, featuring the American Physical Therapy Association's standards for tests and measurements in physical therapy practice. *Amer Physical Therapy Assn*.

Rouhani, H., Favre, J., Crevoisier, X., Joles, B., & Aminian, K. (2011). Segmentation of foot and ankle complex based on kinematic criteria. *Comput Methods Biomech Biomed Engin*, 773-781.

Saghazadeh, M., Kitano, N., & Okura, T. (2015). Gender differences of foot characteristics in older Japanese adults using a 3D foot scanner. *Journal of Foot and Ankle Research*, 8-29.

Salbach, N., Mayo, N., Higgins, J., Ahmed, S., Finch, L., & Richards, C. (2001). Responsiveness and predictability of gait speed and other disability measures in acute stroke. *Archives of Physical Medicine and Rehabilitation*, 1204-1212.

Saraswat, P., MacWilliams, B., Davis, R., & D'Astous, J. (2014). Kinematics and kinetics of normal and planovalgus feet during walking. *Gait & Posture*, 339-345.

Sarrafian, S. (1987). Functional characteristics of the foot and plantar aponeurosis under tibiotalar loading. . *Foot Ankle*, 4-18.

Sarrafian, S. (1993). Biomechanics of the subtalar joint complex. . *Clinical Orthopaedics and Related Research*, 17-26.

Schenkman, M., Cutson, T., Kuchibhatla, M., Chandler, J., & Pieper, C. (1997). Reliability of Impairment and Physical Performance Measures for Persons With Parkinson's Disease. *Physical Therapy* , 19-27.

Schmitz, A., Silder, A., Heiderscheit, B., Mahoney, J., & Thelen, D. (2009). Differences in lower-extremity muscular acti- vation during walking between healthy older and young adults. . *J Electromyogr Kinesiol*, 1085-1091.

Schrager, M., Kelly, V., Price, R., Ferrucci, L., & Shumway-Cook, A. (2008). The effects of age on medio-lateral stability during normal and narrow base walking. *Gait & Posture*, 466-471.

Schwartz, M., Rozumalski, A., & Trost, J. (2008). The effect of walking speed on the gait of typically developing children. *Journal of Biomechanics*, 1639-1650.

Scott, G., Menz, H., & Newcombe, L. (2007). Age-related differences in foot structure and function. *Gait&Posture*, 68-75.

Shimada, T. (1996). Factors affecting appearance patterns of hip-flexion contractures and their effects on postural and gait abnormalities. *Kobe J Med Sci*, 271-290.

Shin, H., Lee, J., Kim, E., Kyung, M., Yoo, H., & Lee, D. (2019). Flatfoot deformity affected the kinematics of the foot and ankle in proportion to the severity of deformity. *Gait & posture*, 123-128.

Silder, A., Heiderscheit, B., & Thelen, D. (2008). Active and passive contributions to joint kinetics during walking in older adults. *Journal of Biomechanics*, 1520-1527.

Snyder, K., Earl, J., O'Connor, K., & K., E. (2009). Resistance training is accompanied by increases in hip strength and changes in lower extremity biomechanics during running. *Clinical Biomechanics*, 26-34.

Souza, T., Fonseca, H., Vaz, A., Antero, J., Marinho, C., & Fonseca, S. (2014). Between-Day Reliability of a Cluster-Based Method for Multisegment Kinematic Analysis of the Foot-Ankle Complex. *Am Podiatr Med Assoc*, 601-609.

Spink, M., Fotoohabadi, M., Wee, E., Hill, K., Lord, S., & Menz, H. (2011). Foot and Ankle Strength, Range of Motion, Posture, and Deformity Are Associated With Balance and Functional Ability in Older Adults. *Archives of Physical Medicine and Rehabilitation*, 68-75.

Stansfield, B., Hillman, S., Hazlewood, M., Lawson, A., Mann, A., Loudon, I., & Robb, J. (2001). Normalized speed, not age, characterizes ground reaction force patterns in 5- to 12-year-old children walking at self-selected speeds. *Journal of Pediatric Orthopedics*, 395-402.

Stevens, J., & Choo, K. (1996). Spatial acuity of the body surface over the life span. *Somatosens Mot Res*, 153-166.

Stolze, H., Kuhtz-Buschbeck, J., Mondwurf, C., Boczek-Funcke, A., Johnk, K., Deuschl, G., & Illert, M. (1997). Gait analysis during treadmill and overground locomotion in children and adults. *Electroencephalography and Clinical Neurophysiology/Electromyography and Motor Control*, 490-497.

Sudarsky, L. (2000). Gait disorders: prevalence, morbidity, and etiology. *Adv Neurol*, 111-117.

Sun, D., Fekete, G., Mei, Q., & Gu, Y. (2018). The effect of walking speed on the foot inter-segment kinematics, ground reaction forces and lower limb joint moments. *PeerJ*.

Sushima, H., Morris, M., & McGinley, J. (2003). Test-Retest reliability and inter-tester reliability of kinematic data from a three-dimensional gait analysis system. *Journal of the japanese physical theraphy association*, 9-17.

Sutherland, D. H. (1988). *The Development of mature walking.* Philadelphia: Oxford: McKeith Press.

Takahashi, K., Worster, K., & Bruening, D. (2017). Energy neutral: the human foot and ankle subsections combine to produce near zero net mechanical work during walking. *Scientific Reports*, 1-9.

Telfer, S., & Woodburn, J. (2010). The use of 3D surface scanning for the measurement and assessment of the human foot. *Journal of Foot and Ankle Research*, 3-19.

Thelen, D., Schultz, A., Alexander, N., & Ashton-Miller, J. (1996). Effects of Age on Rapid Ankle Torque Development. *Journal of Gerontoly*, 226-232.

Trombetti, A., Reid, K., Hars, M., Herrman, F., Pasha, E., Phillips, E., & Fielding, R. (2016). Age-associated declines in muscle mass, strength, power,and physical performance: impact on fear of falling and quality of life. *Osteoporos Int*, 463-471.

Tulchin, K., Orendurff, M., & Karol, L. (2010). A comparison of multi-segment foot kinematics during level overground and treadmill walking. *Gait & Posture*, 104-108.

Tulchin, K., Orendurff, M., Adolfsen, S., & Karol, L. (2009). The Effects of Walking Speed on Multisegment Foot Kinematics in Adults. *Human Kinetics*, 377-386.

Tyrell, C., Roos, M., Rudolph, K., & Resiman, D. (2011). Influence of Systematic Increases in Treadmill Walking Speed on Gait Kinematics After Stroke. *Physical Therapy*, 392-403.

Tyson, S., & DeSouza, L. (2004). Reliability and validity of functional balance tests post stroke. *Clinical Rehabilitation*, 916-923.

Umberger, B., & Martin, P. (2007). Mechanical power and efficiency of level walking with different stride rates. *Journal of Experimental Biology*, 3255-3265.

Van Boerum, D., & Sangeorzan, B. (2003). Biomechanics and pathophysiology of flat foot. *Foot Ankle Clin*, 419-430.

Van Hoeve, S., Leenstra, B., Willems, P., Poeze, M., & Meijer, K. (2017). The effect of age and speed on foot and ankle kinematics assessed using a 4-segment foot model. *Medicine*.

Vandervoort, A., Chesworth, B., Cunningham, D., Paterson, D., Rechnitzer, P., & Koval, J. (1992). Age and sex effects on mobility of the human ankle. *Journal of Gerontology*, M17-M21.

Verghese, J., Wang, C., & Holtzer, R. (2011). Relationship of Clinic-Based Gait Speed Measurement to Limitations in Community-Based Activities in Older Adults. *Archives of Physical Medicine and Rehabilitation*, 844-846.

Wagenaar, R., & Beek, W. (1992). Hemiplegic gait: A kinematic analysis using walking speed as a basis. *Journal of Biomechanics*, 1007-1015.

Waite, L., Grayson, D., Piguet, O., Creasey, H., Bennett, H., & Broe, G. (2005). Gait slowing as a predictor of incident dementia: 6-year longitudinal data from the Sydney Older Persons Study. *J Neurol Sci*, 89-93.

Wall, J., Hogan, D., Turnbull, G., & Fox, R. (1991). The kinematics of idiopathic gait disorder. A comparison with healthy young and elderly females. *J Rehabil Med*, 159-164.

White, S., Tucker, C., Brangaccio, J., & Lin, H. (1996). Relation of vertical ground reaction forces to walking speed. *Gait & Posture*.

White, S., Tucker, C., Brangaccio, J., & Lin, H. (1996). Relation of vertical ground reaction forces to walking speed. *Gait & Posture*.

Wilken, J., Rao, S., Saltzman, C., & Yack, J. (2011). The effect of arch height on kinematic coupling during walking. *Clinical Biomechanics*, 318-323.

Williams, D. M., Hamill, J., & Buchanan, T. (2001). Lower extremity kinematic and kinetic differences in runners with high and low arches. *Journal of Applied Biomechanics*, 153-163.

Williams, D., & McClay, I. (2000). Measurements used to characterie the foot and the medial longitudinal arch: reliability and validity. *Phys Ter*, 864-871.

Winter, D. (1983a). Biomechanical motor patterns in normal walking. . *J Motor Behav*, 302-330.

Winter, D. (1983b). Energy generation and absorption at the ankle and knee during fast, natural, and slow cadences. *Clin Orthop.*, 147-154.

Winter, D. (1988). *The biomechanics and motor control of human gait.* Waterloo: University of Waterloo Press.

Winter, D. (1991). *The biomechanics and motor control of human gait : normal, elderly and pathological.* Waterloo: University of Waterloo Press.

Winter, D., Patla, A., Frank, J., & Walt, S. (1990). Biomechanical walking pattern changes in the fit and healthy elderly. *Phys Ter*, 340-347.

Witana, C., Xiong, S., Zhao, J., & Goonetilleke, R. (2006). Foot measurements from three-dimensional scans: A comparison and evaluation of different methods. *Int. J. Ind. Ergon.*, 789-807.

Woodhull-McNeal, A. (1992). Changes in posture and balance with age. *Aging*, 219-225.

Woollacott, M., & Shumway-Cook, A. (1990). Changes in posture control across the life span – a systems approach. *Phys Ther*, 799-807.

Yu, C., & Tu, H. (2009). Foot surface area database and estimation formula. *Appl. Ergon.*, 767-774.

Zelik, K., & Honert, E. (2018). Ankle and foot power in gait analysis: Implications for science, technology and clinical assessment. *Journal of Biomechanics* , 1-12.

Zeni Jr, J., Richards, J., & Higginson, J. (2008). Two simple methods for determining gait events during treadmill and overground walking using kinematic data. *Gait & Posture*, 710-714.

Zeni Jr., J., & Higginson, J. (2009). Differences in gait parameters between healthy subjects and persons with moderate and severe knee osteoarthritis: A result of altered walking speed? *Clin Biomech*, 372-378.

Zhao, X., Tjusimoto, T., Kim, B., Katayama, Y., Ogiso, K., Takenaka, M., & Tanaka, K. (2018). Does Weight Reduction Affect Foot Structure and the Strength of the Muscles That Move the Ankle in Obese Japanese Adults? *The Journal of Foot & Ankle Surgery*, 281-284.

ZIPAPP.CO. (2018, December 13). *Fashion Figure Templates Front And Back* . Retrieved from http://zippapp.co/get/

Curriculum Vitae

Candidate's full name: Nayeli Guadalupe Marcial Muñoz

Education: Biomedical Engineer, Tecnológico de Monterrey (2013-2018)

Conference Presentations and Publications:

- Marcial, N., Chester, V., & Kuruganti, U. (2021). A comparison of multisegment foot kinematics between younger and older adults during walking. *International Society of Biomechanics*. Stockholm.
- Marcial, N., Kuruganti, U., & Chester, V. (2021). Age-related differences in foot structure and mobility. *The Canadian Medical and Biological Engineering Society*. Montreal.
- Marcial, N., Kieley, M., Sembinelli, D., & Chester, V. (2021). Inter- and Intra-rater reliability and validity of real-time 3D foot scanner in non-weight bearing and weight bearing conditions. *Canadian Society for Biomechanics*. Montreal.
- Marcial, N., & Chester, V. (2020). Sex and age-related differences in foot structure using a 3D scanner. *New Brunswick Health Research Foundation - Health Research Week.* Fredericton: NBHRF.
- Marcial, N., Kieley, M., & Chester, V. (2020). Differences in foot structure between younger and older adults using a 3D foot scanner. *International Society of Electrophysiology and Kinesiology*. Tokyo.
- Marcial, N., Kieley, M., Sembinelli, D., & Chester, V. (2020). Inter-and Intra-Rater Reliability and Validity of a 3D body segment scanner to obtain foot anthropometrics. *International Society of Electrophysiology and Kinesiology*. Tokyo.

Research Projects:

- *Inter- and Intra-Examiner Reliability and Validity of Real-Time 3D Foot Scanning in Nonweight Bearing and Weight Bearing Conditions (*July '19-January'20)
  Responsible for ethics applications, literature reviews, protocols, recruitment of participants, as well as the collection, process and analysis of data collected from 3D scanner.
- *Walking patterns in children with autism and cerebral palsy (*Sept '18 – Dec '19)
  Responsible for collecting and processing gait data from autistic children and with cerebral palsy. The project involved working directly with engineers and physiotherapists to provide clinicians the information they requested for their patients, as well as the interaction with patients and their families.
- *Measuring physiological and biomechanical performance data during a two-month competitive season period in varsity female hockey players. (*Jan '19-March '19)
  Responsible for ethics applications, literature reviews, protocols, recruitment of participants, as well as collecting and processing data collected from varsity female hockey players at the University of New Brunswick. The project involved working directly with the athletes of the team, as well as the strength and conditioning coach.